FAULT ESTIMATION AND FAULT TOLERANT CONTROL WITH APPLICATION TO WIND TURBINE SYSTEMS

XIAOXU LIU

PhD

2017

Fault Estimation and Fault Tolerant Control with Application to Wind Turbine Systems

Xiaoxu Liu

A thesis submitted in partial fulfilment of the requirements of the University of Northumbria at Newcastle for the degree of Doctor of Philosophy

Research undertaken in the Faculty of Engineering and Environment

August 2017

Abstract

In response to the high demand of the operation reliability by implementing real-time monitoring and system health management, the three-year PhD project focuses on developing robust fault diagnosis and fault tolerant control strategies for complex systems with high-nonlinearities, stochastic Brownian perturbations, and partially decoupled unknown inputs, which are then applied to wind turbine energy systems.

Integration of serval advanced approaches, including the augmented system method, unknown input observer design, Takagi-Sugeno fuzzy logic, linear matrix inequality optimization, and signal compensation techniques enable us to achieve robust estimations of both the system states and the faults concerned simultaneously, while removing/reducing the adverse influences from faults to the system dynamics. Prior to the existing work, the considered unknown inputs can be partially decoupled rather than completely decoupled, which can meet a wider practical requirement. Moreover, the systems under investigation can be linear, Lipschitz nonlinear, quadratic inner-bounded nonlinear, high-nonlinear characterized by a Takagi-Sugeno fuzzy model, and stochastic with Brownian perturbations, which can cover a wide range of real industrial plants.

Specifically, the augmented system method is used to construct an augmented plant with the concerned faults and system states being the augmented states. Unknown input observer technique is thus utilized to estimate the augmented states and decouple unknown inputs that can be decoupled. Linear matrix inequality approach is further addressed to ensure the stability of the estimation error dynamics and attenuate the influences from the unknown inputs that cannot be decoupled. As a result, the robust estimates of the faults concerned and system states can be obtained simultaneously. Based on the fault estimates, a signal compensation scheme is developed to remove/offset the effects of the faults to the system dynamics and outputs, leading to a stable dynamic satisfying the expected performance.

A case study on a 4.8 MW wind turbine benchmark system is proposed to illustrate and demonstrate the proposed integrated fault tolerant control techniques. Takagi-Sugeno modelling of a wind turbine system is presented as a by-product.

To summarize, the proposed integrated fault estimation and fault tolerant control strategy can handle a system with highly nonlinear dynamics in a strong disturbance/noise environment (e.g., partially-decoupled process disturbances and stochastic parameter perturbations), which is validated by a real-time wind turbine system. As a result, the presented methods/algorithms have enriched fault diagnosis and tolerant control theory with high-novelty and great potentials for practical applications.

Keywords: Fault estimation; unknown input observer; signal compensation; wind turbines; nonlinear systems; partially decoupled unknown inputs; stochastic Brownian motion.

Contents

Abstract i
Acknowledgements vii
Declaration viii
List of notifications ix
Chapter 1 1
Introduction 1
1.1 Research motivations 1
1.2 Summary of contributions of the thesis 2
1.3 Organisation of the thesis 4
1.4 List of publications 5
1.4.1 Journal articles 5
1.4.2 Conference articles 5
Chapter 2 7
Literature Review 7
2.1 Review of fault diagnosis and fault tolerant control techniques 7
2.1.1 Model-based approaches 7
2.1.2 Signal-based approaches 10
2.1.3 Data-driven approaches 12
2.1.4 Hybrid approaches 13
2.2 Construction of wind turbine and typical faults. 13
2.3 Fault diagnosis and fault tolerant control techniques for wind turbine systems 16
2.3.1 Model-based approaches for wind turbines 16
2.3.2 Signal-based approaches for wind turbines 18
2.3.3 Data-driven approaches for wind turbines 18
2.3.4 Hybrid approaches for wind turbines 18
2.4 Summary 19

Chapter 3 20
Robust fault estimation for linear system and Lipschitz nonlinear system 20
3.1 Fault estimation for linear system 20
3.1.1 System description and augmented system 20
3.1.2 Novel unknown input observer (UIO) 21
3.1.3 Design procedure of the UIO for fault estimation 26
3.2 UIO-based fault estimation for Lipschitz nonlinear system 26
3.2.1 Nonlinear system subjected to process disturbances 26
3.2.2 Nonlinear system with process and sensor disturbances 29
3.2.3 Design procedure of the Nonlinear UIO for fault estimation 32
3.3 Illustration examples 32
3.3.1 Three-shaft gas turbine engine 32
3.3.2 Single-link flexible joint robot 37
3.4 Summary 40
Chapter 4. 42
Integrated fault tolerant control for Takagi-Sugeno system 42
4.1 Robust fault estimation of T-S fuzzy System 43
4.2 Tolerant design with signal compensation 49
4.3 Summary 54
Chapter 5. 56
Fault estimation for stochastic system 56
5.1 Preliminaries and problem formulation 57
5.2 Lyapunov function-based properties of finite-time stochastic input-to-state-stability 60
5.3 Robust fault estimation for quadratic inner bounded nonlinear system 64
5.4 Robust fault estimation of Takagi-Sugeno stochastic system 72
5.5 Illustration examples 78
5.6 Summary 90

Chapter 6 91
Integrated fault tolerant control of stochastic system 91
6.1 Integrated fault tolerant control of linear stochastic system 92
6.1.1 Joint observer for robust fault estimation 93
6.1.2 Robust estimation-based fault tolerant control 95
6.2 Integrated fault tolerant control of Lipschitz nonlinear stochastic system 102
6.3 Integrated fault tolerant control of quadratic inner-bounded nonlinear stochastic system 111
6.4 Integrated fault tolerant control of T-S fuzzy nonlinear stochastic system 120
6.4.1 Joint observer techniques for robust fault estimation 120
6.4.2 Design of observer-based control law 124
6.4.3 Reachability of the sliding mode surface 132
6.5 Summary 142
Chapter 7 143
Case study on benchmark wind turbine 143
7.1 System overview of benchmark wind turbine 143
7.1.1. Blade and pitch system 144
7.1.2. Drive train model 145
7.1.3. Generator and converter model 146
7.1.4. Controller 146
7.2 Takagi-Sugeno modelling of benchmark wind turbine 148
7.3 Fault estimation and signal compensation of wind turbine 153
7.3.1. Fault estimation/reconstruction 154
7.3.2. Fault tolerance by signal compensation 157
7.4 Robust fault estimation and fault tolerant control for drive train system subject to stochastic perturbations 159
7.5 Summary 163

Chapter 8 164
Conclusions 164
8.1 Thesis summary 164
8.2 Further research 166
Appendix 1 168
System coefficients of *Example 5.5.3* 168
Appendix 2 172
Simulink blocks of T-S fuzzy modelling 172
Appendix 3 174
System coefficients of benchmark wind turbine characterized by T-S fuzzy model 174
Appendix 4 178
Simulink blocks of fault estimation of benchmark wind turbine 178
Appendix 5 181
Simulink blocks of signal compensation of benchmark wind turbine 181
References 182

Acknowledgements

This thesis would not have been possible without the encouragement and input of many people. I am grateful to several individuals who have supported me in various ways during my PhD period and would like to hereby acknowledge their assistance.

First and foremost, I wish to express my deep thanks to my supervisor, Dr. Zhiwei Gao for his enlightening guidance, invaluable discussions and insightful ideas on my research work. Without his constructive advice and encouraging supervision, I cannot make this study possible. What I have benefited most from him is the rigorous and diligent attitude to scientific research. He also gave me quite a lot of support on both my research, teaching experiences and future plan. He makes me find a better and confident me than I ever imagined.

Especially, I would like to express my heartfelt appreciation to Dr. Hui Shao who provided me valuable support for the wind turbine fuzzy modelling, which is an important part of my PhD work. She also gave me a lot of guidance to both my research and life.

Furthermore, I would like to thank Prof. Ghanim Putrus for his kind advice and support of my PhD experience.

I would like to extend my gratitude to Prof. Steven Ding in AKS, for his guidance and support. I also thank all AKS members who provided me kind help, discussion, and valuable idea during my visit.

Thanks to Dr. Dapeng Zhang, Dr. Zhiling Lin, Prof. Yanling Li, Dr. Sarah Odofin, and Mr. Yichuan Fu who provided me good research atmosphere and make my research time enjoyable. I also express my thanks to the other members of the research group who provided me helpful ideas and discussions.

I gratefully acknowledge Northumbria University for providing me the scholarship and facilities to carry out my research. I also express my gratitude to the supporting staffs in Faculty of Engineering and Environment for their kind help.

Last but far from least, I wish to devote my special thanks to my parents and my husband for their love, encouragement and support.

Declaration

I declare that the work contained in this thesis is my own work, and to the best of my knowledge, it reproduces no material previously published or written, nor material has not been submitted for any other degree.

Any ethical clearance for the research presented in this thesis has been approved. Approval has been sought and granted by the University Ethics Committee on 14^{th} November, 2014.

I declare that the word count of this thesis is 34,120 words.

Name: ______________________________

Date: ________________________________

List of notifications

$\mathcal{R}^n$	n-dimentional Euclidean space
$\mathcal{R}^{n\times m}$	Set of $n \times m$ real matrices
I_n	Identity matrix with dimension of $n \times n$
0	A scalar zero or a zero matrix with appropriate zero entries
Superscript T	The transpose of matrices or vectors
$X > Y$	Symmetric matrix $X - Y$ is positive definite
$\mathrm{Re}(s)$	The real part of the complex number s
$\leftrightarrow$	The left side of the arrow is equivalent to the right side
$\forall$	For all
$\lVert . \rVert$	Standard norm of vectors or matrices $\lVert d \rVert_{Tf} = (\int_0^{Tf} d^T(\tau)\, d(\tau) d\tau)^{1/2}$
L_∞^m	Essentially bounded m-dimentional functions
$\lvert \xi(t) \rvert$	$\mathrm{ess.\,sup.}\{\lVert \xi(t) \rVert, t \geq 0\}$
$\mathbb{E}(\cdot)$	Expectation of a stochastic process
$\langle\, , \rangle$	Inner product
$\left(\Omega, \mathcal{F}, \{\mathcal{F}_t\}_{t \geq t_0}, \mathcal{P}\right)$	A complete probability space with Ω being a sample space, $\mathcal{F}$ being a σ-field, $\{\mathcal{F}_t\}_{t \geq t_0}$ being a filtration and $\mathcal{P}$ being a probability measure
$\psi \circ \varphi: A \to C$	The composition of two functions $\varphi: A \to B$ and $\psi: B \to C$
$\begin{bmatrix} M_1 & M_2 \\ * & M_3 \end{bmatrix}$	Simplification of $\begin{bmatrix} M_1 & M_2 \\ M_2^T & M_3 \end{bmatrix}$ in large matrix expression

Chapter 1

Introduction

1.1 Research motivations

Along with the development of advanced technologies to increase production, the complexity and the expense of industrial systems are growing correspondingly. The components of control systems are prone to malfunction, which could bring unanticipated economic cost due to the unscheduled shutdown and repairing/maintenance. Therefore, it is of particular interest to design advanced fault diagnosis and fault tolerant control programs to automatically monitor the behavior of industrial systems and prevent extensive damage caused by unexpected faults.

A fault in dynamical systems is unpermitted deviation of the system structure or the system parameters from the nominal situation. The objectives of fault diagnosis include fault detection to detect the occurrence of faults, fault isolation to locate the faulty components, and fault identification to recognize the specific features such as types, magnitudes and patterns of the faults at an early stage. Fault tolerant control (FTC) aims to preserve the functionalities of a faulty system with acceptable performance. With the aid of an advanced fault diagnosis block providing the online information of faulty features, FTC can real-time reconfigure controller laws such that the influences from the unforeseen faults to the system dynamics are eliminated/relieved, and the system stability is guaranteed.

Fault estimation can achieve multi-task of fault diagnosis, provide rich knowledge about faults, and generate auxiliary full state estimation as a by-product. In consequence, it is motivated to develop integrated fault estimation and fault tolerant control techniques for industrial dynamics to make the system resilient to unexpected faults. It is paramount for fault estimators to possess a good capability to attenuate the effects from various disturbance sources. Unknown input observer (UIO) is well recognized owing to its ability to decouple the influences from the unknown inputs, resulting from the modeling errors, parameter perturbations, and exogenous disturbances. As a result, UIO-based fault reconstruction is able to provide the rich information of the concerned faults (e.g., types, sizes and shapes) under noisy environments. It is noticed that not all process disturbances can be decoupled by the UIO techniques in some engineering systems. Therefore, additional techniques such as robust optimal techniques are also required such that the disturbances that cannot be decoupled can be further attenuated.

Because of wide existence of random factors in real plants, stochastic systems subject to Brownian motion can describe real plants more practically. Nevertheless, this class of systems is formulated in It$\hat{o}$-type stochastic differential equations rather than conventional differential equations, hence make many effective techniques for deterministic dynamics invalid in stochastic plants. Moreover, many practical systems are nonlinear. However, there is few powerful and systematic tool to handle nonlinearities of systems so far, especially for those with high-nonlinearities. Therefore, advanced fault estimation and fault tolerant control strategies are challenging but in stringent requirement for nonlinear industrial systems subject to stochastic perturbations.

Nowadays, wind energy conversion industry has drawn tremendous attention worldwide along with increasing concerns of clean sources of electricity. Wind turbine systems are complex and remotely installed structures. Working under harsh environment and operating load conditions, wind turbine components are inevitably subject to a variety of possible faults. As is known, it is of high cost to maintain wind turbines, especially for those built offshore. It was reported that the operation and maintenance costs for onshore and offshore wind turbines made up 10%–15% and 20%–35%, respectively, of the total life costs of wind conversion systems. Therefore, implementing real-time fault estimation techniques, which allows early diagnosis of the unexpected behaviors of turbine dynamics, and appropriate fault tolerant control, which compensates occurred faults, can improve reliability of wind turbine, reduce maintenance cost and extract maximum amount of energy from the wind.

Based on the aforementioned facts, the PhD project focuses on developing novel unknown input observer-based fault estimation and fault tolerant control strategies for systems subject to partially decoupled unknown inputs, faults, nonlinear properties and stochastic perturbations, which can be applied to wind turbines to prevent high cost of maintenance caused by faults, and increase system reliability and safety.

1.2 Summary of contributions of the thesis

- A novel unknown input observer-based fault estimation technique

The constraints of traditional unknown input observer techniques are relaxed from completely decoupled to partially decoupled, which can meet practical requirements better. Integration of augmented system approach and unknown input observer techniques provides simultaneous estimations of system states and concerned faults, and decouple a part of unknown inputs. Linear matrix inequality (LMI) algorithms are associated to eliminate the rest of unknown inputs that cannot be decoupled by the UIO. The novel UIO-based fault estimation techniques are developed for linear systems, Lipschitz nonlinear systems, and Takagi-Sugeno (T-S) fuzzy nonlinear systems.

- Signal compensation for tolerant control design

  Based on robust fault estimation mentioned above, signal compensation technique is developed to remove adverse effects caused by actuator faults and sensor faults. One advantage is that the signal compensation technique is based on a pre-designed controller, hence will not change the original controller and healthy system trajectories of the plant, and can work effectively under both healthy and faulty situations.

- Takagi-Sugeno fuzzy modelling of nonlinear system

  Takagi-Sugeno fuzzy logic is adopted to model high-nonlinear systems by convex combination of a set of linear systems valid around corresponding operating points. The modelling errors are regarded as a part of unknown inputs, and can be attenuated or decoupled by the developed UIO-based fault estimation. The modelling process is demonstrated via case study on wind turbines.

- Lyapunov-based criteria of stochastically input-to-state stability and finite-time stochastically input-to-state stability

  In order to achieve better robustness against unknown inputs for fault estimation of stochastic system, stochastically input-to-state stability and finite-time stochastically input-to-state stability are investigated. Stochastically input-to-state stability takes the influences of disturbances on stability into account, and reflects that bounded disturbances result in bounded stochastic system states. It is stronger than traditional asymptotic stability in probability, hence reflects better estimation performance. Finite-time stochastically input-to-state stability further requires that the stochastic convergence time is finite. The thesis provided criteria based on Lyapunov theory, which is simple and straightforward for the observer design.

- Observer-based fault tolerant control for stochastic systems

  Based on the developed criterion of stochastically input-to-state stability, UIO-based fault estimation and fault tolerant control methods are designed for stochastic linear time invariant system, stochastic Lipschitz nonlinear system and stochastic quadratic inner-bounded nonlinear system, respectively. Siding mode unknown input observer-based fault estimation and fault tolerant control is developed for stochastic Takagi-Sugeno fuzzy nonlinear system. Because of the influences of Brownian motions, the separate design process of observer-based control cannot work for stochastic systems. The original plant after signal compensation and estimation error dynamic make up an overall closed-loop system. The observer gains and controller gains are designed to meet stability and robustness requirement of the closed-system, such that both estimation and fault tolerant control can achieve expected performance.

- Application of the integrated fault tolerant control techniques to wind turbines

  A case study on benchmark wind turbine model is investigated to illustrate the successful application of the proposed methods. The nonlinear benchmark wind turbine is firstly modeled by a T-S fuzzy system. Based on the built T-S fuzzy model, the developed fuzzy unknown input observer-based fault tolerant control method is then applied to compensate generator torque actuator faults, and rotor rotational speed sensor faults. Furthermore, the integrated fault tolerant control designed for stochastic system is applied to stochastic drive train system in presence of Brownian motion. The simulation results can well demonstrate that the T-S fuzzy modelling algorithms and the integrated fault tolerant control techniques are effective.

1.3 Organisation of the thesis

This thesis is divided into eight chapters. Following introduction in Chapter 1, Chapter 2 reviews recent fault diagnosis and fault tolerant control techniques, their application to wind turbines, and the current challenges to be solved. Robust fault estimation approaches for linear system and Lipschitz nonlinear system in presence of faults and partially decoupled unknown inputs are addressed in Chapter 3. Chapter 4 introduces robust fault estimator-based fault tolerant control techniques for Takagi-Sugeno fuzzy dynamic plant, which can well describe general nonlinear engineering systems. Chapter 5 focuses on robust fault estimation for nonlinear stochastic system with Brownian motion. Specially, stochastically input-to-state stability and finite-time stochastically input-to state stability along with their Lyapunov function-based criteria are proposed and proved firstly. Then based on the criteria, robust unknown input observer-based fault estimation techniques are designed for stochastic quadratic inner-bounded nonlinear system and stochastic Takagi-Sugeno fuzzy nonlinear model. In Chapter 6, integrated fault tolerant control methods of stochastic dynamics are introduced in terms of linear, Lipschitz nonlinear, quadratic inner-bounded nonlinear and Takagi-Sugeno fuzzy nonlinear plants. A case study on wind turbine is presented in Chapter 7, which can validate the effectiveness of the proposed techniques. The PhD thesis ends with conclusions and future work in Chapter 8.

1.4 List of publications

1.4.1 Journal articles

1. **X. Liu**, Z. Gao and Z. Q. Chen, "Takagi-Sugeno fuzzy model based fault estimation and signal compensation with application to wind Turbines," *IEEE Trans. Ind. Electron*., vol. 64, no. 7, pp. 5678-5689, Jul. 2017.

2. **X. Liu** and Z. Gao, "Robust finite-time fault estimate on for stochastic nonlinear systems with Brownian motions," *Journal of the Franklin Institute,* vol. 354, no. 6, pp. 2500-2523, Apr. 2016

3. Z. Gao, **X. Liu** and Z. Q. Chen, "Unknown input observer-based robust fault estimation for systems corrupted by partially decoupled disturbances," *IEEE Trans. Ind. Electron.*, vol. 63, no. 4, pp. 2537-2547, Apr. 2016.

1.4.2 Conference articles

1. **X. Liu**, Z. Gao, A. Zhang and Y. Li, "Robust Fault Tolerant Control for Drive Train in Wind Turbine Systems with Stochastic Perturbations," in *Proc. IEEE Conf. Ind. Inf.*, Emden, Germany, Jul. 2017.

2. **X. Liu**, Z. Gao and A. Zhang, "Robust fault estimation and fault tolerant control for Lipschitz nonlinear Brownian systems," in *Proc. IEEE Chinese Control and Decision Conference,* Chongqing, China, May 2017

3. **X. Liu**, Z. Gao, R. Binns, and H. Shao, "Robust fault estimation for stochastic Takagi-Sugeno fuzzy systems," in *Proc. IEEE Conf. Ind. Electron. Society*, pp. 453-458, Florence, Italy, Oct. 2016.

4. **X. Liu**, Z. Gao and S. Odofin, “Robust fault estimation for stochastic nonlinear systems with Brownian perturbations,” in *Proc. IEEE Conf. Ind. Engineering and Applications*, pp. 438-443, Hefei, China, Jun. 2016.
5. **X. Liu** and Z. Gao, “Takagi-Sugeno fuzzy modelling and robust fault reconstruction for wind turbine systems,” in *Proc. IEEE Conf. Ind. Inf.*, pp. 492-495, Poitiers, France, Jul. 2016
6. **X. Liu** and Z. Gao, “Novel unknown input observer for fault estimation of gas turbine dynamic systems”, in *Proc. IEEE Conf. Ind. Inf.,* pp. 562-567, Cambridge, UK, Jul. 2015,
7. **X. Liu** and Z. Gao, “Unknown input observers for fault diagnosis in Lipchitz nonlinear systems,” in *Proc. IEEE Int. Conf. Mechatr. Autom.,* pp. 1555-1560, Beijing, China, Aug. 2015.
8. S. Odofin, Z. Gao, **X. Liu** and K. Sun, “Robust actuator fault detection for an induction motor via genetic algorithms optimization,” in *Proc. IEEE Conf. Ind. Engineering and Applications*, pp. 468-473, Hefei, China, Jun. 2016.

Chapter 2

Literature Review

During the past decades, substantial feasible researches have been conducted in the area of fault diagnosis and fault tolerant control. This chapter aims to review different types of fault diagnosis and fault tolerant control approaches and their application on wind turbines. Section 2.1 introduces various fault diagnosis and fault tolerant control strategies and the current problems to be solved. The construction of wind turbines and possible faults are presented in section 2.2. Section 2.3 is to review the fault diagnosis and fault tolerant control techniques that have been applied to wind turbines, followed by section 2.4 to conclude this chapter.

2.1 Review of fault diagnosis and fault tolerant control techniques

The approaches of fault diagnosis can be classified into various categories from different perspectives. According to the recent two part survey papers [1, 2], fault diagnosis approaches can be categorized into model-based methods, signal-based methods, knowledge-based methods, and hybrid/active methods.

2.1.1 Model-based approaches

Model-based fault diagnosis is suitable for non-stationary operation for engineering plants and can provide systematic design solutions. This method requires a well-developed model of engineering systems established by using either physical principles or systems identification techniques. A model-based fault diagnosis process is usually composed of two parts: residual generation and residual evaluation. The real operation data, reflecting anomaly features, are compared with those of a designed model, describing a healthy working condition, to generate residual signals, which increase with the level of faults. A threshold is then set to determine whether the faults should make alarms. The schematic diagram of model-based fault diagnosis is illustrated in Fig. 2.1.1. Well-known model-based fault diagnosis techniques include observer/filter-based techniques (e.g. proportional integral (PI) observer [3], sliding mode observer [4, 5], descriptor observer [6] and Kalman filter [7]), parity space approaches [8, 9], and parameter estimation approaches [10]. Specifically, observer-based techniques have better sensitivity to faults and robustness against disturbances compared with parity space approach. Moreover, they are less dependent on accuracy of measured parameters along with an explicit mapping to the physical coefficients than parameter estimation approaches. As a result, observer-based fault diagnosis becomes popular and leads to fruitful results.

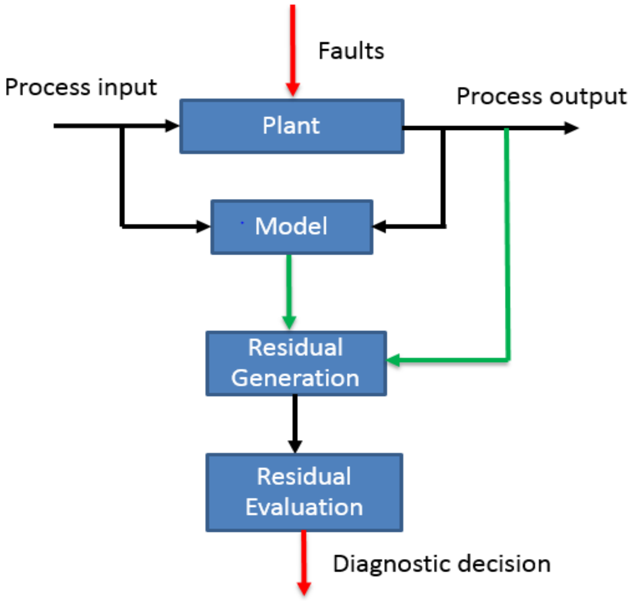

Fig. 2.1.1. Schematic diagram of model-based fault diagnosis

As is known that a real dynamic is unavoidably influenced by unknown inputs, such as perturbations, uncertainties, and modelling errors, which are acceptable in the system and should not be regarded as faults. Therefore, the robustness of an observer does always shave a vital status to make the diagnosis accurate against false alarms from unknown inputs. In order to attenuate the influences from the disturbances/uncertainties, one solution is to carry out various optimization calculations to make the residual sensitive to faults, but robust against the disturbances/uncertainties (e.g. [11-14]). Alternatively, decomposition techniques such as unknown input observers (UIO) [15], can be utilized to decouple the process disturbances so that the effects of the disturbances on the residual are removed. The UIO methods were employed either for robust state estimation [16, 17] or robust fault diagnosis [15, 18-24]. Specifically, an UIO-based fault detection filter was proposed for linear time-invariant systems in [15]. UIO techniques were developed in [18-21] for robust fault detection and isolations for a class of nonlinear systems.

Signal compensation is a powerful fault tolerant control technique, which is capable to work along with a pre-existing controller designed for healthy working condition of the system, and eliminate the influences from the occurred faults. Before implementing signal compensation, the size and shape of the faults should be available. Advanced observer methods, such as adaptive observer [25], sliding mode observer [26], and augmented system observer (including descriptor observer) [27-31] are capable to achieve fault estimation/reconstruction which can provide rich knowledge about faults (shapes, sizes, types, etc.) for implementation of signal compensation. Among those, augmented system approach takes advantage to generate auxiliary full state estimation as a by-product at the mean time of fault estimation. By using estimated faults, the effects from the faulty signals to the system dynamics can be then compensated to realize a fault tolerant operation no matter faults occur or not [29-31].

As a result, it is a common trend to join augmented observer approach and unknown input observer to provide simultaneous estimation of the concerned faults and system state under noisy environments. UIO based fault/disturbance estimation and reconstruction were addressed in [22-24]. It is noticed that all the unknown input observers and UIO-based fault diagnosis methods mentioned above are based on the assumption that the process disturbances can be decoupled completely. Unfortunately, this assumption cannot always be met in many engineering systems. As a result, there is a motivation to develop UIO techniques to handle the systems in the presence of more general form of disturbances. So far, few results have been reported on unknown input observer design for systems subject to partially decoupled process disturbances [32, 33]. Specifically, in [32], partial disturbance decoupled UIO was addressed for state estimation in linear time-invariant systems by attenuating un-decoupled process disturbances using linear matrix inequality (LMI) techniques. In [33], for linear systems subject to both process and sensor disturbances that cannot be decoupled completely, UIO methods were developed for state estimates by using linear transformation and descript system methods. It is noted that the partial decoupled unknown input observers in [32, 33] were proposed for state estimates only, which were not employed for fault diagnosis. Therefore, it is motivated to pay efforts to investigate UIO-based fault estimation and fault tolerant control issues for systems subject to partially decoupled disturbances/uncertainties.

Many industrial processes are of high-nonlinear, which cannot be expressed by linearized models or Lipschitz models. Therefore, the linearized or Lipschitz model based fault diagnosis methods fail to handle high-nonlinear systems. Therefore, robust fault diagnosis for general nonlinear systems is a challenging problem and worthy of further research. Takagi-Sugeno (T-S) fuzzy model was initialized in [34], which has been widely used to approximate a variety of high-nonlinear engineering systems through weighted aggression of a set of linear models valid around selected operating points, such that the complexity of nonlinear problems can be reduced to linear range. As a result, a variety of T-S fuzzy model based fault diagnosis approaches were developed during the last decades, e.g., see [35-38]. Moreover, T-S fuzzy model based UIOs were investigated in [39-42]. To the best of our knowledge, no effort has been paid on T-S fuzzy UIO-based fault estimation and signal compensation for high-nonlinear systems subject to partially decoupled unknown disturbances.

Stochastic dynamics widely exist in many industrial processes such as nuclear systems, chemical processes, biological systems, thermal systems, wind energy conversion systems, and so forth. Therefore, research on fault diagnosis and tolerant control for industrial processes with stochastic natures is well motivated, and some interesting results were reported for systems with various stochastic descriptions such white noises [43, 44], Markovian jump distributions [45, 46], non-Gaussian disturbances [47] and Brownian parameter perturbations [35, 36]. It is worthy to point out that stochastic systems formulated by It$\hat{o}$-type stochastic differential equations have attracted much attention recently [48, 49] due to their flexibility to describe a wide range of stochastic processes. Nevertheless, due to the influences of Brownian motions, techniques suitable for deterministic systems become invalid for stochastic systems. Because of the complexity of stochastic properties, fault estimation and fault tolerant control become challenging, hence limited work has been reported so far. Specifically, [35] presented a fault tolerant control scheme based on state estimation to handle sensor faults for stochastic T-S fuzzy dynamics, and actuator faults have also been considered in [36]; [49] investigated stability of stochastic systems and proposed a sequential design technique to solve observer and controller gains in case of Brownian motions. However, robustness of fault estimation and fault tolerant control against partially decoupled unknown inputs has not been considered in the above mentioned work, hence still an open problem.

2.1.2 Signal-based approaches

Signal-based fault diagnosis is dependent on appropriate sensors installed in plant components, rather than explicit input-output models. A diagnostic decision can be made by comparing the measured signals such as vibrations, sounds and electrical signals, which reflect faulty features, with prior knowledge of symptom of healthy systems via symptom analysis. Schematic diagram is demonstrated in Fig. 2.1.2 to show its methodology. In general, signal-based fault diagnosis can be classified into time-domain (broadband-based) approach, frequency-domain (spectral line analysis) approach, and time-frequency approach.

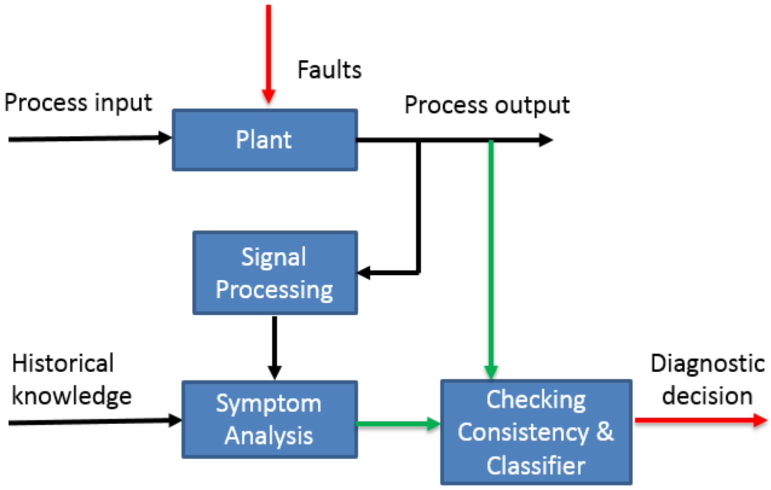

Fig. 2.1.2. Schematic diagram of signal-based fault diagnosis

Time-domain signal-based fault diagnosis utilizes time-domain parameters reflecting component failures such as root mean square [50], slop [51] and kurtosis [52] straightforwardly to monitor the dynamics. Widely used time-domain signal-based diagnostic methods includes scale-invariant feature transform [53] and fast dynamic time warping [52].

Frequency-domain signal-based fault diagnosis employs a variety of spectrum analysis tools, such as discrete Fourier transformation (DFT) which can be computed by fast Fourier transformation (FFT) [54] to convert a time-domain waveform into its frequency-domain equivalence for monitoring the systems.

In order to improve the processing ability for signals, time-frequency analysis approaches by combining both time-domain waveform and corresponding frequency spectrum become a hot issue. Among them, short-time Fourier transform (STFT) [55], wavelet transform (WT) [56], Hilbert–Huang transform (HHT) [57], and Wigner–Ville distribution (WVD) [58] are the most commonly used approaches. Integration of different signal–based diagnosis approaches to achieve better diagnostic performance is also a trend recently.

2.1.3 Data-driven approaches

In contrast to model-based and signal-based diagnosis requiring either mathematical models or extracted signal patterns, a data-driven approach relies on a large volume of historic data available to train universal approximations in order to recognize faulty patterns. The schematic diagram of data-driven fault diagnosis is shown in Fig. 2.1.3. Data-driven fault diagnosis methods can be qualitative (e.g. Expert-system-based method [59]) and quantitative. Quantitative data-driven methods can be either statistical-analysis-based or non-statistical-analysis-based.

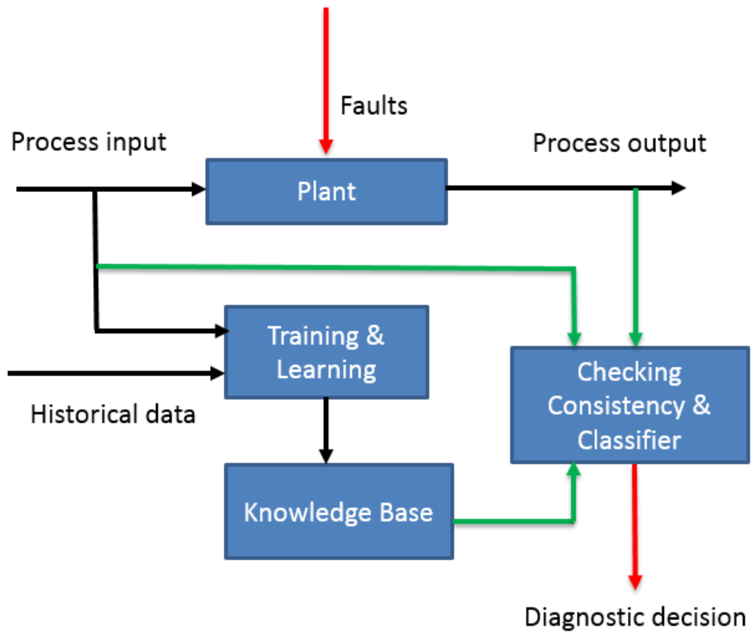

Fig. 2.1.3. Schematic diagram of data-driven fault diagnosis

Principle component analysis (PCA), independent component analysis (ICA), partial least squares, subspace aided approach (SAP), fisher discriminant analysis (FDA), and support vector machine (SVM) are commonly used statistical data-driven fault diagnosis techniques. An introduction of these methods and comparison of their advantages have been shown in [60]. The basic idea of PCA, ICA, SAP and FDA is to utilize various dimensionality reduction techniques to preserve the significant trends of original data set and have produced promising results in fault extraction. The SVM is a nonparametric statistical method to capture the faulty response using its excellence ability in classification process. Associated with appropriate nonlinear kernels tested on the dataset, statistical-analysis-based methods can achieve more accurate and reliable identifications.

In addition to the above statistical data-driven diagnostic techniques, non-statistical approaches such as neural network (NN) [61] and fuzzy logic (FL) [62] are widely utilized to do fault diagnosis. Recent development has shown an interest on adaptive Neuro-Fuzzy Inference System (ANFIS) to combine these two methods, such that better diagnosis performance can be achieved (e.g. [63]).

2.1.4 Hybrid approaches

Model-based fault diagnosis has capability to detect unknown types of faults and requires small amount of online data. However, precise physical models are required. Signal-based approaches and data-driven approaches are independent of explicit mathematical models. Nevertheless, without considering system inputs, the performance of signal-based fault diagnosis can be degraded by extra disturbances. Data-driven approaches require a vast value of reliable historic data and can be time consuming. In consequence, hybrid approaches by adopting more than one of the methods are exploited in practice to enhance diagnosis performance, and lead to fruitful results (e. g. [64-67]).

2.2 Construction of wind turbine and typical faults.

A wind turbine is a complex electromechanical system that converts wind energy to electrical power. Most wind turbines are three–blade unites composed of a number of components and subsystems including blades, rotor, gearbox, generator, yaw, tower etc. and a typical structure is shown in Fig. 2.2.1. The wind flow in the nature drives the blades and rotor to rotate, converting wind power into mechanical energy transmitted via the main shaft supported through the gearbox to the generator, resulting in electrical output. Pitch angle varies to adjust to the change of wind speed, while yaw system aims to align turbine with the direction of the wind detected by anemometer. The controller is to guarantee stable electricity and the housing (or “nacelle”) covering most of these components is mounted at the top of a tower.

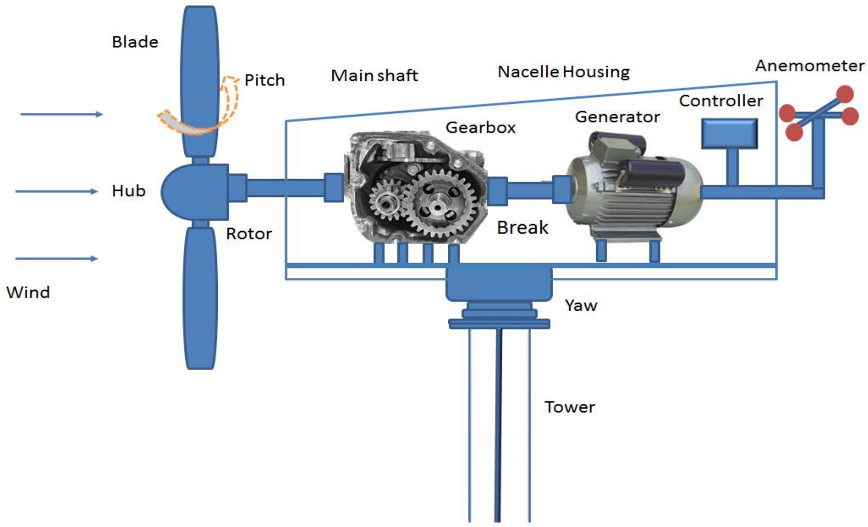

Fig. 2.2.1 wind turbine systems

In practice, wind turbine components might fail due to either momentary events or aging degradation, and consequently lead to system interruptions as well as a huge amount of economic losses. Abnormal behaviours of wind turbines can be classified into faults and failures. Faults in wind turbines are short-term, temporary events caused by factors such as wind speed fluctuation, thermal issue, grid disturbances, temporary wrong sensor readings, etc. Fig. 2.2.2 shows a breakdown of faults in wind turbines, and the causes of typical faults are listed in Table 2.2.1. If an occurred fault is not detected and reacted in time, it may cause consequent failures, which require repairing or replacing of the degraded components and induce additional costs and loss of energy production.

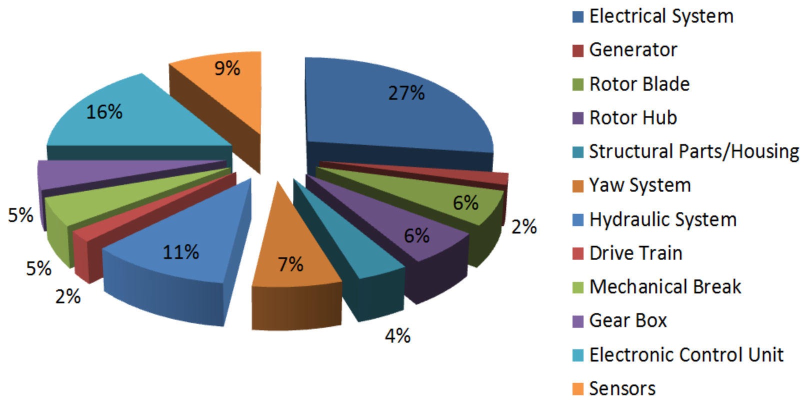

Fig. 2.2.2 Breakdown of faults in wind turbines [68]

Table 2.2.1. Typical faults in wind turbines [69,70]

Fault types	Causes
Rotor and blade faults	Rotor imbalance, blade and hub corrosion, crack, reduced stiffness, increased surface roughness, and deformation of blades, errors of pitch angle, etc.
Gearbox faults	Shaft imbalance, shaft misalignment, shaft damage, bearing damage, gear damage, leaking oil, high oil temperature, and poor lubrication, etc.
Generator faults	Generator excessive vibrations, generator overheating, bearing overheating, abnormal noises and insulation damage, etc.
Bearing faults	Overheating and premature wear caused by unpredictable stress, etc.
Main shaft faults	Corrosion, crack, misalignment, and coupling failure, etc.
Hydraulic faults	Oil leakage and sliding valve blockage, etc.
Mechanical braking faults	Wind speed exceeding the limit, hydraulic failures, etc.
Tower faults	Poor quality control during the manufacturing process, improper installation, loading, harsh environment fire, etc.
Electrical faults	Broken buried metal lines, corrosion or crack of traces, board delamination, component misalignment, electrical leaks, cold-solder joints, etc.
Sensor faults	Malfunction or physical failure of a sensor, the data processing hardware, the communication link, or malfunction of the

	data processing or communication software, etc.

2.3 Fault diagnosis and fault tolerant control techniques for wind turbine systems

During the past decades, substantial feasible researches have been conducted in the area of fault diagnosis and fault tolerant control for wind energy systems which have been reviewed in several literature surveys [69-80]. In this chapter, fault diagnosis and fault tolerant control strategies are reviewed from the perspective of information redundancy classified in section 2.1.

2.3.1 Model-based approaches for wind turbines

As mentioned in section 2.1, model-based methods depend on a well-designed physical model. A benchmark model of a generic three-blade horizontal wind turbine with a full converter coupling and a rated power of 4.8 MW was originally introduced in [81], and the model has been described in more details along with proposed fault diagnosis schemes in [82]. Subsequently, based on wind turbine modelling software FAST, a model of 5 MW electrical output has been built in [83]. In addition to these popular models, there have been other wind turbine models built via physical principles [84], various systems identification approaches [85], or simulation tools [86, 87].

These models provide grounds to implement developed model-based fault diagnosis methods on wind turbines to validate the developed methodologies, and fruitful achievements of fault detection, isolation and accommodation of wind turbines have been recorded. Advanced observer/filter techniques, such as sliding mode observer [88], Kalman filter [85], unknown input observer [89] and PI observer [90] have been successfully applied to monitor wind turbine components. Due to complexity of wind turbines, although some components are linear, the overall wind turbines are nonlinear; hence bring challenges to observer/filter design. Cascaded Kalman filter [91] and cascaded unscented Kalman filter [92] have been developed in order to handle nonlinearities. A nonlinear parameter estimation technique was designed for wind turbine generator by monitoring temperature trend in [93]. T-S fuzzy model-based fault diagnosis methods have been developed in [37] and [94] for nonlinear wind turbines.

The controller pre-designed in the wind turbine model has already been known to work well in fault-free case. Therefore, it is reasonable to require the controller retain in the designed fault tolerant control schemes. Signal compensation can work along with a pre-designed controller, hence can meet the practical requirement of fault tolerant control for wind turbines. As mentioned in section 2.1, signal compensation is based on well-designed fault estimation approaches. Augmented approach associated with high-gain observer [95] and proportional, integral and derivative observer [96] have been successfully applied to converter and pitch system in benchmark wind turbines for fault estimation-based signal compensation purpose. For the overall nonlinear wind turbines, nonlinear geometric approach [97], linear parameter varying techniques [98, 99], and T-S fuzzy modelling strategies [90, 100,101] have been adopted to handle nonlinearities in the process of estimation-based signal compensation. Specifically, T-S fuzzy modelling logics can enhance flexibility when designing observer-based fault estimation. Because based on well–developed T-S fuzzy model, various sophistically designed observer-based fault estimation techniques for linear system can be employed to nonlinear wind turbines.

Working under harsh environment and operation load, the unknown input disturbances are unavoidable. Therefore, the robustness of fault estimation against unknown inputs is of critical importance for wind turbines. It is worthy to notice that T-S fuzzy model cannot be exactly the same with original nonlinear wind turbines. The modelling errors can also be recognized as part of unknown inputs. Optimization algorithm has been adopted in [102] to achieve robustness of fault estimation against disturbances. Integration of augmented approach and unknown input observer for robust fault estimation of whole benchmark wind turbine system with completely decoupled unknown inputs has been addressed in [24]. However, the unknown inputs in wind turbines cannot always be completely decoupled by the UIO. Hence, it is motivated join optimization methods and unknown input observer approaches to handle partially decoupled unknown inputs for robust fault estimation of high-nonlinear systems like wind turbines.

Since wind turbines are more or less in presence of random factors caused by stochastic noises in either wind speed or measurements, the dynamics are usually not deterministic. Kalmen filter techniques and parameter estimation methods can solve fault diagnosis of a class of stochastic systems subject to white noises. Nevertheless, stochastic systems subject to Brownian motions can describe real wind turbines more practically, but design of fault estimation and fault tolerant control for this class of systems becomes more challenging. To the best of our knowledge, no effort has been paid on fault estimation-based fault tolerant control for stochastic wind turbines with Brownian motions, hence this topic is worthy of investigation.

2.3.2 Signal-based approaches for wind turbines

Signal-based fault diagnosis have also been widely used for monitoring wind turbines. For instance, HHT has been utilized in [103] to detect gear-pitting faults. Empirical wavelet transform has been adopted in [104] for generator bearing diagnosis. A two-stage diagnosis framework for wind turbine gearbox was presented in [105], where FFT was employed to convert raw time domain vibration signals to frequency spectrum, and the kurtosis values were used to calculate severity factors and levels by comparing with desired frequencies of fault-free conditions. Gear tooth damages were detected in a [106] by checking gear vibration spectra consisting of tooth meshing frequencies, their harmonics and the sidebands.

2.3.3 Data-driven approaches for wind turbines

Data-driven approaches including PCA [107], ICA [108], SAP [109], FDA [110], and SVM [111, 112] have also been successfully applied to monitor wind turbines. Least squares SVM was used in [111] to train the function of the weather and the turbine response variables, and distinguish faulty conditions from normal conditions. A comparative study has been investigated in [112] to show the advantages of a kernel-based SVM implemented in wind turbines over traditional methods without kernels. [113] compared different neural networks methods, while further development leads to a fault diagnosis scheme by using multiple extreme learning machines layers for feature learning and fault classification in [114]. Implementation of Adaptive Neuro-Fuzzy Inference System for fault diagnosis of wind turbines can be found in [63]. Additionally, jointly data-driven algorithms (PCA, k-nearest neighbor algorithms, and evolutionary strategy) have been adopted in [115] to monitor operation of a wind farm.

2.3.4 Hybrid approaches for wind turbines

To overcome difficulties in model-based fault diagnosis due to the wind turbine complexity and strong non-stationary characters, clustering and classification has been combined with benchmark model to learn drift-like faulty features of pitch systems in [116]. Fuzzy/Bayesian networks have been introduced in [117, 118] to detect and isolate faults based on benchmark model. Kalman-like observers and SVM have been implemented together in [119] to achieve robust fault detection and isolation. Model-based and signal-based techniques have been applied in [120] to monitor three-phase hydraulic pump motor of the brake system. In [121], parity space is identified directly from data, and observer-based approach was used to generate residuals. [122] identified sparse features by learning algorithms to identify gearbox faults. Singular value decomposition has been used to select appropriate transform scale of Morlet wavelet in [123] to diagnosing impulsive faults in rolling bearing of wind turbine gearbox. A hybrid diagnosis approach was addressed on diagonal spectrum and clustering binary tree SVM in [124].

2.4 Summary

Signal-based monitoring methods require the installation of a large number of sensors, which increase the operation difficulty and costs. Another drawback is that they do not consider the dynamic interrelationship between the different measured signals of the system. In addition, for detecting abrupt changes, signal analysis methods are not as fast as model-based approaches. Data-driven monitoring methods rely on large volume of reliable data, which can be difficult to obtain. Moreover, this class of methods require long time for the training or learning process. These two methods are suitable to use when the physical models cannot be achieved. Therefore, as long as the input-output model can be constructed, model-based fault diagnosis and fault tolerant control methods become more effective, systemic, and efficient for real plants.

In many industrial systems such as wind turbine systems, robotic systems, and aerospace systems, the explicit physical models can be obtained. Therefore, model-based fault diagnosis and fault tolerant control techniques have wide application in industrial area. One challenge of this type of techniques is that when the system complexity increases due to nonlinearities, diversity of unknown input disturbances, and stochastic perturbations, the design of observer becomes more difficult.

According to the aforementioned concerns, this PhD project aims to design robust fault estimation and fault tolerant control strategies for systems in presence of partially decoupled unknown inputs, faults, nonlinearities and stochastic Brownian perturbations. Then the developed methods can be applied to wind turbines to enhance the system reliability and reduce maintenance cost.

Chapter 3

Robust fault estimation for linear system and Lipschitz nonlinear system

In this chapter, robust fault estimation strategies are addressed for linear system and Lipschitz nonlinear system to simultaneously estimate the system states and the concerned faults, while eliminate the influences of caused process and sensor disturbances. Specifically, the augmented system is constructed by forming an augmented state vector composed of original system states and concerned faults. A novel unknown input observer is next designed for the augmented system by decoupling partial disturbances and attenuating the other disturbances through optimization algorithms, leading to a simultaneous estimate of the original system states and concerned faults. In order to meet the practical engineering situations, the process disturbances in this study are assumed not to be decoupled completely. In section 3.1 of the chapter, the existence condition of such an unknown input observer is proposed to facilitate the fault estimation for linear systems subjected to process disturbances. In section 3.2, robust fault estimation techniques are addressed for Lipschitz nonlinear systems subjected to both process and sensor disturbances. The proposed techniques are demonstrated by the simulation studies of a three-shaft gas turbine engine and a single link flexible joint robot in section 3.3.

3.1 Fault estimation for linear system

3.1.1 System description and augmented system

Consider the dynamic systems described in the form of:

$$\begin{cases} \dot{x}(t) = Ax(t) + Bu(t) + B_d d(t) + B_f f(t) \\ y(t) = Cx(t) + Du(t) + D_f f(t) \end{cases} \tag{3-1}$$

where $x(t) \in \mathcal{R}^n$ represents unmeasurable state vector with initial value of $x(0) \in \mathcal{R}^n$; $u(t) \in \mathcal{R}^m$ and $y(t) \in \mathcal{R}^p$ stand for control input vector and measurement output vector, respectively; $d(t) \in \mathcal{R}^{l_d}$ is a bounded unknown input vector caused by either disturbances or modelling errors, $f \in \mathcal{R}^{l_f}$ is the fault vector involving actuator faults and sensor faults, A, B, C, D, B_d, B_f and D_f are known constant coefficient matrices with appropriate dimensions. For the simplicity of presentation, the symbol t will be omitted in the rest of this chapter.

Incipient faults are slowly developing faults, whereas an abrupt fault will approach a step signal. In this study, the faults concerned are assumed either to be incipient faults or abrupt faults, which are two typical faults in industrial processes. These two types of faults do not vary too fast, therefore, the second-order derivative of f should be zero piecewise. In other words, $\ddot{f} = 0$. For faults whose second order derivatives are not zero but bounded, the bounded signals could be regarded as a part of unknown inputs. In addition, $B_d = [B_{d1} \;\; B_{d2}]$, $d = [d_1 \;\; d_2]^T$, $d_1 \in \mathcal{R}^{l_{d1}}$ and $d_2 \in \mathcal{R}^{l_{d2}}$, where d_1 rather than d_2 is assumed to be decoupled, and B_{d1} is of full column rank.

Define an augmented state vector as

$$\bar{x} = [x^T \quad \dot{f}^T \quad f^T]^T \in \mathcal{R}^{\bar{n}} \tag{3-2}$$

where $\bar{n} = n + 2l_f$.

As a result, we can construct an equivalent augmented system as follows:

$$\begin{cases} \dot{\bar{x}} = \bar{A}\bar{x} + \bar{B}u + \bar{B}_d d \\ y = \bar{C}\bar{x} + Du \end{cases} \tag{3-3}$$

where

$$\bar{A} = \begin{bmatrix} A & 0 & B_f \\ 0 & 0 & 0 \\ 0 & I_{l_f} & 0 \end{bmatrix} \in \mathcal{R}^{\bar{n}\times\bar{n}},\ \bar{B} = \begin{bmatrix} B \\ 0 \\ 0 \end{bmatrix} \in \mathcal{R}^{\bar{n}\times m},$$

$$\bar{B}_d = \begin{bmatrix} B_d \\ 0 \\ 0 \end{bmatrix} \in \mathcal{R}^{\bar{n}\times l_d}, \text{ and } \bar{C} = [C \quad 0 \quad D_f] \in \mathcal{R}^{p\times\bar{n}}.$$

Clearly, $\bar{x}$ contains the original state vector x, the concerned fault vector f, and its first order derivative $\dot{f}$. As a result, these three components can be estimated simultaneously by designing an observer for the augmented system (3-3).

3.1.2 Novel unknown input observer (UIO)

Consider the following unknown input observer (UIO):

$$\begin{cases} \dot{\bar{z}} = R\bar{z} + T\bar{B}u + (K_1 + K_2)(y - Du) \\ \hat{\bar{x}} = \bar{z} + H(y - Du) \end{cases} \tag{3-4}$$

in which $\bar{z} \in \mathcal{R}^{\bar{n}}$ is the state vector of dynamic system (3-4) and $\hat{\bar{x}} \in \mathcal{R}^{\bar{n}}$ represents the estimation of $\bar{x} \in \mathcal{R}^{\bar{n}}$, while $R \in \mathcal{R}^{\bar{n}\times\bar{n}}, K_1 \in \mathcal{R}^{\bar{n}\times p}$, $K_2 \in \mathcal{R}^{\bar{n}\times p}$, $T \in \mathcal{R}^{\bar{n}\times m}$ and $H \in \mathcal{R}^{\bar{n}\times p}$ are the gain matrices to be designed.

Letting estimation error $\bar{e} = \bar{x} - \hat{\bar{x}}$, and using the output equation in (3-4), one has

$$\begin{aligned}\bar{e} &= \bar{x} - \hat{\bar{x}} \\ &= \bar{x} - \bar{z} - H\bar{C}\bar{x} \\ &= (I_{\bar{n}} - H\bar{C})\bar{x} - \bar{z}\end{aligned} \tag{3-5}$$

Using (3-3) to (3-5), the derivative of $\bar{e}$ can be thus calculated as

$$\begin{aligned}\dot{\bar{e}} &= (I_{\bar{n}} - H\bar{C})\dot{\bar{x}} - \dot{\bar{z}} \\ &= (I_{\bar{n}} - H\bar{C})(\bar{A}\bar{x} + \bar{B}u + \bar{B}_d d) - R\bar{z} - T\bar{B}u - K_1\bar{C}\bar{x} - K_2(y - Du) \\ &= (\bar{A} - H\bar{C}\bar{A} - K_1\bar{C})\bar{e} + (\bar{A} - H\bar{C}\bar{A} - K_1\bar{C} - R)\bar{z} \\ &\quad +[(\bar{A} - H\bar{C}\bar{A} - K_1\bar{C})H - K_2](y - Du) + [(I_{\bar{n}} - H\bar{C})\bar{B} - T\bar{B}]u \\ &\quad +(I_{\bar{n}} - H\bar{C})\bar{B}_{d1}d_1 + (I_{\bar{n}} - H\bar{C})\bar{B}_{d2}d_2\end{aligned} \tag{3-6}$$

where $[\bar{B}_{d1} \quad \bar{B}_{d2}] = \bar{B}_d$.

If one can make the following relationships hold,

$$(I_{\bar{n}} - H\bar{C})\bar{B}_{d1} = 0 \tag{3-7}$$

$$R = \bar{A} - H\bar{C}\bar{A} - K_1\bar{C} \tag{3-8}$$

$$T = I_{\bar{n}} - H\bar{C} \tag{3-9}$$

$$K_2 = RH \tag{3-10}$$

the state estimation error dynamics (3-6) reduces to

$$\dot{\bar{e}} = R\bar{e} + (I_{\bar{n}} - H\bar{C})\bar{B}_{d2}d_2 \tag{3-11}$$

From (3-11), one can see d_1 has been decoupled under the conditions (3-7) to (3-10), but d_2 still exists. Therefore, the observer design is transformed to seek the solution to (3-7), and design an algorithm to make the observer system matrix R stable, and minimize the influence from the unknown input d_2.

It is ready to develop the existence condition of the UIO with original system matrices, and the following lemma is useful for the proof of *Theorem 3.1.1*

Lemma 3.1.1 [11, 15].

The sufficient and necessary conditions for the existence of the UIO (3-4) for the system (3-3) are:

(i) $\mathrm{rank}(\bar{C}\bar{B}_{d1}) = \mathrm{rank}(\bar{B}_{d1})$;

(ii) $(\bar{C}, \bar{A}_1)$ is a detectable pair, where $\bar{A}_1 = (I_n - H\bar{C})\bar{A}$.

***Remark 3.1.1* [15]**

(a) Condition (i) in *Lemma 3.1.1* can ensure equation (3-7) is solvable, and a special solution is:

$$H_* = \bar{B}_{d1}[(\bar{C}\bar{B}_{d1})^T(\bar{C}\bar{B}_{d1})]^{-1}(\bar{C}\bar{B}_{d1})^T \tag{3-12}$$

The design of observer gain H will be used to design other observer gains. In some cases, a general solution $H = \bar{B}_M(\bar{C}\bar{B}_M)^+ + N(I - (\bar{C}\bar{B}_M)(\bar{C}\bar{B}_M)^+)$, where $(\bar{C}\bar{B}_M)^+ = [(\bar{C}\bar{B}_M)^T(\bar{C}\bar{B}_M)]^{-1}(\bar{C}\bar{B}_M)^T$ and N is a compatible matrix of proper dimension, can be considered to make the design of remaining observer gains more flexible.

(b) Condition (ii) in *Lemma 3.1.1* is standard for assigning the unstable poles of R arbitrarily. Moreover, the condition (ii) is equivalent to the condition that the transmission zeros from the unknown inputs to the measurements must be stable, *i.e.*,

$$\begin{bmatrix} sI_{\bar{n}} - \bar{A} & \bar{B}_{d1} \\ \bar{C} & 0 \end{bmatrix} \tag{3-13}$$

is of full column rank for all s with $\mathrm{Re}(s) \geq 0$.

Theorem 3.1.1

The sufficient and necessary conditions for the existence of the UIO (3-4) for the system (3-3) are

(i) $\mathrm{rank}(CB_{d1}) = \mathrm{rank}(B_{d1})$;

(ii) $\begin{bmatrix} A & B_f & B_{d1} \\ C & D_f & 0 \end{bmatrix}$ is of full column rank;

(iii) $\mathrm{rank}\begin{bmatrix} sI_n - A & B_{d1} \\ C & 0 \end{bmatrix} = n + l_{d1}$ for all s with $\mathrm{Re}(s) \geq 0$, but $s \neq 0$.

Proof

It is noted that

$$\bar{C}\bar{B}_{d1} = [C \quad 0 \quad D_f]\begin{bmatrix} B_{d1} \\ 0 \\ 0 \end{bmatrix} = CB_{d1},$$

and

$$\text{rank}(\bar{B}_{d1}) = \text{rank}(B_{d1}).$$

Therefore one can know that condition (i) in *Lemma 3.1.1*, that is $\text{rank}(\bar{C}\bar{B}_{d1}) = \text{rank}(\bar{B}_{d1})$, is equivalent to the condition (i) in *Theorem 3.1.1*, that is, $\text{rank}(CB_{d1}) = \text{rank}(B_{d1})$.

It is noticed that

$$\text{rank}\begin{bmatrix} sI_{\bar{n}} - \bar{A} & \bar{B}_{d1} \\ \bar{C} & 0 \end{bmatrix} = \text{rank}\begin{bmatrix} sI_n - A & 0 & -B_f & B_{d1} \\ 0 & sI_{l_f} & 0 & 0 \\ 0 & -I_{l_f} & sI_{l_f} & 0 \\ C & 0 & D_f & 0 \end{bmatrix}$$

$$= \begin{cases} \text{rank}\begin{bmatrix} A & B_f & B_{d1} \\ C & D_f & 0 \end{bmatrix} + l_f, \ s = 0 \\ \text{rank}\begin{bmatrix} sI_n - A & B_{d1} \\ C & 0 \end{bmatrix} + 2l_f, \ s \neq 0 \end{cases} \tag{3-14}$$

Therefore, (3-14) implies that the conditions (ii) and (iii) in *Theorem 3.1.1* are equivalent to (3-13) being full of column rank for all s with $\text{Re}(s) \geq 0$, which is also equivalent to (ii) in *Lemma 3.1.1*.

This completes the proof.

The next challenge for designing robust observer (3-4) is to make the matrix R stable and reduce the influence from the un-decoupled disturbance d_2. H can be obtained from (3-12). The following theorem is provided to solve observer gain K_1.

Theorem 3.1.2

For system (3-3), there exists a robust UIO in the form of (3-4) such that $\|\bar{e}\|_{Tf} \leq r\|d_2\|_{Tf}$, if there exists a positive definite matrix P and matrix Q, such that

$$\begin{bmatrix} I_{\bar{n}} + \bar{A}_1^T P + P\bar{A}_1 - \bar{C}^T Q^T - Q\bar{C} & P(I_{\bar{n}} - H\bar{C})\bar{B}_{d2} \\ * & -r^2 I_{l_{d2}} \end{bmatrix} < 0 \tag{3-15}$$

where $\bar{A}_1 = (I_n - H\bar{C})\bar{A}$, and $Q = PK_1$. Then we can obtain $K_1 = P^{-1}Q$

Proof

Take the following Lyapunov function candidate for error dynamic system (3-11):

$$V(\bar{e}) = \bar{e}^T P \bar{e} \tag{3-16}$$

Using (3-11) and (3-16), one has

$$\begin{aligned}\dot{V}(\bar{e}) &= \bar{e}^T P \dot{\bar{e}} + \dot{\bar{e}}^T P \bar{e} \\ &= \bar{e}^T(\bar{A}_1^T P + P\bar{A}_1 - \bar{C}^T Q^T - Q\bar{C})\bar{e} + 2\bar{e}^T P(I_{\bar{n}} - H\bar{C})\bar{B}_{d2} d_2\end{aligned} \tag{3-17}$$

Form (3-15), one can see

$$I_{\bar{n}} + \bar{A}_1^T P + P\bar{A}_1 - \bar{C}^T Q^T - Q\bar{C} < 0,$$

indicating $\bar{A}_1^T P + P\bar{A}_1 - \bar{C}^T Q^T - Q\bar{C} < 0$.

Apparently, when $d_2 = 0$, one can get $\dot{V}(\bar{e}) < 0$, implying the error dynamics in (3-11) is asymptotically stable.

Let

$$\Gamma = \int_0^{Tf} (\bar{e}^T \bar{e} - r^2 d_2^T d_2) dt \tag{3-18}$$

By using (3-17) and (3-18), one can have:

$$\begin{aligned}\Gamma &= \int_0^{f} \left(\bar{e}^T \bar{e} - r^2 d_2^T d_2 + \dot{V}(\bar{e})\right) dt - \int_0^{Tf} \dot{V}(\bar{e}) dt \\ &= \int_0^{Tf} [\bar{e}^T (I_{\bar{n}} + \bar{A}_1^T P + P\bar{A}_1 - \bar{C}^T Q^T - Q\bar{C})\bar{e} \\ &\quad + 2\bar{e}^T P(I_{\bar{n}} - H\bar{C})\bar{B}_{d2} d_2 - \gamma^2 d_2^T d_2] dt - \int_0^{Tf} \dot{V}(\bar{e}) dt \\ &= \int_0^{Tf} [\bar{e}^T \quad d_2^T] \Pi \begin{bmatrix} \bar{e} \\ d_2 \end{bmatrix} dt - \int_0^{Tf} \dot{V}(\bar{e}) dt\end{aligned} \tag{3-19}$$

where

$$\Pi = \begin{bmatrix} I_{\bar{n}} + \bar{A}_1^T P + P\bar{A}_1 - \bar{C}^T Q^T - Q\bar{C} & P(I_{\bar{n}} - H\bar{C})\bar{B}_{d2} \\ * & -r^2 I_{l_{d2}} \end{bmatrix}.$$

Under zero initial condition $\bar{e}(0) = 0$,

$$\begin{aligned}\int_0^{Tf} \dot{V}(\bar{e}) dt &= \bar{e}^T(T_f) P \bar{e}(T_f) - \bar{e}^T(0) P \bar{e}(0) \\ &= V(\bar{e}(T_f)\,) > 0\end{aligned} \tag{3-20}$$

Since $\Pi < 0$ in terms of (3-15), and from (3-19) and (3-20), one can have $\Gamma < 0$, which indicates $\|\bar{e}\|_{Tf} \leq r\|d_2\|_{Tf}$.

The proof is completed.

3.1.3 Design procedure of the UIO for fault estimation

Based on *Theorems 3.1.1* and *Theorems 3.1.2,* we can summarize the design procedure of the UIO as follows.

Procedure 3.1.1 *The design of robust UIO for fault estimation*

i) Construct the augmented system in the form of (3-3).

ii) Select the matrix H_* in the form of (3-12).

iii) Solve the LMI (3-15) to obtain the matrices P and Q, and calculate the gain $K_1 = P^{-1}Q$.

iv) Calculate the other gain matrices R, T and K_2 following the formulae (3-8)-(3-10), respectively.

v) Implement the robust UIO (3-4), and get the augmented estimate $\hat{\bar{x}}$, leading to the simultaneous state and fault estimates as follows:

$$\hat{x} = \begin{bmatrix} I_n & 0_{n\times 2l_f} \end{bmatrix} \hat{\bar{x}} \tag{3-21}$$

$$\hat{f} = \begin{bmatrix} 0_{n\times(n+l_f)} & I_{l_f} \end{bmatrix} \hat{\bar{x}} \tag{3-22}$$

3.2 UIO-based fault estimation for Lipschitz nonlinear system

It is well-known that nonlinear properties widely exist in many practical dynamics, which motivates us to extend the approach proposed in Section 3.1 to nonlinear system. Many nonlinearities of engineering systems satisfy Lipschitz condition, hence make Lipschitz nonlinear system popular for study of fault diagnosis. In this section, robust UIO-based fault estimation approach is to be developed for Lipschitz nonlinear system. In subsection 3.2.1, we consider the system is in presence of process disturbances, while in subsection 3.2.2, sensor noises are also taken into account.

3.2.1 Nonlinear system subjected to process disturbances

In this subsection, novel UIO-based fault estimation approaches are to be proposed for Lipschitz nonlinear system subjected to process disturbances. The Lipschitz nonlinear system under consideration is represented as follows:

$$\begin{cases} \dot{x} = Ax + Bu + B_d d + B_f f + \Phi(t, x, u) \\ y = Cx + Du + D_f f \end{cases} \tag{3-23}$$

where $\Phi(t, x, u) \in \mathcal{R}^n$ is a real nonlinear vector function with Lipschitz constant θ, namely,

$$\|\Phi(t, x, u) - \Phi(t, \hat{x}, u)\| \leq \theta \|x - \hat{x}\|,$$

$$\forall (t, x, u), (t, \hat{x}, u) \in \mathcal{R} \times \mathcal{R}^n \times \mathcal{R}^m, \tag{3-24}$$

and the other symbols are the same as defined as (3-1). Lipschitz nonlinear systems, locally Lipschitz nonlinear systems at least, can be found in many practical systems. All the results derived for a globally Lipschitz system can be applied to a locally Lipschitz system directly.

Defining an augmented state vector in the form of (3-2), one can obtain an equivalent augmented system as follow:

$$\begin{cases} \dot{\bar{x}} = \bar{A}\bar{x} + \bar{B}u + \bar{B}_d d + \bar{\Phi}(t, x, u) \\ y = \bar{C}\bar{x} + Du \end{cases} \tag{3-25}$$

where $\bar{\Phi}(t, x, u) = [\Phi^T(t, x, u) \quad 0 \quad 0]^T \in \mathcal{R}^{\bar{n}}$, and the other symbols are defined as the same as those in (3-3).

An nonlinear UIO is in the form of

$$\begin{cases} \dot{\bar{z}} = R\bar{z} + T\bar{B}u + (K_1 + K_2)(y - Du) + T\bar{\Phi}(t, \hat{x}, u) \\ \hat{\bar{x}} = \bar{z} + H(y - Du) \end{cases} \tag{3-26}$$

where the gains H, R, T, and K_2 satisfy (3-7) to (3-10).

The estimation error is defined in (3-5). In terms of (3-5), (3-25) and (3-26), the estimation error dynamics is represented as :

$$\begin{aligned} \dot{\bar{e}} = {} & (\bar{A} - H\bar{C}\bar{A} - K_1\bar{C})\bar{e} + (\bar{A} - H\bar{C}\bar{A} - K_1\bar{C} - R)\bar{z} \\ & + [(\bar{A} - H\bar{C}\bar{A} - K_1\bar{C})H - K_2](y - Du) + [(I_{\bar{n}} - H\bar{C})\bar{B} - T\bar{B}]u \\ & + (I_{\bar{n}} - H\bar{C})\bar{B}_{d1}d_1 + (I_{\bar{n}} - H\bar{C})\bar{B}_{d2}d_2 \ + (I_{\bar{n}} - H\bar{C})\tilde{\Phi} \end{aligned} \tag{3-27}$$

in which $\tilde{\Phi} = \bar{\Phi}(t, x, u) - \bar{\Phi}(t, \hat{x}, u)$. Substitution (3-7) to (3-10) into (3-27) yields

$$\dot{\bar{e}} = R\bar{e} + (I_{\bar{n}} - H\bar{C})\bar{B}_{d2}d_2 + (I_{\bar{n}} - H\bar{C})\widetilde{\Phi} \tag{3-28}$$

It is time to design the observer K_1 to ensure the estimation error dynamics above to be asymptotically stable and satisfy robust performance index. The following two lemmas are useful to derive *Theorem 3.2.1*.

Lemma 3.2.1 [125].

For any matrices $X \in \mathcal{R}^{s\times t}, Y \in \mathcal{R}^{t\times s}$, a time-varying matrix $F(t) \in \mathcal{R}^{t\times t}$ with $\|F(t)\| \leq 1$ and any scalar $\varepsilon > 0$, we have:

$$XF(t)Y + Y^T F^T(t) X^T \leq \varepsilon^{-1} XX^T + \varepsilon Y^T Y.$$

Lemma 3.2.2 (Schur complement**)** [126].

Let $S = \begin{bmatrix} S_{11} & S_{12} \\ * & S_{22} \end{bmatrix}$ to be a symmetric matrix, then the LMI $S < 0$ is equivalent to $S_{22} < 0$ and $S_{11} - S_{12}S_{22}^{-1}S_{12}^T < 0$.

Theorem 3.2.1

For system (3-25), there exists a robust observer in the form of (3-26), such that $\|\bar{e}\|_{Tf} \leq r\|d_2\|_{Tf}$,if there exists a positive definite matrix P and matrix Q, such that

$$\begin{bmatrix} \Lambda & P(I_{\bar{n}} - H\bar{C})\bar{B}_{d2} & P(I_{\bar{n}} - H\bar{C}) \\ * & -r^2 I_{l_{d2}} & 0 \\ * & * & -\varepsilon I_{\bar{n}} \end{bmatrix} < 0 \tag{3-29}$$

where $\Lambda = (\varepsilon\theta^2 + 1)I_{\bar{n}} + \bar{A}_1^T P + P\bar{A}_1 - \bar{C}^T \mathrm{Q}^T - \mathrm{Q}\bar{C}$, $\bar{A}_1 = (I_{\bar{n}} - H\bar{C})\bar{A}$, $Q = PK_1$, ε is a given positive number, r is a performance index, standing for the magnitude of error compared with disturbances. Then we can obtain $K_1 = P^{-1}Q$.

Proof

Choosing the Lyapunov function in the form of (3-16), and using (3-28), and notice that $R = \bar{A}_1 - K_1\bar{C}$, one has

$$\begin{aligned}\dot{V}(\bar{e}) = \bar{e}^T(\bar{A}_1^T P + P\bar{A}_1 - \bar{C}^T Q^T - Q\bar{C})\bar{e} + 2\bar{e}^T P(I_{\bar{n}} - H\bar{C})\bar{B}_{d2}d_2 \\ +\bar{e}^T P(I_{\bar{n}} - H\bar{C})\widetilde{\Phi} \;\; + \widetilde{\Phi}^T (I - H\bar{C})^T P\bar{e}\end{aligned} \tag{3-30}$$

Applying *Lemma 3.2.1* to the last two terms in (3-30) and using (3-24), one has

$$\dot{V}(\bar{e}) \leq \bar{e}^T(\bar{A}_1^T P + P\bar{A}_1 - \bar{C}^T Q^T - Q\bar{C} + \varepsilon\theta^2 I_{\bar{n}} + \varepsilon^{-1} P(I_{\bar{n}} - H\bar{C})(I_{\bar{n}} - H\bar{C})^T P)\bar{e}$$

$$+2\bar{e}^T P(I_{\bar{n}} - H\bar{C})\bar{B}_{d2}d_2 \tag{3-31}$$

In terms of *Lemma 3.2.2*, one can see (3-29) implies that

$$\Lambda + \varepsilon^{-1}P(I_{\bar{n}} - H\bar{C})(I_{\bar{n}} - H\bar{C})^T P < 0, \tag{3-32}$$

which leads to

$$\bar{A}_1^T P + P\bar{A}_1 - \bar{C}^T Q^T - Q\bar{C} + \varepsilon\theta^2 I_{\bar{n}} + \varepsilon^{-1}P(I_{\bar{n}} - H\bar{C})(I_{\bar{n}} - H\bar{C})^T P < 0 \tag{3-33}$$

When $d_2 = 0$, from (3-31) and (3-33) one can have $\dot{V}(\bar{e}) < 0$, indicating the error dynamics is asymptotically stable.

Letting

$$\Gamma_a = \int_0^{Tf} \left(\bar{e}^T\bar{e} - r^2 d_2^T d_2 + \dot{V}(\bar{e})\right) dt - \int_0^{Tf} \dot{V}(\bar{e})dt \tag{3-34}$$

and using (3-31), one has

$$\begin{aligned}\Gamma_a \leq \int_0^{Tf} [\bar{e}^T(&I_{\bar{n}} + \bar{A}_1^T P + P\bar{A}_1 - \bar{C}^T Q^T - Q\bar{C} + \varepsilon\theta^2 I_{\bar{n}} \\ &+\varepsilon^{-1}P(I_{\bar{n}} - H\bar{C})(I_{\bar{n}} - H\bar{C})^T P)\bar{e} + 2\bar{e}^T P(I_{\bar{n}} - H\bar{C})\bar{B}_{d2}d_2 \\ &-r^2 d_2^T d_2]dt - \int_0^{Tf} \dot{V}(\bar{e})dt \\ = \int_0^{Tf} [\bar{e}^T \quad &d_2^T]\Omega \begin{bmatrix}\bar{e} \\ d_2\end{bmatrix} dt - \int_0^{Tf} \dot{V}(\bar{e})dt\end{aligned} \tag{3-35}$$

where

$$\Omega = \begin{bmatrix}\Lambda + \varepsilon^{-1}P(I_{\bar{n}} - H\bar{C})(I_{\bar{n}} - H\bar{C})^T P & P(I_{\bar{n}} - H\bar{C})\bar{B}_{d2} \\ * & -r^2 I_{l_{d2}}\end{bmatrix} \tag{3-36}$$

In terms of *Lemma 3.2.2*, the inequality (3-29) implies $\Omega < 0$. It is also noted that $\int_0^{Tf} \dot{V}(\bar{e})dt = V\left(\bar{e}(t_f)\right) > 0$ under zero initial condition. As a result, from (3-35) one has $\Gamma_a < 0$, implying

$$\|\bar{e}\|_{Tf} \leq r\|d_2\|_{Tf} \tag{3-37}$$

This completes the proof.

3.2.2 Nonlinear system with process and sensor disturbances

In this subchapter, a more general case is taken into consideration, that is, Lipschitz nonlinear system corrupted by both process and sensor disturbances, which is described by

$$\begin{cases} \dot{x} = Ax + Bu + B_f f + B_d d + \Phi(t, x, u) \\ y = Cx + Du + D_d d_s + D_f f \end{cases} \tag{3-38}$$

where D_d is constant known matrix, standing for coefficient matrix of the measurement noise $d_s \in \mathcal{R}^s$, and the other symbols are the same as defined before.

Defining an augmented state vector in the form of (3-2), an equivalent augmented system is given as

$$\begin{cases} \dot{\bar{x}} = \bar{A}\bar{x} + \bar{B}u + \bar{B}_d d + \bar{\Phi}(t, x, u) \\ y = \bar{C}\bar{x} + Du + D_d d_s \end{cases} \tag{3-39}$$

where the symbols are the same as defined in (3-25) except for D_d and d_s.

The nonlinear UIO is taken the same form as (3-26). From (3-26) and (3-39), one can see the estimation error as

$$\begin{aligned} \bar{e} &= \bar{x} - \hat{\bar{x}} \\ &= \bar{x} - \bar{z} - H(y - Du) \\ &= (I_{\bar{n}} - H\bar{C})\bar{x} - \bar{z} - HD_d d_s \end{aligned} \tag{3-40}$$

Furthermore, in terms of (3-26), (3-39) and (3-40), one can obtain the estimation error dynamic equation as follows:

$$\dot{\bar{e}} = R\bar{e} + (I_{\bar{n}} - H\bar{C})\bar{B}_{d2}d_2 + (I_{\bar{n}} - H\bar{C})\tilde{\bar{\Phi}} - K_1 D_d d_s - HD_d \dot{d}_s \tag{3-41}$$

where $\tilde{\bar{\Phi}} = \bar{\Phi}(t, x, u) - \bar{\Phi}(t, \hat{x}, u)$.

To design the parameters of observer (3-26), the following theorem is addressed.

Theorem 3.3.1

For system (3-39), there exists a robust observer in the form of (3-26) such that $\|\bar{e}\|_{Tf} \leq r\|\bar{d}\|_{Tf}$,if there exists a positive definite matrix P and matrix Q, such that

$$\begin{bmatrix} \Lambda & P(I_{\bar{n}} - H\bar{C})\bar{B}_{d2} & P(I_{\bar{n}} - H\bar{C}) & -QD_d & -PHD_d \\ * & -r^2 I_{l_{d2}} & 0 & 0 & 0 \\ * & * & -\varepsilon I_{\bar{n}} & 0 & 0 \\ * & * & * & -r^2 I_s & 0 \\ * & * & * & * & -r^2 I_s \end{bmatrix} < 0 \tag{3-42}$$

where $\Lambda = (\varepsilon\theta^2 + 1)I_{\bar{n}} + \bar{A}_1^T P + P\bar{A}_1 - \bar{C}^T \mathrm{Q}^T - \mathrm{Q}\bar{C}$, $\bar{A}_1 = (I_{\bar{n}} - H\bar{C})\bar{A}$, $Q = PK_1$, $\bar{d} = \begin{bmatrix} d_2^T & d_s{}^T & \dot{d}_s^T \end{bmatrix}^T$, ε is a given positive number, r is a performance index, standing for the magnitude of error compared with disturbances.

Proof

Taking the Lyapunov function in the form of (3-16), using (3-41) and the proof manner of (3-30) and (3-31), one has

$$\dot{V}(\bar{e}) \le \bar{e}^T(\bar{A}_1^T P + P\bar{A}_1 - \bar{C}^T Q^T - Q\bar{C} + \varepsilon\theta^2 I_{\bar{n}} + \varepsilon^{-1} P(I_{\bar{n}} - H\bar{C})(I_{\bar{n}} - H\bar{C})^T P)\,\bar{e}$$
$$+2\bar{e}^T P(I - H\bar{C})\bar{B}_{d2} d_2 - 2\bar{e}^T PK_1 D_d d_s - 2\bar{e}^T PHD_d \dot{d}_s \tag{3-43}$$

For $d_2 = 0$, and $d_s = 0$, one can see the error estimation system (3-41) is asymptotically stable, similar to the proof in *Theorem 3.3.1*.

Letting

$$\Gamma_b = \int_0^{Tf} \left(\bar{e}^T\bar{e} - r^2\bar{d}^T\bar{d} + \dot{V}(\bar{e})\right)dt - \int_0^{Tf} \dot{V}(\bar{e})dt \tag{3-44}$$

and using (3-43), we can have

$$\Gamma_b = \int_0^{Tf} [\bar{e}^T \quad d_2^T \quad d_s^T \quad \dot{d}_s^T]\Psi \begin{bmatrix} \bar{e} \\ d_2 \\ d_s \\ \dot{d}_s \end{bmatrix} dt - \int_0^{Tf} \dot{V}(\bar{e})dt \tag{3-45}$$

where

$$\Psi = \begin{bmatrix} \Sigma & P(I_{\bar{n}} - H\bar{C})\bar{B}_{d2} & -QD_d & -PHD_d \\ * & -r^2 I_{l_{d2}} & 0 & 0 \\ * & * & -r^2 I_s & 0 \\ * & * & * & -r^2 I_s \end{bmatrix} \tag{3-46}$$

$$\Sigma = \Lambda + \varepsilon^{-1} P(I_{\bar{n}} - H\bar{C})(I_{\bar{n}} - H\bar{C})^T P \tag{3-47}$$

and Λ is defined in (3-42).

In terms of *Lemma 3.3.2*, the inequality (3-42) implies $\Psi < 0$. It is also noted that $\int_0^{Tf} \dot{V}(\bar{e})dt = V\left(\bar{e}(t_f)\right) > 0$ under zero initial condition. Therefore from (3-45) one has $\Gamma_b < 0$, indicating $\|\bar{e}\|_{Tf} \leq r\|\bar{d}\|_{Tf}$.

This completes the proof.

In the LMIs (3-15), (3-29), and (3-42), H can be obtained from (3-12). r is given performance index, and ε is a given positive number. Therefore, these three variables are fixed before handing them in LMIs. The positive definite matrix P and matrix Q are decision variables. Observer gain K_1 can be then obtained by $K_1 = P^{-1}Q$.

3.2.3 Design procedure of the Nonlinear UIO for fault estimation

On the basis of *Theorems 3.2.1* and *Theorems 3.2.2,* we can summarize the design procedure of the robust nonlinear UIO estimator as follows.

Procedure 3.2.1 *The design of nonlinear UIO for fault estimation*

i) Construct the augmented system in the form of (3-25) or (3-39), respectively for systems subjected to either process disturbances or both disturbances in the process and measurement.

ii) Select the matrix H_* in the form of (3-12).

iii) Solve the LMI (3-29) or (3-42) to obtain the matrices P and Q, and calculate the gain $K_1 = P^{-1}Q$.

iv) Calculate the other gain matrices R, T and K_2 following the formulae (3-8)-(3-10), respectively.

v) Implement the robust UIO (3-26), and get the augmented estimate $\hat{\bar{x}}$, leading to the simultaneous state and fault estimates in the forms of (3-21) and (3-22), respectively.

3.3 Illustration examples

In this section, the proposed techniques are to be applied to two engineering-oriented systems: three-shaft gas turbine engine and single link flexible joint robot, to validate the effectiveness.

3.3.1 Three-shaft gas turbine engine

A three-shaft gas turbine engine can be characterized by a 14-order linearized model:

$$\begin{cases} \dot{x} = Ax + Bu + B_a f_a + B_d d \\ y = Cx + Du + D_a f_a + D_s f_s \end{cases} \quad (3\text{-}48)$$

where the state vector, input vector and output vector are defined respectively as

$$x = [N_L, N_I, N_H, P_{2LM}, P_{2I}, P_2, T_3, P_{4H}, P_{4I}, P_{4M}, W_H, W_C, P_5, T_6]^T,$$

$$u = [W_{FE}, W_{FR}, A_J]^T,$$

$$y = [W_1, W_2, P_6, T_{2LM}, T_{2I}, T_H]^T,$$

The meanings of the symbols above can be found in Table 3.3.1. The coefficient matrices $A, B, C,$ and D are provided by [30, 127].

In this simulation study, three actuator faults and two sensor faults are to be considered. Therefore, $B_a = B, D_s = \begin{bmatrix} 1 & 0 & 0 & 0 & 0 & 0 \\ 0 & 1 & 0 & 0 & 0 & 0 \end{bmatrix}^T$.

Denote $f = [f_a^T \quad f_s^T]^T$, we can have $B_f = [B_a \quad 0]$ and $D_f = [D_a \quad D_s]$, correspondingly.

Table 3.3.1 Parameter symbols of gas turbine engine

A_J	Nozzle area	T_{2LM}	LP/IP inter-compressor temperature
N_H	HP shaft speed	T_3	Combustor outlet temperature
N_I	IP shaft speed	T_6	Jet pipe outlet temperature
N_L	LP shaft speed	W_1	Fan mass flow
P_{2I}	IP/P inter-compressor pressure	W_2	HP compressor mass flow
P_{2LM}	LP/IP inter-compressor pressure	W_C	Cold stream mass flow
P_{4H}	HP/IP inter-turbine pressure	W_{FE}	Engine fuel
P_{4M}	Post-turbine pressure	W_{FR}	Reheat fuel
P_5	Jet pipe pressure	W_H	Hot stream mass flow
P_6	Nozzle pressure	T_H	Thrust
P_2	Combustor pressure	T_{2I}	LP/HP inter-compressor temperature
P_{4I}	IP/LP inter-turbine pressure		

The unknown input disturbance vector is $d = [d_1^T \quad d_2^T \quad d_3^T]^T$, where $d_1 = 5\sin(10t)$, d_2 is random number between -0.5 to 0.5, and $d_3 = 0.5\sin(50t)$. The control input vector is $u = [2 \quad 2 \quad 2]^T$.

The three actuator faults are:

$$f_{a1}=\begin{cases}0, & t<10\\ t-10, & 10\le t<15\\ 20-t, & 15\le t<20\\ 0, & t\ge 20\end{cases} \tag{3-49}$$

$$f_{a2}=\begin{cases}0, & t<25\\ 25-t, & 25\le t<30\\ -5, & 30\le t<35\\ t-40, & 35\le t<40\\ 0, & t\ge 40\end{cases} \tag{3-50}$$

$$f_{a3}=\begin{cases}0, & t<2\\ 0.2\mathrm{t}-0.4, & 2\le t<6\\ 0.1\sin(2t)+0.8, & t\ge 6\end{cases} \tag{3-51}$$

and the two sensor faults concerned are:

$$f_{s1}=\begin{cases}0, & t<65\\ 1, & t\ge 65\end{cases} \tag{3-52}$$

$$f_{s2}=\begin{cases}0, & t<40\\ 0.1\sin(0.5\mathrm{t})+0.2\sin(\mathrm{t}+\frac{\pi}{2}), & 40\le t<65\\ 0, & t\ge 65\end{cases} \tag{3-53}$$

By using the design *procedure 3.1.1*, we can obtain the robust UIO in the form of (3-4) (the obtained observer gains are omitted here due to the limit of space). The unknown input d_1 is decoupled whereas the influences of d_2 and d_3 are attenuated via the designed observer gains. Due to the limit of space, we only give the curves of the three dominant states (*i.e.*, states corresponding to the three dominant poles) and their estimates, shown by Fig.3.3.1-Fig. 3.3.3, showing excellent estimation performance. The estimates of the three actuator faults and two sensor faults are depicted by Fig.3.3.4-Fig.3.3.8, respectively. It can be seen that the proposed UIO-based fault estimation techniques can successfully estimate abrupt faults, incipient faults and even sinusoidal faults.

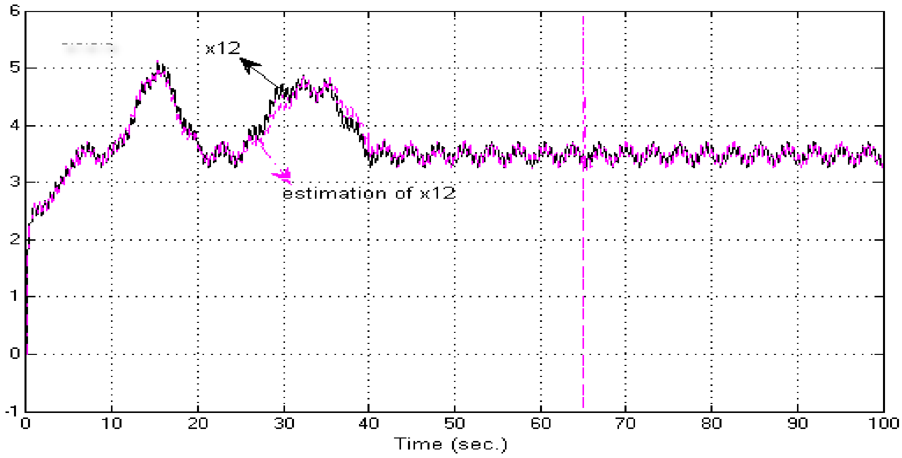

Fig. 3.3.1. x_{12} (the 12th state) and its estimation

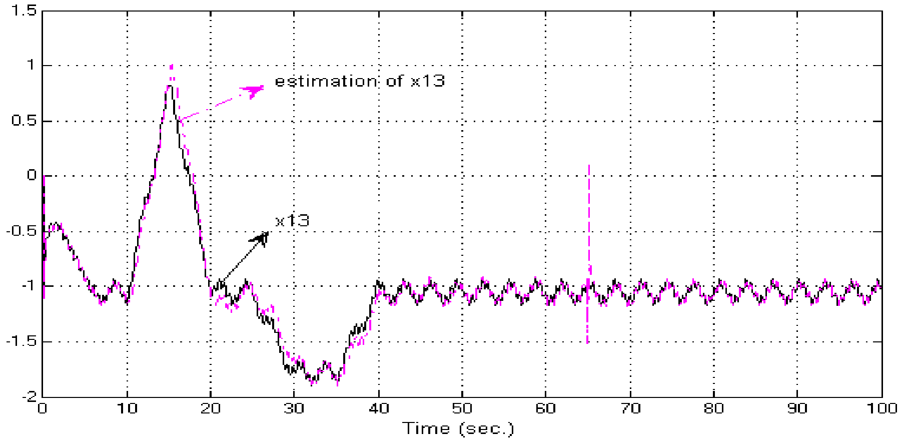

Fig. 3.3.2. x_{13} (the 13th state) and its estimation

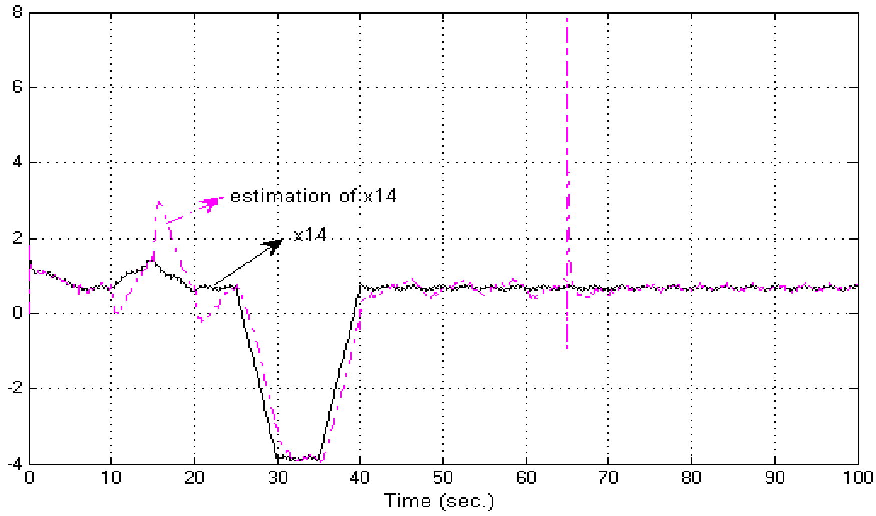

Fig. 3.3.3. x_{14} (the 14th state) and its estimation

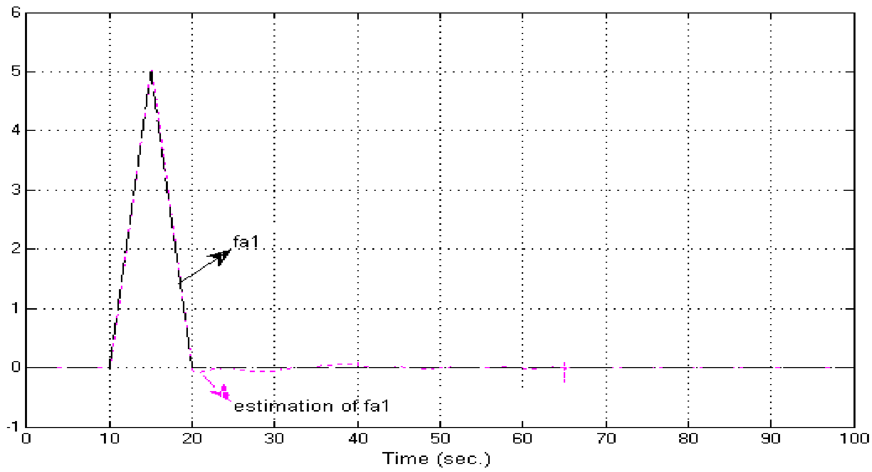

Fig. 3.3.4. f_{a1} (engine fuel actuator fault) and its estimation

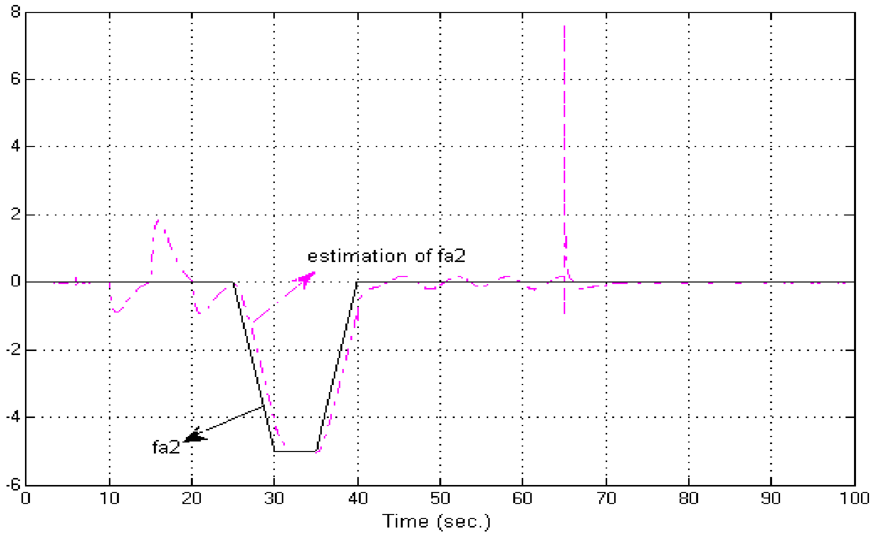

Fig. 3.3.5. f_2 (reheat fuel actuator fault) and its estimation

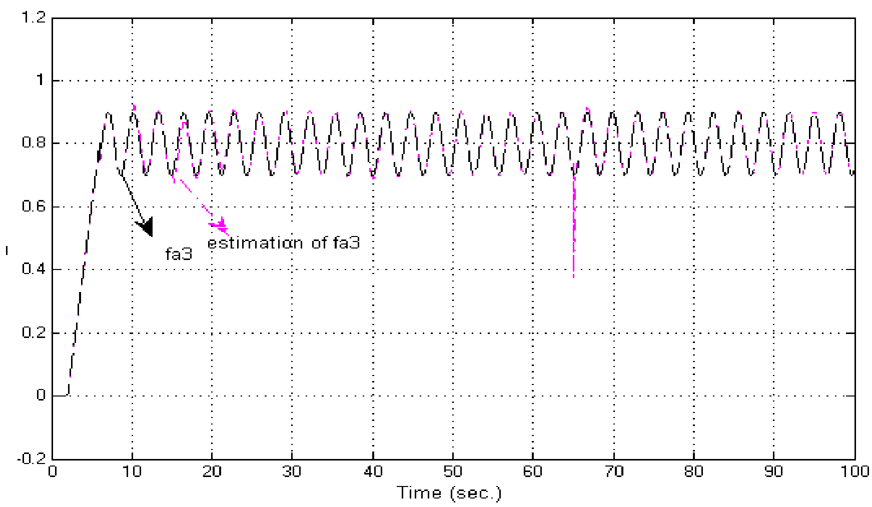

Fig.3.3.6. f_{a3} (nozel area actuator fault) and its estimation

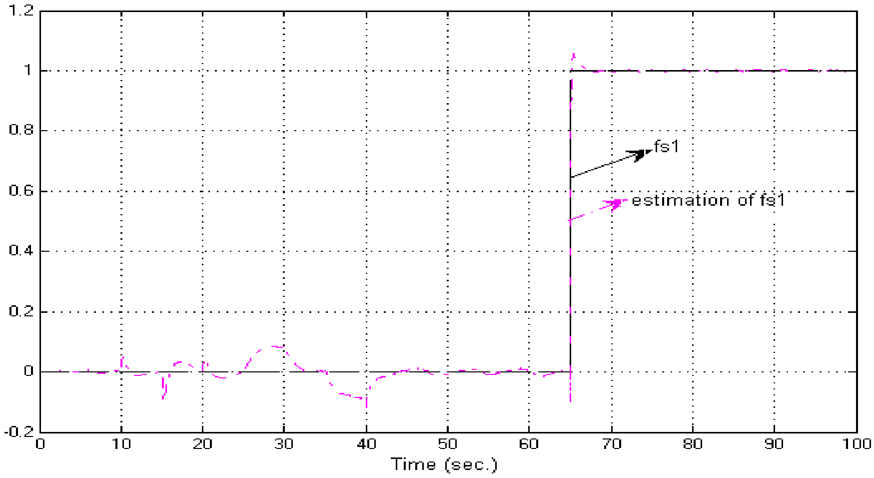

Fig.3.3.7. f_{s1} (fan mass flow sensor fault) and its estimation

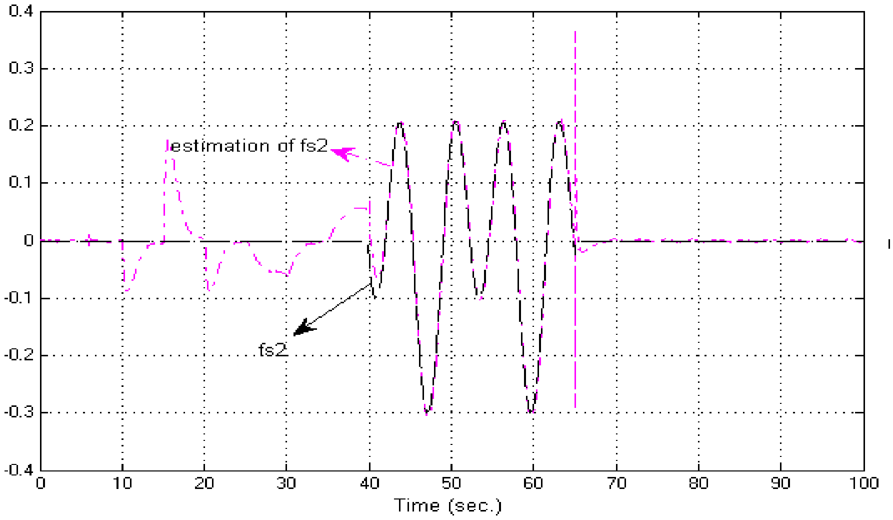

Fig.3.3.8. f_{s2} (HP compressor mass flow sensor fault) and its estimation

3.3.2 Single-link flexible joint robot

The single-link manipulator with revolute joints actuated by a DC motor can be described by a Lipschtiz nonlinear system [128, 129]:

$$\begin{cases} \dot{\theta}_m = \omega_m \\ \dot{\omega}_m = \frac{k}{J_m}(\theta_l - \theta_m) - \frac{G}{J_m}\omega_m + \frac{k_\tau}{J_m}u \\ \dot{\theta}_l = \omega_l \\ \dot{\omega}_l = -\frac{k}{J_l}(\theta_l - \theta_m) - \frac{mgh}{J_l}\sin(\theta_l) \end{cases} \tag{3-54}$$

where J_m represents the inertia of the DC motor, J_l is the inertia of the link, θ_m and θ_l denote the angles of the rotations of the motor and link, respectively, ω_m and ω_l are the angular velocities of the motor and link, respectively, k is torsional spring constant, k_τ is the amplifier gain, $G$is the viscous friction, m is the pointer mass, g is the gravity constant, and h is the distance from the rotor to the gravity center of the link, and u is the control input (DC voltage) to produce the motor torque. Let $x = [\theta_m \quad \omega_m \quad \theta_l \quad 0.1\omega_l]$, the system can be written in the form of (3-38), where

$$A = \begin{bmatrix} 0 & 1 & 0 & 0 \\ -48.6 & -1.25 & 48.6 & 0 \\ 0 & 0 & 0 & 10 \\ 1.95 & 0 & -1.95 & 0 \end{bmatrix}, B = \begin{bmatrix} 0 \\ 21.6 \\ 0 \\ 0 \end{bmatrix},$$

$$C = \begin{bmatrix} 1 & 0 & 0 & 0 \\ 0 & 1 & 0 & 0 \end{bmatrix}, \Phi(x) = \begin{bmatrix} 0 \\ 0 \\ 0 \\ -0.333\sin(x_3) \end{bmatrix}.$$

The fault and disturbance distribution matrices are respectively $B_{fa} = B$, and

$$B_d = \begin{bmatrix} -0.2 & 0.01 & -0.02 \\ -0.1 & 0.02 & -0.04 \\ 0.1 & -0.02 & 0.04 \\ 0.2 & 0.02 & -0.04 \end{bmatrix}, D_d = \begin{bmatrix} 0.1 \\ -0.02 \end{bmatrix}.$$

The actuator fault is:

$$f_a = \begin{cases} 1 + 0.1\sin(4t) & t \geq 4 \\ 0.5(t-2) & 2 \leq t < 4, \\ 0 & t < 2 \end{cases}$$

The unknown input disturbances are as follows: $d_1 = 5\sin(10t)$, corrupted by a uniform-random-number signal, $d_2 = 2\sin(10t), d_3 = \sin(20t)$ and $d_s = 0.1\sin(10t)$. The control input is added as $u = 2\sin(2\pi t)$ and the initial state value is given as $x(0) = [0.01 \ \ -5 \ \ 0.01 \ \ 5 \ ]^T$.

Choose $r = 0.58$, $\varepsilon = 50$, and using the *procedure 3.2.1*, we can obtain the observer gains as follows:

$$H = \begin{bmatrix} 0.8000 & 0.4000 \\ 0.4000 & 0.2000 \\ -0.4000 & -0.2000 \\ -0.8000 & -0.4000 \\ 0 & 0 \\ 0 & 0 \end{bmatrix},$$

$$T = \begin{bmatrix} 0.2000 & -0.4000 & 0 & 0 & 0 & 0 \\ -0.4000 & 0.8000 & 0 & 0 & 0 & 0 \\ 0.4000 & 0.2000 & 1 & 0 & 0 & 0 \\ 0.8000 & 0.4000 & 0 & 1 & 0 & 0 \\ 0 & 0 & 0 & 0 & 1 & 0 \\ 0 & 0 & 0 & 0 & 0 & 1 \end{bmatrix},$$

$$K = K_1 + K_2 = \begin{bmatrix} -2851.2 & 5761.3 \\ 396.33 & -910.70 \\ 3172.4 & -6393.8 \\ -1638.4 & 3224.6 \\ -6308.5 & 12617 \\ -14930 & 29859 \end{bmatrix},$$

$$R = \begin{bmatrix} -1595.9 & -7993.9 & -19.440 & 0 & 0 & -8.6400 \\ 210.82 & 1232.3 & 38.880 & 0 & 0 & 17.280 \\ 1781.0 & 8875.5 & 9.7200 & 10 & 0 & 4.3200 \\ -924.22 & -4496.9 & 17.490 & 0 & 0 & 8.6400 \\ -3540.0 & -17541 & 0 & 0 & 0 & 0 \\ -8378.3 & -41513 & 0 & 0 & 1 & 0 \end{bmatrix}$$

In this example, we choose $r = 0.58$, $\varepsilon = 50$, such that the unknown inputs can be mitigated, meanwhile, there are applicable solutions of LMI.

By choosing the above parameters, d_1 is decoupled and the influences of d_2, d_3 and d_s are minimized. The curves displayed in Figs. 3.3.9-3.3.11 exhibit the estimation performance for angular velocities of the motor and link, and actuator fault respectively.

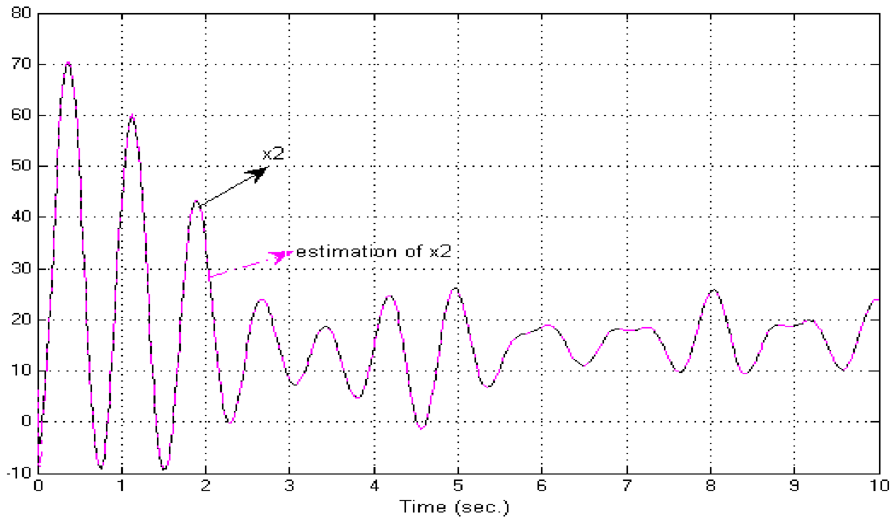

Fig. 3.3.9: x_2 (motor angular velocity) and its estimation

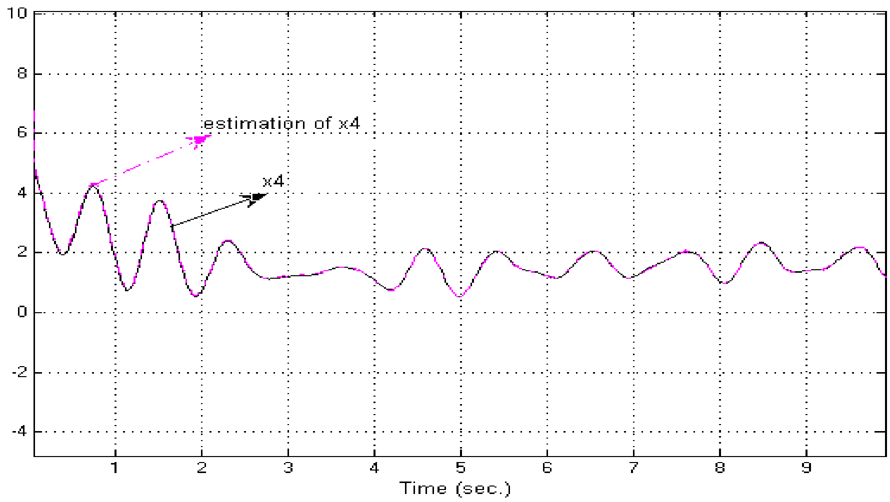

Fig. 3.3.10. x_4 (10% link angular velocity) and its estimation

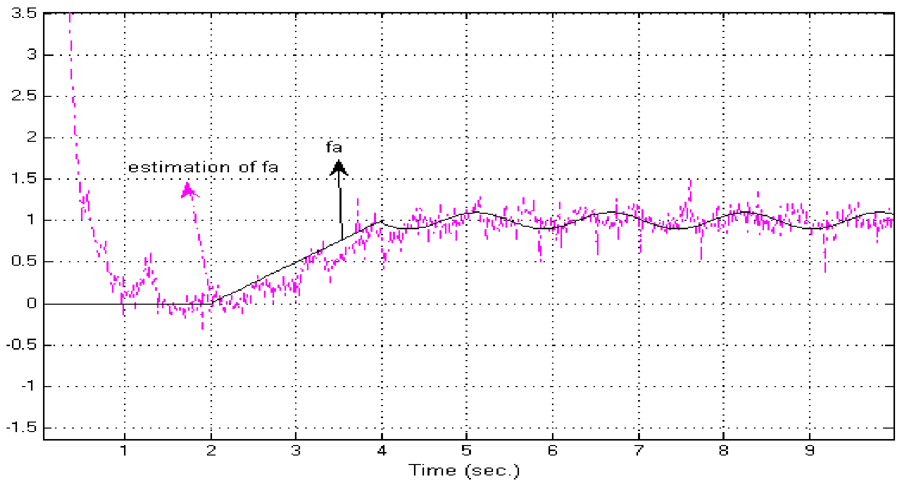

Fig. 3.3.11. f_a (DC input voltage actuator fault) and its estimation

3.4 Summary

In this chapter, a novel UIO-based simultaneous state and fault estimation techniques have been proposed which can be utilized to handle systems subjected to partially decoupled process disturbances and even sensor disturbances. The design procedures of the estimators for both linear and nonlinear systems are presented. The robustness is ensured by decoupling partial process disturbances with the UIO approach, and attenuating un-decoupled process disturbances and sensor disturbances with LMI optimization technique. The simultaneous estimation is realized with the integration of the system augmentation and the estimator design for the augmented system. The proposed techniques have been illustrated by using two engineering-oriented examples: three-shaft gas turbine engine and single link robot. The proposed techniques have great potentials to apply to various engineering systems. It is encouraged to extend the proposed techniques to more complex systems such as time-delay nonlinear systems, distributed control systems and fault tolerant control design.

Chapter 4.

Integrated fault tolerant control for Takagi-Sugeno system

Based on well-developed fault estimation, signal compensation can be implemented to achieve integrated fault tolerant control. In Chapter 3, robust UIO based fault estimation approaches have been proposed for linear system and Lipschitz nonlinear system with partially decoupled unknown inputs. Many industrial processes are of high-nonlinear, which cannot be expressed by linearized models or Lipschitz models. Therefore, the linearized or Lipschitz model based fault diagnosis methods will become invalid to handle high-nonlinear systems. Due to lack of powerful and systematic tools to handle general nonlinearities directly, robust fault estimation for general nonlinear systems is a challenging problem and worthy of further research. Takagi-Sugeno (T-S) fuzzy model [34] has been widely used to approximate a variety of high-nonlinear engineering systems by using a convex combination of a set of local linearized systems. This idea can reduce complication of nonlinear problems. As a result, a variety of T-S fuzzy model based fault diagnosis approaches were developed during the last decades, e.g., see [35-38]. Moreover, T-S fuzzy model based UIOs were investigated in [39-42]. To the best of our knowledge, no effort has been paid on T-S fuzzy UIO-based fault estimation and signal compensation for high-nonlinear systems subject to partially decoupled unknown disturbances. In this chapter, a robust fault estimation and fault tolerant control approach is proposed for Takagi-Sugeno fuzzy systems, by integrating augmented system method, unknown input fuzzy observer design, linear matrix inequality optimization, and signal compensation techniques. In section 4.1, fuzzy augmented system method is used to construct an augmented plant with the concerned faults and system states being the augmented states. Unknown input fuzzy observer technique is thus utilized to estimate the augmented states and decouple unknown inputs that can be decoupled. Linear matrix inequality approach is further addressed to ensure the global stability of the estimation error dynamics and attenuate the influences from the unknown inputs that cannot be decoupled. As a result, the robust estimates of the faults concerned and system states can be obtained simultaneously. Based on the fault estimates, signal compensation scheme is developed in section 4.2 to remove the effects of the faults to the system dynamics and outputs, leading to a stable dynamic satisfying the expected performance. Finally, section 4.3 concludes this chapter.

4.1 Robust fault estimation of T-S fuzzy System

This section presents the approach for robust state/fault estimation for T-S fuzzy system subjected to partially decoupled unknown inputs. Consider the following nonlinear system characterized by T-S fuzzy model:

IF μ_1 is M_{1i} and …μ_q is M_{qi}, THEN

$$\begin{cases} \dot{x}(t) = A_i x(t) + B_i u(t) + B_{di} d(t) + B_{fi} f(t) \\ y(t) = Cx(t) + D_f f(t) + D_d d_w(t) \end{cases} \tag{4-1}$$

where $x(t) \in \mathcal{R}^n$ represents the state vector; $u(t) \in \mathcal{R}^m$ stands for the control input vector and $y(t) \in \mathcal{R}^p$ is the measurement output vector; $d(t) \in \mathcal{R}^{l_d}$, $d_w(t) \in \mathcal{R}^{l_{d_w}}$ are the bounded unknown disturbance vectors from plant and sensors, respectively; $f(t) \in \mathcal{R}^{l_f}$ means the fault vector including actuator faults and sensor faults. $i = 1, 2, \dots r$, and r is the total number of local models, depending on the precision requirement for modelling, the complexity of the nonlinear system and the choice of structure of weighting functions. M_{ji} are fuzzy sets and μ denotes the decision vector containing all individual elements μ_j, $j = 1, 2, \dots q$ which are known premise variables that may be the functions of the measurable state variables, external inputs, and/or time. A_i, B_i, B_{di}, B_{fi}, C, D_d, D_f can be obtained by using the direct linearization of a nonlinear system or alternatively by using an identification procedure. For the simplification of description, in the rest of the chapter, the time symbol t is omitted.

From (4-1), the final fuzzy system is inferred as follows:

$$\begin{cases} \dot{x} = \sum_{i=1}^{r} h_i(\mu) \left(A_i x + B_i u + B_{di} d + B_{fi} f\right) \\ y = Cx + D_f f + D_d d_w \end{cases} \tag{4-2}$$

where $h_i(\mu)$ are weighting functions, quantifying the membership of the current operation point of the system at a zone of operation, which are selected following the convex sum properties: $\sum_{i=1}^{r} h_i(\mu) = 1$ and $0 \le h_i(\mu) \le 1$.

The faults concerned are either abrupt or incipient, which have the same assumption with those in Chapter 3. Moreover, denote $B_{di} = [B_{di1} \;\; B_{di2}]$ and $d = [d_1 \;\; d_2]^T$. We assume that $d_1 \in \mathcal{R}^{l_{d1}}$ rather than $d_2 \in \mathcal{R}^{l_{d2}}$ can be decoupled. In addition, we also assume both the f and $\dot{f}$ are bounded.

In order to estimate faults and system states at the same time, an augmented system can be constructed as:

$$\begin{cases} \dot{\bar{x}} = \sum_{i=1}^{r} h_i(\mu)\,(\bar{A}_i\bar{x} + \bar{B}_i u + \bar{B}_{di} d) \\ y = \bar{C}\bar{x} + D_d d_w \end{cases} \tag{4-3}$$

where

$$\bar{n} = n + 2l_f,$$

$$\bar{x} = [x^T \quad \dot{f}^T \quad f^T]^T \in \mathcal{R}^{\bar{n}}$$

$$\bar{A}_i = \begin{bmatrix} A_i & 0_{n\times l_f} & B_{fi} \\ 0_{l_f\times n} & 0_{l_f\times l_f} & 0_{l_f\times l_f} \\ 0_{l_f\times n} & I_{l_f} & 0_{l_f\times l_f} \end{bmatrix} \in \mathcal{R}^{\bar{n}\times\bar{n}}$$

$$\bar{B}_i = \begin{bmatrix} B_i^T & 0_{m\times l_f} & 0_{m\times l_f} \end{bmatrix}^T \in \mathcal{R}^{\bar{n}\times m}$$

$$\bar{B}_{di} = \begin{bmatrix} B_{di}^T & 0_{l_d\times l_f} & 0_{l_d\times l_f} \end{bmatrix}^T \in \mathcal{R}^{\bar{n}\times l_d}$$

$$\bar{C} = \begin{bmatrix} C & 0_{p\times l_f} & D_f \end{bmatrix} \in \mathcal{R}^{p\times\bar{n}}$$

An unknown input observer in the following form can be designed for (4-3):

$$\begin{cases} \dot{\bar{z}} = \sum_{i=1}^{r} h_i(\mu)[R_i\bar{z} + T\bar{B}_i u + (K_{i1} + K_{i2})y] \\ \hat{\bar{x}} = \bar{z} + Hy \end{cases} \tag{4-4}$$

Let the estimation error to be $\bar{e} = \bar{x} - \hat{\bar{x}}$, leading to its derivative calculated as follows:

$$\begin{aligned} \dot{\bar{e}} = \sum_{i=1}^{r} h_i(\mu)\,\{ & (\bar{A}_i - H\bar{C}\bar{A}_i - K_{i1}\bar{C})\bar{e} + (\bar{A}_i - H\bar{C}\bar{A}_i - K_{i1}\bar{C} - R_i)\bar{z} \\ & + [(\bar{A}_i - H\bar{C}\bar{A}_i - K_{i1}\bar{C})H - K_{i2}]y + [(I_{\bar{n}} - H\bar{C}) - T]\bar{B}_i u + (I_{\bar{n}} - H\bar{C})\bar{B}_{di1} d_1 \\ & + (I_{\bar{n}} - H\bar{C})\bar{B}_{di2} d_2 - K_{i1} d_s - HD_d \dot{d}_s \} \end{aligned} \tag{4-5}$$

If the observer gains satisfy the following conditions:

$$(I_{\bar{n}} - H\bar{C})\bar{B}_{di1} = 0 \tag{4-6}$$

$$R_i = \bar{A}_i - H\bar{C}\bar{A}_i - K_{i1}\bar{C} \tag{4-7}$$

$$T = I_{\bar{n}} - H\bar{C} \tag{4-8}$$

$$K_{i2} = R_i H \tag{4-9}$$

the state estimation error can be reduced to

$$\dot{\bar{e}} = \sum_{i=1}^{r} h_i(\mu)\,[R_i\bar{e} + (I_{\bar{n}} - H\bar{C})\bar{B}_{di2}d_2 - K_{i1}d_w - HD_d\dot{d}_w] \tag{4-10}$$

In order to meet the conditions (4-6)-(4-9), we have the following assumptions:

Assumption 4.1.1

$$\mathrm{rank}\big(\bar{C}(\bar{B}_{d11}\ \ \bar{B}_{d21}\cdots\ \bar{B}_{dr1})\big) = \mathrm{rank}\big((\bar{B}_{d11}\ \ \bar{B}_{d21}\cdots\ \bar{B}_{dr1})\big);$$

Assumption 4.1.2

For $\forall\, i,\ \begin{bmatrix} A_i & B_{fi} & B_{di1} \\ C & D_{fi} & 0 \end{bmatrix}$ is of full column rank;

Assumption 4.1.3

For $\forall\, i,\ \mathrm{rank}\begin{bmatrix} sI_n - A_i & B_{di1} \\ C & 0 \end{bmatrix} = n + l_{d1}.$

According to Chapter 3, the above assumptions are to ensure that for each local model, equation (4-6) can be solved, and the model is observable.

Equation (4-6) implies that

$$H\bar{C}(\bar{B}_{d11}\ \ \bar{B}_{d21}\cdots\ \bar{B}_{dr1}) = (\bar{B}_{d11}\ \ \bar{B}_{d21}\cdots\ \bar{B}_{dr1}) \tag{4-11}$$

For $(\bar{B}_{d11}\ \bar{B}_{d21}\cdots\ \bar{B}_{dr1})$, there exists a non-singular matrix M such that $(\bar{B}_{d11}\ \ \bar{B}_{d21}\cdots\ \bar{B}_{dr1})M = (\bar{B}_M\ \ 0)$, where $\bar{B}_M$ is of full column rank. *Assumption 4.1.1* indicates $\mathrm{rank}\big((\bar{C}\bar{B}_M\ \ 0)\big) = \mathrm{rank}\big((\bar{B}_M\ \ 0)\big)$, which implies that $\bar{C}\bar{B}_M$ is of full column rank, hence $(\bar{C}\bar{B}_M)^{+}$ exists. By right multiplying M on the both sides of (4-11), we have $H\bar{C}\bar{B}_M = \bar{B}_M$. Therefore, by choosing different compatible matrix N of proper dimension, all possible solutions of H can be obtained as follows:

$$H = \bar{B}_M(\bar{C}\bar{B}_M)^{+} + N(I - (\bar{C}\bar{B}_M)(\bar{C}\bar{B}_M)^{+}) \tag{4-12}$$

where $(\bar{C}\bar{B}_M)^{+} = [(\bar{C}\bar{B}_M)^T(\bar{C}\bar{B}_M)]^{-1}(\bar{C}\bar{B}_M)^T$. Here, a general solution is used to make the design of fuzzy observer gains more flexible.

By deriving H from (4-12) to satisfy condition (4-6), a part of unknown inputs d_1 are decoupled, however, un-decoupled unknown inputs d_2 and d_w still exist in error dynamic and influence the performance of the estimator. To achieve robustness to d_2 and d_w, the following *Theorem 4.1* is addressed to attenuate their influences on estimation error.

Theorem 4.1

For system (4-3), there exists a robust UIO in the form of (4-4), such that $\|\bar{e}\|_{Tf} \leq \gamma\|\bar{d}\|_{Tf}$, if $\forall\, i$, there exist a positive definite matrix P, matrices Y_i, and Z such that

$$\begin{bmatrix} \Lambda_i & (PF - ZG\bar{C})\bar{B}_{di2} & -Y_i & -(P\bar{B}_M Q - ZG)D_d \\ * & -\gamma^2 I_{l_{d2}} & 0 & 0 \\ * & * & -\gamma^2 I_{l_{dw}} & 0 \\ * & * & * & -\gamma^2 I_{l_{dw}} \end{bmatrix} < 0 \tag{4-13}$$

where $\Lambda_i = I_{\bar{n}} + \bar{A}_i^T F^T P - \bar{A}_i^T \bar{C}^T G^T Z^T + PF\bar{A}_i - ZG\bar{C}\bar{A}_i - \bar{C}^T Y_i^T - Y_i\bar{C}$, $Y_i = PK_{i1}$, $Z = PN$, $F = I_{\bar{n}} - \bar{B}_M(\bar{C}\bar{B}_M)^+\bar{C}$, $G = I - (\bar{C}\bar{B}_M)(\bar{C}\bar{B}_M)^+$, $Q = (\bar{C}\bar{B}_M)^+$, $i = 1,2,\ldots r$, $\bar{d} = \begin{bmatrix} d_2^T & d_w{}^T & \dot{d}_w^T \end{bmatrix}^T$, and γ is a performance index, standing for the magnitude of the error compared with unknown inputs. Therefore, we have $N = P^{-1}Z$ and $K_{i1} = P^{-1}Y_i, i = 1,2,\ldots r$.

Proof

Choose a Lyapunov function $V(\bar{e}) = \bar{e}^T P\bar{e}$, and it is easy to verity that $V(\bar{e}) > 0$ for any nonzero $\bar{e}$. With the aid of (4-10), the derivative of $V(\bar{e})$ can be derived as:

$$\begin{aligned}
\dot{V}(\bar{e}) &= \textstyle\sum_{i=1}^r h_i(\mu)\{\left[R_i\bar{e} + T\bar{B}_{di2}d_2 - K_{i1}d_w - HD_d\dot{d}_w\right]^T P\bar{e} \\
&\quad + \bar{e}^T P\left[R_i\bar{e} + T\bar{B}_{di2}d_2 - K_{i1}d_w - HD_d\dot{d}_w\right]\} \\
&= \textstyle\sum_{i=1}^r h_i(\mu)[\,\bar{e}^T(R_i^T P + PR_i)\bar{e} + 2\bar{e}^T PT\bar{B}_{di2}d_2 - 2\bar{e}^T PK_{i1}d_w \\
&\quad -2\bar{e}^T PHD_d\dot{d}_w \\
&= \textstyle\sum_{i=1}^r h_i(\mu)\,[\bar{e}^T(\bar{A}_i^T T^T P - \bar{C}^T K_{i1}^T P + PT\bar{A}_i - PK_{i1}\bar{C})\bar{e} + 2\bar{e}^T PT\bar{B}_{di2}d_2 \\
&\quad -2\bar{e}^T PK_{i1}d_w - 2\bar{e}^T PHD_d\dot{d}_w] \\
&= \textstyle\sum_{i=1}^r h_i(\mu)[\,\bar{e}^T(\bar{A}_i^T F^T P - \bar{A}_i^T\bar{C}^T G^T Z^T + PF\bar{A}_i - ZG\bar{C}\bar{A}_i - \bar{C}^T Y_i^T - Y_i\bar{C})\bar{e} \\
&\quad +2\bar{e}^T(PF - ZG\bar{C})\bar{B}_{di2}d_2 - 2\bar{e}^T PK_{i1}d_w - 2\bar{e}^T PHD_d\dot{d}_w]
\end{aligned} \tag{4-14}$$

where $Y_i = PK_{i1}$,$Z = PN$, $F = I_{\bar{n}} - \bar{B}_M(\bar{C}\bar{B}_M)^+\bar{C}$, $G = I - (\bar{C}\bar{B}_M)(\bar{C}\bar{B}_M)^+$.

It can be seen from the condition that $\Lambda_i < 0$, which implies $\bar{A}_i^T F^T P - \bar{A}_i^T \bar{C}^T G^T Z^T + PF\bar{A}_i - ZG\overline{C}\bar{A}_i - \bar{C}^T Y_i^T - Y_i\bar{C} < 0$. Apparently, when $d_2 = 0$ and $d_w = 0$, $\dot{V}(\bar{e}) < 0$. Based on Lyaponov stability theory, the error dynamic system (4-10) is stable.

Now let us verify the robustness of the estimator. Let $\Gamma = \int_0^{Tf} \left(\bar{e}^T\bar{e} - \gamma^2\bar{d}^T\bar{d}\right)dt$, and by adding and subtracting $\int_0^{Tf} \dot{V}(\bar{e})dt$ into Γ, we can have:

$$\Gamma = \int_0^{Tf} \left(\bar{e}^T\bar{e} - \gamma^2\bar{d}^T\bar{d} + \dot{V}(\bar{e})\right)dt - \int_0^{Tf} \dot{V}(\bar{e})dt$$

$$= \int_0^{Tf} \sum_{i=1}^{r} h_i(\mu)\,[\,\bar{e}^T(\bar{A}_i^T F^T P - \bar{A}_i^T \bar{C}^T G^T Z^T + PF\bar{A}_i - ZG\overline{C}\bar{A}_i - \bar{C}^T Y_i^T - Y_i\bar{C})\bar{e}$$

$$+2\bar{e}^T(PF - ZG\bar{C})\bar{B}_{di2}d_2 - 2\bar{e}^T PK_{i1}d_w - 2\bar{e}^T P(\bar{B}_M Q + NG)D_d\dot{d}_w$$

$$-\gamma^2\bar{d}^T\bar{d}]dt - \int_0^{Tf} \dot{V}(\bar{e})dt$$

$$= \int_0^{Tf} [\bar{e}^T \quad \bar{d}^T][\textstyle\sum_{i=1}^{r} h_i(\mu)\,\Phi_i]\begin{bmatrix}\bar{e}\\ \bar{d}\end{bmatrix}dt - \int_0^{Tf} \dot{V}(\bar{e})dt \tag{4-15}$$

where

$$\Phi_i = \begin{bmatrix} \Lambda_i & (PF - ZG\bar{C})\bar{B}_{di2} & -Y_i & -(P\bar{B}_M Q - ZG)D_d \\ * & -\gamma^2 I_{l_{d2}} & 0 & 0 \\ * & * & -\gamma^2 I_{l_{dw}} & 0 \\ * & * & * & -\gamma^2 I_{l_{dw}} \end{bmatrix} \tag{4-16}$$

$\Lambda_i = I_{\bar{n}} + \bar{A}_i^T F^T P - \bar{A}_i^T \bar{C}^T G^T Z^T + PF\bar{A}_i - ZG\overline{C}\bar{A}_i - Y_i\bar{C} - \bar{C}^T Y_i^T$, and $Q = (\bar{C}\bar{B}_M)^+$.

Under zero initial condition $\bar{e}(0) = 0$, therefore,

$$\int_0^{Tf} \dot{V}(\bar{e})dt = V(\bar{e}) \geq 0 \tag{4-17}$$

Since $\Phi_i < 0$ in terms of (4-13), then $\sum_{i=1}^{r} h_i(\mu)\,\Phi_i < 0$. From (4-15) and (4-17), one has $\Gamma < 0$, which indicates $\|\bar{e}\|_{Tf} \leq \gamma\|\bar{d}\|_{Tf}$. As a result, for any given performance index γ, the estimation error can be reduced to be less than certain value by choosing observer gains according to LMIs (4-13).

Remark 4.1

In the aforementioned fault estimation approach design, we consider system for all local models with $C_1 = C_2 = \cdots = C_r$, $D_{f1} = D_{f2} = \cdots = D_{fr}$ and $D_{d1} = D_{d2} = \cdots = D_{dr}$. This kind of models are widely used to represent real industrial systems, such as wind turbines, robotic systems, and electrical models. For more general situations, when C_i, D_{fi} and D_{di}, $i = 1,2,\cdots r$, are not equal among different local models, the system can be represented as follows

$$\begin{cases} \dot{x} = \sum_{i=1}^{r} h_i(\mu)\,(A_i x + B_i u + B_{di} d + B_{fi} f) \\ y = \sum_{i=1}^{r} h_i(\mu)\,(C_i x + D_{fi} f + D_{di} d_w) \end{cases} \tag{4-18}$$

To make the problem easier to tackle, the following augmented system can be constructed

$$\begin{cases} \dot{\bar{x}} = \sum_{i=1}^{r} h_i(\mu)\,(\bar{A}_i \bar{x} + \bar{B}_i u + \bar{B}_{di} d) \\ y = \bar{C}\bar{x} + d_s \end{cases} \tag{4-19}$$

where $\bar{C}$ is chosen from any $\bar{C}_i$, $\bar{C}_i = \begin{bmatrix} C_i & 0_{p\times l_f} & D_{fi} \end{bmatrix} \in \mathcal{R}^{p\times\bar{n}}$, and $d_s = \sum_{i=1}^{r} h_i(\mu)[(\bar{C}_i - \bar{C})\bar{x} + D_{di} d_w]$. As a matter of fact, a pre-designed controller (see (4-20) in Section 4.2) can make the system dynamics stable, therefore, the influences from the system states due to different system output matrices can be regarded as the disturbances. In this case, d_w in Theorem 1 should be replaced by d_s, and D_d should be replaced by I_p. In the stability analysis, when $d_s = 0$, it means $d_w = 0$, and $\bar{C}_1 = \bar{C}_2 = \cdots = \bar{C}_r$. When $d_s \neq 0$, it implies $d_w \neq 0$ and/or $\bar{C}_i$, $i = 1,2,\cdots r$, are not equal. As a result, the methods used in *Theorem 4.1* can be directly applied to prove the robust stability of the estimation error dynamics.

Now the design procedure of the T-S fuzzy model based fault estimation for general nonlinear systems can be summarized as follows:

Procedure 4.1 *Robust state/faults estimation*

i) Construct the augmented system in the form of (4-3) for the T-S fuzzy model (4-2).

ii) For system with fuzzy output, rewrite the augmented system in the form of (4-19).

iii) Solve the LMIs (4-13) to obtain the matrices P, Y_i and Z, and calculate the gain $K_{i1} = P^{-1}Y_i$ and $N = P^{-1}Z$.

iv) Use N to solve H from Equation (4-12).

v) Calculate the other gain matrices R_i, T and K_{i2} following the formulae (4-6) to (4-9), respectively.

vi) Obtain the augmented estimate $\hat{\bar{x}}$ by implementing UIO (4-4), leading to the simultaneous estimates of state and fault as $\hat{x} = \begin{bmatrix} I_n & 0_{n\times 2l_f} \end{bmatrix}\hat{\bar{x}}$ and $\hat{f} = \begin{bmatrix} 0_{l_f\times(n+l_f)} & I_{l_f} \end{bmatrix}\hat{\bar{x}}$.

4.2 Tolerant design with signal compensation

In the last section, a robust fault estimation technique was proposed. In this section, we will apply the obtained estimates to compensate faulty signals. Assume there is a pre-existing nonlinear dynamic output feedback controller characterized by T-S fuzzy model, designed for normal operating conditions (i. e., fault free scenario), in the following format:

$$\begin{cases} \dot{x}_c = \sum_{l=1}^{r_c} h_{cl}(\mu_c)\,(A_{cl}x_c + B_{cl}y) \\ \quad u = \sum_{l=1}^{r_c} h_{cl}(\mu_c)\,C_{cl}x_c \end{cases} \tag{4-20}$$

where $x_c \in \mathcal{R}^{n_c}$ is the state of dynamic controller (4-20), $l = 1, 2, \cdots r_c$, $h_{cl}(\mu_c)$ are membership functions satisfying $\sum_{l=1}^{r_c} h_{cl}(\mu_c) = 1$ and $0 \le h_{cl}(\mu_c) \le 1$, A_{cl}, B_{cl} and C_{cl} are control gains of appropriate dimensions which are pre-designed in absence of faults, whose designs are beyond the concern in this study.

On the basis of the estimation of augmented state $\hat{\bar{x}}$, the fault term can be reconstructed as

$$\hat{f} = \begin{bmatrix} 0_{l_f\times\bar{n}} & 0_{l_f\times l_f} & I_{l_f} \end{bmatrix}\hat{\bar{x}} \tag{4-21}$$

The measurement output can thus be compensated as follows:

$$\begin{aligned} y_c &= y - \sum_{i=1}^{r} h_i(\mu)\,D_{fi}J\hat{\bar{x}} \\ &= Cx + \textstyle\sum_{i=1}^{r} h_i(\mu)\,D_{fi}J\bar{e} + d_c \\ &= Cx + \bar{e}_1 + d_c \end{aligned} \tag{4-22}$$

where $J = \begin{bmatrix} 0_{l_f\times\bar{n}} & 0_{l_f\times l_f} & I_{l_f} \end{bmatrix}$, $C = \bar{C}\begin{bmatrix} I_n & 0_{n\times l_f} & 0_{n\times l_f} \end{bmatrix}^T$, $d_c = \sum_{i=1}^{r} h_i(\mu)[(C_i - C)x + D_{di}d_w]$, $\bar{e}_1 = \sum_{i=1}^{r} h_i(\mu)\,D_{fi}J\bar{e}$.

Suppose

$$\text{rank}\begin{bmatrix} B_h & B_{fh} \end{bmatrix} = \text{rank}\, B_h \tag{4-23}$$

where $B_h = \sum_{i=1}^{r} h_i(\mu)B_i$, $B_{fh} = \sum_{i=1}^{r} h_i(\mu)B_{fi}$. The compensated signal for the actuator is designed as $u_f = K_f\hat{f}$, where

$$K_f = B_h^+ B_{fh} \tag{4-24}$$

Therefore, it is clear that

$$\sum_{i=1}^{r} h_i(\mu)\left(B_{fi} - B_iK_f\right) = B_{fh} - B_hB_h^+B_{fh} = 0. \tag{4-25}$$

Subtracting u_f from the actuator input, and using the compensated measurement output y_c to replace the actual measurement y, the controller can be compensated as follows:

$$\begin{cases} \dot{x}_c = \sum_{l=1}^{r_c} h_{cl}(\mu_c)\,(A_{cl}x_c + B_{cl}y_c) \\ u = \sum_{l=1}^{r_c} h_{cl}(\mu_c)\,(C_{cl}x_c - K_fJ\hat{\bar{x}}) \end{cases} \tag{4-26}$$

Substituting (4-26) into (4-2), the following closed-loop system can be formulated as:

$$\begin{cases} \dot{\tilde{x}} = \sum_{i=1}^{r} h_i(\mu)\sum_{l=1}^{r_c} h_{cl}(\mu_c)\,(\tilde{A}_{il}\tilde{x} + \tilde{B}_{dil}\tilde{d} + B_{eil}\tilde{e}) \\ y_c = \tilde{C}\tilde{x} + J_e\tilde{e} + J_c\tilde{d} \end{cases} \tag{4-27}$$

where $\tilde{x} = [x^T \quad x_c^T]^T$, $\tilde{e} = [\bar{e}_1^T \quad \bar{e}_2^T]^T$, $\bar{e}_2 = K_fJ\bar{e}$, $\tilde{A}_{il} = \begin{bmatrix} A_i & B_iC_{cl} \\ B_{cl}C & A_{cl} \end{bmatrix}$, $\tilde{B}_{dil} = \begin{bmatrix} B_{di} & 0 \\ 0 & B_{cl} \end{bmatrix}$, $\tilde{C} = [C \quad 0_{p\times n_c}]$ $\tilde{d} = [d^T \quad d_c^T]^T$, $B_{eil} = \begin{bmatrix} 0 & B_i \\ B_{cl} & 0 \end{bmatrix}$, $J_e = [I_p \quad 0_{p\times m}]$, and $J_c = [0_{p\times l_d} \quad I_p]$.

Now it is ready to discuss the stability and robustness of the dynamic system (4-27).

Theorem 4.2

If there is a pre-existing controller in the form of (4-20) to ensure plant (4-2) to be stable and satisfy the following robust performance index

$$\|y\|_{Tf}^2 \leq \gamma_p^2\left\|\tilde{d}\right\|_{Tf}^2 \tag{4-28}$$

in fault free case, where γ_p is a positive scalar, then based on the robust fault estimation scheme designed following *Theorem 4.1*, the controller (4-26) can drive the trajectories of compensated system (4-27) to be stable and satisfy the following robust performance index:

$$\|y_c\|_{Tf}^2 \leq \gamma_0^2\left\|\tilde{d}\right\|_{Tf}^2 + \gamma_{0e}^2\|\tilde{e}\|_{Tf}^2 \tag{4-29}$$

where $\gamma_0^2 > \gamma_p^2 + \alpha_2 + \alpha_0(\alpha_3 + \alpha_4)$, $\gamma_{0e}^2 > \alpha_1 + \alpha_2 + \alpha_3 + \alpha_4$, $\alpha_1 = \|J_e^T J_e\|$, $\alpha_2 = \|J_e^T J_c\|$, $\alpha_3 = \|\tilde{C}^T J_e\|$, and$\alpha_4$ is a positive scalar such that

$$\sum_{i=1}^{r} h_i(\mu) \sum_{l=1}^{r_c} h_{cl}(\mu_c) \left\|\tilde{P} B_{eil}\right\| \le \alpha_4.$$

Proof

(i) Proof of the closed-loop stability by assuming $d = 0$ and $d_c = 0$.

Choose Lyapunov function as

$$\tilde{V} = V_c + \xi V = \tilde{x}^T \tilde{P} \tilde{x} + \xi \bar{e}^T P \bar{e} \quad (4\text{-}30)$$

where ξ is a positive scalar, $\tilde{P}$ and P are positive-definite matrices with appropriate dimensions. From *Theorem 4.1*, there exists a positive scalar φ_0 such that

$$\dot{V} \le -\varphi_0 \|\bar{e}\|^2 \quad (4\text{-}31)$$

It can be derived that

$$\|\tilde{e}\|^2 = \|\bar{e}_1\|^2 + \|\bar{e}_2\|^2 \le \varphi_e \|\bar{e}\|^2 \quad (4\text{-}32)$$

where φ_e is a positive scalar such that $\varphi_e \ge (\sum_{i=1}^{r} h_i(\mu) \left\|D_{fi} J\right\|)^2 + \left\|K_f J\right\|^2$. Therefore,

$$\dot{V} \le -\varphi_0 \|\bar{e}\|^2 \le -\frac{\varphi_0}{\varphi_e} \|\tilde{e}\|^2 \quad (4\text{-}33)$$

Using (4-27), (4-30) and (4-33), one can yield

$$\dot{\tilde{V}} \le \sum_{i=1}^{r} h_i(\mu) \sum_{l=1}^{r_c} h_{cl}(\mu_c) \left[\tilde{x}^T \left(\tilde{A}_{il}^T \tilde{P} + \tilde{P} \tilde{A}_{il}\right) \tilde{x} + 2\tilde{x}^T \tilde{P} B_{eil} \tilde{e}\right] - \xi \frac{\varphi_0}{\varphi_e} \|\tilde{e}\|^2 \quad (4\text{-}34)$$

Since system (4-2) is stable under controller (4-20) in fault free case, there is a positive scalar φ_c such that $\forall\ i, l$, there is a positive scalar φ_c such that

$$\sum_{i=1}^{r} h_i(\mu) \sum_{l=1}^{r_c} h_{cl}(\mu_c) \tilde{x}^T \left(\tilde{A}_{il}^T \tilde{P} + \tilde{P} \tilde{A}_{il}\right) \tilde{x} \le -\varphi_c \|\tilde{x}\|^2 \quad (4\text{-}35)$$

As a result, we have

$$\begin{aligned} \dot{\tilde{V}} &\le \sum_{i=1}^{r} h_i(\mu) \sum_{l=1}^{r_c} h_{cl}(\mu_c) \left(2\tilde{x}^T \tilde{P} B_{eil} \tilde{e}\right) - \varphi_c \|\tilde{x}\|^2 - \xi \frac{\varphi_0}{\varphi_e} \|\tilde{e}\|^2 \\ &\le -\varphi_c \|\tilde{x}\|^2 + \xi_f \|\tilde{x}\| \|\tilde{e}\| - \xi \frac{\varphi_0}{\varphi_e} \|\tilde{e}\|^2 \end{aligned} \quad (4\text{-}36)$$

where $\xi_f \ge 2 \sum_{i=1}^{r} h_i(\mu) \sum_{l=1}^{r_c} h_{cl}(\mu_c) \left\|\tilde{P} B_{eil}\right\|$. Selecting

$$\xi \geq \frac{\xi_f^2 \varphi_e}{\varphi_0 \varphi_c} \tag{4-37}$$

it follows that

$$\dot{\tilde{V}} \leq -\frac{\varphi_c}{2}\|\tilde{x}\|^2 - \frac{\xi\varphi_0}{2\varphi_e}\|\tilde{e}\|^2 \tag{4-38}$$

which indicates the compensated system (4-27) is stable.

(ii) Proof of the robust performance when $d \neq 0$ and $d_c \neq 0$.

From (4-27) and (4-30), one has

$$\begin{aligned}
\dot{V}_c &= \textstyle\sum_{i=1}^{r} h_i(\mu) \sum_{l=1}^{r_c} h_{cl}(\mu_c)\, [\tilde{x}^T\big(\tilde{A}_{il}^T\tilde{P} + \tilde{P}\tilde{A}_{il}\big)\tilde{x} + 2\tilde{x}^T\tilde{P}\tilde{B}_{dil}\tilde{d} + 2\tilde{x}^T\tilde{P}B_{eil}\tilde{e}] \\
&= \textstyle\sum_{i=1}^{r} h_i(\mu) \sum_{l=1}^{r_c} h_{cl}(\mu_c)\, [\tilde{x}^T\big(\tilde{A}_{il}^T\tilde{P} + \tilde{P}\tilde{A}_{il}\big)\tilde{x} + 2\tilde{x}^T\tilde{P}\tilde{B}_{dil}\tilde{d} + 2\tilde{x}^T\tilde{P}B_{eil}\tilde{e}] \\
&\quad + {y_c}^T y_c - \gamma_0^2\tilde{d}^T\tilde{d} - \gamma_{0e}^2\tilde{e}^T\tilde{e} - {y_c}^T y_c + \gamma_0^2\tilde{d}^T\tilde{d} + \gamma_{0e}^2\tilde{e}^T\tilde{e} \\
&= \textstyle\sum_{i=1}^{r} h_i(\mu) \sum_{l=1}^{r_c} h_{cl}(\mu_c)\, [\tilde{x}^T\big(\tilde{A}_{il}^T\tilde{P} + \tilde{P}\tilde{A}_{il}\big)\tilde{x} + 2\tilde{x}^T\tilde{P}\tilde{B}_{dil}\tilde{d} + 2\tilde{x}^T\tilde{P}B_{eil}\tilde{e}] \\
&\quad + y^T y + \tilde{e}^T J_e^T J_e\tilde{e} + 2\tilde{e}^T J_e^T J_c\tilde{d} + 2\tilde{x}^T\tilde{C}^T J_e\tilde{e} - \gamma_0^2\tilde{d}^T\tilde{d} - \gamma_{0e}^2\tilde{e}^T\tilde{e} - {y_c}^T y_c \\
&\quad + \gamma_0^2\tilde{d}^T\tilde{d} + \gamma_{0e}^2\tilde{e}^T\tilde{e} \\
&\leq \textstyle\sum_{i=1}^{r} h_i(\mu) \sum_{l=1}^{r_c} h_{cl}(\mu_c)\, \big[\tilde{x}^T\big(\tilde{A}_{il}^T\tilde{P} + \tilde{P}\tilde{A}_{il}\big)\tilde{x} + 2\tilde{x}^T\tilde{P}\tilde{B}_{dil}\tilde{d}\big] + \|y\|^2 \\
&\quad + \|J_e^T J_e\|\|\tilde{e}\|^2 + 2\|J_e^T J_c\|\|\tilde{e}\|\|\tilde{d}\| \\
&\quad + 2\textstyle\sum_{i=1}^{r} h_i(\mu) \sum_{l=1}^{r_c} h_{cl}(\mu_c)\, \big(\|\tilde{C}^T J_e\| + \|\tilde{P}B_{eil}\|\big)\|\tilde{e}\|\|\tilde{x}\| \\
&\quad - \gamma_0^2\tilde{d}^T\tilde{d} - \gamma_{0e}^2\tilde{e}^T\tilde{e} - {y_c}^T y_c + \gamma_0^2\tilde{d}^T\tilde{d} + \gamma_{0e}^2\tilde{e}^T\tilde{e}
\end{aligned} \tag{4-39}$$

Since (4-28) holds by pre-designed controller in fault-free case, we have

$$\textstyle\sum_{i=1}^{r} h_i(\mu) \sum_{l=1}^{r_c} h_{cl}(\mu_c)\, [\tilde{x}^T\big(\tilde{A}_{il}^T\tilde{P} + \tilde{P}\tilde{A}_{il}\big)\tilde{x} + 2\tilde{x}^T\tilde{P}\tilde{B}_{dil}\tilde{d}] + \|y\|^2 \leq \gamma_p^2\|\tilde{d}\|^2 \tag{4-40}$$

Substituting (4-40) into (4-39), one can have

$$\begin{aligned}
\dot{V}_c &\leq \gamma_p^2\|\tilde{d}\|^2 + \|J_e^T J_e\|\|\tilde{e}\|^2 + 2\|J_e^T J_c\|\|\tilde{e}\|\|\tilde{d}\| \\
&\quad + 2\textstyle\sum_{i=1}^{r} h_i(\mu) \sum_{l=1}^{r_c} h_{cl}(\mu_c)\, (\|\tilde{C}^T J_e\| + \|\tilde{P}B_{eil}\|)\|\tilde{e}\|\|\tilde{x}\| \\
&\quad - \gamma_0^2\tilde{d}^T\tilde{d} - \gamma_{0e}^2\tilde{e}^T\tilde{e} - {y_c}^T y_c + \gamma_0^2\tilde{d}^T\tilde{d} + \gamma_{0e}^2\tilde{e}^T\tilde{e}
\end{aligned}$$

$$\leq \gamma_p^2\|\tilde{d}\|^2 + \|J_e^T J_e\|\|\tilde{e}\|^2 + \|J_e^T J_c\|\left(\|\tilde{e}\|^2 + \|\tilde{d}\|^2\right)$$

$$+\sum_{i=1}^{r} h_i(\mu)\sum_{l=1}^{r_c} h_{cl}(\mu_c)\,(\|\tilde{C}^T J_e\| + \|\tilde{P}B_{eil}\|)\,(\|\tilde{e}\|^2 + \|\tilde{x}\|^2)$$

$$-\gamma_0^2\tilde{d}^T\tilde{d} - \gamma_{0e}^2\tilde{e}^T\tilde{e} - {y_c}^T y_c + \gamma_0^2\tilde{d}^T\tilde{d} + \gamma_{0e}^2\tilde{e}^T\tilde{e}$$

$$\leq [(\gamma_p^2 + \|J_e^T J_c\|)\|\tilde{d}\|^2 + (\|J_e^T J_e\| + \|J_e^T J_c\| + \|\tilde{C}^T J_e\|$$

$$+\sum_{i=1}^{r} h_i(\mu)\sum_{l=1}^{r_c} h_{cl}(\mu_c)\,\|\tilde{P}B_{eil}\|)\|\tilde{e}\|^2$$

$$+\left(\|\tilde{C}^T J_e\| + \sum_{i=1}^{r} h_i(\mu)\sum_{l=1}^{r_c} h_{cl}(\mu_c)\,\|\tilde{P}B_{eil}\|\right)\|\tilde{x}\|^2$$

$$-\gamma_0^2\tilde{d}^T\tilde{d} - \gamma_{0e}^2\tilde{e}^T\tilde{e} - {y_c}^T y_c + \gamma_0^2\tilde{d}^T\tilde{d} + \gamma_{0e}^2\tilde{e}^T\tilde{e}$$

$$\leq (\gamma_p^2 + \alpha_2 - \gamma_0^2)\|\tilde{d}\|^2 + (\alpha_1 + \alpha_2 + \alpha_3 + \alpha_4 - \gamma_{0e}^2)\|\tilde{e}\|^2$$

$$+(\alpha_3 + \alpha_4)\|\tilde{x}\|^2 - {y_c}^T y_c + \gamma_0^2\tilde{d}^T\tilde{d} + \gamma_{0e}^2\tilde{e}^T\tilde{e} \tag{4-41}$$

where $\alpha_1 = \|J_e^T J_e\|$, $\alpha_2 = \|J_e^T J_c\|$, $\alpha_3 = \|\tilde{C}^T J_e\|$, and α_4 is a positive scalar such that $\sum_{i=1}^{r} h_i(\mu)\sum_{l=1}^{r_c} h_{cl}(\mu_c)\,\|\tilde{P}B_{eil}\| \leq \alpha_4$.

From (4-28), we know $\|y\|^2 \leq \gamma_p\|\tilde{d}\|^2$, which means

$$\tilde{x}^T\tilde{C}^T\tilde{C}\tilde{x} + \tilde{d}^T J_c^T J_c\tilde{d} + 2\tilde{x}^T\tilde{C}^T J_c\tilde{d} \leq \gamma_p\|\tilde{d}\|^2 \tag{4-42}$$

From (4-42), we can have

$$\lambda_{min}(\tilde{C}^T\tilde{C})\|\tilde{x}\|^2 + \lambda_{min}(J_c^T J_c)\|\tilde{d}\|^2 - 2\|\tilde{C}^T J_c\|\|\tilde{x}\|\|\tilde{d}\|$$

$$\leq \tilde{x}^T\tilde{C}^T\tilde{C}\tilde{x} + \tilde{d}^T J_c^T J_c\tilde{d} + 2\tilde{x}^T\tilde{C}^T J_c\tilde{d} \leq \gamma_p\|\tilde{d}\|^2 \tag{4-43}$$

Notice that $J_c = [0_{p\times l_d} \quad I_p]$, which means $\lambda_{min}(J_c^T J_c) = 0$. This implies there exists a positive scalar α_0, such that $\|\tilde{x}\|^2 \leq \alpha_0\|\tilde{d}\|^2$ by simple calculation. Therefore, (4-41) indicates

$$\dot{V}_c \leq [\gamma_p^2 + \alpha_2 + \alpha_0(\alpha_3 + \alpha_4) - \gamma_0^2]\|\tilde{d}\|^2 + (\alpha_1 + \alpha_2 + \alpha_3 + \alpha_4 - \gamma_{0e}^2)\|\tilde{e}\|^2$$

$$-{y_c}^T y_c + \gamma_0^2\tilde{d}^T\tilde{d} + \gamma_{0e}^2\tilde{e}^T\tilde{e} \tag{4-44}$$

From (4-44), we have

$$0 \leq V_c \leq \int_0^{Tf}\{[\gamma_p^2 + \alpha_2 + \alpha_0(\alpha_3 + \alpha_4) - \gamma_0^2]\|\tilde{d}\|^2$$

$$+(\alpha_1 + \alpha_2 + \alpha_3 + \alpha_4 - \gamma_{0e}^2)\|\tilde{e}\|^2 - {y_c}^T y_c$$

$$+\gamma_0^2 \tilde{d}^T \tilde{d} + \gamma_{0e}^2 \tilde{e}^T \tilde{e}\}dt \tag{4-45}$$

If we make $\gamma_0^2 \geq \gamma_p^2 + \alpha_2 + \alpha_0(\alpha_3 + \alpha_4)$ and $\gamma_{0e}^2 \geq \alpha_1 + \alpha_2 + \alpha_3 + \alpha_4$, (4-45) can be reduced to

$$0 \leq V_c \leq \int_0^{Tf} (-{y_c}^T y_c + \gamma_0^2 \tilde{d}^T \tilde{d} + \gamma_{0e}^2 \tilde{e}^T \tilde{e})dt \tag{4-46}$$

which means

$$\int_0^{Tf} {y_c}^T y_c \, dt \leq \int_0^{Tf} \gamma_0^2 \tilde{d}^T \tilde{d} \, dt + \int_0^{Tf} \gamma_{0e}^2 \tilde{e}^T \tilde{e} dt \tag{4-47}$$

Therefore, we can derive $\|y_c\|_{Tf}^2 \leq \gamma_0^2 \|\tilde{d}\|_{Tf}^2 + \gamma_{0e}^2 \|\tilde{e}\|_{Tf}^2$, which completes the proof.

Now the procedure of signal compensation can be summarized as follows:

Procedure 4.2 *Tolerant control with signal compensation*

i) Obtain the estimates of the augmented state vector $\hat{\bar{x}}$ from the robust estimation algorithm described in *Procedure 4.1*.
ii) Implement the sensor compensation in terms of (4-22).
iii) Based on a pre-existing controller (4-20), implement a compensation controller in the form (4-26) to plant (4-2).

Remark 4.2

Based on robust fault estimation scheme designed in Chapter 3, signal compensation can also be implemented on linear system and Lipschitz nonlinear system through similar method with T-S fuzzy systems. To avoid repetitive statement, we do not give much detail about this part.

The experimental work to demonstrate the above techniques is based on a case study on wind turbine benchmark model, which can be found in Chapter 7.

4.3 Summary

In this study, integrated robust fault estimation and signal compensation techniques for tolerant control have been addressed for T-S fuzzy systems corrupted by simultaneous actuator faults, sensor faults, and partially decoupled unknown uncertainties, which would find applications in wide industrial systems. Augmented system approach, jointly with T-S fuzzy UIOs and robust optimization technique provides robust estimates of the considered faults and the system states, which are then utilized for signal compensation to remove the influences from the faults to the system dynamics and outputs. A remarkable advantage of the proposed fault tolerant control approach is that the pre-existing controller can work well by integrating the proposed signal compensation technique under both faulty and fault-free scenarios.

Chapter 5.

Fault estimation for stochastic system

Owing to the widespread presence of random factors in the operation of systems, stochastic systems formulated in It$\hat{o}$-type stochastic differential equations have played crucial roles in modelling practical systems. However, the existence of stochastic perturbations make fault estimation for this class of systems difficult, thus few related work has been recorded. Robust UIO-based fault estimation for stochastic systems with partially decoupled unknown inputs and Brownian motions becomes more challenging hence remains to be an open problem.

Stability plays the most fundamental role in systems control and estimation theory. Global asymptotically stability in probability can be used to analyze the convergence system in absence of disturbances considering that a small enough perturbation should not destroy the stability properties. However, for robust fault estimation, understanding how large can the perturbations change the phase portrait is beneficial to enhance estimation performances. Input-to-state stability was firstly introduced in [130] to capture the idea of bounded input bounded state behavior together with the decay of states under small inputs, and a series of results centralizing on the theory of input-to-state stability-Lyapunov functions were reported in the literature [131-135]. The input-to-state stability paradigm was generalized to finite-time stochastic input-to-state stability in [136, 137], and a couple of interesting results were reported in [138-142], which will facilitate to address a variety of control and estimation problems for stochastic systems.

In this chapter, the criteria of stochastic input-to-state stability and finite-time stochastic input-to-state stability are addressed with the aid of Lyapunov theory. Based on the criteria, robust fault estimation techniques are developed for stochastic systems in presence of faults, partially decoupled unknown inputs and Brownian motions. Section 5.1 is dedicated to the problem statement and needed preliminaries. Sufficient conditions of both stochastic input-to-state-stability and finite-time stochastic input-to-state-stability are presented in Section 5.2. Section 5.3 and 5.4 state the methodologies to design UIO-based fault estimator for stochastic quadratic inner-bounded nonlinear systems and stochastic T-S fuzzy nonlinear systems, respectively, applying the results in Section 5.2 to analyze the stability of error dynamic. Both the synthesis of the stability and robustness will be on the basis of LMI algorithms. Section 5.5 provides simulation examples to show the estimation performance, followed by Section 5.6 to conclude the whole contents of this chapter.

5.1 Preliminaries and problem formulation

Consider a stochastic nonlinear system in the form of:

$$dx(t) = l(t, x(t), v(t))dt + h\big(t, x(t), v(t)\big)dw(t), \;\; t \geq t_0 \qquad \text{(5-1-1)}$$

where $x(t) \in \mathcal{R}^n$ is system state; $v(t)$ is input, where $\mathbb{E}[v(t)] \in L_\infty^m$; $w(t)$ represents Brownian motions defined on the probability space $\big(\Omega, \mathcal{F}, \{\mathcal{F}_t\}_{t \geq t_0}, \mathcal{P}\big)$; $l(t, x(t), v(t))$ and $h(t, x(t), v(t))$ stand for system dynamic function and stochastic perturbation distribution function, respectively. For system (5-1-1), the following lemmas and definitions are introduced:

Lemma 5.1.1 [143].

Assume that $l(t, x(t), v(t))$ and $h(t, x(t), v(t))$ are all continuous in $x(t)$. Further, for each $N = 1, 2, \ldots$, and each $0 \leq T < \infty$, if the following conditions hold:

(i) $\|l(t, x, v)\| \leq c(t)(1 + \|x\|)$ (5-1-2)

(ii) $\|h(t, x, v)\|^2 \leq c(t)(1 + \|x\|^2)$ (5-1-3)

(iii) $2\langle x_1 - x_2, l(t, x_1, v) - l(t, x_2, v)\rangle + \|h(t, x_1, v) - h(t, x_2, v)\|^2$

$$\leq c_T^N(t)\rho_T^N(\|x_1 - x_2\|^2) \qquad \text{(5-1-4)}$$

as $\|x_i\| \leq N, i = 1, 2, t \in [0, T]$, where $c(t)$ and $c_T^N(t)$ are nonnegative functions such that $\int_0^T c(t)\,dt < \infty$ and $\int_0^T c_T^N(t)\,dt < \infty$; $\rho_T^N(s) \geq 0$, as $s \geq 0$, is non-random, strictly increasing, continuous and concave such that $\int_0^T ds/\rho_T^N(s) = \infty$. Then for any given $x_0 \in \mathcal{R}^n$, Equation (5-1-1) has a path-wise unique strong solution.

It should be mentioned that the existence of a unique solution for a stochastic nonlinear system is the precondition of discussing the stochastic input-to-state stability and finite-time stochastic input-to-state stability.

Definition 5.1.1 [144]

A function $\gamma: \mathcal{R}^+ \longrightarrow \mathcal{R}^+$ is said to be a generalized $\mathcal{K}$-function if it is continuous with $\gamma(0) = 0$, and satisfies:

$$\begin{cases} \gamma(\sigma_1) > \gamma(\sigma_2), \ \ if\ \gamma(\sigma_1) \neq 0 \\ \gamma(\sigma_1) = \gamma(\sigma_2) = 0, if\ \gamma(\sigma_1) = 0 \end{cases}, \forall \sigma_1 > \sigma_2 \geq 0 \tag{5-1-5}$$

$\mathcal{K}_\infty$ is the subset of $\mathcal{K}$-functions that are unbounded. Note that if γ is of class generalized $\mathcal{K}_\infty$, then its inverse function γ^{-1} is well defined and again of class generalized $\mathcal{K}_\infty$.

Definition 5.1.2 [144]

A function $\beta: \mathcal{R}^+ \times \mathcal{R}^+ \longrightarrow \mathcal{R}^+$ is said to be a generalized $\mathcal{KL}$-function if for each fixed $t \geq 0$, the function $\beta(s, t)$ is a generalized $\mathcal{K}$-function, and for each fixed $s \geq 0$, it decreases to zero as $t \longrightarrow T$ for some constant $T > 0$.

Definition 5.1.3 [137]

System (5-1-1) is said to be stochastic input-to-state stable, if $\forall \varepsilon > 0$, there exist functions $\beta \in \mathcal{KL}$ and $\gamma \in \mathcal{K}_\infty$, such that for any initial condition $x(t_0) = x_0$, one has

$$\mathcal{P}\{\|x(t)\| \leq \beta(\|x_0\|, t - t_0) + \gamma(|v|)\} \geq 1 - \varepsilon, \forall t \geq t_0, \forall x_0 \in \mathcal{R}^n \tag{5-1-6}$$

Remark 5.1.1

Since $\gamma(0) = 0$, it can be found that, in zero input situation, stochastic input-to-state stability can necessarily lead to globally asymptotically stability in probability stated in [145]. But in general, globally asymptotically stability in probability does not imply stochastic input-to-state stability.

For system (5-1-1), given any function $V(t, x) \in \mathcal{C}^{2\times1}\{\mathcal{R}^n \times [t_0, \infty] \to \mathcal{R}^+\}$, the infinitesimal generator $\mathcal{L}V(t, x)$ is defined as:

$$\mathcal{L}V(t, x) = \frac{\partial V(t,x)}{\partial t} + \left[\frac{\partial V(t,x)}{\partial x}\right]^T l + \frac{1}{2} trace\left\{h^T \frac{\partial^2 V(t,x)}{\partial x^2} h\right\} \tag{5-1-7}$$

where $trace\left\{h^T \frac{\partial^2 V(t,x)}{\partial x^2} h\right\}$ is called as the Hessian term of $\mathcal{L}$.

Lemma 5.1.2 [138]

For any continuous convex function $q(\cdot) \in \mathcal{K}$, there exists a generalized class $\mathcal{KL}$ function β satisfying

$$\mathbb{E}(Y(t)) \leq \beta(\mathbb{E}(Y_0), t - t_0), t \geq t_0 \tag{5-1-8}$$

if for process $Y(t)$ with $\mathbb{E}(Y(t))$ being (locally) absolutely continuous and $0 \leq \mathbb{E}(Y(t)) < \infty$ and for any $t \geq t_0$

$$\mathbb{E}[\mathcal{L}Y(t)] \leq -\mathbb{E}\big[q\big(Y(t)\big)\big] \tag{5-1-9}$$

Especially, when $t = t_0, \mathbb{E}(Y_0) = \beta(\mathbb{E}(Y_0),0)$.

Lemma 5.1.3 [140]

Assume that $\phi(\cdot): \mathcal{R} \to \mathcal{R}$ and $\chi(\cdot,\cdot): \mathcal{R}^n \to \mathcal{R}$ are two smooth functions and x is the solution of system (5-1-1). Then the following equality holds:

$$\mathcal{L}\big(\phi \circ \chi(t,x)\big) = \frac{d\phi}{d\chi}\mathcal{L}\big(\chi(t,x)\big) + \frac{1}{2}\frac{d^2\phi}{d\chi^2} trace\left\{\left(\frac{\partial\chi}{\partial x}h\right)^T \left(\frac{\partial\chi}{\partial x}h\right)\right\}$$

(5-1-10)

Definition 5.1.4 **[**145**]**

System (5-1-1) is said to be finite-time stochastic input-to-state stable, if $\forall\varepsilon > 0$, there exists function $\gamma \in \mathcal{K}_\infty$, such that

$$\mathcal{P}\{\|x(t)\| \leq \gamma(|v|)\} \geq 1 - \varepsilon, \forall t \geq t_0, \forall x_0 \in \mathcal{R}^n \tag{5-1-11}$$

Remark 5.1.2

The difference between stochastic input-to-state stability and finite-time stochastic input-to-state stability is the finite-time convergence of β. Finite-time stochastic input-to-state stability says,

$$\beta(\|x_0\|, t - t_0) = 0, t \geq t_0 + T_0(t_0, x_0, v) \tag{5-1-12}$$

Lemma 5.1.4 (Jensen's inequality) [146]

If X to be a random variable and let φ to be a convex function, then

$$\mathbb{E}[\varphi(X)] \geq \varphi\big(\mathbb{E}(X)\big) \tag{5-1-13}$$

Lemma 5.1.5 (Chebychev's inequality)[146]

Let X to be a random variable and let φ to be a nonnegative function. Then, for any positive real number a,

$$\mathcal{P}\{\varphi(X) \geq a\} \leq \frac{\mathbb{E}[\varphi(X)]}{a} \tag{5-1-14}$$

Lemma 5.1.6 (It$\hat{o}$ formula) [146]

Given Itô process in the form of (5-1-1), then function $\mu(t, x)$ is again an Itô process with differential given by

$$d(\mu(t,x)) = \mathcal{L}(\mu(t,x))dt + \frac{\partial \mu}{\partial x} hdw \tag{5-1-15}$$

The above preliminaries are the same with most previous literatures. Note that the class of conventional $\mathcal{K}_\infty$ functions mentioned in some papers is certainly the class of generalized $\mathcal{K}_\infty$ functions. Stochastic input-to-state stability reflects the fact that bounded initial condition and bounded input result in bounded state in probability, and the trajectories will decay under small inputs. Further, finite-time stochastic input-to-state stability says that the bounded state will converge to a function of input alone after the finite stochastic settling time.

5.2 Lyapunov function-based properties of finite-time stochastic input-to-state-stability

In this section, based on the above definitions and lemmas, we shall derive some sufficient conditions for checking the stochastic input-to-state stability and finite-time stochastic input-to-state stability properties, associated with Lyapunov theory.

Definition 5.2.1

A function V is called a stochastic input-to-state stability-Lyapunov function if there exist $\mathcal{K}_\infty$ functions $\psi_1, \psi_2, \psi_3, \psi_4$ such that for all $x \in \mathcal{R}^n$, $v \in L_\infty^m$ and $t \geq t_0$,

(i) $\psi_1(\|x\|) \leq V(t,x) \leq \psi_2(\|x\|)$ (5-2-1)

(ii) $\mathcal{L}V(t,x) \leq -\psi_3(\|x\|) + \psi_4(|v|)$ (5-2-2)

Theorem 5.2.1

System (5-1-1) is stochastic input-to-state stable if there is a stochastic input-to-state stability-Lyapunov function V.

Proof

Let $\tau_0 \in [t_0, \infty)$ denote a time at which the system trajectory x enters the set

$$\mathcal{B} = \left\{x \in \mathcal{R}^n : \psi_3(\|x\|) \leq \tilde{\psi}_4(|v|)\right\} \tag{5-2-3}$$

where $\tilde{\psi}_4$ is a generalized $\mathcal{K}$ function and $\tilde{\psi}_4 = \frac{(1+\sigma_0)}{1-\lambda}\psi_4$, $\sigma_0 > 0, 0 < \lambda < 1$. In the following analysis, we consider two cases: $x_0 \in \mathcal{B}^c$ and $x_0 \in \mathcal{B}$, respectively, where $\mathcal{B}^c$ denotes the complementary set of $\mathcal{B}$.

Case 1. $x_0 \in \mathcal{B}^c$

In this case, for any $t \in [t_0, \tau_0)$,

$$\psi_3(\|x\|) > \frac{(1+\sigma_0)}{1-\lambda}\psi_4(|v|) \tag{5-2-4}$$

Then

$$-\psi_3(\|x\|) < -\lambda\psi_3(\|x\|) - (1+\sigma_0)\psi_4(|v|) \tag{5-2-5}$$

According to (5-2-2), we can derive

$$\mathcal{L}V(t,x) < -\lambda\psi_3(\|x\|) - (1+\sigma_0)\psi_4(|v|) + \psi_4(|v|) \tag{5-2-6}$$

thus

$$\mathcal{L}V(t,x) < -\lambda\psi_3(\|x\|) - \sigma_0\psi_4(|v|) \tag{5-2-7}$$

Because ψ_4 is of $\mathcal{K}_\infty$, then

$$\mathcal{L}V(t,x) < -\lambda\psi_3(\|x\|) < -\lambda\psi_3 \circ \psi_2^{-1}\big(V(t,x)\big) \tag{5-2-8}$$

From *Lemma 5.1.2* and *Lemma 5.1.4*, there exists a generalized $\mathcal{KL}$ function $\tilde{\beta}$ satisfying the following condition:

$$\mathbb{E}\big(V(t,x)\big) \le \tilde{\beta}\,(V_0, t-t_0)\,,$$

$$t \in \big[t_{0,}\tau_0\big), x_0 \in \mathcal{B}^c \tag{5-2-9}$$

For any $\varepsilon \in (0,1)$, take $\bar{\beta} = \frac{\tilde{\beta}}{\varepsilon} \in \mathcal{KL}$. Applying *Lemma 5.1.5*, we have

$$\mathcal{P}\big\{V(t,x) \ge \bar{\beta}(V_0, t-t_0)\big\} \le \frac{\mathbb{E}\big(V(t,x)\big)}{\bar{\beta}} \le \frac{\tilde{\beta}}{\bar{\beta}} = \varepsilon$$

$$t \in \big[t_{0,}\tau_0\big), x_0 \in \mathcal{B}^c \tag{5-2-10}$$

which leads to

$$\mathcal{P}\big\{V(t,x) \le \bar{\beta}(V_0, t-t_0)\big\} > 1-\varepsilon,\ t \in \big[t_{0,}\tau_0\big), x_0 \in \mathcal{B}^c \tag{5-2-11}$$

To be mentioned that ε can be made arbitrarily small by an appropriate choice of $\bar{\beta}$. Hence for all $\varepsilon > 0$, there exists $\beta = \psi_1^{-1} \circ \bar{\beta} \circ \psi_2$, such that

$$\mathcal{P}\{|x| \le \beta(\|x_0\|, t - t_0)\} \ge 1 - \varepsilon, t \in [t_{0,}\tau_0), x_0 \in \mathcal{B}^c \tag{5-2-12}$$

Now let us consider the interval $t \in [\tau_0, \infty)$, where $\psi_3(\|x\|) \le \tilde{\psi}_4(|v|)$. Based on *Lemma 5.1.5*, it follows that

$$\mathcal{P}\{\psi_3(\|x\|) \ge \bar{\psi}_4(|v|)\} \le \frac{\tilde{\psi}_4(|v|)}{\bar{\psi}_4(|v|)} = \varepsilon_0, t \in [\tau_0, \infty), x_0 \in \mathcal{B}^c \tag{5-2-13}$$

where $\bar{\psi}_4$ is a $\mathcal{K}$ function. By choosing $\bar{\psi}_4$ we can make $\varepsilon_0 < \varepsilon$. Since ψ_3^{-1} is of class $\mathcal{K}_\infty$, we can yield

$$\mathcal{P}\{\|x\| \le \psi_3^{-1} \circ \bar{\psi}_4(|v|)\} \ge 1 - \varepsilon_0, t \in [\tau_0, \infty), x_0 \in \mathcal{B}^c \tag{5-2-14}$$

Define $\gamma = \psi_3^{-1} \circ \bar{\psi}_4$ leading to

$$\mathcal{P}\{\|x\| \le \gamma(|v|)\} \ge 1 - \varepsilon_0, t \in [\tau_0, \infty), x_0 \in \mathcal{B}^c \tag{5-2-15}$$

Combined with (5-2-12),

$$\mathcal{P}\{\|x\| \le \beta(|x_0|, t - t_0) + \gamma(|v|)\} \ge \max\{1 - \varepsilon, 1 - \varepsilon_0\} = 1 - \varepsilon_0,$$
$$t \in [t_0, \infty), x_0 \in \mathcal{B}^c \tag{5-2-16}$$

Case 2. $x_0 \in \mathcal{B}$

In this case, $\tau_0 = t_0$. Then $\mathcal{P}\{t \in [\tau_0, \infty)\} = \mathcal{P}\{t \in [t_0, \infty)\} = 1$. Following the proof of Case 1, we know that (5-2-15) still holds, and then

$$\mathcal{P}\{\|x\| \le \beta(\|x_0\|, t - t_0) + \gamma(|v|)\} \ge \mathcal{P}\{\|x\| \le \gamma(|v|)\} \ge 1 - \varepsilon_0,$$
$$t \in [t_0, \infty), x_0 \in \mathcal{B} \tag{5-2-17}$$

To sum up, by (5-2-16) and (5-2-17) we have

$$\mathcal{P}\{\|x\| \le \beta(\|x_0\|, t - t_0) + \gamma(|v|)\} \ge 1 - \varepsilon_0$$
$$t \in [t_0, \infty], x_0 \in \mathcal{R}^n \tag{5-2-18}$$

which yields system (5-1-1) is stochastic input-to-state stable.

Now, on the basis of *Theorem 5.2.1*, let us turn our attention to the finite convergence and give sufficient conditions of finite-time stochastic input-to-state stability for system (5-1-1). This can be accomplished by making the stochastic settling time finite.

Theorem 5.2.2

System (5-1-1) is finite-time stochastic input-to-state stable if there is a stochastic input-to-state stability-Lyapunov function V, and $\mathcal{K}_\infty$ functions $\psi_1, \psi_2, \psi_3, \psi_4$ such that for all $x \in \mathcal{R}^n, v \in L_\infty^m$ and $t \geq t_0$,

(i) $\psi_1(\|x\|) \leq V(t,x) \leq \psi_2(\|x\|)$ (5-2-19a)

(ii) $\mathcal{L}V(t,x) \leq -\psi_3(\|x\|) + \psi_4(|v|)$ (5-2-19b)

(iii) $\int_0^\epsilon \frac{1}{\psi_3(s)} ds < +\infty, \forall \epsilon \in [0,+\infty)$ (5-2-19c)

Proof

Condition (5-2-19) implies that there exists a function $\eta(V) = \int_0^V \frac{1}{\psi_3(s)} ds, V \in [0,\infty)$. Applying *Lemma 5.1.4* along with system (5-1-1), we have

$$d\eta(V(t,x)) = \mathcal{L}\eta(V(t,x))dt + \frac{d\eta}{dV}\frac{\partial V}{\partial x} h dw \tag{5-2-20}$$

then for all $t \geq t_0$

$$\eta(V(t,x)) = \eta(V(t_0,x_0)) + \int_{t_0}^t \mathcal{L}\eta(V(s,x(s)))ds + \int_{t_0}^t \frac{d\eta}{dV}\frac{\partial V}{\partial x} h dw \tag{5-2-21}$$

Let $t_k = \inf\{s \geq t_0 : \beta(\|x_0\|, s - t_0) < 1/k, k \in \{1, 2, 3, \cdots\}\}$ to be an increasing stop time sequence. If t is replaced by t_k in the above, the stochastic integral in (5-2-21) defines a martingale [143], which means when we take expectation, the second integral should be zero, i.e.

$$\mathbb{E}(\eta(V(t_k, x(t_k)))) = \mathbb{E}(\eta(V(t_0,x_0))) + \mathbb{E}\left(\int_{t_0}^{t_k} \mathcal{L}\eta(V(s,x(s)))ds\right) \tag{5-2-22}$$

When $t \leq t_k$, according to *Lemma 5.1.3*,

$$\mathcal{L}(\eta(V(t,x))) = \frac{d\eta}{dV}\mathcal{L}(V(t,x)) - \frac{d\psi_3}{dV}\frac{1}{2\psi_3^2} trace\left\{\left(\frac{\partial V}{\partial x}h\right)^T \left(\frac{\partial V}{\partial x}h\right)\right\} \tag{5-2-23}$$

Since $\frac{d\eta}{dV} = \frac{1}{\psi_3}$ and $\frac{d\psi_3}{dV} > 0$, which means $\frac{d\psi_3}{dV}\frac{1}{2\psi_3^2} trace\left\{\left(\frac{\partial V}{\partial x}h\right)^T \left(\frac{\partial V}{\partial x}h\right)\right\} > 0$, we can easily find

$$\mathbb{E}\left[\mathcal{L}\left(\eta\left(V(t,x)\right)\right)\right] < \mathbb{E}\left[\frac{1}{\psi_3}\mathcal{L}\left(V(t,x)\right)\right] \leq -1 \tag{5-2-24}$$

then we have

$$\mathbb{E}(\eta(V(t_k, x(t_k)))) - \mathbb{E}(\eta(V(t_0, x_0))) = \mathbb{E}(\int_{t_0}^{t_k} \mathcal{L}\eta\left(V\big(s, x(s)\big)\right) ds))$$

$$< E(\int_{t_0}^{t_k}(-1)ds) = t_0 - t_k \quad (5\text{-}2\text{-}25)$$

Considering $\mathbb{E}(\eta(V(t_k, x(t_k)))) \geq 0$, we get

$$t_k \leq t_0 + \mathbb{E}(\eta(V(t_0, x_0))) \quad (5\text{-}2\text{-}26)$$

Let $k \to \infty$, we have $t_k \to T_0(t_0, x_0, v)$.Thus

$$T_0(t_0, x_0, v) \leq t_0 + \mathbb{E}(\eta(V(t_0, x_0))) < \infty \quad (5\text{-}2\text{-}27)$$

which implies the system is stochastic settling time is finite. Combined with *Theorem 5.2.1*, system (5-1-1) is finite-time stochastic input-to-state stable.

5.3 Robust fault estimation for quadratic inner-bounded nonlinear system

In last section, sufficient conditions for stochastically input-to-state stability and finite-time stochastically input-to-state stability are provided and proved. Based on the developed criteria, UIO-based fault estimation technique is to be designed for quadratic inner-bounded nonlinear stochastic system.

Consider the following stochastic nonlinear system in the form of differential equation:

$$\begin{cases} dx(t) = (Ax(t) + Bu(t) + B_d d(t) + B_f f(t) + g(x(t)))\, dt + Wx(t)dw(t) \\ y(t) = Cx(t) + Du(t) + D_f f(t) + Gw(t) \end{cases}$$

(5-3-1)

where $x(t) \in \mathcal{R}^n$ represents the state vector; $u(t) \in \mathcal{R}^m$ stands for control input vector and $y(t) \in \mathcal{R}^p$ is measurement output vector; $d(t) \in L_\infty^{l_d}$ is unknown input vector; $f(t) \in \mathcal{R}^{l_f}$ represents the means of the faults (e.g., actuator faults and/or sensor faults); $g\big(x(t)\big): \mathcal{R}^n \longrightarrow \mathcal{R}^n$ is a continuous function satisfying $g(0) = 0$; $w(t)$ is a standard one-dimensional Brownian motions with $\mathbb{E}[w(t)] = 0$ and $\mathbb{E}[w^2(t)] = t$; A, B, C, D, B_d, B_f, D_f, W and G are known coefficient matrices with appropriate dimensions. We assume that in system (5-3-1), $\mathbb{E}[\|x(t)\|] < \infty$. In this section, the main goal is to design a robust unknown input observer for system (5-3-1) to estimate system states and the means of considered faults simultaneously. In the rest of the section, the symbol t in vectors will be omitted for the simplicity of presentation.

The means of the faults concerned are assumed either to be incipient or abrupt, which generally exist in industrial processes. Therefore, the second-order derivatives of their means should be zero piecewise. For faults whose second order derivatives of the means are not zero but bounded signals, the bounded signals could be regarded as a part of unknown inputs d. Moreover, $B_d = [B_{d1}\ \ B_{d2}]$, $d = [d_1\ \ d_2]^T$, $d_1 \in \mathcal{R}^{l_{d1}}$ and $d_2 \in \mathcal{R}^{l_{d2}}$. We assume that d_1 rather than d_2 can be decoupled, which means B_{d1} is of full column rank whereas B_d is not.

Assumption 5.3.1

For all $x \in \mathcal{R}^n$, $g(x)$ satisfies the following conditions:

(i) $\|g(x)\| < c(1 + \|x\|)$ (5-3-2)

(ii) $\|g(x_1) - g(x_2)\|^2 \leq \rho_1 \|x_1 - x_2\|^2 + \rho_2\langle x_1 - x_2, g(x_1) - g(x_2)\rangle$ (5-3-3)

where $\rho_1, \rho_2 \in \mathcal{R}$, $c > 0$.

Remark 5.3.1

In *Assumption 5.3.1*, condition (ii) implies $g(x)$ is quadratic inner-bounded [147]. Unlike the well-known Lipschtiz condition, the constants ρ_1, ρ_2 can be positive, negative or zero. In addition, if $g(x)$ is Lipschitz, then it is also quadratic inner-bounded with $\rho_1 > 0$ and $\rho_2 = 0$. Thus, quadratic inner-bounded condition provides a less conservative condition than Lipschitz one. According to *Lemma 5.1.1*, *Assumption 5.3.1* can ensure that for any $x_0 \in \mathcal{R}^n$, system (5-3-1) has a path-wise strong solution.

In order to estimate the trends of system states and faults simultaneously, an augmented plant of system (5-3-1) can be constructed as follows:

$$\begin{cases} d\bar{x} = [\bar{A}\bar{x} + \bar{B}u + \bar{B}_d d + \bar{g}(x)]dt + \bar{W}\bar{x}dw \\ y = \bar{C}\bar{x} + Du + Gw \end{cases} \tag{5-3-4}$$

where

$$\bar{n} = n + 2l_f,$$

$$\bar{x} = \begin{bmatrix} x^T & df/dt^T & f^T \end{bmatrix}^T \in \mathcal{R}^{\bar{n}},$$

$$\bar{A} = \begin{bmatrix} A & 0 & B_f \\ 0 & 0 & 0 \\ 0 & I_{l_f} & 0 \end{bmatrix} \in \mathcal{R}^{\bar{n}\times\bar{n}}$$

$$\bar{B} = [B^T \quad 0 \quad 0]^T \in \mathcal{R}^{\bar{n} \times m},$$

$$\bar{B}_d = [B_d^T \quad 0 \quad 0]^T \in \mathcal{R}^{\bar{n} \times l_d},$$

$$\bar{g}(x) = [g(x)^T \quad 0 \quad 0]^T \in \mathcal{R}^{\bar{n}},$$

$$\bar{W} = \begin{bmatrix} W & 0 & 0 \\ 0 & 0 & 0 \\ 0 & 0 & 0 \end{bmatrix} \in \mathcal{R}^{\bar{n} \times \bar{n}},$$

and

$$\bar{C} = [C \quad 0 \quad D_f] \in \mathcal{R}^{p \times \bar{n}}$$

Consider the following unknown input observer in the form of

$$\begin{cases} d\bar{z} = [R\bar{z} + T\bar{B}u + (K_1 + K_2)(y - Du) + T\bar{g}(\hat{x})]dt \\ \hat{\bar{x}} = \bar{z} + H(y - Du) \end{cases} \tag{5-3-5}$$

where $\bar{z} \in \mathcal{R}^{\bar{n}}$ is the state of observer, $\hat{\bar{x}} \in \mathcal{R}^{\bar{n}}$ is the estimation of $\bar{x}$ which is composed of the system states and the concerned fault trends. In this way, the unmeasurable states and fault trends can be estimated provided that the estimated state vector $\hat{\bar{x}}$ is available. The observer parameters of R, T, K_1, K_2, H need to be designed.

Let

$$\bar{e} = \bar{x} - \hat{\bar{x}} = (I_{\bar{n}} - H\bar{C})\bar{x} - \bar{z} - HGw \tag{5-3-6}$$

$$\tilde{g}(x) = \bar{g}(x) - \bar{g}(\hat{x}) \tag{5-3-7}$$

Subtracting (5-3-5) from (5-3-4), the state estimation error system can be characterized as:

$$\begin{aligned} d\bar{e} &= (I_{\bar{n}} - H\bar{C})\, d\bar{x} - d\bar{z} - HGdw \\ &= \{(I_{\bar{n}} - H\bar{C})\, [\bar{A}\bar{x} + \bar{B}u + \bar{B}_d d + \bar{g}(x)] - R\bar{z} - T\bar{B}u - (K_1 + K_2)(y - Du) \\ &\quad -T\bar{g}(\hat{x})\}dt + (I_{\bar{n}} - H\bar{C})\bar{W}\bar{x}dw - HGdw \\ &= \{(I_{\bar{n}} - H\bar{C})\bar{A}\bar{x} - K_1\bar{C}\bar{x} - K_1Gw + (I_{\bar{n}} - H\bar{C})\bar{B}u + (I_{\bar{n}} - H\bar{C})\bar{B}_d d \\ &\quad +(I_{\bar{n}} - H\bar{C})\bar{g}(x) - R\bar{z} - T\bar{B}u - K_2(y - Du) - T\bar{g}(\hat{x})\}dt \\ &\quad +(I_{\bar{n}} - H\bar{C})\bar{W}\bar{x}dw - HGdw \\ &= \{[(I_{\bar{n}} - H\bar{C})\bar{A} - K_1\bar{C}]\bar{x} - R\hat{\bar{x}} + [(I_{\bar{n}} - H\bar{C}) - T]\bar{B}u + (I_{\bar{n}} - H\bar{C})\bar{B}_{d1}d_1 \end{aligned}$$

$$+(I_{\bar{n}} - H\bar{C})\bar{B}_{d2}d_2 + [(I_{\bar{n}} - H\bar{C})\bar{g}(x) - T\bar{g}(\hat{x})]$$

$$+(HR - K_2)(y - Du) - K_1 Gw\}dt + (I_{\bar{n}} - H\bar{C})\bar{W}\bar{x}dw - HGdw$$

$$= [R\bar{e} + T\bar{B}_{d2}d_2 + T\tilde{g}(x) - K_1 Gw]dt + \widetilde{W}\tilde{x}dw \tag{5-3-8}$$

where $\widetilde{W} = [T\bar{W} \quad -HG]$, $\tilde{x} = [\bar{x}^T \quad 1]^T \in \mathcal{R}^{\bar{n}+1}$, if the following conditions should be held:

$$(I_{\bar{n}} - H\bar{C})\bar{B}_{d1} = 0 \tag{5-3-9}$$

$$R = \bar{A} - H\bar{C}\bar{A} - K_1\bar{C} \tag{5-3-10}$$

$$T = I_{\bar{n}} - H\bar{C} \tag{5-3-11}$$

$$K_2 = RH \tag{5-3-12}$$

For error dynamic (5-3-8), our main problem is to design H, R, T, K_1, K_2 such that $\bar{e}$ is bounded in presence of bounded unknown inputs, and converge in finite time, which can be expressed by finite-time stochastic input-to-state stability of system (5-3-8). To meet this objective, the following assumptions are given:

Assumption 5.3.2

$$\mathrm{rank}(CB_{d1}) = \mathrm{rank}(B_{d1});$$

Assumption 5.3.3

$$\begin{bmatrix} A & B_f & B_{d1} \\ C & D_f & 0 \end{bmatrix} \text{ is of full column rank;}$$

Assumption 5.3.4

$$\mathrm{rank}\begin{bmatrix} sI_n - A & B_{d1} \\ C & 0 \end{bmatrix} = n + l_{d1}.$$

Remark 5.3.3

According to Chapter 3, *Assumption 5.3.2* is to guarantee that Equation (5-3-9) can be solved, and a special solution is

$$H^* = \bar{B}_{d1}[(\bar{C}\bar{B}_{d1})^T(\bar{C}\bar{B}_{d1})]^{-1}(\bar{C}\bar{B}_{d1})^T \tag{5-3-13}$$

while *Assumptions 5.3.3* and *5.3.4* are to ensure $(\bar{C}, \bar{A}_1)$ to be an observable pair, where $\bar{A}_1 = \bar{A} - H\bar{C}\bar{A}$. Based on these assumptions, we can decouple d_1 by solving H from condition (5-3-9), and assign the poles of R arbitrarily. The next step is to ensure the error dynamic is stochastic input-to-state stable with respect to d_2 and Brownian motions, which means $\bar{e}$ will be bounded if un-decoupled unknown inputs are bounded. For this purpose, we shall introduce the following *Theorem 5.3.1*.

Theorem 5.3.1

For system (5-3-1), there exists a robust observer in the form of (5-3-5) yields estimation error dynamic system (5-3-8) that is stochastic input-to-state stable and satisfies $\mathbb{E}(\|\bar{e}\|_{Tf}) \leq \mathbb{E}(\bar{\gamma}|v|_{Tf})$, if there exist positive definite matrices $P$and Q, matrix Y and positive real number τ, such that

$$\begin{bmatrix} \Lambda & PT+\tau\rho_2 I_{2\bar{n}} & PT\bar{B}_{d2} & -YG & 0 \\ * & -2\tau I_{2\bar{n}} & 0 & 0 & 0 \\ * & * & -\bar{\gamma}_1^2 I_{l_{d_2}} & 0 & 0 \\ * & * & * & -\bar{\gamma}_1^2 & 0 \\ * & * & * & * & \widetilde{W}^T P\widetilde{W} - \bar{\gamma}_1^2 I_{\bar{n}+1} \end{bmatrix} < 0 \qquad (5\text{-}3\text{-}14)$$

where $\Lambda = \bar{A}_1^T P + P\bar{A}_1 - \bar{C}^T Y^T - Y\bar{C} + 2\tau\rho_1 I_{\bar{n}} + Q$, $\bar{A}_1 = T\bar{A}$, $Y = PK_1$, ρ_1 and ρ_2 are given real numbers, $\bar{\gamma}$ and $\bar{\gamma}_1$ are positive scalars, $\bar{\gamma}_1 = \lambda_{min}(Q)\bar{\gamma}$.

Proof

Choose Lyapunov function $V(\bar{e}) = \bar{e}^T P\bar{e}$. It is not hard to obtain that:

$$\lambda_{min}(P)\|\bar{e}\|^2 \leq V(\bar{e}) \leq \lambda_{max}(P)\|\bar{e}\|^2 \qquad (5\text{-}3\text{-}15)$$

which implies we can define $\psi_1 = \lambda_{min}(P)\|\bar{e}\|^2$, ψ_2=$\lambda_{max}(P)\|\bar{e}\|^2$ in Theorem 5.2.1. Then, according to (5-1-8), $\mathcal{L}V(\bar{e})$ can be calculated as:

$$\begin{aligned} \mathcal{L}V(\bar{e}) &= \left[\frac{\partial V(\bar{e})}{\partial \bar{e}}\right]^T [R\bar{e} + T\bar{B}_{d2}d_2 + T\tilde{g}(x) - K_1 G w] + \frac{1}{2} trace\left\{\tilde{x}^T \widetilde{W}^T \frac{\partial^2 V(\bar{e})}{\partial x^2}\widetilde{W}\tilde{x}\right\} \\ &= \bar{e}^T(R^T P + PR)\bar{e} + 2\bar{e}^T PT\bar{B}_{d2}d_2 + 2\bar{e}^T PT\tilde{g} - 2\bar{e}^T YGw + \tilde{x}^T\widetilde{W}^T P\widetilde{W}\tilde{x} \end{aligned}$$

(5-3-16)

Assumption 5.3.1 implies that for any positive scalar τ, we have

$$2\tau(\rho_1\bar{e}^T\bar{e} + \rho_2\bar{e}^T\tilde{g} - \tilde{g}^T\tilde{g}) \geq 0 \qquad (5\text{-}3\text{-}17)$$

Adding (5-3-17) to the right side of (5-3-16) , and then adding and subtracting $\bar{e}^T Q\bar{e}$, we can derive:

$$\mathcal{L}V(\bar{e}) \leq \bar{e}^T(\bar{A}_1^T P + P\bar{A}_1 - \bar{C}^T Y^T - Y\bar{C} + 2\tau\rho_1 I_{\bar{n}} + Q)\bar{e} - \bar{e}^T Q\bar{e} - 2\tau\tilde{g}^T\tilde{g}$$

$$+2\bar{e}^T(PT + \tau\rho_2 I_{2\bar{n}})\tilde{g} \ +2\bar{e}^T PT\bar{B}_{d2}d_2 - 2\bar{e}^T YGw + \tilde{x}^T\widetilde{W}^T P\widetilde{W}\tilde{x}$$

$$-\bar{\gamma}_1^2 v^T v + \bar{\gamma}_1^2 v^T v$$

$$= [\bar{e}^T \quad \tilde{g}^T \quad v^T]\ \Psi \begin{bmatrix} \bar{e} \\ \tilde{g} \\ v \end{bmatrix} - \bar{e}^T Q\bar{e} + \bar{\gamma}_1^2 v^T v \tag{5-3-18}$$

where

$$\Psi = \begin{bmatrix} \Lambda & PT + \tau\rho_2 I_{2\bar{n}} & PT\bar{B}_{d2} & -YG & 0 \\ * & -2\tau I_{2\bar{n}} & 0 & 0 & 0 \\ * & * & -\bar{\gamma}_1^2 I_{l_{d_2}} & 0 & 0 \\ * & * & * & -\bar{\gamma}_1^2 & 0 \\ * & * & * & * & \widetilde{W}^T P\widetilde{W} - \bar{\gamma}_1^2 I_{\bar{n}+1} \end{bmatrix}$$

$v = [d_2^T \quad w^T \quad \tilde{x}^T]^T$, and $\Lambda = (\bar{A}_1^T P + P\bar{A}_1 - \bar{C}^T Y^T - Y\bar{C} + 2\tau\rho_1 I_{\bar{n}} + Q)$. LMI (5-3-14) implies that $\Psi < 0$, indicating

$$\mathcal{L}V(\bar{e}) \leq -\bar{e}^T Q\bar{e} + \bar{\gamma}_1^2 v^T v \tag{5-3-19}$$

Since Q is positive, it is easy to find a scale $\bar{\lambda} > 0$ such that

$$\begin{aligned} \mathcal{L}V(\bar{e}) &\leq -\bar{\lambda}\, \|\bar{e}\|^2 + \bar{\gamma}_1^2 \|v\|^2 \\ &\leq -\bar{\lambda}\, \|\bar{e}\|^2 + \bar{\gamma}_1^2 |v|^2 \end{aligned} \tag{5-3-20}$$

According to *Theorem 5.2.1*, dynamic system (5-3-8) is stochastic input-to-state stable with $\psi_3(\bar{e}) = \bar{\lambda}\|\bar{e}\|^2$ and $\psi_4(|v|) = \bar{\gamma}_1^2|v|^2$.

Now we move on to attenuate the influences of v on estimation error. Define the following performance index of the error dynamic

$$\Gamma = \mathbb{E}\left(\int_0^{Tf}(\bar{e}^T Q\bar{e} - \bar{\gamma}_1^2 v^T v)dt\right) \tag{5-3-21}$$

Then adding and subtracting $\mathbb{E}(\int_0^{Tf} \mathcal{L}V(\bar{e})dt)$, yields:

$$\Gamma = \mathbb{E}\left(\int_0^{Tf}\left(\bar{e}^T Q\bar{e} - \bar{\gamma}_1^2 v^T v + \mathcal{L}V(\bar{e})\right)dt\right) - \mathbb{E}\left(\int_0^{Tf}\mathcal{L}V(\bar{e})dt\right)$$

$$\leq \mathbb{E}(\int_0^{Tf}[\bar{e}^T \quad \tilde{g}^T \quad v^T]\ \Psi \begin{bmatrix} \bar{e} \\ \tilde{g} \\ v \end{bmatrix})dt) \ - \mathbb{E}(\int_0^{Tf}\mathcal{L}V(\bar{e})dt) \tag{5-3-22}$$

Under zero initial condition $\bar{e}(0) = 0$,

$$\mathbb{E}\left(\int_0^{Tf} \mathcal{L}V(\bar{e})dt\right) = \mathbb{E}\big(\bar{e}^T(Tf)P\bar{e}(Tf)\big) - \mathbb{E}\big(\bar{e}^T(0)P\bar{e}(0)\big)$$

$$= \mathbb{E}(V(\bar{e})) > 0 \tag{5-3-23}$$

thus $\Psi < 0$ indicates $\Gamma < 0$, leading to

$$\mathbb{E}(\int_0^{Tf} \bar{e}^T Q\bar{e}dt) \leq \mathbb{E}(\int_0^{Tf} \bar{\gamma}_1^2 v^T v dt) \tag{5-3-24}$$

which means

$$\sqrt{\lambda_{min}(Q)}\mathbb{E}(\|\bar{e}\|_{Tf}) \leq \mathbb{E}(\bar{\gamma}_1\|v\|_{Tf}) \tag{5-3-25}$$

Then we have

$$\mathbb{E}(\|\bar{e}\|_{Tf}) \leq \mathbb{E}(\bar{\gamma}|v|_{Tf}) \tag{5-3-26}$$

where $\bar{\gamma} = \frac{\bar{\gamma}_1}{\lambda_{min}(Q)}$.

Theorem 5.3.1 can be applied to prove the asymptotic stability of the estimation error as well, by letting the disturbances be zero. Such a result holds because the stochastic input-to-state stability implies global asymptotic stability in probability which is a special case that the input is zero [130]. In other words, a stochastic input-to-state stable state estimator behaves like an asymptotically stable observer in the absence of system and measurement noises.

Now we are in the position to study the finite-time stochastic input-to-state stability of (5-3-8), which implies the stochastic setting time is finite.

Theorem 5.3.2

For system (5-3-1), there exists a robust observer in the form of (5-3-5) yields estimation error dynamic system (5-3-8) that is finite-time stochastic input-to-state stable and satisfies $\mathbb{E}(\|\bar{e}\|_{Tf}) \leq \mathbb{E}(\bar{\gamma}\|v\|_{Tf})$, if there exist positive definite matrices P and Q, positive real number τ, and matrix Y, such that LMI (5-3-14) holds.

Proof

$\forall\ \varepsilon_e$, we can find positive scalar $k_0 = \varepsilon_e\,\bar{\gamma}_1^2 v^T v$. When $\|\bar{e}\| \leq k_0$, Based on *Lemma 5.1.5*

$$\mathcal{P}\{\|\bar{e}\| \geq \bar{\gamma}_1^2 v^T v\} \leq \frac{\mathbb{E}(\|\bar{e}\|)}{\bar{\gamma}_1^2 v^T v} \leq \frac{k_0}{\bar{\gamma}_1^2 v^T v} = \varepsilon_e \tag{5-3-27}$$

which means

$$\mathcal{P}\{\|\bar{e}\| \leq \bar{\gamma}_1^2 v^T v\} \geq 1 - \varepsilon_e \tag{5-3-28}$$

According to (5-1-11), (5-3-8) is finite-time stochastic input-to-state stable. In the following proof, we consider the case $\|\bar{e}\| > k_0$. From *Theorem 5.3.1*, it has been obtained that $\mathcal{L}V(\bar{e}) \leq -\bar{e}^T Q \bar{e} + \bar{\gamma}_1^2 v^T v$. Thus for $0 < \theta < \frac{1}{2}$, we can derive

$$\begin{aligned}\mathcal{L}V(\bar{e}) &\leq -\frac{\lambda_{min}(Q)}{\lambda_{max}(P)} \bar{e}^T P \bar{e} + \bar{\gamma}_1^2 v^T v \\ &= -\frac{\lambda_{min}(Q)}{\lambda_{max}(P)} (\bar{e}^T P \bar{e})^{\theta} (\bar{e}^T P \bar{e})^{1-\theta} + \bar{\gamma}_1^2 v^T v \\ &\leq -\frac{\lambda_{min}(Q)\lambda_{min}^{1-\theta}(P)}{\lambda_{max}(P)} (\bar{e}^T P \bar{e})^{\theta} (\|\bar{e}\|)^{2(1-\theta)} + \bar{\gamma}_1^2 v^T v \end{aligned} \tag{5-3-29}$$

Then we have

$$\begin{aligned}\mathcal{L}V(\bar{e}) &= -\frac{\lambda_{min}(Q)\lambda_{min}^{1-\theta}(P)}{\lambda_{max}(P)} \left[(\bar{e}^T P \bar{e})^{\theta} (\|\bar{e}\|)^{2(1-\theta)}\right] + \bar{\gamma}_1^2 v^T v \\ &\leq -\frac{\lambda_{min}(Q)\lambda_{min}^{1-\theta}(P)}{\lambda_{max}(P)} (\bar{e}^T P \bar{e})^{\theta} (\|\bar{e}\|)^{2(1-\theta)} + \bar{\gamma}_1^2 v^T v \end{aligned} \tag{5-3-30}$$

$0 < \theta < \frac{1}{2}$ implies $1 < 2(1-\theta) < 2$. Thus $(\|\bar{e}\|)^{2(1-\theta)}$ is convex, according to *lemma 5.1.4*,

$$(\|\bar{e}\|)^{2(1-\theta)} \geq k_0^{2(1-\theta)} \tag{5-3-31}$$

Then

$$\mathcal{L}V(\bar{e}) \leq -\frac{\lambda_{min}(Q)\lambda_{min}^{1-\theta}(P)}{\lambda_{max}(P)} k_0^{2(1-\theta)} (\bar{e}^T P \bar{e})^{\theta} + \bar{\gamma}_1^2 v^T v \tag{5-3-32}$$

Define $\bar{\lambda}_0 = \frac{\lambda_{min}(Q)\lambda_{min}^{1-\theta}(P)}{\lambda_{max}(P)} k_0^{2(1-\theta)}$, it is not hard to find $\bar{\lambda}_0 > 0$. Then we have:

$$\mathcal{L}\bar{V}(\bar{e}) \leq -\bar{\lambda}_0 V^{\theta}(\bar{e}) + \bar{\gamma}_1 |v|^2 \tag{5-3-33}$$

If we define $\psi_3 = \bar{\lambda}_0 [V(\bar{e})]^{\theta}$, it can be verified that

$$\int_0^{\epsilon} \frac{1}{\psi_3(V)} dV = \int_0^{\epsilon} \frac{1}{\bar{\lambda}_0 V^{\theta}} dV = \frac{\epsilon^{1-\theta}}{\bar{\lambda}_0(1-\theta)} < +\infty \tag{5-3-34}$$

According to *Theorem 5.2.2*, error dynamic (5-3-8) is finite-time **s**tochastic input-to-state stable by setting $\psi_3 = \bar{\lambda}_0[V(\bar{e})]^{\theta}$ and $\psi_4(|v|) = \bar{\gamma}_1|v|^2$.

Theorem 5.3.1 and *5.3.2* provide sufficient conditions for the existence of a robust UIO for system (5-3-1) in terms of a given estimation performance index. The observer gains can be decided by solving LMI (5-3-14) to make the estimation error decrease to a bounded value depending on unknown inputs and only. In addition, the performance index can make the bound as small as possible to achieve robustness. LMI (5-3-14) can guarantee both stochastic input-to-state stability and finite-time stochastic input-to-state stability of the error dynamics. Different claims are made here to show how it satisfies the corresponding conditions.

Based on the above results, we can summarize the procedure to design the UIO for system (5-3-1) as follows.

Procedure 5.3.1 *Finite-time UIO-based fault estimation for stochastic quadratic inner-bounded nonlinear system*

i) Construct an augmented system in the form of (5-3-4).
ii) Solve H from Equation (5-3-9).
iii) Solve the LMI (5-3-14) to obtain the matrices P and Y, and calculate the gain $K_1 = P^{-1}Y$.
iv) Calculate the other gain matrices R, T and K_2 following the formulae (5-3-10) to (5-3-12), respectively.
v) Obtain the augmented estimate $\hat{\bar{x}}$ by implementing UIO (5-3-5), leading to the simultaneous estimates of state and fault as $\hat{x} = \begin{bmatrix} I_n & 0_{n\times 2l_f} \end{bmatrix}\hat{\bar{x}}$ and $\hat{f} = \begin{bmatrix} 0_{n\times(n+l_f)} & I_{l_f} \end{bmatrix}\hat{\bar{x}}$, respectively.

5.4 Robust fault estimation of Takagi-Sugeno stochastic system

In this section, robust UIO-based fault estimation is to be developed for T-S fuzzy systems subject to faults, partially decoupled unknown inputs, and stochastic Brownian motions, which can be implemented on a variety of real nonlinear plants.

Consider stochastic T-S fuzzy models suffering from faults and unknown inputs in the form of It$\hat{o}$-type differential equations as follows:

IF μ_1 is M_{1i} and $\dots\mu_q$ is M_{qi}, THEN

$$\begin{cases} dx(t) = [A_i x(t) + B_i u(t) + B_{di} d(t) + B_{fi} f(t)]dt + W_i x(t) dw(t) \\ y(t) = C_i x(t) + D_{fi} f(t) + D_{di} d_w(t) \end{cases} \tag{5-4-1}$$

where $x(t) \in \mathcal{R}^n$ represents state vector with initial value of $x_0 \in \mathcal{R}^n$ at initial time t_0; We assume that there exists a pre-designed controller such that $\mathbb{E}[\|x(t)\|] < \infty$; the $w(t)$ is a standard one-dimensional Brownian motion on the complete probability space $(\Omega, \mathcal{F}, \{\mathcal{F}_t\}_{t\geq t_0} \mathcal{P})$, with Ω being a sample space, $\mathcal{F}$ being a σ-field, $\{\mathcal{F}_t\}_{t\geq t_0}$ being a filtration and $\mathcal{P}$ being a probability measure. $w(t)$ satisfies $\mathbb{E}[w(t)] = 0$ and $\mathbb{E}[w^2(t)] = t$. $u(t) \in \mathcal{R}^m$ stands for control input vector and $y(t) \in \mathcal{R}^p$ is measurement output vector; $d(t) \in \mathcal{R}^{l_{d_u}}$, $d_w(t) \in \mathcal{R}^{l_{d_w}}$ are bounded unknown input vectors from plant and sensors, respectively; $f(t) \in \mathcal{R}^{l_f}$ includes the means of faults from both actuators and sensors with the same assumption of those in section 5.3. $i = 1, 2, \dots r$, and r is the total number of local models, M_{ji} are fuzzy sets and decision vector μ involves all individual premise variables μ_j, $j = 1, 2, \dots q$. A_i, B_i, B_{di}, B_{fi}, C_i, D_{di}, D_{fi} and $W_i$can be obtained by linearization or identification of nonlinear systems. In the rest of this section, the symbol t in vectors will be omitted for the simplicity of presentation. By using the standard fuzzy blending method, the global model of system (5-4-1) can be inferred as:

$$\begin{cases} dx = \sum_{i=1}^{r} h_i(\mu) \left[(A_i x + B_i u + B_{di} d + B_{fi} f)dt + W_i x dw\right] \\ y = \sum_{i=1}^{r} h_i(\mu) \left(C_i x + D_{fi} f + D_{di} d_w\right) \end{cases} \tag{5-4-2}$$

where $h_i(\mu)$ are weighting functions, following the convex sum properties: $\sum_{i=1}^{r} h_i(\mu) = 1$ and $0 \leq h_i(\mu) \leq 1$.

As aforementioned that unknown inputs usually consist of parameter perturbations, exogenous disturbances, measurement errors, and other uncertainties. A T-S fuzzy representation is an approximate of the real model, hence the modelling errors can also be regarded as a part of unknown inputs d and d_w. In this way, plant (5-4-2) can describe a wide range of nonlinear engineering systems in presence of faults and extra disturbances.

In order to estimate the means of faults and system states at the same time, an auxiliary system is constructed as follows, by considering the faults as augmented system states:

$$\begin{cases} d\bar{x} = \sum_{i=1}^{r} h_i(\mu)\,[(\bar{A}_i\bar{x} + \bar{B}_i u + \bar{B}_{di}d)dt + \bar{W}_i\bar{x}dw] \\ y = \sum_{i=1}^{r} h_i(\mu)\,(\bar{C}_i\bar{x} + D_{di}d_w) \end{cases} \tag{5-4-3}$$

where

$$\bar{n} = n + 2l_f,$$

$$\bar{x} = [x^T \quad \dot{f}^T \quad f^T]^T \in \mathcal{R}^{\bar{n}}$$

$$\bar{A}_i = \begin{bmatrix} A_i & 0 & B_{fi} \\ 0 & 0 & 0 \\ 0 & I_{l_f} & 0 \end{bmatrix} \in \mathcal{R}^{\bar{n}\times\bar{n}},$$

$$\bar{B}_i = [B_i^T \quad 0 \quad 0]^T \in \mathcal{R}^{\bar{n}\times m}$$

$$\bar{B}_{di} = [B_{di}^T \quad 0 \quad 0]^T \in \mathcal{R}^{\bar{n}\times l_d}$$

$$\bar{C}_i = [C_i \quad 0 \quad D_{fi}] \in \mathcal{R}^{p\times\bar{n}}$$

$$\bar{W}_i = \begin{bmatrix} W_i & 0 & 0 \\ 0 & 0 & 0 \\ 0 & 0 & 0 \end{bmatrix} \in \mathcal{R}^{\bar{n}\times\bar{n}}$$

To reduce the level of complication for observer design, we can choose any $\bar{C}$ from $\bar{C}_i$ as the output coefficient, and the differences between other local outputs with the selected one are regarded as measurement perturbations. In this way, systems (5-4-3) is equivalent to the following expression:

$$\begin{cases} d\bar{x} = \sum_{i=1}^{r} h_i(\mu)\,[(\bar{A}_i x + \bar{B}_i u + \bar{B}_{di}d)dt + \bar{W}_i\bar{x}dw] \\ y = \sum_{i=1}^{r} h_i(\mu)\,[\bar{C}x + (\bar{C}_i - \bar{C})x + D_{di}d_w] \end{cases} \tag{5-4-4}$$

By letting $d_s = \sum_{i=1}^{r} h_i(\mu)[(\bar{C}_i - \bar{C})\bar{x} + D_{di}d_w]$, system (5-4-4) can be simplified as:

$$\begin{cases} d\bar{x} = \sum_{i=1}^{r} h_i(\mu)[\,(\bar{A}_i\bar{x} + \bar{B}_i u + \bar{B}_{di}d)dt + \bar{W}_i\bar{x}dw] \\ y = \bar{C}\bar{x} + d_s \end{cases} \tag{5-4-5}$$

In system (5-4-5), the component of state vector $\bar{x}$ involves both original state x and fault f. By designing unknown input observer in the following form

$$\begin{cases} \dot{\bar{z}} = \sum_{i=1}^{r} h_i(\mu)[R_i\bar{z} + T\bar{B}_i u + (K_{i1} + K_{i2})y] \\ \hat{\bar{x}} = \bar{z} + Hy \end{cases} \tag{5-4-6}$$

where $\bar{z}$ stands for its state vector and $\hat{\bar{x}}$ is the estimation of $\bar{x}$, simultaneous estimation of x and f can be achieved. Matrices R_i, T, K_{i1} and K_{i2}, $i = 1, 2, \dots r$, are observer gains to be designed such that $\hat{\bar{x}}$ is close enough to $\bar{x}$. Obviously, the global unknown input observer is also a fuzzy aggression of a set of local observers with the same weights of (5-4-2).

Defining estimation error to be $\bar{e} = \bar{x} - \hat{\bar{x}}$, and subtracting (5-4-6) from (5-4-5) leads to the following error dynamic:

$$d\bar{e} = \sum_{i=1}^{r} h_i(\mu) \{\{(\bar{A}_i - H\bar{C}\bar{A}_i - K_{i1}\bar{C})\bar{e} + (\bar{A}_i - H\bar{C}\bar{A}_i - K_{i1}\bar{C} - R_i)\bar{z}$$

$$+[(\bar{A}_i - H\bar{C}\bar{A}_i - K_{i1}\bar{C})H - K_{i2}]y + [(I_{\bar{n}} - H\bar{C}) - T]\bar{B}_i u + (I_{\bar{n}} - H\bar{C})\bar{B}_{di1}d_1$$

$$+(I_{\bar{n}} - H\bar{C})\bar{B}_{di2}d_2 - K_{i1}d_s - H\dot{d}_s\}dt + (I_{\bar{n}} - H\bar{C})\bar{W}_i\bar{x}dw\} \quad (5\text{-}4\text{-}7)$$

If for all $i = 1, 2, \dots r$ the observer gains satisfy the following conditions:

$$(I_{\bar{n}} - H\bar{C})\bar{B}_{di1} = 0 \quad (5\text{-}4\text{-}8)$$

$$R_i = \bar{A}_i - H\bar{C}\bar{A}_i - K_{i1}\bar{C} \quad (5\text{-}4\text{-}9)$$

$$T = I_{\bar{n}} - H\bar{C} \quad (5\text{-}4\text{-}10)$$

$$K_{i2} = R_i H \quad (5\text{-}4\text{-}11)$$

the state estimation error can be reduced to

$$d\bar{e} = \sum_{i=1}^{r} h_i(\mu) \{[R_i\bar{e} + (I_{\bar{n}} - H\bar{C})\bar{B}_{di2}d_2 - K_{i1}d_s$$

$$-H\dot{d}_s]dt + (I_{\bar{n}} - H\bar{C})\bar{W}_i\bar{x}dw\} \quad (5\text{-}4\text{-}12)$$

In order to meet the conditions (5-4-8) to (5-4-11), we have the following assumptions:

(1)rank$\left(\bar{C}(\bar{B}_{d11}\ \ \bar{B}_{d21} \cdots\ \bar{B}_{dr1})\right) = $ rank$\left((\bar{B}_{d11}\ \ \bar{B}_{d21} \cdots\ \bar{B}_{dr1})\right)$;

(2) For $\forall\ i$, $\begin{bmatrix} A_i & B_{fi} & B_{di1} \\ C & D_{fi} & 0 \end{bmatrix}$ is of full column rank;

(3) For $\forall\ i$, rank$\begin{bmatrix} sI_n - A_i & B_{di1} \\ C & 0 \end{bmatrix} = n + l_{di1}$.

According to Chapter 3, the above assumptions are to ensure that for each local model, equation (5-4-8) can be solved, and one solution of H can be obtained as

$$H^* = \bar{B}_M[(\bar{C}\bar{B}_M)^T(\bar{C}\bar{B}_M)]^{-1}(\bar{C}\bar{B}_M)^T \quad (5\text{-}4\text{-}13)$$

where $B_M$is of full column rank, obtained by a non-singular matrix M such that

$$(\bar{B}_{d11}\ \ \bar{B}_{d21} \cdots \ \bar{B}_{dr1})M = (\bar{B}_M\ \ 0) \tag{5-4-14}$$

Moreover, the model is observable. A special solution of (5-4-8), shown as (5-4-13) is used here, as it can already make the design of other observer gains flexible in this chapter. In terms of more flexible requirements, a general solution can be used as $H = \bar{B}_M(\bar{C}\bar{B}_M)^+ + N(I - (\bar{C}\bar{B}_M)(\bar{C}\bar{B}_M)^+)$, where $(\bar{C}\bar{B}_M)^+ = [(\bar{C}\bar{B}_M)^T(\bar{C}\bar{B}_M)]^{-1}(\bar{C}\bar{B}_M)^T$, and N is a compatible matrix of proper dimension.

Under these necessary assumptions, d_1 has been decoupled by settling H, however, d_2, d_s and the Brownian motion still affect the error dynamic. As a good observer should lead to the convergence of error $\bar{e}$, the design of robust fault estimation scheme is converted into attenuating the influences of un-decoupled unknown inputs and the Brownian motion.

For bounded unknown inputs, our target is to design observer gains such that estimation error can be mapped around equilibrium around a certain distance, which is a function of the unknown inputs.

Theorem 5.4.1

For system (5-4-2), there exists a fuzzy unknown input observer in the form of (5-4-6), resulting in a stochastic input-to-state stable error dynamic (5-4-12) which satisfies $\mathbb{E}(\|\bar{e}\|_{Tf}) \leq \mathbb{E}(\bar{\gamma}\|v\|_{Tf})$, if $\forall\ i$, there exist positive definite matrices $P$and $\bar{P}$, matrices Y_i, such that

$$\begin{bmatrix} \Lambda_i & (I_{\bar{n}} - H\bar{C})\bar{B}_{di2} & -Y_i & -PH & 0 \\ * & -\bar{\gamma}^2 I_{l_{d2}} & 0 & 0 & 0 \\ * & * & -\bar{\gamma}^2 I_s & 0 & 0 \\ * & * & * & -\bar{\gamma}^2 I_s & 0 \\ * & * & * & * & \Pi_i \end{bmatrix} < 0 \tag{5-4-15}$$

where $\Lambda_i = I_{\bar{n}} + \bar{A}_{i1}^T P + P\bar{A}_{i1} - \bar{C}^T Y_i^T - Y_i\bar{C} + \bar{P}$, $Y_i = PK_{i1}$ $\bar{A}_{i1} = (I_{\bar{n}} - H\bar{C})\bar{A}_i$, $\Pi_i = \bar{W}_i^T T^T P T \bar{W}_i - \gamma^2 I_{\bar{n}}$ $i = 1,2, \ldots r$, $v = [d_2 \quad d_s \quad \dot{d}_s \quad \bar{x}]$, and $\bar{\gamma}$ is a performance index indicating the level of noise attenuation.

Proof

Based on the *Theorem 5.2.1*, the proof involves establishing a dissipation inequality via a suitable storage function. Here, we choose the function as $V(\bar{e}) = \bar{e}^T P\bar{e}$, and it is not hard to obtain that:

$$\lambda_{min}(P)\|\bar{e}\|^2 \leq V(\bar{e}) \leq \lambda_{max}(P)\|\bar{e}\|^2 \tag{5-4-16}$$

which means it meets (5-2-1). Taking the infinitesimal operator along the state trajectories of dynamic (5-4-12), by using the It$\hat{o}$ formula, $\mathcal{L}V(\bar{e})$ can be calculated as:

$$\begin{aligned}\mathcal{L}V(\bar{e}) &= \textstyle\sum_{i=1}^{r} h_i(\mu)\,[\bar{e}^T P(R_i\bar{e} + T\bar{B}_{di2}d_2 - K_{i1}d_s - H\dot{d}_s) \\ &\quad +(R_i\bar{e} + T\bar{B}_{di2}d_2 - K_{i1}d_s - H\dot{d}_s)^T P\bar{e} + \bar{x}^T\bar{W}_i^T T^T PT\bar{W}_i\bar{x}] \\ &= \textstyle\sum_{i=1}^{r} h_i(\mu)[\,\bar{e}^T\left(\bar{A}_{i1}^T P + P\bar{A}_{i1} - \bar{C}^T Y_i^T - Y_i\bar{C}\right)\bar{e} + 2\bar{e}^T PT\bar{B}_{di2}d_2 \\ &\quad -2\bar{e}^T PK_{i1}d_s - 2\bar{e}^T PH\dot{d}_s + \bar{x}^T\bar{W}_i^T T^T PT\bar{W}_i\bar{x}]\end{aligned} \tag{5-4-17}$$

Adding and subtracting $\bar{e}^T\bar{P}\bar{e} - \bar{\gamma}^2 v^T v$ yields:

$$\mathcal{L}V(\bar{e}) = [\bar{e}^T \quad v^T](\textstyle\sum_{i=1}^{r} h_i(\mu)\,\Psi_i)\begin{bmatrix}\bar{e}\\ v\end{bmatrix} - \bar{e}^T\bar{P}\bar{e} + \bar{\gamma}^2 v^T v \tag{5-4-18}$$

where

$$\Psi_i = \begin{bmatrix}\Theta_i & (I_{\bar{n}} - H\bar{C})\bar{B}_{di2} & -Y_i & -PH & 0\\ * & -\bar{\gamma}^2 I_{l_{d2}} & 0 & 0 & 0\\ * & * & -\bar{\gamma}^2 I_s & 0 & 0\\ * & * & * & -\bar{\gamma}^2 I_s & 0\\ * & * & * & * & \Pi_i\end{bmatrix} \tag{5-4-19}$$

and $\Theta_i = \bar{A}_{i1}^T P + P\bar{A}_{i1} - \bar{C}^T Y_i^T - Y_i\bar{C} + \bar{P}$. LMIs (5-4-15) implies that $\Psi_i < 0$, which means

$$\mathcal{L}V(\bar{e}) \leq -\bar{e}^T\bar{P}\bar{e} + \bar{\gamma}^2 v^T v \tag{5-4-20}$$

Since $\bar{P}$ is positive, a positive scale $\bar{\lambda}$ can be found such that

$$\mathcal{L}V(\bar{e}) \leq -\bar{\lambda}\,\bar{e}^T\bar{e} + \bar{\gamma}^2 v^T v \tag{5-4-21}$$

Therefore, $V(\bar{e})$ is a stochastic input-to-state stability-Lyapunov function with $\psi_3(\bar{e}) = \bar{\lambda}\|\bar{e}\|^2$ and $\psi_4(|v|) = \bar{\gamma}^2|v|^2$. According to the *Theorem 5.2.1*, dynamic (5-4-12) is stochastically input-to-state stable.

We are now in a position to attenuate the influences of v on estimation error. Choose $\bar{\gamma}$ as a performance index, and then we define:

$$\Gamma = \mathbb{E}\left(\int_0^{Tf}(\bar{e}^T\bar{e} - \bar{\gamma}^2 v^T v)dt\right) \tag{5-4-22}$$

It follows that:

$$\Gamma = \mathbb{E}\{\int_0^{Tf}[\bar{e}^T\bar{e} - \bar{\gamma}^2 v^T v + \mathcal{L}V(\bar{e})]dt\} - \mathbb{E}[\int_0^{Tf}\mathcal{L}V(\bar{e})dt]$$

$$= \mathbb{E}\int_0^{Tf}\sum_{i=1}^r h_i(\mu)\,[\,\bar{e}^T(I_{\bar{n}} + \bar{A}_{i1}^T P + P\bar{A}_{i1} - \bar{C}^T Y_i^T - Y_i\bar{C}$$

$$+\bar{P})\bar{e} - \bar{e}^T\bar{P}\bar{e} + 2\bar{e}^T PT\bar{B}_{di2}d_2 - 2\bar{e}^T PK_{i1}d_s$$

$$-2\bar{e}^T PH\dot{d}_s + \bar{x}^T\bar{W}_i^T T^T PT\bar{W}_i\bar{x}]\,dt - \mathbb{E}\int_0^{Tf}\mathcal{L}V(\bar{e})dt$$

$$\leq \mathbb{E}\{\int_0^{Tf}[\bar{e}^T \quad v^T](\sum_{i=1}^r h_i(\mu)\,\Omega_i)\begin{bmatrix}\bar{e}\\ v\end{bmatrix})dt\} - \mathbb{E}[\int_0^{Tf}\mathcal{L}V(\bar{e})dt] \quad (5\text{-}4\text{-}23)$$

where

$$\Omega_i = \begin{bmatrix} \Lambda_i & (I_{\bar{n}} - H\bar{C})\bar{B}_{di2} & -Y_i & -PH & 0 \\ * & -\bar{\gamma}^2 I_{l_{d2}} & 0 & 0 & 0 \\ * & * & -\bar{\gamma}^2 I_s & 0 & 0 \\ * & * & * & -\bar{\gamma}^2 I_s & 0 \\ * & * & * & * & \Pi_i \end{bmatrix}$$

in which $\Lambda_i = I_{\bar{n}} + \bar{A}_{i1}^T P + P\bar{A}_{i1} - \bar{C}^T Y_i^T - Y_i\bar{C} + \bar{P}$.

Under zero initial condition $\bar{e}(0) = 0$,

$$\mathbb{E}(\int_0^{Tf}\mathcal{L}V(\bar{e})dt) = V(\bar{e}) > 0 \quad (5\text{-}4\text{-}24)$$

thus $\Omega_i < 0$ leads to $\Gamma < 0$, i.e. LMIs (5-4-15) is sufficient to make (5-4-12) satisfy

$$\mathbb{E}(\|\bar{e}\|_{Tf}) \leq \mathbb{E}(\bar{\gamma}\|v\|_{Tf}) \quad (5\text{-}4\text{-}25)$$

As a result, for given performance index $\bar{\gamma}$, LMIs (5-4-15) can make sure the estimation error to convergence to equilibrium within a certain distance, and the error to be reduced to certain value.

It is obvious that conditions in the above theorem can also lead to a proof of global asymptotic stability in probability by choosing $\bar{P}$ specially to be null matrix.

5.5 Illustration examples

Example 5.5.1

Consider a single-link robot with flexible joints actuated by a DC motor. The plant can be modelled as the following stochastic nonlinear system [128, 129]:

$$\begin{cases} d\theta_m = \omega_m dt + (0.1\omega_m - 0.2\theta_l)dw \\ d\omega_m = \left[\frac{k_0}{J_m}(\theta_l - \theta_m) - \frac{Z}{J_m}\omega_m + \frac{k_\tau}{J_m}u\right]dt + (-0.1\omega_m + 0.1\omega_l)dw \\ d\theta_l = \omega_l dt + 0.1\theta_l dw \\ d\omega_l = \left[-\frac{k_0}{J_l}(\theta_l - \theta_m) - \frac{mgh}{J_l}\sin(\theta_l)\right] + (-0.3\omega_m + 0.1\omega_l)dw \end{cases} \tag{5-5-1}$$

where θ_m and θ_l denote the angles of the rotations of the motor and link, respectively, ω_m and ω_l are the angular velocities of the motor and link, respectively, J_m represents the inertia of the DC motor (actuator), J_l is the inertia of the link, k_0 is torsional spring constant, k_τ is the amplifier gain, Z is the viscous friction, m is the pointer mass, g is the gravity constant, and h is the length of the link, and u is the control input (DC voltage). Let $x = [\theta_m \quad \omega_m \quad \theta_l \quad 0.1\omega_l]$, the system can be written in the form of (5-3-1), where

$$A = \begin{bmatrix} 0 & 1 & 0 & 0 \\ -48.6 & -1.25 & 48.6 & 0 \\ 0 & 0 & 0 & 10 \\ 1.95 & 0 & -1.95 & 0 \end{bmatrix}, B = \begin{bmatrix} 0 \\ 21.6 \\ 0 \\ 0 \end{bmatrix}, C = \begin{bmatrix} 1 & 0 & 0 & 0 \\ 0 & 1 & 0 & 0 \end{bmatrix},$$

$$g(x) = \begin{bmatrix} 0 \\ 0 \\ 0 \\ -0.333\sin(x_3) \end{bmatrix}, W = \begin{bmatrix} 0.1 & 0 & -0.2 & 0 \\ 0 & -0.1 & 0 & 0.1 \\ 0 & 0 & 0.1 & 0 \\ 0 & -0.3 & 0 & 0.1 \end{bmatrix}, D = \begin{bmatrix} 0 \\ 0 \end{bmatrix},$$

The fault and disturbance distribution matrices are respectively $B_f = B_{fa} = B$, $D_f = \begin{bmatrix} 0 \\ 0 \end{bmatrix}$, $G = \begin{bmatrix} 0.1 & 0 \\ 0 & 0.2 \end{bmatrix}$ and

$$B_d = \begin{bmatrix} -0.2 & 0.01 & -0.02 \\ -0.1 & 0.02 & -0.04 \\ 0.1 & -0.02 & 0.04 \\ 0.2 & 0.02 & -0.04 \end{bmatrix}$$

The actuator fault is:

$$f_a = \begin{cases} 0 & t \geq 80s \\ -0.05(t-80) & 60s \leq t < 80s \\ 1 & 40s \leq t < 60s \\ 0.05(t-20) & 20s \leq t < 40s \\ 0 & 0s \leq t < 20s \end{cases} \tag{5-5-2}$$

and the unknown input disturbances are random numbers from $[-1,1]$ measurement noises are random numbers from $[-0.1,0.1]$. The initial state value is given as $x_0 = [0.1 \quad -1 \quad 0.1 \quad 0.2\ ]^T$ corrupted by random noises. A controller $u = Fy$, where $F = [-0.5 \quad -1]$, can be pre-designed to make the system stable.

$$\|g(x)\| \leq 0.333 \leq 0.333(1 + \|x\|)$$

So let $c = 0.333$, $\rho_1 = 0.11$ and $\rho_2 = 0$, we can easily find $g(x)$ satisfy the (5-3-2) and (5-3-3) in *Assumption 5.3.1*. By choosing $\bar{\gamma} = 3$, we can obtain $\tau = 20$ and the observer gains as follows:

$$H = \begin{bmatrix} 0.8000 & 0.4000 \\ 0.4000 & 0.2000 \\ -0.4000 & -0.2000 \\ -0.8000 & -0.4000 \\ 0 & 0 \\ 0 & 0 \end{bmatrix},$$

$$T = \begin{bmatrix} 0.2000 & -0.4000 & 0 & 0 & 0 & 0 \\ -0.4000 & 0.8000 & 0 & 0 & 0 & 0 \\ 0.4000 & 0.2000 & 1 & 0 & 0 & 0 \\ 0.8000 & 0.4000 & 0 & 1 & 0 & 0 \\ 0 & 0 & 0 & 0 & 1 & 0 \\ 0 & 0 & 0 & 0 & 0 & 1 \end{bmatrix},$$

$$K = K_1 + K_2 = \begin{bmatrix} 60.79 & -62.57 \\ -119.0 & 199.9 \\ 96.77 & -242.6 \\ -193.3 & 334.5 \\ -248.1 & 496.2 \\ -484.2 & 968.4 \end{bmatrix},$$

$$R = \begin{bmatrix} 12.86 & 90.38 & -19.44 & 0 & 0 & -8.640 \\ -31.00 & -176.8 & 38.88 & 0 & 0 & 17.28 \\ -24.05 & 283.9 & 9.720 & 10 & 0 & 4.320 \\ -0.9442 & -422.6 & 17.49 & 0 & 0 & 8.640 \\ 21.49 & -609.4 & 0 & 0 & 0 & 0 \\ 42.05 & -1190 & 0 & 0 & 1 & 0 \end{bmatrix}$$

By choosing the above parameters, d_1 is decoupled and the influences of d_2 and Brownian motion are attenuated. Using the Euler–Maruyama method [148] to simulate the standard Brownian motions, one can obtain the simulated curves of the stochastic state responses (40 state trajectories). The curves displayed in Figs. 5.5.1-5.5.5 exhibit the estimation performances for the trends of full system states, and actuator fault respectively.

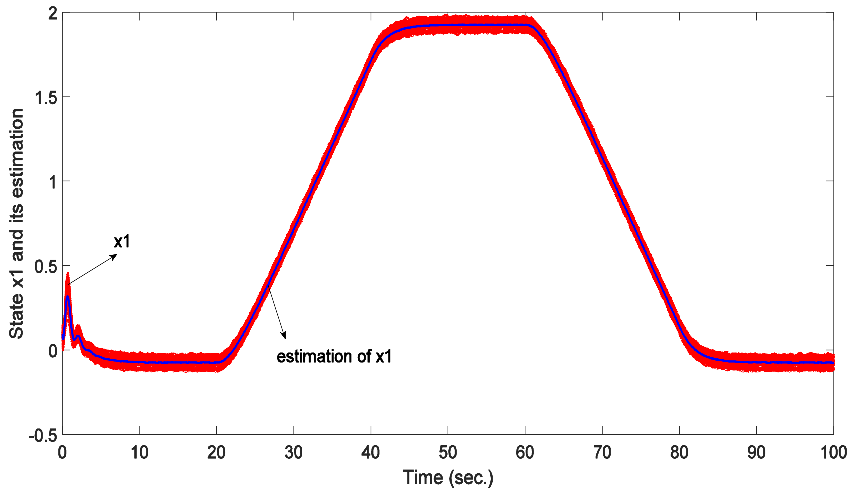

Fig. 5.5.1. State x_1 and its estimation

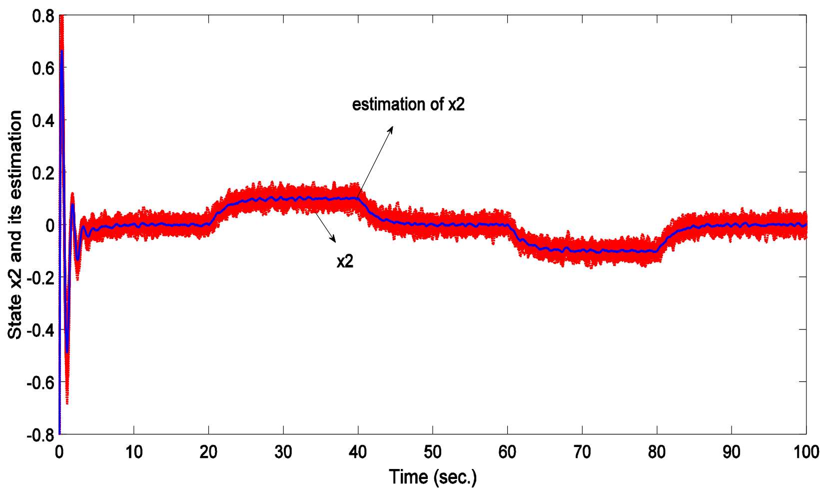

Fig. 5.5.2. State x_2 and its estimation

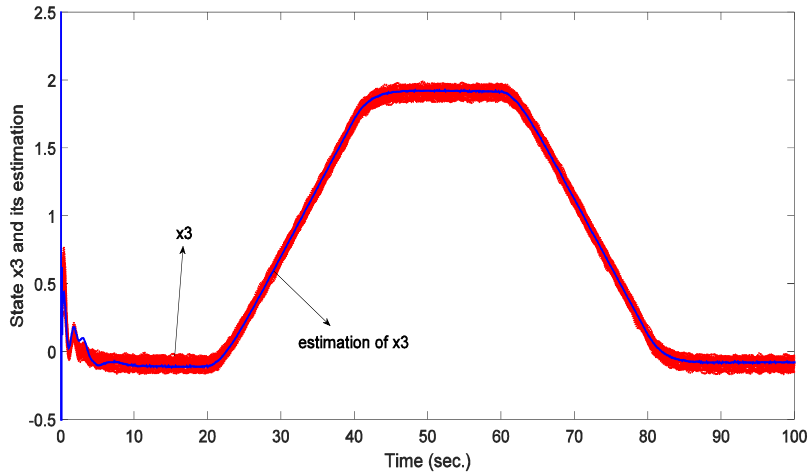

Fig. 5.5.3. State x_3 and its estimation

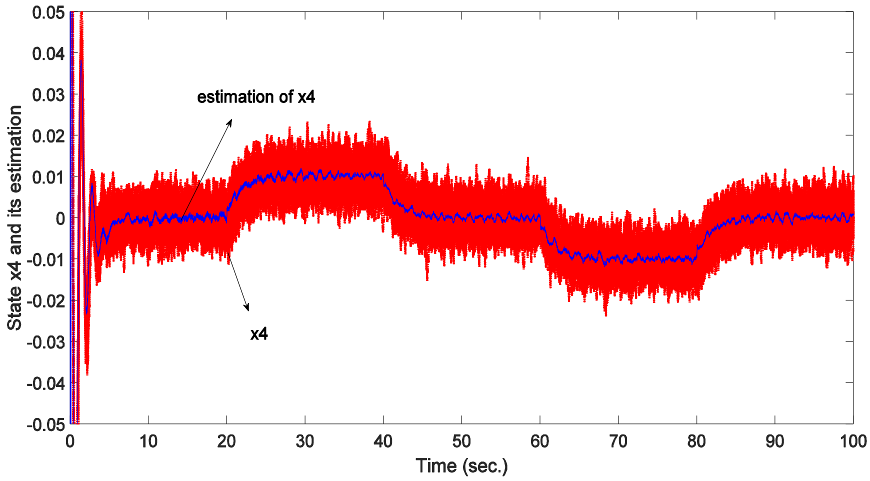

Fig. 5.5.4. State x_4 and its estimation

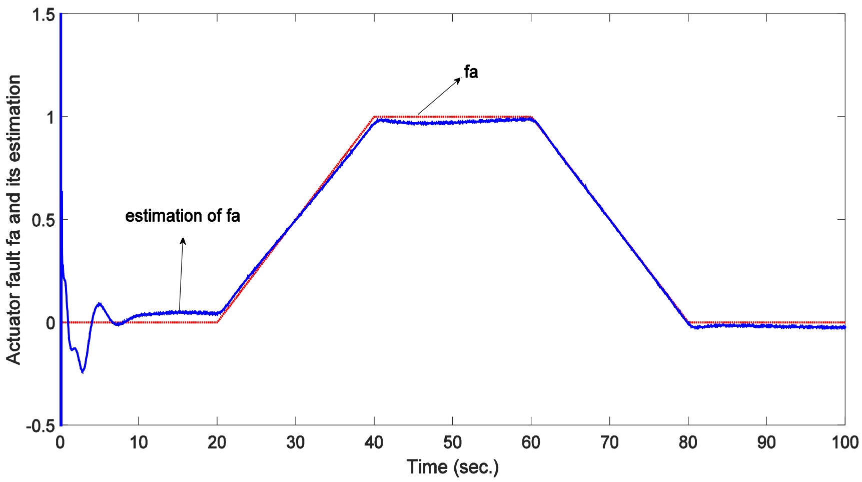

Fig. 5.5.5. f_a and its estimation

Applying the suggested fault-reconstruction approach, the means of actuator fault and full system states can be estimated simultaneously and the trajectories of estimation error can be mapped quite closed to equilibrium in finite time. Since the concerned unknown inputs are not constrained to be completely decoupled as most previous results, and the un-decoupled part of unknown inputs can be attenuated successfully by the solving LMI conditions, the presented methods have wider application on practical dynamic.

Example 5.3.2

We can find the nonlinear component of *Example 5.3.1* satisfies Lipschitz constrict which is a special situation of quadratic inner boundedness. In this example, we consider a more general condition. The plant is in the form of (5-3-1) with the following parameters:

$$A = \begin{bmatrix} -1 & -8 & 1 \\ 2 & -1 & 2 \\ 0 & 0 & -2 \end{bmatrix}, B = \begin{bmatrix} 1 \\ 0 \\ 0 \end{bmatrix}, C = \begin{bmatrix} 1 & 0 & 0 \\ 0 & 1 & 0 \\ 0 & 0 & 1 \end{bmatrix}, g(x) = \begin{bmatrix} -x_1(x_1^2 + x_2^2 + x_3^2) \\ -x_2(x_1^2 + x_2^2 + x_3^2) \\ -x_3(x_1^2 + x_2^2 + x_3^2) \end{bmatrix},$$

$$W = \begin{bmatrix} 0.3 & 0 & -0.2 \\ 0 & 0.1 & 0.4 \\ 0.5 & 0 & 0.1 \end{bmatrix}, B_{f_a} = B, D_{f_s} = \begin{bmatrix} 1 \\ 0 \\ 0 \end{bmatrix}, B_d = \begin{bmatrix} -0.3 & -0.1 & -0.05 \\ 0.1 & -0.2 & 0.1 \\ -0.2 & -0.4 & 0.2 \end{bmatrix},$$

$$D = \begin{bmatrix} 0 \\ 0 \\ 0 \end{bmatrix}, G = \begin{bmatrix} 0.1 & 0 & 0 \\ 0 & 0 & 0 \\ 0 & 0 & 0 \end{bmatrix}$$

In this case, $B_f = [B_{f_a}\ 0]$, $D_f = [0\ \ D_{f_s}]$. The actuator fault is defined as:

$$f_a = \begin{cases} 0 & t \geq 70s \\ -0.02(t-70) & 40s \leq t < 70s \\ 0.02(t-10) & 10s \leq t < 40s \\ 0 & 0s \leq t < 10s \end{cases} \tag{5-5-3}$$

and the sensor fault is 50% deviation of the real output, while the control input $u = 1$ and the unknown input disturbances and measurement noises are random numbers from $[-0.01,0.01]$ The initial state value is given as $x_0 = [0.1 \quad -0.05 \quad 0\ ]^T$ corrupted by random noises. Considering the set $\widetilde{D} = \{x \in R^3 \colon \|x\|) \leq \vartheta\}$, we have $\|g(x)\| = \|x\|^3 < \vartheta^2(1 + \|x\|)$. It is not hard to find that $g(x)$ is not Lipschitz convergence. Let is verify the quadratic inner boundedness according to [147]. After some algebraic manipulations, we can obtain

$$\||g(x_1) - g(x_2)|\|^2 = (\|x_1\|^2 - \|x_2\|^2)^2(\|x_1\|^2 + \|x_2\|^2) + \|x_1 - x_2\|^2\|x_1\|^2\|x_2\|^2$$

$$\rho_1\,\|x_1 - x_2\|^2 + \rho_2\langle x_1 - x_2, g(x_1) - g(x_2)\rangle$$
$$= \|x_1 - x_2\|^2\left[\rho_1 - \frac{\rho_2}{2}(\|x_1\|^2 + \|x_2\|^2)\right] - \frac{\rho_2}{2}(\|x_1\|^2 - \|x_2\|^2)^2$$

In order to make (5-3-3) hold, we have to find ρ_1 and ρ_2 such that

$$\|x_1\|^2 + \|x_2\|^2 \leq -\tfrac{\rho_2}{2}, \|x_1\|^2 \cdot \|x_2\|^2 \leq \rho_1 - \tfrac{\rho_2}{2}[\|x_1\|^2 + \|x_2\|^2]^2 \leq \rho_1 + \tfrac{\rho_2^2}{4}$$

hold in set $\widetilde{D}$. It suffices to have $\rho_2 \leq -4\vartheta^2$and $\rho_1 \geq \vartheta^4 - \frac{\rho_2^2}{4}$. For given set $\widetilde{D}$ with $\vartheta = 1.4$, which is large enough in terms of the considered system, we can find $\rho_1 = -7$ and $\rho_2 = -8.4$ to make $g(x)$ satisfy the quadratic inner-bounded condition. Then by choosing $\bar{\gamma} = 9$, we can obtain $\tau = 82.12$ and the observer gains as follows:

$$H = \begin{bmatrix} 0.6429 & -0.2143 & 0.4286 \\ -0.2143 & 0.0714 & -0.1429 \\ 0.4286 & -0.1429 & 0.2857 \\ 0 & 0 & 0 \\ 0 & 0 & 0 \\ 0 & 0 & 0 \\ 0 & 0 & 0 \end{bmatrix},$$

$$T = \begin{bmatrix} 0.3571 & 0.2143 & -0.4286 & 0 & 0 & 0 & -0.6429 \\ 0.2143 & 0.9286 & 0.1429 & 0 & 0 & 0 & 0.2143 \\ -0.4286 & 0.1429 & 0.7143 & 0 & 0 & 0 & -0.4286 \\ 0 & 0 & 0 & 1 & 0 & 0 & 0 \\ 0 & 0 & 0 & 0 & 1 & 0 & 0 \\ 0 & 0 & 0 & 0 & 0 & 1 & 0 \\ 0 & 0 & 0 & 0 & 0 & 0 & 1 \end{bmatrix},$$

$$K = K_1 + K_2 = \begin{bmatrix} -19.35 & -230.8 & 147.7 \\ -122.2 & 1131 & 754.2 \\ -167.5 & 870.0 & 684.1 \\ 0.3586 & 5.770 & 2.347 \\ 20.67 & -106.8 & -84.39 \\ 2.493 & 32.88 & 12.70 \\ 79.06 & -393.1 & -315.1 \end{bmatrix},$$

$$R = \begin{bmatrix} -0.7785 & -227.1 & -159.5 & 0 & -0.6429 & 0.3571 & -0.8500 \\ 6.350 & 1094 & -830.7 & 0 & 0.2143 & 0.2143 & 4.707 \\ 7.401 & -813.1 & -792.8 & 0 & -0.4286 & -0.4286 & 6.687 \\ 0.0428 & -5.904 & -2.080 & 0 & 0 & 0 & 0.0428 \\ -0.9818 & 100.2 & 97.52 & 0 & 0 & 0 & -0.9818 \\ -0.0644 & -33.69 & -11.08 & 1 & 0 & 0 & -0.0644 \\ -3.555 & 367.9 & 365.5 & 0 & 1 & 0 & -3.555 \end{bmatrix}$$

By choosing the above parameters, and using the Euler–Maruyama method to simulate the standard Brownian motions with 50 state trajectories, we can obtain Figs. 5.5.6-5.5.10 to exhibit the estimation performances for the trends of full system states, actuator fault and sensor fault, respectively. Like *Example 5.5.1*, d_1 is decoupled while the influences of d_2 and Brownian motions are attenuated. Normally, large gains should be avoided in the design of controllers. In this Chapter, K is designed as an observer gain. Therefore, it should be fine to have large elements in K.

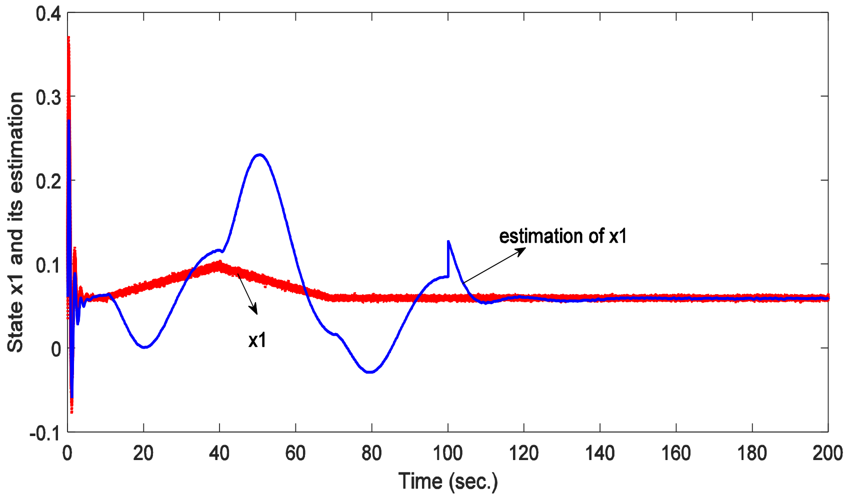

Fig. 5.5.6. State x_1 and its estimation

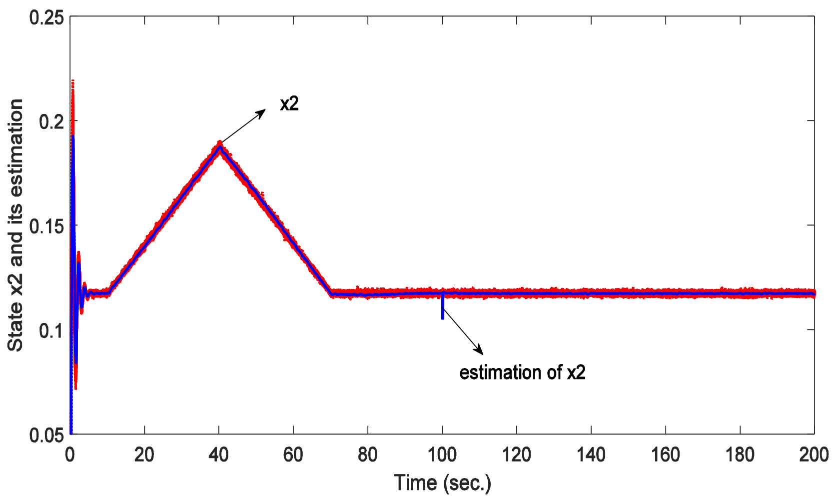

Fig. 5.5.7. State x_2 and its estimation

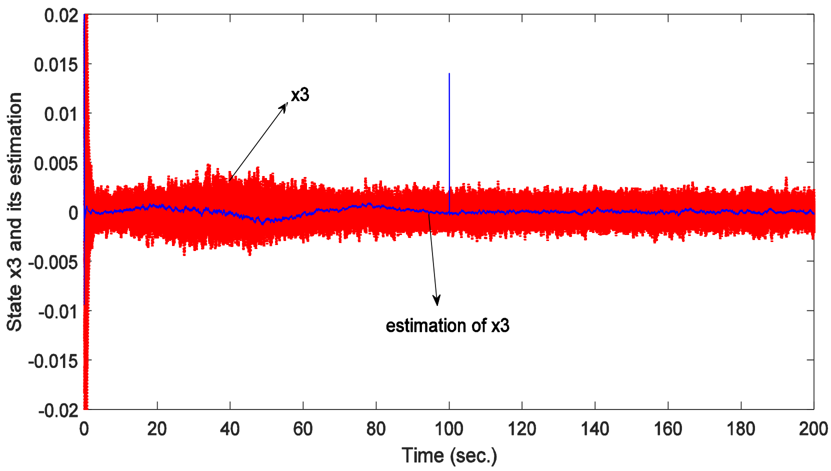

Fig. 5.5.8. State x_3 and its estimation

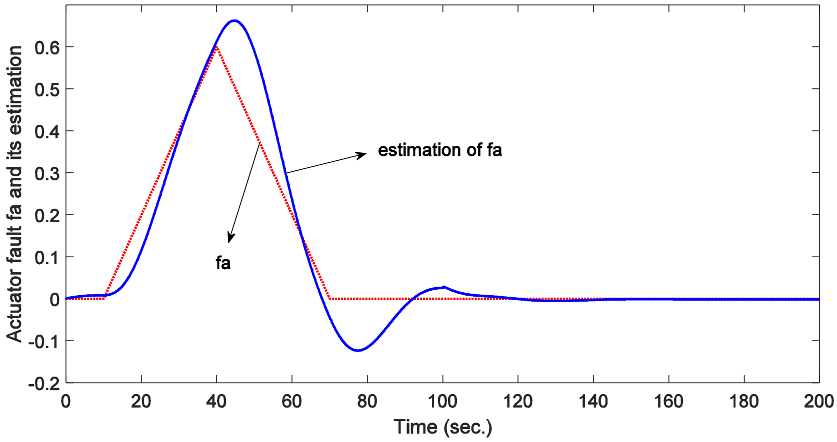

Fig. 5.5.9. f_a and its estimation

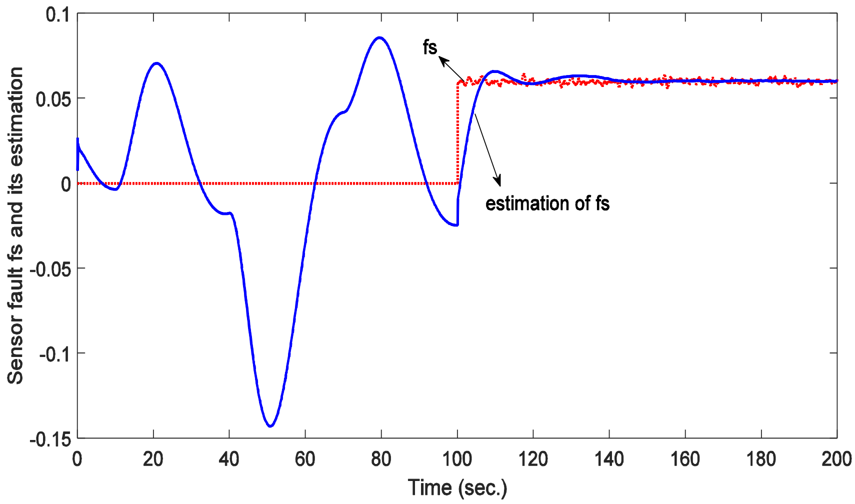

Fig. 5.5.10. f_s and its estimation

From the above figures, we can find the proposed scheme work excellent on quadratic inner-bounded nonlinear systems, which are more general than Lipschitz and one-side Lipschitz nonlinear systems considered in majority of existing literatures about nonlinear systems. Both actuator fault and sensor fault can be estimated simultaneously with system states robustly. The influences from unknown inputs and Brownian motions have been attenuated significantly and the convergence time of estimation error is finite.

Example 5.5.3

In this example, robust fault estimation of stochastic T-S fuzzy systems will be demonstrated through a numerical example. The system can be described in the form of plant (5-4-2) with 18 IF-THEN rules. The coefficients are presented in Appendix 1. The actuator fault taken into account occurs in the first input with the following value:

$$f_a = \begin{cases} 0 & 0s \le t < 1500s \\ -0.2(t-1500) & 1500s \le t < 2000s \\ -100+\sin(0.1t) & 2000s \le t < 2500s \\ 0.2(t-2500)-100 & 2500s \le t < 3000s \\ 0 & t \ge 3000s \end{cases} \tag{5-5-4}$$

And the sensor fault is assumed to be 20% decrease of the first output. The estimation results of full system states and concerned faults are shown in Figs. 5.5.11-5.5.18.

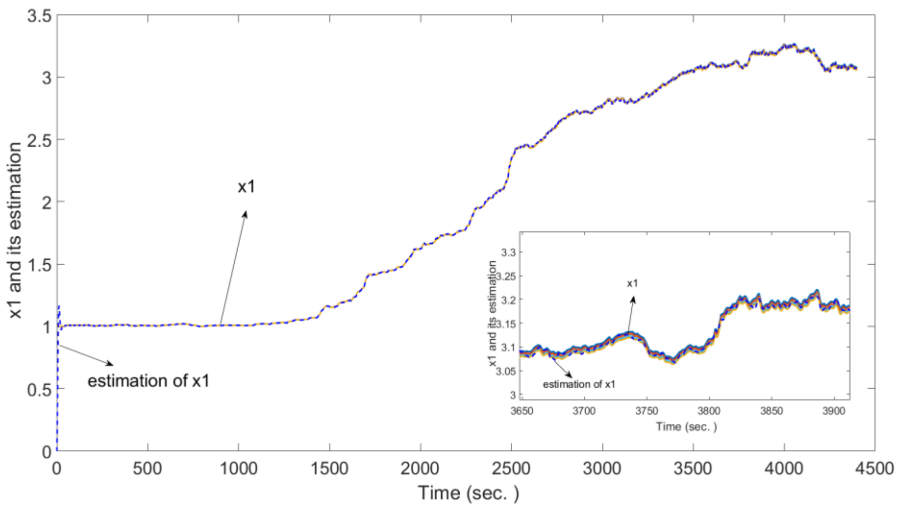

Fig. 5.5.11 state x_1 and its estimation

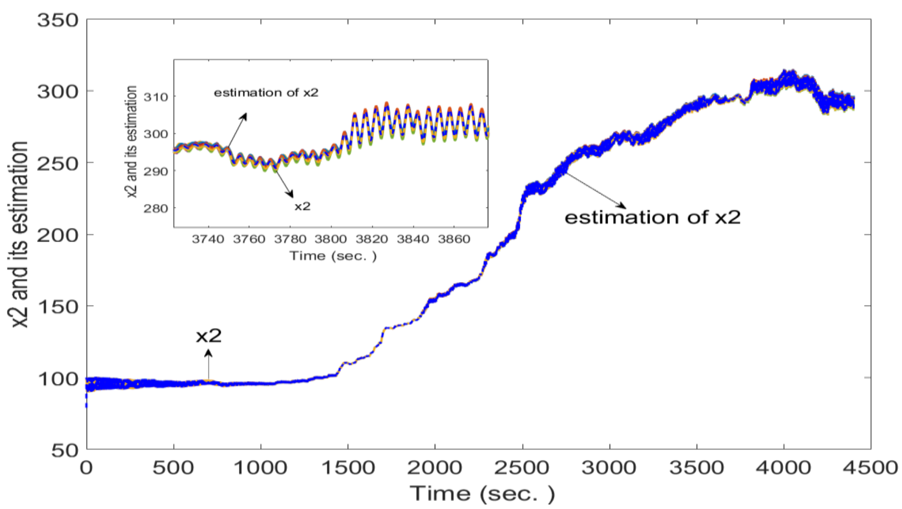

Fig. 5.5.12 state x_2 and its estimation

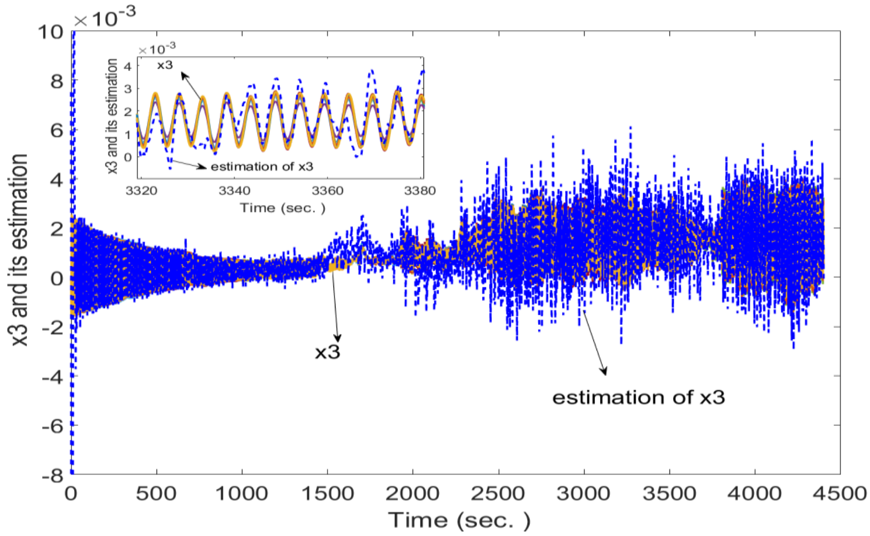

Fig. 5.5.13 state x_3 and its estimation

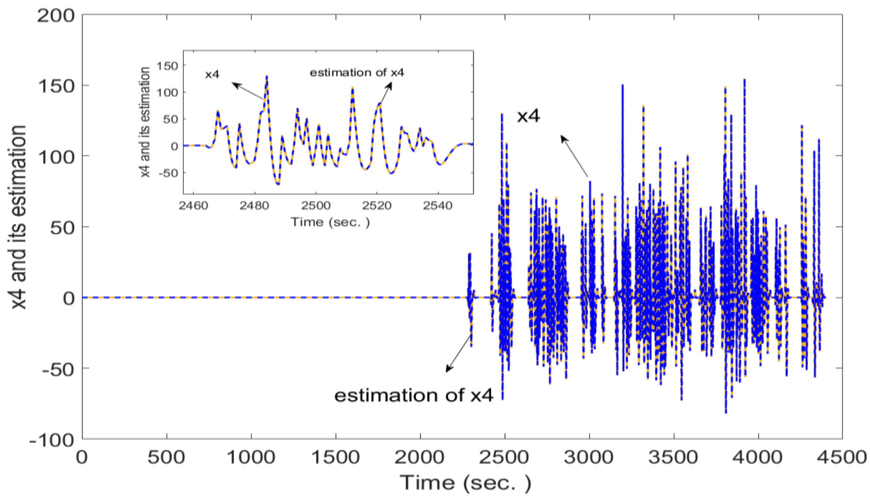

Fig.5.5.14 state x_4 and its estimation

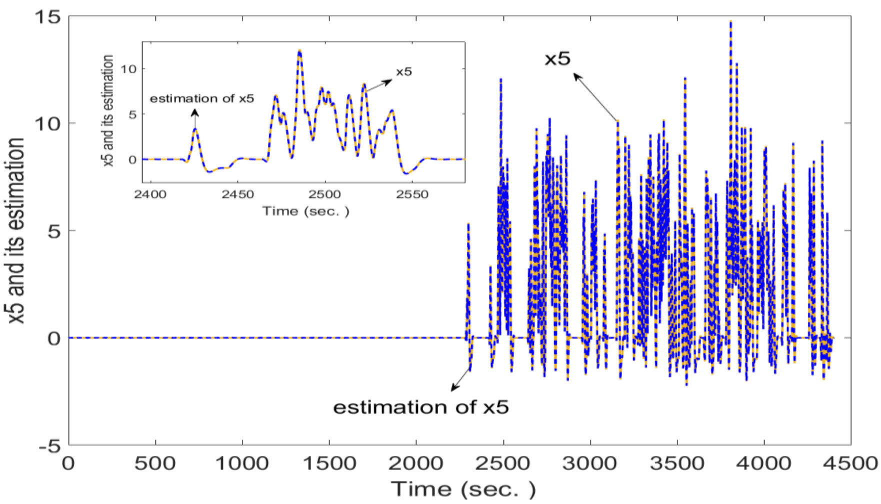

Fig.5.5.15 state x_5 and its estimation

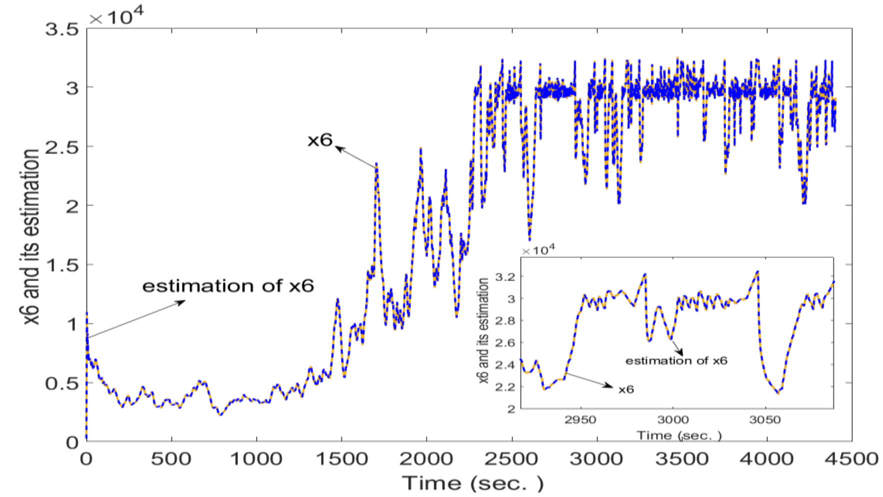

Fig. 5.5.16 state x_6 and its estimation

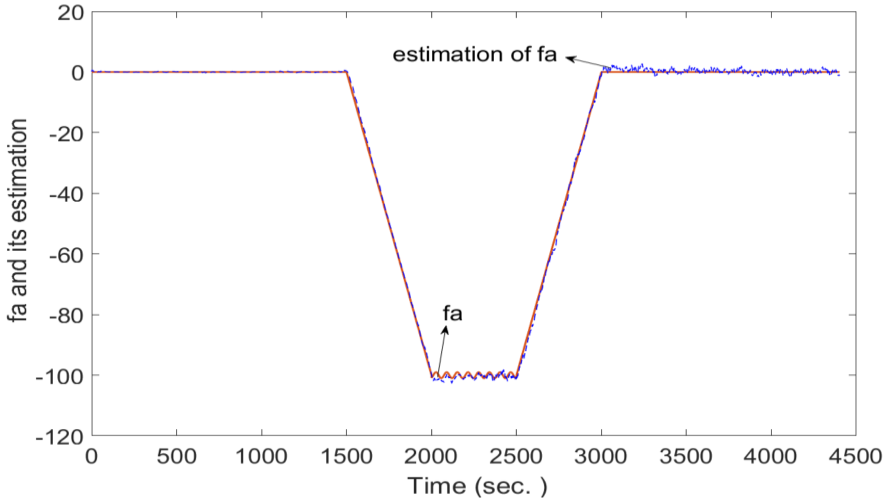

Fig. 5.5.17. f_a and its estimation

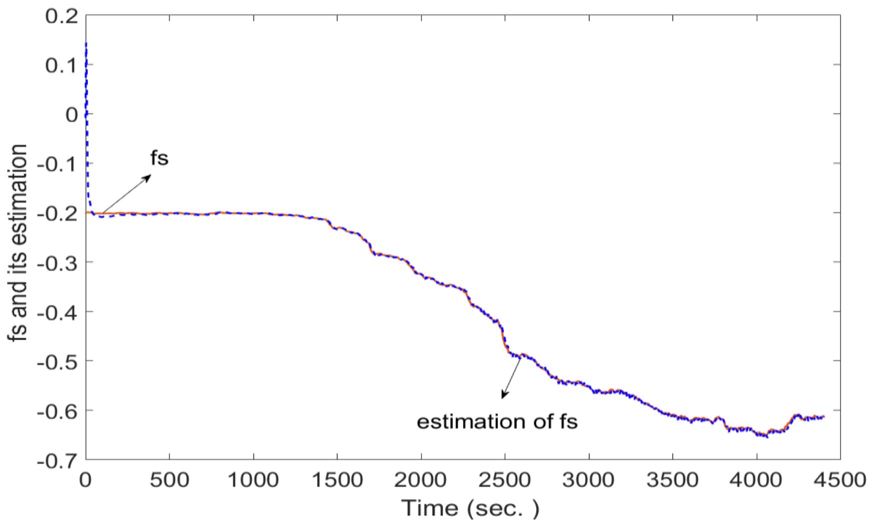

Fig.5.5.18. f_s and its estimation

As shown in the above figures, the estimation of both system states and considered faults are excellent. For given performance index, the estimation errors can converge to equilibrium of a certain distance determined by the index, and the un-decoupled unknown inputs are attenuated by LMIs successfully.

5.6 Summary

This chapter dealt with the problem of robust fault estimation for stochastic nonlinear systems subject to unknown inputs, faults and Brownian motion. Firstly, sufficient conditions of the stochastic input-to-state stable and finite-time stochastic input-to-state stable for stochastic nonlinear systems have been addressed with rigorous and completed proofs. Then UIO-based fault estimation technique has been proposed for the considered systems to estimate the means of considered faults and system states. By solving LMIs, the observer gains can be obtained sequentially to guarantee the convergence of estimation error. Significantly, the proposed methodology has been applied to simulations to illustrate the estimation performance.

Chapter 6

Integrated fault tolerant control of stochastic system

This chapter presents an integrated fault tolerant control technique for stochastic systems subjected to Brownian parameter perturbations. For fault estimation of stochastic systems, because of the existence of Brownian motion, the trajectory of estimation error is influenced by not only observer gains, but also the convergence of original system state. In Chapter 5, robust fault estimation for stochastic systems have been introduced based on assumption that a pre-designed controller can guarantee the stability of original plant. In this chapter, we will relax this assumption, and observer-based control is considered to meet the stability requirement of the plant after implementing the integrated fault tolerant control.

Firstly, UIO-based fault estimation approach is utilized to achieve a robust simultaneous estimate of the system states and the means of faults concerned. Estimation of system state is then used to do observer-based control. In the meanwhile, a robust fault tolerant control strategy is developed by using actuator and sensor signal compensation techniques based on estimation of faults. Fig. 6 can demonstrate the structure of the observer-based fault estimation and fault tolerant control. It is worthy to point out that the well-known separation theory for observer-based control in deterministic systems becomes invalid in stochastic Brownian systems. Therefore, the observer gains and control gains are determined to guarantee the stability and robustness of the overall closed-loop systems consisting original plant after fault tolerant control and the estimation error dynamic.

Stochastic linear time-invariant system (section 6.1), stochastic system with Lipschitz nonlinear constraint (section 6.2), stochastic system with quadratic inner-bounded nonlinear constraint (section 6.3), and stochastic T-S fuzzy nonlinear approximation (section 6.4) are respectively investigated, and the corresponding fault-tolerant control algorithms are addressed with illustration examples. The chapter ends with a conclusion in section 6.5.

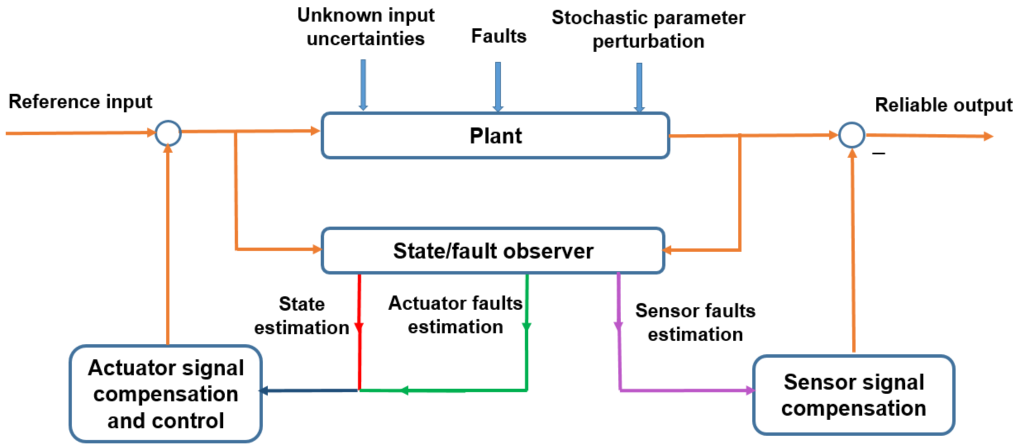

Fig. 6 The structure of observer-based fault tolerant control

6.1 Integrated fault tolerant control of linear stochastic system

Consider the following stochastic linear system in the form of It$\hat{o}$-type stochastic differential equation:

$$\begin{cases} dx(t) = [Ax(t) + Bu(t) + B_d d(t) + B_f f(t)]\, dt + Wx(t)dw(t) \\ y(t) = Cx(t) + D_f f(t) \end{cases}$$

(6-1-1)

where $x(t) \in \mathcal{R}^n$ represents the state vector; $u(t) \in \mathcal{R}^m$ stands for the control input vector and $y(t) \in \mathcal{R}^p$ is the measurement output vector; $d(t) \in L_\infty^{l_d}$ is unknown disturbance vectors; $f(t) \in \mathcal{R}^{l_f}$ represents the means of the faults (e.g., actuator faults and/or sensor faults); $w(t)$ is a standard one-dimensional Brownian motion with $\mathbb{E}[w(t)] = 0$ and $\mathbb{E}[w^2(t)] = t$; A, B, C, B_d, B_f, D_f and W are known coefficient matrices with appropriate dimensions. For the simplification of description, in the rest of paper, the time symbol t is omitted.

Similar with Chapter 5, the means of the faults concerned are assumed to be either incipient or abrupt. Moreover, we still denote $B_d = [B_{d1} \;\; B_{d2}]$ and $d = [d_1 \;\; d_2]^T$. We assume that $d_1 \in \mathcal{R}^{l_{d1}}$ rather than $d_2 \in \mathcal{R}^{l_{d2}}$ can be decoupled.

The aim of this section is to design a robust fault estimation based tolerant controller for system (6-1-1). The main objectives include: (i) Estimate full system states and the means of concerned faults simultaneously, and eliminate the influences of the unknown inputs. (ii) Design an observe-based fault tolerant control strategy to guarantee the stochastically input-to-state stability of the closed-loop system, and eliminate the adverse effects from the faults to the system dynamics with the aid of signal compensations.

6.1.1 Joint observer for robust fault estimation

This section is to introduce the integration of the augmented system approach and the UIO technique. The former can establish an auxiliary system vector composed of the original system states and the means of the concerned faults, while the latter is to decouple the unknown inputs that can be decoupled.

For system (6-1-1), the following augmented system can be constructed by describing the means of faults as auxiliary states

$$\begin{cases} d\bar{x} = (\bar{A}\bar{x} + \bar{B}u + \bar{B}_d d)dt + \bar{W}xdw \\ y = \bar{C}\bar{x} \end{cases} \tag{6-1-2}$$

where

$$\bar{n} = n + 2l_f,$$

$$\bar{x} = [x^T \quad \dot{f}^T \quad f^T]^T \in \mathcal{R}^{\bar{n}},$$

$$\bar{A} = \begin{bmatrix} A & 0_{n\times l_f} & B_f \\ 0_{l_f\times n} & 0_{l_f\times l_f} & 0_{l_f\times l_f} \\ 0_{l_f\times n} & I_{l_f} & 0_{l_f\times l_f} \end{bmatrix} \in \mathcal{R}^{\bar{n}\times\bar{n}},$$

$$\bar{B} = \begin{bmatrix} B^T & 0_{m\times l_f} & 0_{m\times l_f} \end{bmatrix}^T \in \mathcal{R}^{\bar{n}\times m},$$

$$\bar{B}_d = \begin{bmatrix} B_d^T & 0_{l_d\times l_f} & 0_{l_d\times l_f} \end{bmatrix}^T \in \mathcal{R}^{\bar{n}\times l_d},$$

$$\bar{W} = \begin{bmatrix} W^T & 0_{n\times l_f} & 0_{n\times l_f} \end{bmatrix}^T \in \mathcal{R}^{\bar{n}\times n},$$

$$\bar{C} = \begin{bmatrix} C & 0_{p\times l_f} & D_f \end{bmatrix} \in \mathcal{R}^{p\times\bar{n}}$$

For the augmented system (6-1-2), we design the following unknown input observer:

$$\begin{cases} d\bar{z} = [R\bar{z} + T\bar{B}u + (L_1 + L_2)y]dt \\ \hat{\bar{x}} = \bar{z} + Hy \end{cases} \tag{6-1-3}$$

where $\bar{z}$ is the state vector of (6-1-3), $\hat{\bar{x}}$ is the estimation of $\bar{x}$, and R, T, L_1, L_2 and H are all observer gains with appropriate dimensions to be designed.

Let $\bar{e} = \bar{x} - \hat{\bar{x}}$ which represents the estimation error. In terms of (6-1-2) and (6-1-3), we have:

$$
\begin{aligned}
d\bar{e} &= (I_{\bar{n}} - H\bar{C})\, d\bar{x} - d\bar{z} \\
&= \{(I_{\bar{n}} - H\bar{C})\, (\bar{A}\bar{x} + \bar{B}u + \bar{B}_d d) - R\bar{z} - T\bar{B}u - (L_1 + L_2)y\}dt \\
&\quad +(I_{\bar{n}} - H\bar{C})\bar{W}xdw \\
&= \{(I_{\bar{n}} - H\bar{C})\bar{A}\bar{x} - L_1\bar{C}\bar{x} + (I_{\bar{n}} - H\bar{C})\bar{B}u + (I_{\bar{n}} - H\bar{C})\bar{B}_d d - R\bar{z} - T\bar{B}u \\
&\quad -L_2 y\}dt + (I_{\bar{n}} - H\bar{C})\bar{W}xdw \\
&= \{[(I_{\bar{n}} - H\bar{C})\bar{A} - L_1\bar{C}]\bar{x} - R\hat{\bar{x}} + [(I_{\bar{n}} - H\bar{C}) - T]\bar{B}u + (I_{\bar{n}} - H\bar{C})\bar{B}_{d1}d_1 \\
&\quad +(I_{\bar{n}} - H\bar{C})\bar{B}_{d2}d_2 + (RH - L_2)y\}dt + (I_{\bar{n}} - H\bar{C})\bar{W}xdw
\end{aligned} \tag{6-1-4}
$$

If the observer gains satisfy the following conditions:

$$(I_{\bar{n}} - H\bar{C})\bar{B}_{d1} = 0 \tag{6-1-5}$$

$$R = \bar{A} - H\bar{C}\bar{A} - L_1\bar{C} \tag{6-1-6}$$

$$T = I_{\bar{n}} - H\bar{C} \tag{6-1-7}$$

$$L_2 = RH \tag{6-1-8}$$

the state estimation error can be simplified as

$$d\bar{e} = (R\bar{e} + T\bar{B}_{d2}d_2)dt + T\bar{W}xdw \tag{6-1-9}$$

In order to make (6-1-5) to (6-1-8) solvable, we have the following assumptions:

Assumption 6.1.1

$$\mathrm{rank}(CB_{d1}) = \mathrm{rank}(B_{d1}).$$

Assumption 6.1.2

$$\begin{bmatrix} A & B_f & B_{d1} \\ C & D_f & 0 \end{bmatrix} \text{ is of full column rank.}$$

Assumption 6.1.3

$$\mathrm{rank}\begin{bmatrix} sI_n - A & B_{d1} \\ C & 0 \end{bmatrix} = n + l_{d1}.$$

In terms of Chapter 3, the above assumptions are to ensure that (6-1-5) can be solved, and the augmented system model is observable. Moreover, and a special solution of (6-1-5) is

$$H^* = \bar{B}_{d1}[(\bar{C}\bar{B}_{d1})^T(\bar{C}\bar{B}_{d1})]^{-1}(\bar{C}\bar{B}_{d1})^T \tag{6-1-10}$$

By deriving H from (6-1-10) to satisfy condition (6-1-5), d_1 can decoupled. However, the unknown inputs d_2 are not decoupled which still exist in the error dynamics. It is evident that additional optimization approach should be employed to determine other observer gains so that the influence of d_2 can be attenuated. Furthermore, it is noticed that the stochastic perturbation term $T\bar{W}xdw$ exists in the error dynamic equation (6-1-9), therefore, the performance of the estimator depends not only on appropriate observer gains, but also on controlled states. As a result, before we choose the observer gains, a proper controller should be taken into account.

A special solution of (6-1-5), shown as (6-1-10) is used here, as it can already make the design of other observer gains flexible in this chapter. In terms of more flexible requirements, a general solution can be used as $H = \bar{B}_M(\bar{C}\bar{B}_M)^+ + N(I - (\bar{C}\bar{B}_M)(\bar{C}\bar{B}_M)^+)$, where $(\bar{C}\bar{B}_M)^+ = [(\bar{C}\bar{B}_M)^T(\bar{C}\bar{B}_M)]^{-1}(\bar{C}\bar{B}_M)^T$, and N is a compatible matrix of proper dimension.

6.1.2 Robust estimation-based fault tolerant control

As stated in the aforementioned part, the estimation error dynamics rely on the design of observer gains and the controlled states. Therefore, observer-based controller should be designed as a whole. Now let us move on to deal with the observer-based fault tolerant control method.

Consider the following control law

$$u = \bar{K}\hat{\bar{x}} = [K \quad 0 \quad K_f]\begin{bmatrix}\hat{x}\\ \hat{\dot{f}}\\ \hat{f}\end{bmatrix} = K\hat{x} + K_f\hat{f} \tag{6-1-11}$$

where K and K_f are control gains to be determined, $\hat{x}$, $\hat{\dot{f}}$ and $\hat{f}$ represent the estimates of x, $\dot{f}$ and f respectively. Moreover, K should be selected to guarantee the convergence of the closed-loop system, while K_f is designed to compensate the influences of the faults.

Based on the estimation of $\hat{\bar{x}}$, the estimates of the original system states and the mean of fault vector can be reconstructed as

$$\hat{x} = \begin{bmatrix} I_n & 0_{n\times l_f} & 0_{n\times l_f} \end{bmatrix} \hat{\bar{x}} \tag{6-1-12}$$

and

$$\hat{f} = \begin{bmatrix} 0_{l_f\times \bar{n}} & 0_{l_f\times l_f} & I_{l_f} \end{bmatrix} \hat{\bar{x}} \tag{6-1-13}$$

Suppose

$$\mathrm{rank}[B \quad B_f] = \mathrm{rank}\, B \tag{6-1-14}$$

and let

$$K_f = -B^{+}B_f \tag{6-1-15}$$

Therefore, it is clear that

$$B_f f + BK_f\hat{f} = B_f f - BB^{+}B_f\hat{f} = B_f J_2 \bar{e} \tag{6-1-16}$$

where $J_2 = \begin{bmatrix} 0_{l_f\times n} & 0_{l_f\times l_f} & I_{l_f} \end{bmatrix}$. This implies that the effects from the actuator faults to the system dynamics are eliminated.

Using $-D_f\hat{f}$ to compensate the measurement output, we have

$$y_c = y - D_f J_2 \hat{\bar{x}} = Cx + D_f f - D_f\hat{f} = Cx + D_f J_2 \bar{e} \tag{6-1-17}$$

As a result, the influences from the sensor faults to the system outputs are removed.

Substituting (6-1-11) into system (6-1-1) and using the compensated measurement output y_c to replace the actual measurement y, the following closed-loop system can be established

$$\begin{cases} dx = [(A+BK)x - B_e\bar{e} + B_d d]dt + Wxdw \\ d\bar{e} = (R\bar{e} + T\bar{B}_{d2}d_2)dt + T\bar{W}xdw \\ y_c = Cx + D_e\bar{e} \end{cases} \tag{6-1-18}$$

where $B_e = BKJ_0 - B_f J_2, J_0 = \begin{bmatrix} I_n & 0_{n\times l_f} & 0_{n\times l_f} \end{bmatrix}, D_e = D_f J_2$.

It is obvious that by using signal compensation approach, actuator and sensor faults have been removed successfully from the closed-loop system except for estimation errors. The next step is to design the observer and controller gains to make system (6-1-18) stochastically input-to-state stable, attenuate the influences of the unknown inputs on the closed-loop system, and satisfy the robust performance index:

$$\mathbb{E}\left(\|y_c\|_{Tf}^2\right) < \gamma_1^2 \mathbb{E}\left(\|d_1\|_{Tf}^2\right) + \gamma_2^2 \mathbb{E}\left(\|d_2\|_{Tf}^2\right) \tag{6-1-19}$$

It should be mentioned that, although d_1 can be decoupled in observer-based fault estimator. However, it still exists in the original plant. Hence, d_1 should be considered in the robustness analysis of the overall closed-loop system.

It is noticed that both the system dynamics and error dynamics are subject to state stochastic fluctuation, which makes it challenging to design observer and controller gains simultaneously. In order to simplify the challenging matrix problem, we firstly design control gain K such that $A + BK$ is a Hurwitz matrix, then choose a proper observer gain L_1 to guarantee the stochastically input-to-state stability of closed-loop plant (6-1-18) with robust performance index (6-1-19). Furthermore, in the case of observer-based fault tolerant control, the design of observer gain L_1 should make the estimation error dynamics reaches the steady states faster than those of the control system dynamics. Therefore, before we determine the observer gain L_1, the following lemma is introduced:

Lemma 6.1.1 ([149])

Consider the vertical strip defined by $\mathcal{D}(a) = \{x + jy \in \mathcal{C}: x < -a, a > 0\}$, a matrix A has all its eigenvalues in $\mathcal{D}(a)$ if and only if there exists a positive definite matrix X, such that

$$A^T X + XA + 2aX < 0 \tag{6-1-20}$$

Therefore, based on a designed K, the following theorem is proposed to design L_1.

Theorem 6.1.1

For system (6-1-1), there exists an unknown input observer in the form of (6-1-3), and the tolerant control laws in the form of (6-1-11) and (6-1-17), so that the closed-loop system (6-1-18) is stochastically input-to-state stable satisfying the robust performance index (6-1-19), if there exist positive definite matrices P, $\bar{P}$, Q, and $\bar{Q}$, matrix Y, such that

$$\begin{bmatrix} \Omega_{11} & -PB_e + C^T D_e & PB_{d1} & PB_{d2} \\ * & \Omega_{22} & 0 & \bar{P}T\bar{B}_{d2} \\ * & * & -\gamma_1^2 I_{l_{d_1}} & 0 \\ * & * & * & -\gamma_2^2 I_{l_{d_2}} \end{bmatrix} < 0 \tag{6-1-21}$$

and

$$\bar{P}T\bar{A} + \bar{A}^T T^T \bar{P} - Y\bar{C} - \bar{C}^T Y^T + 2a\bar{P} < 0 \tag{6-1-22}$$

where

$\Omega_{11} = P(A + BK) + (A + BK)^T P + W^T PW + \bar{W}^T T^T \bar{P}T\bar{W} + Q + C^T C,$

$\Omega_{22} = \bar{P}T\bar{A} + \bar{A}^T T^T \bar{P} - Y\bar{C} - \bar{C}^T Y^T + \bar{Q} + D_e^T D_e,$

$Y = \bar{P}L_1,$

$a = \beta\theta_l, \theta_l = -\min Re[\lambda_i\,(A + BK)] > 0, i = \{1, 2, \cdots n\}$ and $\beta > 1$.

We can thus calculate $L_1 = \bar{P}^{-1}Y$.

Proof

According to *Theorem 5.3.1*, to prove the stability, we should establish a Lyapunov function satisfying (5-2-1) and (5-2-2). Without loss of generality, we choose the candidate as $V = V_1 + V_2$, where $V_1 = x^T Px$ and $V_2 = \bar{e}^T P\bar{e}$. We can notice

$$V = \tilde{x}^T \tilde{P}\tilde{x} \tag{6-1-23}$$

where $\tilde{x} = [x^T \quad \bar{e}^T]^T$, $\tilde{P} = \begin{bmatrix} P & 0 \\ 0 & \bar{P} \end{bmatrix}$. In the choice of V, a special form of $\tilde{P}$ is selected as $\tilde{P} = \begin{bmatrix} P & 0 \\ 0 & \bar{P} \end{bmatrix}$ to reduce design complexity. Then we can find

$$\lambda_{min}(\tilde{P})\|\tilde{x}\|^2 \leq V \leq \lambda_{max}(\tilde{P})\|\tilde{x}\|^2 \tag{6-1-24}$$

which implies V satisfy (5-2-1) with $\psi_1 = \lambda_{min}(\tilde{P})\|\tilde{x}\|^2$, $\psi_2 = \lambda_{max}(\tilde{P})\|\tilde{x}\|^2$ in *Definition 5.2.1*. Taking infinitesimal generator (5-1-7) along the state trajectories of (6-1-18), by using It$\hat{o}$ formula, it follows that:

$$\mathcal{L}V_1 = x^T[P(A + BK) + (A + BK)^T P]x - 2x^T PB_e\bar{e} + 2x^T PB_a d + x^T W^T PWx \tag{6-1-25}$$

and

$$\mathcal{L}V_2 = \bar{e}^T(\bar{P}R + R^T\bar{P})\bar{e} + 2\bar{e}^T\bar{P}T\bar{B}_{d2}d_2 + x^T\bar{W}^T T^T\bar{P}T\bar{W}x \qquad (6\text{-}1\text{-}26)$$

Therefore, we have

$$\begin{aligned}\mathcal{L}V &= \mathcal{L}V_1 + \mathcal{L}V_2 \\ &= \{x^T[P(A+BK) + (A+BK)^T P + W^T PW + \bar{W}^T T^T\bar{P}T\bar{W}]x - 2x^T PB_e\bar{e} \\ &\quad + 2x^T PB_d d + \bar{e}^T(\bar{P}R + R^T\bar{P})\bar{e} + 2\bar{e}^T\bar{P}T\bar{B}_{d2}d_2 \qquad (6\text{-}1\text{-}27)\end{aligned}$$

Adding and subtracting $x^T Qx + \bar{e}^T\bar{Q}\bar{e} - \gamma_1^2 d_1^T d_1 - \gamma_2^2 d_2^T d_2$ to $\mathcal{L}V$, we can obtain

$$\mathcal{L}V = [x^T \quad \bar{e}^T \quad d_1^T \quad d_2^T]\,\Psi\begin{bmatrix} x \\ \bar{e} \\ d_1 \\ d_2 \end{bmatrix} - x^T Qx - \bar{e}^T\bar{Q}\bar{e} + \gamma_1^2 d_1^T d_1 + \gamma_2^2 d_2^T d_2$$

(6-1-28)

where

$$\Psi = \begin{bmatrix} \Psi_{11} & -PB_e & PB_{d1} & PB_{d2} \\ * & \Psi_{22} & 0 & \bar{P}T\bar{B}_{d2} \\ * & * & -\gamma_1^2 I_{l_{d_1}} & 0 \\ * & * & * & -\gamma_2^2 I_{l_{d_2}} \end{bmatrix} \qquad (6\text{-}1\text{-}29)$$

$$\Psi_{11} = P(A+BK) + (A+BK)^T P + W^T PW + \bar{W}^T T^T\bar{P}S\bar{W} + Q,$$

$$\Psi_{22} = \bar{P}T\bar{A} + \bar{A}^T T^T\bar{P} - \bar{P}L_1\bar{C} - \bar{C}^T L_1^T\bar{P}^T + \bar{Q}.$$

From the LMI (6-1-27), one has

$$\Psi < 0 \qquad (6\text{-}1\text{-}30)$$

which indicates

$$\begin{aligned}\mathcal{L}V &\le -x^T Qx - \bar{e}^T\bar{Q}\bar{e} + \gamma_1^2 d_1^T d_1 + \gamma_2^2 d_2^T d_2 \\ &= -[x^T \quad \bar{e}^T]\begin{bmatrix} Q & 0 \\ 0 & \bar{Q} \end{bmatrix}\begin{bmatrix} x \\ \bar{e} \end{bmatrix} + \gamma_1^2 d_1^T d_1 + \gamma_2^2 d_2^T d_2 \qquad (6\text{-}1\text{-}31)\end{aligned}$$

Since Q and $\bar{Q}$ are both positive definite, we have

$$\tilde{Q} = \begin{bmatrix} Q & 0 \\ 0 & \bar{Q} \end{bmatrix} > 0 \qquad (6\text{-}1\text{-}32)$$

indicating we can find a scalar $\bar{\lambda} > 0$ such that

$$\mathcal{L}V \le -\bar{\lambda}\,\|\tilde{x}\|^2 + \gamma_1^2|d_1|^2 + \gamma_2^2|d_2|^2 \qquad (6\text{-}1\text{-}33)$$

As a result, we can conclude the closed-loop system (6-1-18)is stochastically input-to-state sable with

$$\psi_3(\tilde{x}) = \bar{\lambda}\|\tilde{x}\|^2 \tag{6-1-34}$$

and

$$\psi_4(|d|) = \gamma_1^2|d_1|^2 + \gamma_2^2|d_2|^2 \tag{6-1-35}$$

Now we move on to discuss the robustness of the observer-based fault tolerant control. Consider the following performance index:

$$\begin{aligned}
\Gamma &= \mathbb{E}\{\int_0^{Tf}[y_c^T(\tau)y_c(\tau) - \gamma_1^2 d_1^T(\tau)d_1(\tau) - \gamma_2^2 d_2^T(\tau)d_2(\tau)]d\tau\} \\
&= \mathbb{E}\{\int_0^{Tf}[x^T(\tau)C^TCx(\tau) + \bar{e}^T(\tau)D_e^TD_e\bar{e}(\tau) + 2x^T(\tau)C^TD_e\bar{e}(\tau) \\
&\quad -\gamma_1^2 d_1^T(\tau)d_1(\tau) - \gamma_2^2 d_2^T(\tau)d_2(\tau)]d\tau\}
\end{aligned} \tag{6-1-36}$$

It is obvious that condition (6-1-19) is equivalent to the condition $\Gamma < 0$.Then, adding and subtracting $\mathbb{E}(\int_0^t \mathcal{L}V\, d\tau)$ to Γ, and using $Y = \bar{P}L_1$, one has:

$$\begin{aligned}
\Gamma = \mathbb{E}\{\int_0^{Tf}[x^T \quad \bar{e}^T \quad d_1^T \quad d_2^T]\,\Omega\begin{bmatrix} x \\ \bar{e} \\ d_1 \\ d_2 \end{bmatrix} - x^T(\tau)Qx(\tau) - \bar{e}^T(\tau)\bar{Q}\bar{e}(\tau)]d\tau\} \\
-\mathbb{E}(\int_0^{Tf} \mathcal{L}V\, d\tau)
\end{aligned} \tag{6-1-37}$$

Where

$$\Omega = \begin{bmatrix} \Omega_{11} & -PB_e + C^TD_e & PB_{d1} & PB_{d2} \\ * & \Omega_{22} & 0 & \bar{P}T\bar{B}_{d2} \\ * & * & -\gamma_1^2 I_{l_{d_1}} & 0 \\ * & * & * & -\gamma_2^2 I_{l_{d_2}} \end{bmatrix} \tag{6-1-38}$$

$$\Omega_{11} = P(A+BK) + (A+BK)^TP + W^TPW + \bar{W}^TT^T\bar{P}T\bar{W} + Q + C^TC,$$

$$\Omega_{22} = \bar{P}T\bar{A} + \bar{A}^TT^T\bar{P} - Y\bar{C} - \bar{C}^TY^T + \bar{Q} + D_e^TD_e.$$

It is not hard to find

$$\mathbb{E}(\int_0^{Tf} \mathcal{L}V\, d\tau) = \mathbb{E}(V) > 0 \tag{6-1-39}$$

One can have $\Omega < 0$ from the LMI (6-1-21), thus one can $\Gamma < 0$, which indicates the (6-1-19) can be satisfied.

From *Lemma 6.1.1*, the LMI (6-1-22) implies

$$Re[\lambda_i(R)] < -a, \quad i = \{1, 2, \cdots \bar{n}\} \tag{6-1-40}$$

Noticing that $a = \beta\theta_l$, where $\theta_l = -\min Re[\lambda_i\,(A + BK)] > 0$ and $\beta > 1$, one can know the response of the estimation error dynamics is faster than the system dynamics. This completes the proof.

Remark 6.1.1

As aforementioned, control gain K should be designed to make $A + BK$ Hurwitz, which means the eigenvalues of the matrix $A + BK$ are located on the left half complex plane. For some practical applications, it can be required that the eigenvalues of the matrix $A + BK$ are settled in a specific region $\mathcal{D}(c, \mu, \delta) = \{x + jy \in \mathcal{C}: x < -c, |x + jy| < \mu, \tan(\delta)x < -|y|\}$, where c, μ and $\delta$are positive scalars, which is to ensure a minimum decay rate c, a minimum damping ratio $\varsigma = \cos(\delta)$, and a maximum un-damped natural frequency $\omega_d = \mu\sin(\delta)$. According to [149], we can derive that if there exists a positive definite matrix X and matrix Z such that

$$AX + BZ + XA^T + XZ^T + 2cX < 0 \tag{6-1-41}$$

$$\begin{bmatrix} -\mu X & AX + BZ \\ * & -\mu X \end{bmatrix} < 0 \tag{6-1-42}$$

$$\begin{bmatrix} \Delta_{11} & \Delta_{12} \\ \Delta_{21} & \Delta_{22} \end{bmatrix} < 0 \tag{6-1-43}$$

where $Z = KX$, $\Delta_{11} = \sin(\delta)(AX + BZ + XA^T + Z^T B^T)$, $\Delta_{12} = \cos(\delta)(AX + BZ - XA^T - Z^T B^T)$, $\Delta_{21} = \cos(\delta)(XA^T + Z^T B^T - AX - BZ)$, and $\Delta_{22} = \sin(\delta)(AX + BZ + XA^T + Z^T B^T)$, then $\lambda_i(A + BK) \in \mathcal{D}(c, \mu, \delta), \forall i = \{1, 2, \cdots n\}$. After obtaining X and Z, the control gain K can be calculated as $K = ZX^{-1}$ to constrain the poles of $A + BK$ to lie in a prescribed stable region $\mathcal{D}(c, \mu, \delta)$. This design bounds the maximum overshoot, the frequency of oscillatory modes, the delay time, rise time, and the settling time.

Now, it is time to conclude the design procedure of the robust fault estimation and fault tolerant control strategies.

Procedure 6.1.1 *(Fault tolerant control algorithm by integrating state/fault estimation and signal compensation for stochastic linear systems)*

i) Construct the augmented system in the form of (6-1-2) for system (6-1-1).

ii) Select the matrix H^* in the form of (6-1-10), and T can be calculated in terms of $T = I_{\bar{n}} - H\bar{C}$.

iii) Design control gain K to make $A + BK$ Hurwitz. For a certain desired region $\mathcal{D}(c, \mu, \delta)$, solve LMIs (6-1-41)-(6-1-43) to determine the control gain K such that all poles of $A + BK$ are settled in $\mathcal{D}(c, \mu, \delta)$. Denote $\theta_l = -\min Re[\lambda_i\,(A + BK)]$, and $a = \beta\theta_l$. β can be chosen between 2 and 5 such that the response of the estimation error is reasonably faster than that of the system dynamics.

iv) Solve the LMIs (6-1-21) and (6-1-22) to obtain P, Q, $\bar{P}$, $\bar{Q}$ and matrix Y. The observer gain is thus calculated as $L_1 = \bar{P}^{-1}Y$.

v) Calculate the other observer gains R and L_2 following the formulas (6-1-6) and (6-1-8), respectively.

vi) Implement the robust unknown input observer (6-1-3) to produce the augmented estimate $\hat{\bar{x}}$, leading to the simultaneous estimates of the system states and faults $\hat{x}$ and $\hat{f}$ in the forms of (6-1-12) and (6-1-13), respectively.

vii) Implement the tolerant control law $u = \bar{K}\hat{\bar{x}}$ and $y_c = y - D_f\hat{f}$, where $\bar{K} = [K \quad 0 \quad K_f]$ and $K_f = -B^+B_f$.

6.2 Integrated fault tolerant control of Lipschitz nonlinear stochastic system

In the last section, a robust fault tolerant control technique has been developed for stochastic linear systems. It is well-known nonlinear properties widely exist in many practical dynamics, therefore this motivates us to extend the approach proposed in Section 6.1 to nonlinear systems. In this section, robust fault estimation-based fault tolerant control approach is proposed for Lipschitz nonlinear systems subject to unexpected faults, unknown inputs and stochastic parameter perturbations. The considered stochastic nonlinear systems can be represented by the following It$\hat{o}$-type differential equations:

$$\begin{cases} dx = [Ax + Bu + B_d d + B_f f + \phi(t, x, u)]dt + Wxdw \\ y = Cx + D_f f \end{cases} \tag{6-2-1}$$

where $\phi(t, x, u) \in \mathcal{R}^n$ is a real nonlinear vector function with Lipschitz constant θ, namely,

$$\|\phi(t, x, u) - \phi(t, \hat{x}, u)\| \le \theta\|x - \hat{x}\|,$$

$$\forall(t, x, u),\ (t, \hat{x}, u)\ \in \mathcal{R} \times \mathcal{R}^n \times \mathcal{R}^m \tag{6-2-2}$$

and the other symbols are the same as defined as system (6-1-1).

In order to estimate the means of faults and system states at the same time, an auxiliary system is constructed as follows, by considering the faults as augmented system states:

$$\begin{cases} d\bar{x} = [\bar{A}\bar{x} + \bar{B}u + \bar{B}_d d + \bar{\phi}(t,x,u)]dt + \bar{W}xdw \\ y = \bar{C}\bar{x} \end{cases} \tag{6-2-3}$$

where

$$\bar{\phi}(t,x,u) = \begin{bmatrix} \bar{\phi}^T(t,x,u) & 0_{1\times l_f} & 0_{1\times l_f} \end{bmatrix}^T \in \mathcal{R}^{\bar{n}} \tag{6-2-4}$$

and the other symbols are defined the same as those in system (6-1-2). In the rest of this paper, the symbols are of the same meanings with those defined in section 6.1 if not stated specifically.

For system (6-2-3), the following unknown input observer is constructed:

$$\begin{cases} d\bar{z} = [R\bar{z} + T\bar{B}u + (L_1 + L_2)y + T\bar{\phi}(t,\hat{x},u)]dt \\ \hat{\bar{x}} = \bar{z} + Hy \end{cases} \tag{6-2-5}$$

Defining the estimation error to be $\bar{e} = \bar{x} - \hat{\bar{x}}$, $\tilde{\phi} = \bar{\phi}(t,x,u) - \bar{\phi}(t,\hat{x},u)$. Then the following error dynamics can be obtained if (6-1-5) to (6-1-8) are satisfied

$$d\bar{e} = \left(R\bar{e} + T\bar{B}_{d2}d_2 + T\tilde{\phi}\right)dt + T\bar{W}xdw \tag{6-2-6}$$

Under the designed observer-based fault tolerant controller (6-1-11) and (6-1-17), the overall closed-loop system can be obtained as follows:

$$\begin{cases} dx = [(A + BK)x - B_e\bar{e} + B_d d + \phi(t,x,u)]dt + Wxdw \\ d\bar{e} = (R\bar{e} + T\bar{B}_{d2}d_2 + T\tilde{\phi})dt + T\bar{W}xdw \\ y_c = Cx + D_e\bar{e} \end{cases} \tag{6-2-7}$$

It is obvious that both actuator and sensor faults can be well compensated as long as the estimation is good enough. Based on Section 6.1, the control gain K can be selected to make $A + BK$ Hurwitz. To meet some instantaneous response requirements, the eigenvalue of $A + BK$ can be located within certain region by solving LMIs (6-1-41) to (6-1-43). Therefore, based on the designed K, we aim to determine proper observer gains such that: (i) the overall closed-loop system (6-2-7) is stochastically input-to-state stable; (ii) condition (6-1-19) is satisfied, which means the controlled output is robust against unknown perturbations.

It can be noticed that the existence of nonlinear item $\phi(t, x, u)$ and $\tilde{\phi}$ in plant (6-2-7) make the linear method to design observer gain not applicable. In consequence, when we design observer gain L_1, additional technique should be employed to deal with the nonlinearities.

Lemma 6.2.1 ([125])

For any matrices $M \in \mathcal{R}^{s\times t}, N \in \mathcal{R}^{t\times s}$, a time-varying matrix $F(t) \in \mathcal{R}^{t\times t}$ with $\|F(t)\| \leq 1$ and any scalar $\varepsilon > 0$, we have:

$$MF(t)N + N^T F^T(t) M^T \leq \varepsilon^{-1} M M^T + \varepsilon N^T N \tag{6-2-8}$$

Lemma 6.2.2 (Schur complement, [126])

Let $S = \begin{bmatrix} S_{11} & S_{12} \\ * & S_{22} \end{bmatrix}$ be a symmetric matrix. $S < 0$ is equivalent to $S_{22} < 0$ and $S_{11} - S_{12} S_{22}^{-1} S_{12}^T < 0$.

Theorem 6.2.1

For system (6-2-1), there exists an unknown input observer in the form of (6-2-5), and the tolerant control laws in the form of (6-1-11) and (6-1-17), so that the closed-loop system (6-2-7) is stochastically input-to-state stable satisfying the robust performance index (6-1-19), if there exist positive definite matrices P, $\bar{P}$, Q, and $\bar{Q}$, matrix Y, such that

$$\begin{bmatrix} \Xi_{11} & -PB_e + C^T D_e & PB_{d1} & PB_{d2} & P & 0 \\ * & \Xi_{22} & 0 & \bar{P}T\bar{B}_{d2} & 0 & \bar{P}T \\ * & * & -\gamma_1^2 I_{l_{d_1}} & 0 & 0 & 0 \\ * & * & * & -\gamma_2^2 I_{l_{d_2}} & 0 & 0 \\ * & * & * & * & -\varepsilon_1 I_n & 0 \\ * & * & * & * & * & -\varepsilon_2 I_{\bar{n}} \end{bmatrix} < 0 \tag{6-2-9}$$

and

$$\bar{P}T\bar{A} + \bar{A}^T T^T \bar{P} - Y\bar{C} - \bar{C}^T Y^T + 2a\bar{P} < 0 \tag{6-2-10}$$

where

$\Xi_{11} = P(A + BK) + (A + BK)^T P + \varepsilon_1 \theta^2 + W^T P W + \bar{W}^T T^T \bar{P} T \bar{W} + C^T C,$

$\Xi_{22} = \bar{P}T\bar{A} + \bar{A}^T T\bar{P} - Y\bar{C} - \bar{C}^T Y^T + D_e^T D_e + \varepsilon_2 \theta^2 I_{\bar{n}} + \bar{Q},$

$Y = \bar{P}L_1$,

ε_1 and ε_2 are given positive scalars,

$a = \beta\theta_l, \theta_l = -\min Re[\lambda_i\,(A + BK)] > 0, i = \{1, 2, \cdots n\}$ and $\beta > 1$.

One can thus calculate $L_1 = \bar{P}^{-1}Y$.

Proof

Choosing the Lyapunov function in the form of (6-1-23), and similar to the proof of *Theorem 6.1.1*, we can know it satisfies condition (5-2-1) in *Definition 5.2.1*. Taking infinitesimal generator along the state trajectories of (6-2-7), by using It$\hat{o}$ formula, it follows that:

$$\begin{aligned}\mathcal{L}V &= \mathcal{L}V_1 + \mathcal{L}V_2\\ &= x^T[P(A + BK) + (A + BK)^T P]x - 2x^T PB_e\bar{e} + 2x^T PB_d d\\ &\quad +2x^T P\phi(t, x, u) + x^T W^T PWx + \bar{e}^T(\bar{P}R + R^T\bar{P})\bar{e}\\ &\quad +2\bar{e}^T\bar{P}T\bar{B}_{d2}d_2 + 2\bar{e}^T\bar{P}T\tilde{\phi} + x^T\bar{W}^T T^T\bar{P}T\bar{W}x \end{aligned} \tag{6-2-11}$$

According to *Lemma 6.2.1*, we have

$$\begin{aligned}\mathcal{L}V &\le x^T[P(A + BK) + (A + BK)^T P + \varepsilon_1\theta^2 I_n + \varepsilon_1^{-1}PP]x - 2x^T PB_e\bar{e}\\ &\quad +x^T W^T PWx + 2x^T PB_d d + \bar{e}^T(\bar{P}R + R^T\bar{P} + \varepsilon_2\theta^2 I_{\bar{n}} + \varepsilon_2^{-1}\bar{P}TT^T\bar{P})\bar{e}\\ &\quad +2\bar{e}^T\bar{P}T\bar{B}_{d2}d_2 + x^T\bar{W}^T T^T\bar{P}T\bar{W}x\}\\ &= \mathbb{E}\{x^T[P(A + BK) + (A + BK)^T P + \varepsilon_1\theta^2 I_n + \varepsilon_1^{-1}PP + Q\\ &\quad +W^T PW + \bar{W}^T T^T\bar{P}T\bar{W}]x - 2x^T PB_e\bar{e}\\ &\quad +\bar{e}^T(\bar{P}R + R^T\bar{P} + \varepsilon_2\theta^2 I_{\bar{n}} + \varepsilon_2^{-1}\bar{P}TT^T\bar{P} + \bar{Q})\bar{e}\\ &\quad +2x^T PB_d d + 2\bar{e}^T\bar{P}T\bar{B}_{d2}d_2 - x^T Qx - \bar{e}^T\bar{Q}\bar{e}\\ &= [x^T \quad \bar{e}^T \quad d_1^T \quad d_2^T]\Pi\begin{bmatrix} x\\ \bar{e}\\ d_1\\ d_2\end{bmatrix} - x^T Qx - \bar{e}^T\bar{Q}\bar{e} + \gamma_1^2 d_1^T d_1 + \gamma_2^2 d_2^T d_2 \end{aligned} \tag{6-2-12}$$

where

$$\Pi = \begin{bmatrix} \Pi_{11} & -PB_e & PB_{d1} & PB_{d2} \\ * & \Pi_{22} & 0 & \bar{P}T\bar{B}_{d2} \\ * & * & -\gamma_1^2 I_{l_{d_1}} & 0 \\ * & * & * & -\gamma_2^2 I_{l_{d_2}} \end{bmatrix}$$

$\Pi_{11} = P(A+BK) + (A+BK)^T P + \varepsilon_1\theta^2 I_n + \varepsilon_1^{-1}PP + W^T PW + \bar{W}^T T^T \bar{P} T\bar{W} + Q$, $\Pi_{22} = \bar{P}T\bar{A} + \bar{A}^T T\bar{P} - \bar{P}L_1\bar{C} - \bar{C}^T L_1^T \bar{P} + \varepsilon_2\theta^2 I_{\bar{n}} + \varepsilon_2^{-1}\bar{P}TT^T\bar{P} + \bar{Q}$, ε_1 and ε_2 are given positive scalars.

From LMI (6-2-9), we can see $\Pi < 0$, indicating

$$\mathcal{L}V \le -x^T Qx - \bar{e}^T \bar{Q}\bar{e} + \gamma_1^2 d_1^T d_1 + \gamma_2^2 d_2^T d_2$$
$$= -\tilde{x}^T \tilde{Q}\tilde{x} + \gamma_1^2 d_1^T d_1 + \gamma_2^2 d_2^T d_2 \qquad (6\text{-}2\text{-}13)$$

A positive scalar $\bar{\lambda}$ can be found such that

$$\mathcal{L}V \le -\bar{\lambda}\|\tilde{x}\|^2 + \gamma_1^2|d_1|^2 + \gamma_2^2|d_2|^2 \qquad (6\text{-}2\text{-}14)$$

According to *Theorem 5.3.1*, system (6-2-7) is is stochastically input-to-state stable with $\psi_3(\tilde{x}) = \bar{\lambda}\|\tilde{x}\|^2$ and $\psi_4(|d|) = \gamma_1^2|d_1|^2 + \gamma_2^2|d_2|^2$.

In terms of the robustness of tolerant control, we can calculate that

$$\Gamma = \mathbb{E}\{\int_0^{Tf} [y_c^T(\tau)y_c(\tau) - \gamma_1^2 d_1^T(\tau)d_1(\tau) - \gamma_2^2 d_2^T(\tau)d_2(\tau)]d\tau\}$$

$$\le \mathbb{E}\{\int_0^{Tf}[x^T \quad \bar{e}^T \quad d_1^T \quad d_2^T]\,\Lambda \begin{bmatrix} x \\ \bar{e} \\ d_1 \\ d_2 \end{bmatrix} d\tau\} - \mathbb{E}(\int_0^{Tf} \mathcal{L}V\, d\tau) \qquad (6\text{-}2\text{-}15)$$

where

$$\Lambda = \begin{bmatrix} \Lambda_{11} & -PB_e + C^T D_e & PB_{d1} & PB_{d2} \\ * & \Lambda_{22} & 0 & \bar{P}T\bar{B}_{d2} \\ * & * & -\gamma_1^2 I_{l_{d_1}} & 0 \\ * & * & * & -\gamma_2^2 I_{l_{d_2}} \end{bmatrix}$$

$$\Lambda_{11} = P(A+BK) + (A+BK)^T P + \varepsilon_1\theta^2 I_n + \varepsilon_1^{-1}PP + W^T PW + \bar{W}^T T^T \bar{P} T\bar{W} + C^T C,$$

$$\Lambda_{22} = \bar{P}T\bar{A} + \bar{A}^T T\bar{P} - \bar{P}L_1\bar{C} - \bar{C}^T L_1^T \bar{P} + D_e^T D_e + \varepsilon_2\theta^2 I_{\bar{n}} + \varepsilon_2^{-1}\bar{P}TT^T\bar{P}.$$

Since $\mathbb{E}\left(\int_0^{Tf} \mathcal{L}V\, d\tau\right) > 0$, if $\Lambda < 0$, we can get $\Gamma < 0$, leading to $\mathbb{E}\left(\|y_c\|_{Tf}^2\right) < \gamma_1^2\mathbb{E}\left(\|d_1\|_{Tf}^2\right) + \gamma_2^2\mathbb{E}\left(\|d_2\|_{Tf}^2\right)$. Nevertheless, it is noted that $\Lambda < 0$ is not linear and difficult to be solved. According to *Lemma 6.2.2,* and using $Y = \bar{P}L_1$, $\Lambda < 0$ is equivalent with LMI (6-2-9). As a results, LMI (6-2-9) can guarantee the stochastically input-to-state stability of system (6-2-7) and robust fault tolerant control requirement (6-1-19).

Similar to *Theorem 6.1.1*, condition (6-2-10) is to guarantee that the convergence speed of estimation error dynamics is faster than that of the control system dynamics. This completes the proof.

Now, we can conclude the design procedure of the robust fault estimation and fault tolerant control strategies for stochastic Lipschitz nonlinear systems.

Procedure 6.2.1 *(Fault tolerant control algorithm by integrating state/fault estimation and signal compensation for stochastic Lipschitz nonlinear systems)*

i) Construct the augmented system in the form of (6-2-3) for system (6-2-1).
ii) Select observer gains H and T following step ii) in *Procedure 6.1.1*.
iii) Design control gain K in the same way with step iii) in *Procedure 6.1.1*.
iv) Solve the LMIs (6-2-9) and (6-2-10) to obtain P, Q, $\bar{P}$, $\bar{Q}$ and matrix Y. The observer gain is thus calculated as $L_1 = \bar{P}^{-1}Y$.
v) Calculate the other observer gains R and L_2 following the formulas (6-2-6) and (6-2-8), respectively.
vi) Implement the robust unknown input observer (6-2-5) to produce the augmented estimate $\hat{\bar{x}}$, leading to the simultaneous estimates of the system states and faults $\hat{x}$ and $\hat{f}$ in the forms of (6-1-12) and (6-1-13), respectively.
vii) Implement the tolerant control law $u = \bar{K}\hat{\bar{x}}$ and $y_c = y - D_f\hat{f}$, where $\bar{K} = [K \quad 0 \quad K_f]$ and $K_f = -B^{+}B_f$.

Example 6.2.1

Considered the three-tank system modelled in [150] affected by the Brownian motion and nonlinear perturbation term:

$$\begin{cases} dh_1 = \left[-\frac{1}{S_a}az_1S_n\sqrt{2g(h_1^* - h_3^*)} + \frac{1}{S_a}q_1\right]dt + 0.03h_1dw \\ dh_2 = \left[\frac{1}{S_a}az_3S_n\sqrt{2g(h_3^* - h_2^*)} - \frac{1}{S_a}az_2S_n\sqrt{2gh_2^*} + \frac{1}{S_a}q_2\right]dt + 0.01h_2dw \\ dh_3 = \left[\frac{1}{S_a}az_1S_n\sqrt{2g(h_1^* - h_3^*)} - \frac{1}{S_a}az_3S_n\sqrt{2g(h_3^* - h_2^*)} + \frac{1}{S_a}q_3 + 0.05\sin(h_3)\right]dt + 0.05h_3dw \end{cases} \tag{6-2-16}$$

where $\forall i = 1, 2, 3$, h_i represent the liquid level (in m) of the three tanks; q_i are supplying flow rates (in m^3/s) of the three pumps; az_i are outflow coefficients taking values of 0.48, 0.5 and 0.58, respectively; $S_a = 0.0154m^2$ and $S_n = 5 \times 10^{-5}m^2$ are the cross sections; $[h_1^* \quad h_2^* \quad h_3^*]^T = [0.4890 \quad 0.2332 \quad 0.3611]^T$ is an equilibrium point under a nominal control law which is not in our concern.

When the system is subjected to faults and unknown inputs, it can be represented by plant (6-2-1), where $x = [h_1 \quad h_2 \quad h_3]^T$ with initial value $x_0 = [0.4890 \quad 0.2332 \quad 0.3611\ ]^T$ corrupted by random noises; $u = [q_1 \quad q_2 \quad q_3]^T$ with reference input of $[38 \times 10^{-6} \quad 24 \times 10^{-6} \quad 0]^T$; $d = [d_1 \quad d_2 \quad d_3]^T$, d_1, d_2 and d_3 are random signals with range from -10^{-6} to 10^{-6}; $f = [f_{a1} \quad f_{a2}]^T$, and actuator faults f_{a1} and f_{a2} are 50% loss of actuation effectiveness for pump 1 (from 25sec. to 50 sec.) and pump 2 (from 60sec. to 100sec.), respectively; $\phi(x) = [0 \quad 0 \quad 0.05\sin(x_3)]^T$, and the coefficients are as follows:

$$A = \begin{bmatrix} -0.0096 & 0 & 0.0096 \\ 0 & 0.0042 & 0.0117 \\ 0.0096 & 0.0117 & -0.0020 \end{bmatrix}, B = \begin{bmatrix} 64.935 & 0 & 0 \\ 0 & 64.935 & 0 \\ 0 & 0 & 64.935 \end{bmatrix},$$

$$C = \begin{bmatrix} 1 & 0 & 0 \\ 0 & 1 & 0 \\ 0 & 0 & 1 \end{bmatrix},\ W = \begin{bmatrix} 0.03 & 0 & 0 \\ 0 & 0.01 & 0 \\ 0 & 0 & 0.05 \end{bmatrix}, B_f = \begin{bmatrix} 64.935 & 0 \\ 0 & 64.935 \\ 0 & 0 \end{bmatrix},$$

$$B_d = \begin{bmatrix} 0.3 & -0.1 & 0.05 \\ -0.1 & -0.2 & 0.1 \\ -0.2 & -0.04 & 0.02 \end{bmatrix} \text{ and } D_f = \begin{bmatrix} 0 & 0 \\ 0 & 0 \\ 0 & 0 \end{bmatrix}.$$

It is obvious that

$$|\phi(x)| \le 0.05|x - \hat{x}| \tag{6-2-17}$$

So $\phi(x)$ satisfy Lipschitz condtion with $\theta = 0.05$. Select $\mathcal{D}(c, \mu, \delta) = \mathcal{D}(0.25, 2, 60)$ as the region of poles for the plant after implementing control input. Solving LMIs (6-1-41) to (6-1-43), we can obtain observer gain

$$K = \begin{bmatrix} -0.0156 & 0 & -0.0001 \\ 0 & -0.0158 & -0.0002 \\ -0.0001 & -0.0002 & -0.0157 \end{bmatrix}$$

and $\min Re[\lambda_i\,(A + BK)] = -1.0235$. Let $\beta = 2.5$, then $a = 2.5587$. Selecting $\gamma_1 = 1$ and $\gamma_2 = 0.5$, and substituting θ, K and a to the LMIs (6-2-9) and (6-2-10), the observer gain L_1 can be calculated as

$$L_1 = \begin{bmatrix} 38.0427 & 97.8116 & -3.9286 \\ 106.443 & 347.199 & 8.4629 \\ 1.4897 & 25.4615 & 13.7447 \\ 67.869 & 31.2794 & -86.7459 \\ 43.5794 & 193.563 & 28.1524 \\ 19.2956 & 11.5666 & -23.3783 \\ 16.9729 & 70.1258 & 8.4585 \end{bmatrix}$$

Then R and L_2 can be obtained following the formulas (6-1-6) and (6-1-8), respectively.

Using the Euler–Maruyama method to simulate the standard Brownian motion, one can obtain the simulated curves of the stochastic state responses (here we give 15 state trajectories). We employ the controller $u = \overline{K}_0\hat{\bar{x}} + K_p(Cx^* - y_c)$, where K_p is selected as $\begin{bmatrix} 0.0158 & 0 & 0 \\ 0 & 0.0158 & 0 \\ 0 & 0 & 0.0158 \end{bmatrix}$ to drive the trajectory of the state to the equilibrium point x^*, $\overline{K}_0 = [K_0 \quad 0 \quad K_f]$, and $K_0 = K + K_pC$. The curves displayed in Figures 6.2.1 and 6.2.2 exhibit the estimation performance for full system states and the means of actuator faults after implementing the designed estimator-based fault tolerant control method, respectively. Figures 6.2.3 and 6.2.4 show the system outputs with signal compensation and without signal compensation.

From the Figures 6.2.1 and 6.2.2, we can see that both system states and the two actuator faults can be estimated robustly, and the influences of unknown inputs have been attenuated successfully. By comparison of Figures 6.2.3 and 6.2.4, we can find the actuator faults will make deviation of the liquid levels, however, based on accurate estimates of faults, the deviation can be compensated by the proposed fault tolerant control strategy. The differences of tank 1 and tank 2 are more distinguished than tank 3 because the loss of actuation effectiveness occurs in tank 1 and tank 2, hence influences more on the liquid levels of tank 1 and 2 than that of tank 3.

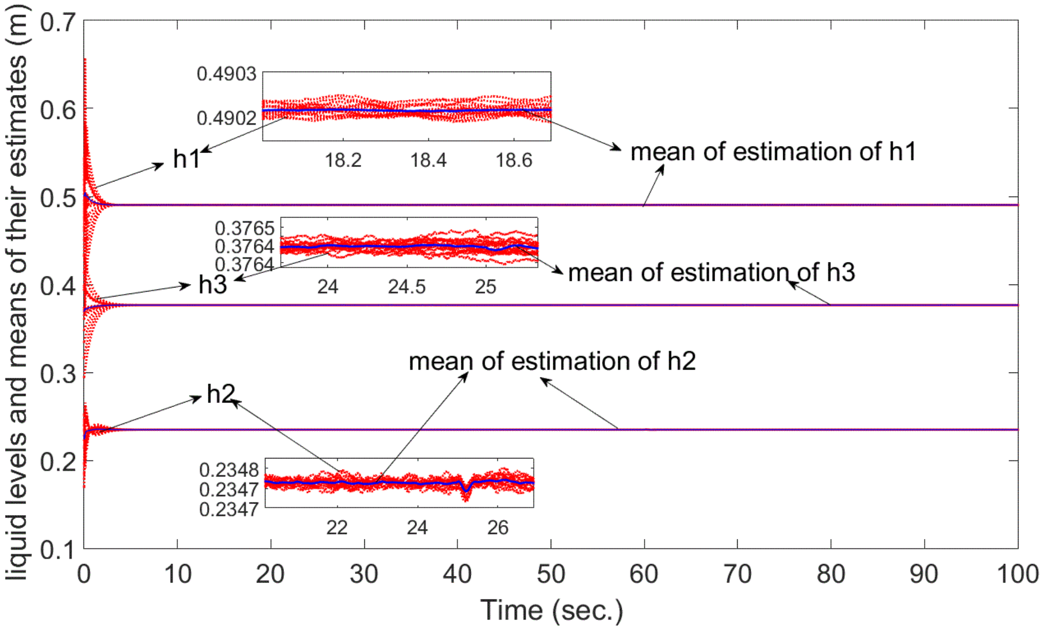

Figure 6.2.1. System states and means of their estimates: three-tank system.

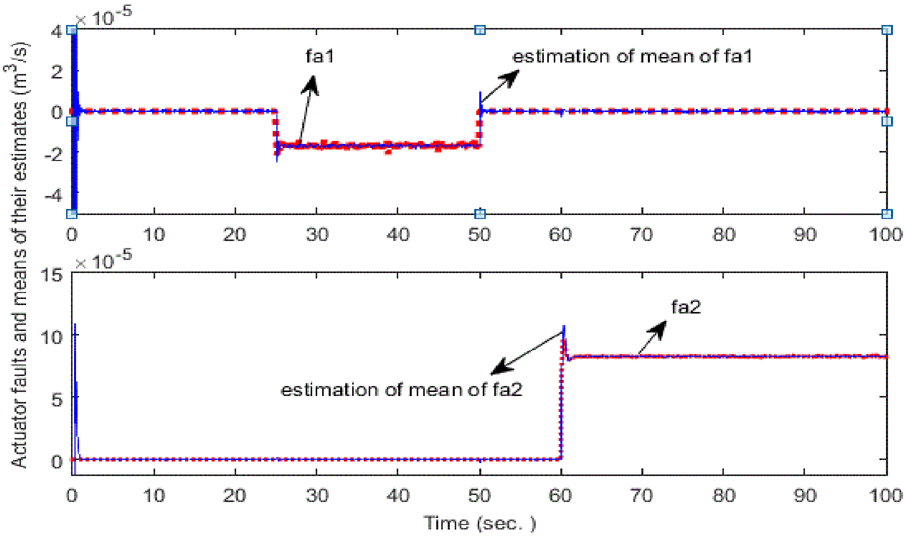

Figure 6.2.2. Actuator faults and estimates of their means: three-tank system.

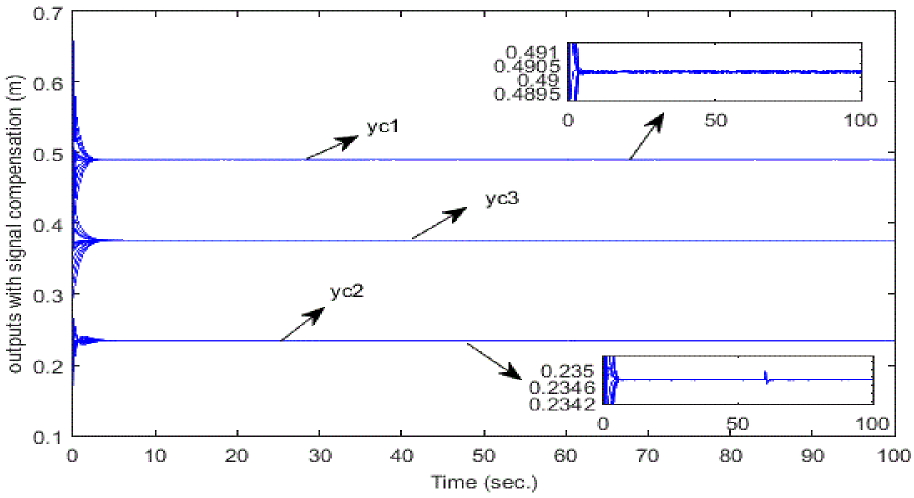

Figure 6.2.3. System outputs with signal compensation: three-tank system.

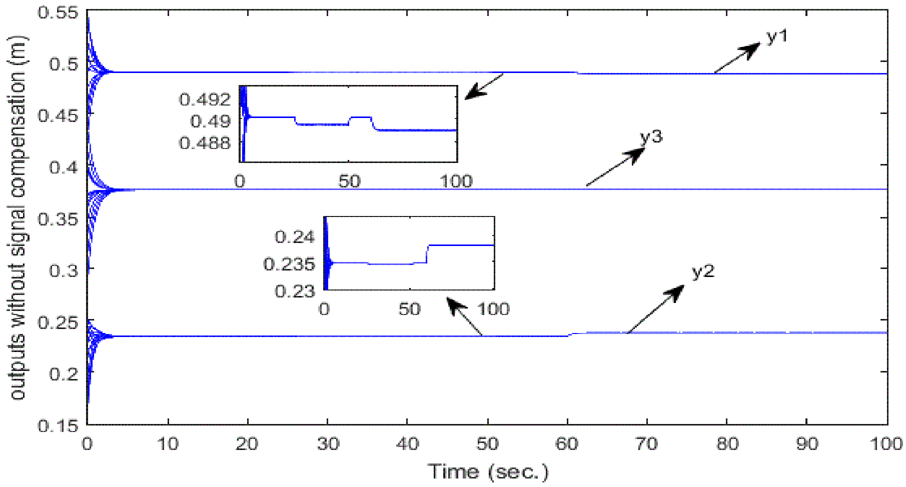

Figure 6.2.4. System outputs without signal compensation: three-tank system.

6.3 Integrated fault tolerant control of quadratic inner-bounded nonlinear stochastic system

In Section 6.2, we consider robust fault tolerant control for Lipschitz stochastic nonlinear systems. In some real plants, the nonlinear items cannot satisfy Lipschitz condition. Recently, one-side Lipschitz systems which are more general than Lipschitz ones have drawn our attention. In this section, we consider robust fault tolerant control for quadratic inner-bounded stochastic nonlinear systems, which describe a more general case than the two above mentioned classes of models. The systems under consideration can be represented in the following form:

$$\begin{cases} dx = [Ax + Bu + B_d d + B_f f + g(t, x, u)]\, dt + Wx dw \\ y = Cx + D_f f \end{cases} \tag{6-3-1}$$

where $g(t,x,u) \in \mathcal{R}^n$ is a nonlinear function satisfies $g(t,0,u) = 0$, and the following conditions:

(i) $\|g(t,x,u)\| < c[1 + \|x\|]$ (6-3-2)

(ii) $\|g(t_1,x_1,u_1) - g(t_2,x_2,u_2)\|^2$

$$\leq \rho_1\|x_1 - x_2\|^2 + \rho_2\langle x_1 - x_2, g(t_1,x_1,u_1) - g(t_2,x_2,u_2)\rangle \quad (6\text{-}3\text{-}3)$$

where $\rho_1, \rho_2 \in \mathcal{R}$, $c > 0$.

Remark 6.3.1

The above assumptions for $g(t,x,u)$ implies that $\forall x_0 \in \mathcal{R}^n$, system (6-3-1) has a path-wise strong solution, and $g(t,x,u)$ is quadratic inner-bounded. The constants ρ_1, ρ_2 can be positive, negative or zero. When $\rho_1 > 0$ and $\rho_2 = 0$, condition (6-3-3) is equivalent to the Lipschitz condition, which means Lipschitz nonlinear system is a specific scenario of quadratic inner-bounded nonlinear system.

For plant (6-3-1), we can construct the following augmented system by representing the means of faults as a part of states:

$$\begin{cases} d\bar{x} = [\bar{A}\bar{x} + \bar{B}u + \bar{B}_d d + \bar{g}(t,x,u)]dt + \bar{W}xdw \\ y = \bar{C}\bar{x} \end{cases} \quad (6\text{-}3\text{-}4)$$

where $\bar{g}(t,x,u) = \begin{bmatrix} g(t,x,u)^T & 0_{1\times l_f} & 0_{1\times l_f} \end{bmatrix}^T \in \mathcal{R}^{\bar{n}}$and other symbols are the same as the above sections.

An unknown input observer in the following form can be designed for (6-3-4):

$$\begin{cases} d\bar{z} = [R\bar{z} + T\bar{B}u + (L_1 + L_2)y + T\bar{g}(t,\hat{x},u)]dt \\ \hat{\bar{x}} = \bar{z} + Hy \end{cases} \quad (6\text{-}3\text{-}5)$$

Let the estimation error be $\bar{e} = \bar{x} - \hat{\bar{x}}$, and $\tilde{g} = (t,x,u) - \bar{g}(t,\hat{x},u)$, we can derive the following error dynamic if conditions (6-1-5) to (6-1-8) hold:

$$d\bar{e} = [R\bar{e} + T\bar{B}_{d2}d_2 + T\tilde{g}]dt + T\bar{W}xdw \quad (6\text{-}3\text{-}6)$$

Substituting (6-1-11) into system (6-3-1) and using the compensated measurement output y_c to replace the actual measurement y, the following closed-loop system can be established

$$\begin{cases} dx = [(A + BK)x - B_e\bar{e} + B_d d + g(t, x, u)]dt + Wxdw \\ d\bar{e} = [R\bar{e} + T\bar{B}_{d2}d_2 + T\tilde{g}]dt + T\bar{W}xdw \\ y_c = Cx + D_e\bar{e} \end{cases} \tag{6-3-7}$$

Since Lipschitz condition (6-2-2) fail to capture the nonlinear features of $g(t, x, u)$, LMIs (6-2-9) and (6-2-10) are invalid for the robust fault tolerant control design. Hence, the design of observer-based fault tolerant control become more challenging and require alternative techniques. For closed-loop system (6-3-7), we firstly design K as in the aforementioned ways in section 6.1 and 6.2. Then, we can employ the following theorem to achieve the stochastic stability and the robustness requirement.

Theorem 6.3.1

For system (6-3-1), there exists an unknown input observer in the form of (6-3-5), and the tolerant control laws in the form of (6-1-11) and (6-1-17), so that the closed-loop system (6-3-7) is stochastically input-to-state stable and satisfy the robust performance index (6-1-19), if there exist positive definite matrices P, $\bar{P}$, Q, and $\bar{Q}$, matrix Y , positive scalars τ_1 and τ_2, such that

$$\begin{bmatrix} \Theta_{11} & -PB_e + C^T D_e & P + \tau_1\rho_2 I_n & 0 & PB_{d1} & PB_{d2} \\ * & \Theta_{22} & 0 & \bar{P}T + \tau_2\rho_2 J_0^T J_0 & 0 & \bar{P}T\bar{B}_{d2} \\ * & * & -2\tau_1 I_n & 0 & 0 & 0 \\ * & * & * & -2\tau_2 I_{\bar{n}} & 0 & 0 \\ * & * & * & * & -\gamma_1^2 I_{l_{d_1}} & 0 \\ * & * & * & * & * & -\gamma_2^2 I_{l_{d_2}} \end{bmatrix} < 0 \tag{6-3-8}$$

and

$$\bar{P}T\bar{A} + \bar{A}^T T^T \bar{P} - Y\bar{C} - \bar{C}^T Y^T + 2a\bar{P} < 0 \tag{6-3-9}$$

where

$\Theta_{11} = P(A + BK) + (A + BK)^T P + W^T PW + \bar{W}^T T^T \bar{P} T\bar{W} + 2\tau_1\rho_1 I_n + Q + C^T C,$

$\Theta_{22} = \bar{P}T\bar{A} + \bar{A}^T T^T \bar{P} - Y\bar{C} - \bar{C}^T Y^T + 2\tau_2\rho_1 J_0^T J_0 + \bar{Q} + D_e^T D_e,$

$Y = \bar{P}L_1;$

$a = \beta\theta_l, \theta_l = -\min Re[\lambda_i\,(A + BK)] > 0, i = \{1, 2, \cdots n\}$ and $\beta > 1$.

One can thus calculate $L_1 = \bar{P}^{-1}Y$.

Proof

Choosing the Lyapunov function in the form of (6-1-23), and with the same proof manner of *Theorem 6.1.1*, we can know it satisfies condition (5-2-1) in *Definition 5.2.1*. Taking the infinitesimal generator along the state trajectories of (6-3-7), by using It$\hat{o}$ formula, it follows that:

$$\begin{aligned}\mathcal{L}V &= x^T[P(A+BK)+(A+BK)^TP+W^TPW+\bar{W}^TT^T\bar{P}T\bar{W}]x-2x^TPB_e\bar{e}\\ &\quad +2x^TPB_dd+2x^TPg(t,x,u)+\bar{e}^T(\bar{P}R+R^T\bar{P})\bar{e}+2\bar{e}^T\bar{P}T\bar{B}_{d2}d_2\\ &\quad +2\bar{e}^T\bar{P}T\tilde{g}\end{aligned} \tag{6-3-10}$$

Condition (6-3-3) implies that

$$\rho_1x^Tx+\rho_2x^Tg(t,x,u)-g^T(t,x,u)g(t,x,u)\geq 0 \tag{6-3-11}$$

We also have

$$\begin{aligned}\tilde{g}^T\tilde{g} &= \|\bar{g}(t,x,u)-\bar{g}(t,\hat{x},u)\|^2\\ &= \left\|\begin{bmatrix} g(t,x,u)-g(t,\hat{x},u)\\ 0_{l_f\times 1}\\ 0_{l_f\times 1}\end{bmatrix}\right\|^2\\ &= \|g(t,x,u)-g(t,\hat{x},u)\|^2\\ &\leq \rho_1\|x-\hat{x}\|^2+\rho_2\langle x-\hat{x},g(t,x,u)-g(t,\hat{x},u)\rangle\end{aligned} \tag{6-3-12}$$

Since

$$\|x-\hat{x}\|^2=\|J_0\bar{e}\|^2=\bar{e}^TJ_0^TJ_0\bar{e} \tag{6-3-13}$$

and

$$\langle x-\hat{x},g(t,x,u)-g(t,\hat{x},u)\rangle=\bar{e}^TJ_0^TJ_0\tilde{g} \tag{6-3-14}$$

we can obtain

$$\tilde{g}^T\tilde{g}\leq\rho_1\bar{e}^TJ_0^TJ_0\bar{e}+\rho_2\bar{e}^TJ_0^TJ_0\tilde{g} \tag{6-3-15}$$

Hence, based on (6-3-11) and (6-3-15), for any positive scalars τ_1, τ_2, we have

$$2\tau_1\big(\rho_1x^Tx+\rho_2x^Tg(t,x,u)-g^T(t,x,u)g(t,x,u)\big)\geq 0 \tag{6-3-16}$$

and

$$2\tau_2(\rho_1\bar{e}^TJ_0^TJ_0\bar{e}+\rho_2\bar{e}^TJ_0^TJ_0\tilde{g}-\tilde{g}^T\tilde{g})\geq 0 \tag{6-3-17}$$

Adding (6-3-16) and (6-3-17) to the right side of (6-3-10), we can derive:

$$
\begin{aligned}
\mathcal{L}V \leq\ & x^T[P(A+BK)+(A+BK)^TP+W^TPW+\bar{W}^TT^T\bar{P}T\bar{W}+2\tau_1\rho_1 I_n+Q]x \\
& -2x^TPB_e\bar{e}+2x^TPB_dd+2x^T(P+\tau_1\rho_2 I_n)g(t,x,u) \\
& +\bar{e}^T(\bar{P}R+R^T\bar{P}+2\tau_2\rho_1 J_0^TJ_0+\bar{Q})\bar{e}+2\bar{e}^T\bar{P}T\bar{B}_{d2}d_2 \\
& +2\bar{e}^T(\bar{P}T+\tau_2\rho_2 J_0^TJ_0)\tilde{g}-2\tau_1 g^Tg-2\tau_2\tilde{g}^T\tilde{g}-x^TQx-\bar{e}^T\bar{Q}\bar{e} \\
=\ & [x^T \quad \bar{e}^T \quad g^T \quad \tilde{g}^T \quad d_1^T \quad d_2^T]\,\Phi\begin{bmatrix} x \\ \bar{e} \\ g \\ \tilde{g} \\ d_1 \\ d_2 \end{bmatrix}-x^TQx-\bar{e}^T\bar{Q}\bar{e}+\gamma_1^2 d_1^Td_1+\gamma_2^2 d_2^Td_2
\end{aligned}
$$

(6-3-18)

where

$$
\Phi=\begin{bmatrix}
\Phi_{11} & -PB_e & P+\tau_1\rho_2 I_n & 0 & PB_{d1} & PB_{d2} \\
* & \Phi_{22} & 0 & \bar{P}T+\tau_2\rho_2 J_0^TJ_0 & 0 & \bar{P}T\bar{B}_{d2} \\
* & * & -2\tau_1 I_n & 0 & 0 & 0 \\
* & * & * & -2\tau_2 I_{\bar{n}} & 0 & 0 \\
* & * & * & * & -\gamma_1^2 I_{l_{d_1}} & 0 \\
* & * & * & * & * & -\gamma_2^2 I_{l_{d_2}}
\end{bmatrix}
$$

$$\Phi_{11}=P(A+BK)+(A+BK)^TP+W^TPW+\bar{W}^TT^T\bar{P}T\bar{W}+2\tau_1\rho_1 I_n+Q$$

$$\Phi_{22}=\bar{P}T\bar{A}+\bar{A}^TT^T\bar{P}-\bar{P}L_1\bar{C}-\bar{C}^TL_1^T\bar{P}^T+2\tau_2\rho_1 J_0^TJ_0+\bar{Q}.$$

From the LMI (6-3-8), one has

$$\Phi<0 \tag{6-3-19}$$

which indicates we can find a positive scalar $\bar{\lambda}$ such that

$$
\begin{aligned}
\mathcal{L}V &\leq -x^TQx-\bar{e}^T\bar{Q}\bar{e}+\gamma_1^2 d_1^Td_1+\gamma_2^2 d_2^Td_2 \\
&\leq -\bar{\lambda}\,\|\tilde{x}\|^2+\gamma_1^2|d_1|^2+\gamma_2^2|d_2|^2
\end{aligned} \tag{6-3-20}
$$

As a result, we can conclude the closed-loop system (6-3-7) is stochastically input-to-state sable with $\psi_3(\tilde{x})=\bar{\lambda}\|\tilde{x}\|^2$ and $\psi_4(|d|)=\gamma_1^2|d_1|^2+\gamma_2^2|d_2|^2$.

Now it is ready to discuss the robustness of the observer-based fault tolerant control:

$$\Gamma=\mathbb{E}\{\int_0^{Tf}[y_c^T(\tau)y_c(\tau)-\gamma_1^2 d_1^T(\tau)d_1(\tau)-\gamma_2^2 d_2^T(\tau)d_2(\tau)]d\tau\}$$

$$\leq \mathbb{E}\{\int_0^{Tf}[x^T \quad \bar{e}^T \quad g^T \quad \tilde{g}^T \quad d_1^T \quad d_2^T]\,\Theta\begin{bmatrix} x \\ \bar{e} \\ g \\ \tilde{g} \\ d_1 \\ d_2 \end{bmatrix} - x^T(\tau)Qx(\tau) - \bar{e}^T(\tau)\bar{Q}\bar{e}(\tau)\}d\tau\}$$

$$-\mathbb{E}(\int_0^{Tf} \mathcal{L}V\, d\tau) \tag{6-3-21}$$

where

$$\Theta = \begin{bmatrix} \Theta_{11} & -PB_e + C^T D_e & P + \tau_1\rho_2 I_n & 0 & PB_{d1} & PB_{d2} \\ * & \Theta_{22} & 0 & \bar{P}T + \tau_2\rho_2 J_0^T J_0 & 0 & \bar{P}T\bar{B}_{d2} \\ * & * & -2\tau_1 I_n & 0 & 0 & 0 \\ * & * & * & -2\tau_2 I_{\bar{n}} & 0 & 0 \\ * & * & * & * & -\gamma_1^2 I_{l_{d_1}} & 0 \\ * & * & * & * & * & -\gamma_2^2 I_{l_{d_2}} \end{bmatrix},$$

$$\Theta_{11} = P(A+BK) + (A+BK)^T P + W^T PW + \bar{W}^T T^T \bar{P} T\bar{W} + 2\tau_1\rho_1 I_n + Q + C^T C,$$

$$\Theta_{22} = \bar{P}T\bar{A} + \bar{A}^T T^T \bar{P} - Y\bar{C} - \bar{C}^T Y^T + 2\tau_2\rho_1 J_0^T J_0 + \bar{Q} + D_e^T D_e,$$

$$Y = \bar{P}L_1.$$

We know $\Theta < 0$ from the LMI (6-3-8) and $\mathbb{E}(\int_0^{Tf} \mathcal{L}V\, d\tau) > 0$, thus we have $\Gamma < 0$, which indicates the performance (6-1-19) can be satisfied. Similar to *Theorems 6.1.1* and *6.2.1*, the LMI (6-3-9) implies the response of the estimation error dynamics is faster than that of the system dynamics.

The proof is completed.

Remark 6.3.2

Since Lipschitz nonlinear condition is a specific scenario of the quadratic inner-bounded one, LMIs (6-3-8) and (6-3-9) are still suitable for application in stochastic Lipschitz nonlinear system (6-2-1), by letting $\rho_1 = \theta^2$ and $\rho_2 = 0$. In other words, LMIs (6-3-8) and (6-3-9) are alternative rules of (6-2-9) and (6-2-10) for robust tolerant control of plant (6-2-1).

Now, the design procedure of the robust fault estimation and fault tolerant control strategies for stochastic quadratic inner-bounded nonlinear systems can be summarized as follows:

Procedure 6.3.1 *(Fault tolerant control algorithm by integrating state/fault estimation and signal compensation for stochastic quadratic inner-bounded nonlinear systems)*

i) Construct the augmented system in the form of (6-3-4) for system (6-3-1).

ii) Select observer gains H and T following step ii) in *Procedure 6.1.1*.

iii) Design control gain K in the same way with step iii) in *Procedure 6.1.1*.

iv) Solve the LMIs (6-3-8) and (6-3-9) to obtain P, Q, $\bar{P}$, $\bar{Q}$ and matrix Y. The observer gain is thus calculated as $L_1 = \bar{P}^{-1}Y$.

v) Calculate the other observer gains R and L_2 following the formulas (6-1-6) and (6-1-8), respectively.

vi) Implement the robust unknown input observer (6-3-5) to produce the augmented estimate $\hat{\bar{x}}$, leading to the simultaneous estimates of the system states and faults $\hat{x}$ and $\hat{f}$ in the forms of (6-1-12) and (6-1-13), respectively.

vii) Implement the tolerant control law $u = \bar{K}\hat{\bar{x}}$ and $y_c = y - D_f\hat{f}$, where $\bar{K} = [K \quad 0 \quad K_f]$ and $K_f = -B^{+}B_f$.

Example 6.3.1 *(A quadratic inner-bounded nonlinear system)*

In this example, we apply the robust observer-based controller to nonlinear system. The considered plant is in the form of (6-3-1) with the following parameters:

$$A = \begin{bmatrix} 1 & 3 & 1 \\ 2 & 0 & 3 \\ 0 & 2 & 5 \end{bmatrix}, B = \begin{bmatrix} 1 \\ 0 \\ 0 \end{bmatrix}, C = \begin{bmatrix} 1 & 0 & 0 \\ 0 & 1 & 0 \\ 0 & 0 & 1 \end{bmatrix},$$

$$W = \begin{bmatrix} 0.03 & 0 & -0.02 \\ 0 & 0.01 & 0.04 \\ 0.05 & 0 & 0.01 \end{bmatrix}, B_d = \begin{bmatrix} 0.3 & 0.1 & -0.02 \\ -0.1 & -0.2 & 0.04 \\ -0.15 & -0.4 & 0.08 \end{bmatrix},$$

$$g(x) = \begin{bmatrix} -0.1x_1(x_1^2 + x_2^2 + x_3^2) \\ -0.1x_2(x_1^2 + x_2^2 + x_3^2) \\ -0.1x_3(x_1^2 + x_2^2 + x_3^2) \end{bmatrix}, \; B_{f_a} = B, D_{f_s} = \begin{bmatrix} 1 \\ 0 \\ 0 \end{bmatrix}.$$

In this case, $B_f = [B_{f_a} \; 0_{3\times1}]$, $D_f = [0_{3\times1} \;\; D_{f_s}]$. The reference input is given as 0.5. The actuator fault and the sensor fault are 50% loss of the actuation effectiveness from 25 sec. to 50 sec., and 30% loss of the sensor efficiency from 70 sec. to 100 sec., respectively, and the unknown input disturbances are random signals ranging from -0.01 to 0.01. The initial state value is given as $x_0 = [-0.1 \quad -0.05 \quad -0.2\ ]^T$ corrupted by random noises. Considering the set $\widetilde{D} = \{x \in R^3 : \|x\| \leq \vartheta\}$, we have $\|g(x)\| < 0.1\vartheta^2[1 + \|x\|]$. After some algebraic manipulations, we can obtain

$$\|g(x_1) - g(x_2)\|^2 = 0.01[(\|x_1\|^2 - \|x_2\|^2)^2(\|x_1\|^2 + \|x_2\|^2) + \|x_1 - x_2\|^2\|x_1\|^2\|x_2\|^2] \quad (6\text{-}3\text{-}22)$$

$$\rho_1 \|x_1 - x_2\|^2 + \rho_2\langle x_1 - x_2, g(x_1) - g(x_2)\rangle = \|x_1 - x_2\|^2 \left[\rho_1 - \frac{0.1\rho_2}{2}(\|x_1\|^2 + \|x_2\|^2)\right] - \frac{0.1\rho_2}{2}(\|x_1\|^2 - \|x_2\|^2)^2 \quad (6\text{-}3\text{-}23)$$

In order to make (6-3-3) hold, we have to find ρ_1 and ρ_2 such that

$$\|x_1\|^2 + \|x_2\|^2 \leq -5\rho_2 \quad (6\text{-}3\text{-}24)$$

$$\|x_1\|^2\|x_2\|^2 \leq 100\rho_1 + 25\rho_2^2 \quad (6\text{-}3\text{-}25)$$

hold in set $\widetilde{D}$. It suffices to have $\rho_2 \leq -0.4\vartheta^2$and $\rho_1 \geq 0.01\vartheta^4 - 0.25\rho_2^2$. For given set $\widetilde{D}$ with $\vartheta = 1.04$, which is large enough in terms of the considered system, we can find $\rho_1 = -0.0373$ and $\rho_2 = -0.44$ to make $g(x)$ satisfy the quadratic inner-bounded condition. Select $\mathcal{D}(c, \mu, \delta) = \mathcal{D}(0.2, 2.8, 55)$ as the region of poles for the original plant after implementing control input. Solving LMIs (6-1-41) to (6-1-43), we can obtain observer gain $K = [-4.7532 \quad -6.9039 \quad -10.8230]$, and $\min Re[\lambda_i\,(A + BK)] = -2.1324$. Let $\beta = 2$, then $a = 4.2648$. Selecting $\gamma_1 = 10$ and $\gamma_2 = 20$, and substituting ρ_1, ρ_2, K and a to LMIs (6-3-8) and (6-3-9), L_1 can be calculated as

$$L_1 = 10^3 \times \begin{bmatrix} 0.1800 & 2.0167 & 0.4592 \\ 0.0182 & 0.2160 & 0.0548 \\ -0.0061 & 0.0346 & 0.0632 \\ -0.1015 & 3.3422 & 2.7269 \\ -0.4043 & -4.8093 & -1.1991 \\ -0.2256 & -1.2118 & 0.3026 \\ -0.1653 & -1.9653 & -0.4700 \end{bmatrix}$$

Then R and L_2 can be obtained following the formulas (6-1-6) and (6-1-8), respectively. The choice of γ_1 and γ_2 has to make the LMI solvable. The choice $\gamma_1 = 10$ and $\gamma_2 = 20$ is the best choice to make LMI solvable and unknown inputs mitigated at mean time.

By choosing the above parameters, and using the Euler–Maruyama method to simulate the standard Brownian motions with 10 state trajectories, we can obtain Figures 6.3.1 and 6.3.2 to exhibit the estimation performance for the means of full system states, actuator fault and sensor fault, respectively. Figures 6.3.3 and 6.3.4 show the system output with and without signal compensation.

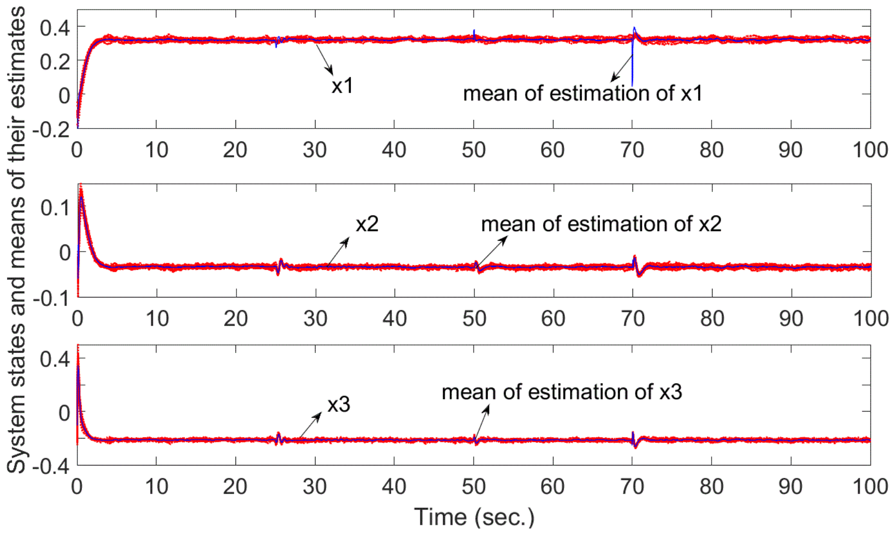

Figure 6.3.1. System states and the means of their estimates: a quadratic inner-bounded nonlinear system.

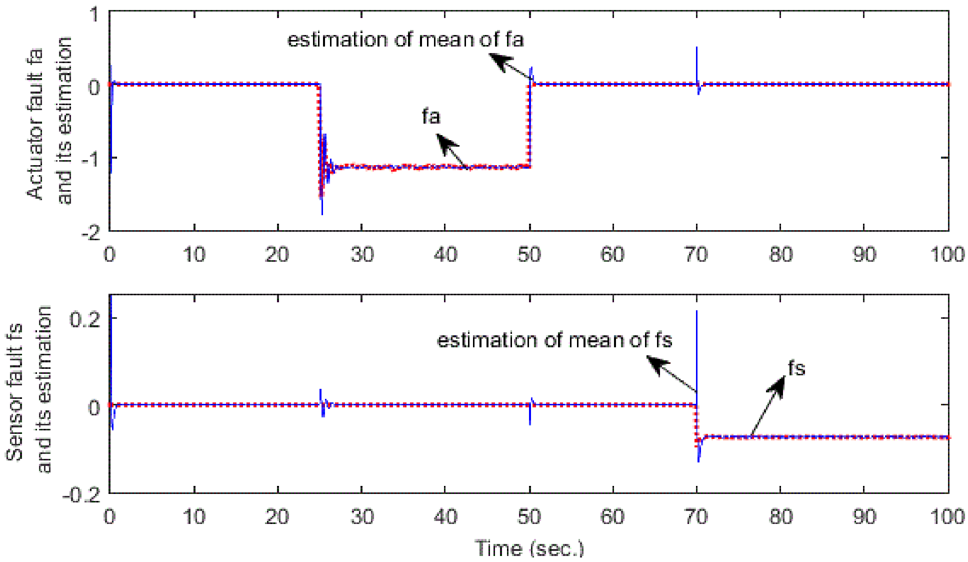

Figure 6.3.2. Faults and the estimates of their means: a quadratic inner-bounded nonlinear system.

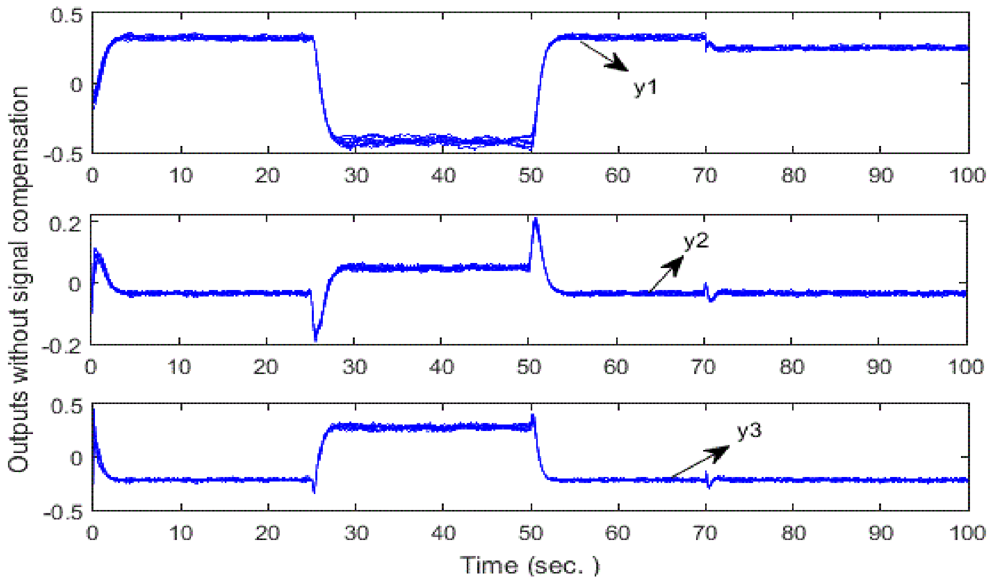

Figure 6.3.3. System outputs without tolerant control: a quadratic inner-bounded nonlinear system.

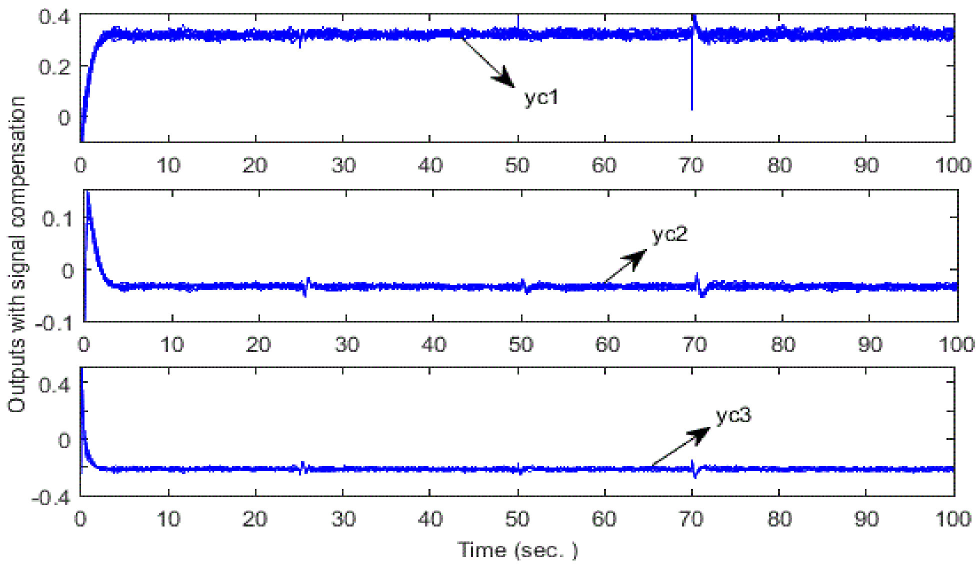

Figure 6.3.4. System outputs with tolerant control: a quadratic inner-bounded nonlinear system.

From Figures 6.3.1 and 6.3.2, the system states and the means of the concerned faults are estimated satisfactorily. Figure 6.3.3 shows the system dynamics are corrupted by the faults, while Figure 6.3.4 indicates the system performance are recovered after the fault-tolerant control.

6.4 Integrated fault tolerant control of T-S fuzzy nonlinear stochastic system

6.4.1 Joint observer techniques for robust fault estimation

Consider stochastic T-S fuzzy models suffering from faults and unknown inputs in the form of It$\hat{o}$-type differential equations as follows:

IF μ_1 is M_{1i} and $\ldots\mu_q$ is M_{qi}, THEN

$$\begin{cases} dx(t) = [A_i x + B_i u + B_{di} d + B_{fi} f]dt + W_i x dw \\ y(t) = Cx + D_f f \end{cases} \tag{6-4-1}$$

By using the standard fuzzy blending method, the global model of system (6-4-1) can be inferred as:

$$\begin{cases} dx = \sum_{i=1}^{r} h_i(\mu)\,[(A_i x + B_i u + B_{di} d + B_{fi} f)dt + W_i x dw] \\ y = Cx + D_f f \end{cases} \tag{6-4-2}$$

where $h_i(\mu)$ are membership functions, following the convex sum properties: $\sum_{i=1}^{r} h_i(\mu) = 1$ and $0 \leq h_i(\mu) \leq 1$.

Lemma 6.4.1 [48]

If there exist a function V, and positive constants c_1, c_2 and c_3, such that

$$c_1\|x\|^2 \leq V \leq c_2\|x\|^2 \tag{6-4-3}$$

and

$$\mathcal{L}V(t,x) \leq -c_3\|x\|^2 \tag{6-4-4}$$

then the solution of stochastic system (6-4-2) is stochastically exponentially stable in mean square.

Remark 6.4.1

In Section 6.1-6.3 stochastically input-to-state stability is considered for the observer-based fault tolerant control. In this section, stochastically exponentially stability in mean square, which is another popular concern for stochastic systems, is under investigation. In other words, the designed scheme is flexible with different stability requirements.

In order to estimate the means of faults and system states at the same time, an auxiliary system is constructed as follows, by considering the faults as augmented system states:

$$\begin{cases} d\bar{x} = \sum_{i=1}^{r} h_i(\mu)\,[\big(\bar{A}_i\bar{x} + \bar{B}_i u + \bar{B}_{di} d + J_1 \ddot{f}\big)dt + \bar{W}_i x dw] \\ y = \bar{C}\bar{x} \end{cases} \tag{6-4-5}$$

where

$$\bar{n} = n + 2l_f,$$

$$\bar{x} = [x^T \quad \dot{f}^T \quad f^T]^T \in \mathcal{R}^{\bar{n}}$$

$$\bar{A}_i = \begin{bmatrix} A_i & 0_{n\times l_f} & B_{fi} \\ 0_{l_f\times n} & 0_{l_f\times l_f} & 0_{l_f\times l_f} \\ 0_{l_f\times n} & I_{l_f} & 0_{l_f\times l_f} \end{bmatrix} \in \mathcal{R}^{\bar{n}\times\bar{n}},$$

$$\bar{B}_i = \begin{bmatrix} B_i^T & 0_{m\times l_f} & 0_{m\times l_f} \end{bmatrix}^T \in \mathcal{R}^{\bar{n}\times m},$$

$$\bar{B}_{di} = \begin{bmatrix} B_{di}^T & 0_{l_d\times l_f} & 0_{l_d\times l_f} \end{bmatrix}^T \in \mathcal{R}^{\bar{n}\times l_d},$$

$$\bar{C} = \begin{bmatrix} C & 0_{p\times l_f} & D_f \end{bmatrix} \in \mathcal{R}^{p\times\bar{n}},$$

$$\bar{W}_i = \begin{bmatrix} W_i^T & 0_{n\times l_f} & 0_{n\times l_f} \end{bmatrix}^T \in \mathcal{R}^{\bar{n}\times n},$$

$$J_1 = \begin{bmatrix} 0_{l_f\times n} & I_{l_f\times l_f} & 0_{l_f\times l_f} \end{bmatrix}^T \in \mathcal{R}^{\bar{n}\times l_f}$$

In system (6-4-5), the components of state vector $\bar{x}$ include original state x, the means of concerned faults, denoted by f, and the first-order differentials of the means of the faults, that is $\dot{f}$. In this section, we assume that $\ddot{f}$ is not zero but bounded and satisfies:

$$\|\ddot{f}\| \le \delta \tag{6-4-6}$$

where δ is a positive scalar. In addition, we suppose that d can be decoupled, whereas $\ddot{f}$ cannot.

For system (6-4-5), the following fuzzy unknown input observer consisting sliding mode terms is constructed:

$$\begin{cases} d\bar{z} = \sum_{i=1}^{r} h_i(\mu)[R_i\bar{z} + T\bar{B}_i u + (L_{i1} + L_{i2})y + L_{si}u_s]dt \\ \hat{\bar{x}} = \bar{z} + Hy \end{cases} \tag{6-4-7}$$

where $\bar{z}$ is a state vector of the observer (6-4-7), $\hat{\bar{x}}$ is the estimation of $\bar{x}$, u_s is a discontinuous control input to compensate the influences of $\ddot{f}$. The matrices H, R_i, T, L_{i1}, L_{i2} and L_{si}, where $i = 1, 2, \ldots r$, are observer gains to be designed such that $\hat{\bar{x}}$ is close enough to $\bar{x}$.

Remark 6.4.2

Using nonlinear discontinuous term u_s, the designed sliding mode unknown input observer constraints the trajectory of the estimation error to remain on a specific surface such that error is insensitive to the disturbances.

Defining estimation error as $\bar{e} = \bar{x} - \hat{\bar{x}}$, and subtracting (6-4-7) from (6-4-5) leads to the following error dynamic:

$$d\bar{e} = \sum_{i=1}^{r} h_i(\mu) \{\{(\bar{A}_i - H\bar{C}\bar{A}_i - L_{i1}\bar{C})\bar{e} + (\bar{A}_i - H\bar{C}\bar{A}_i - L_{i1}\bar{C} - R_i)\bar{z}$$
$$+[(\bar{A}_i - H\bar{C}\bar{A}_i - L_{i1}\bar{C})H - L_{i2}]y + [(I_{\bar{n}} - H\bar{C}) - T]\bar{B}_i u + (I_{\bar{n}} - H\bar{C})\bar{B}_{di} d$$
$$+(I_{\bar{n}} - H\bar{C})J_1\ddot{f} - L_{si}u_s\}dt + (I_{\bar{n}} - H\bar{C})\bar{W}_i x dw\} \quad (6\text{-}4\text{-}8)$$

If the observer gains satisfy the following conditions:

$$(I_{\bar{n}} - H\bar{C})\bar{B}_{di} = 0 \quad (6\text{-}4\text{-}9)$$

$$R_i = \bar{A}_i - H\bar{C}\bar{A}_i - L_{i1}\bar{C} \quad (6\text{-}4\text{-}10)$$

$$T = I_{\bar{n}} - H\bar{C} \quad (6\text{-}4\text{-}11)$$

$$L_{i2} = R_i H \quad (6\text{-}4\text{-}12)$$

the state estimation error can be reduced to

$$d\bar{e} = \sum_{i=1}^{r} h_i(\mu) [(R_i\bar{e} + TJ_1\ddot{f} - L_{si}u_s)dt + T\bar{W}_i x dw] \quad (6\text{-}4\text{-}13)$$

In order to meet the conditions (6-4-9) to (6-4-12), we have the following assumptions in terms of the references:

(1) $\operatorname{rank}\big(\bar{C}(\bar{B}_{d1}\ \ \bar{B}_{d2} \cdots\ \bar{B}_{dr})\big) = \operatorname{rank}\big((\bar{B}_{d1}\ \ \bar{B}_{d2} \cdots\ \bar{B}_{dr})\big)$;

(2) For $\forall\, i$, $\begin{bmatrix} A_i & B_{fi} & B_{di} \\ C & D_f & 0 \end{bmatrix}$ is of full column rank;

(3) For $\forall\, i$, $\operatorname{rank}\begin{bmatrix} sI_n - A_i & B_{di} \\ C & 0 \end{bmatrix} = n + l_d$.

The above assumptions are to ensure that for each local model, equation (6-4-9) can be solved, and one solution of H can be obtained as

$$H^* = \bar{B}_U[(\bar{C}\bar{B}_U)^T(\bar{C}\bar{B}_U)]^{-1}(\bar{C}\bar{B}_U)^T \quad (6\text{-}4\text{-}14)$$

where B_U is of full column rank, obtained by a non-singular matrix U such that

$$(\bar{B}_{d1}\ \ \bar{B}_{d2} \cdots\ \bar{B}_{dr})U = (\bar{B}_U\ \ 0) \quad (6\text{-}4\text{-}15)$$

Moreover, the model is observable.

Under these necessary assumptions, d has been decoupled by selecting suitable H. however, $\ddot{f}$ still affect the error dynamic. As a good observer should lead to the convergence of error $\bar{e}$, the design of robust fault estimation scheme is converted into attenuating the influences of $\ddot{f}$. Now let us discuss how to design the sliding mode controller u_s to eliminate its influence. Define a sliding mode surface

$$s = J_1^T T^T \bar{P} \bar{e} = 0 \tag{6-4-16}$$

where $\bar{P}$ is a positive matrix satisfying

$$J_1^T T^T \bar{P} = N\bar{C} \tag{6-4-17}$$

while N is a parameter matrix to be designed. The sliding surface is defined according to the desired dynamical specifications of the closed-loop error dynamic. Here, the estimation error can be driven around zero on surface (6-4-16). To make sliding mode achieve and maintain on the surface, the discontinuous input law is introduced as follows

$$u_s = (\delta + \varepsilon) sgn(s) \tag{6-4-18}$$

where ε is a parameter to be designed later.

Remark 6.4.3

Since $\bar{e}$ is unknown, s is not available from (6-4-16). Constraint (6-4-17) is introduced such that $\mathrm{s} = N\bar{C}\bar{e} = N\bar{C}\bar{x} - N\bar{C}\hat{\bar{x}} = Ny - N\bar{C}\hat{\bar{x}}$, where y and $\bar{C}\hat{\bar{x}}$ are available in practice.

It is noted that the estimation error dynamics are also subject to stochastic parameter perturbations. Therefore, it is infeasible to design the observer gain independent of the control gains. The integrated design of the observer gain and control gain will be addressed in the next section.

6.4.2 Design of observer-based control law

Now we consider the design of the control law for system (6-4-2), to compensate the effects of the faults, make the trajectories of state stable, and eliminate the influences of unknown inputs.

Firstly, we introduce the following feedback gain $\bar{K}_i = [K_i \quad 0 \quad K_f]$ and construct u in the following fuzzy form:

$$u = \sum_{i=1}^{r} h_i(\mu)\, \bar{K}_i \hat{\bar{x}}$$

$$= \sum_{i=1}^{r} h_i(\mu)\, [K_i \quad 0 \quad K_f] \begin{bmatrix} \hat{x} \\ \hat{\dot{f}} \\ \hat{f} \end{bmatrix}$$

$$= \sum_{i=1}^{r} h_i(\mu)\, (K_i \hat{x} + K_f \hat{f}) \tag{6-4-19}$$

where

$$K_f = -B_h^{+} B_{fh} \tag{6-4-20}$$

with $B_h = \sum_{i=1}^{r} h_i(\mu) B_i$, $B_{fh} = \sum_{i=1}^{r} h_i(\mu) B_{fi}$, and supposing rank$[B_h \quad B_{fh}] =$ rank B_h.

Then it is clear that

$$\sum_{i=1}^{r} h_i(\mu)\left(B_{fi} + B_i K_f\right) = B_{fh} - B_h B_h^{+} B_{fh} = 0 \tag{6-4-21}$$

In order to eliminate the effects caused by sensor faults, the following sensor compensation output are employed:

$$y_c = y - D_f J_2 \hat{\bar{x}} = Cx + D_f f - D_f \hat{f} = Cx + D_f J_2 \bar{e} \tag{6-4-22}$$

where $J_2 = \begin{bmatrix} 0_{l_f \times n} & 0_{l_f \times l_f} & I_{l_f} \end{bmatrix}$, and y_c is called reliable output.

Substituting (6-4-19) into systems (6-4-2) and using the reliable output y_c to replace the actual measurement y, the following closed-loop system can be formulated

$$\begin{cases} dx = \sum_{i=1}^{r} h_i(\mu) \sum_{i=1}^{r} h_j(\mu)\, [(\left(A_i + B_i K_j\right)x - B_{eij}\bar{e} + B_{di} d)dt + W_i x dw] \\ y_c = Cx + D_e \bar{e} \end{cases}$$

(6-4-23)

where $B_{eij} = B_i K_j J_0 - B_{fi} J_2$, $J_0 = \begin{bmatrix} I_n & 0_{n \times l_f} & 0_{n \times l_f} \end{bmatrix}$ and $D_e = D_f J_2$. It can be seen that the fault estimation performance will have an impact on the fault tolerant control performance.

Under the designed observer-based fault tolerant controller, the overall closed-loop system can be obtained as follows:

$$
\begin{cases}
dx = \sum_{i=1}^{r} h_i(\mu) \sum_{i=1}^{r} h_j(\mu) \left\{ \left[\left(A_i + B_i K_j \right) x - B_{eij} \bar{e} + B_{di} d \right] dt + W_i x dw \right\} \\
d\bar{e} = \sum_{i=1}^{r} h_i(\mu) \left[\left(R_i \bar{e} - L_{si} u_s + T J_1 \ddot{f} \right) dt + T \bar{W}_i x dw \right] \\
y_c = Cx + D_e \bar{e}
\end{cases}
$$

(6-4-24)

The next step is to choose appropriate observer and controller gains to make the closed-loop system stable, and satisfy the following performance:

$$
\mathbb{E}(\|y_c\|_{Tf}^2) < \gamma^2 \mathbb{E}(\|d\|_{Tf}^2) \tag{6-4-25}
$$

where $\gamma > 0$ is the H_∞ performance index.

For $\forall\ i$, the coefficient of sliding mode controller is chosen to be $L_{si} = TJ_1$, then we have the following theorem.

Theorem 6.4.1

For system (6-4-2), there exists a tolerant observer-based controller in the form of (6-4-7), (6-4-19) and (6-4-22), making closed-loop system (6-4-24) be stochastic exponentially stable in mean square and satisfy$\mathbb{E}(\|y_c\|_{Tf}^2) < \gamma^2 \mathbb{E}(\|d\|_{Tf}^2)$, if $\forall\ i, j$, there exist positive definite matrices $P$and $\bar{P}$, matrices K_j, and L_{i1} such that

$$
\begin{bmatrix}
\Omega_{ij11} & PB_{di} & -PB_{eij} + C^T D_e \\
* & -\gamma^2 I_{ld} & 0 \\
* & * & \Omega_{ij33}
\end{bmatrix} < 0 \tag{6-4-26}
$$

And

$$
J_1^T T^T \bar{P} = N\bar{C} \tag{6-4-27}
$$

where $\Omega_{ij11} = P\left(A_i + B_i K_j\right) + \left(A_i + B_i K_j\right)^T P + W_i^T P W_i + \bar{W}_i^T T^T \bar{P} T \bar{W}_i + C^T C$, $\Omega_{ij33} = \bar{P} T \bar{A}_i + \bar{A}_i^T T^T \bar{P} - \bar{P} L_{i1} \bar{C} - \bar{C}^T L_{i1}^T \bar{P} + D_e^T D_e$, and $i, j = 1,2, \ldots r$.

Proof

Based on *Lemma 6.4.1*, the proof involves establishing a dissipation inequality via a suitable storage function. Here, we choose the function as $V = V_1 + V_2$, where $V_1 = x^T P x$ and $V_2 = \bar{e}^T P \bar{e}$. We can notice

$$V = \tilde{x}^T \tilde{P} \tilde{x} \tag{6-4-28}$$

where $\tilde{x} = [x^T \quad \bar{e}^T]^T$, $\tilde{P} = \begin{bmatrix} P & 0 \\ 0 & \bar{P} \end{bmatrix}$. It is not hard to find that

$$\lambda_{min}(\tilde{P})\|\tilde{x}\|^2 \leq V \leq \lambda_{max}(\tilde{P})\|\tilde{x}\|^2 \tag{6-4-29}$$

which implies V satisfy (6-4-3) in *Lemma 6.4.1*. Taking infinitesimal generator along the state trajectories of (6-4-24), by using Itô formula, it follows that:

$$\begin{aligned} \mathcal{L}V_1 = &\textstyle\sum_{i=1}^{r} h_i(\mu) \sum_{j=1}^{r} h_j(\mu) \{x^T[P(A_i + B_iK_j) + (A_i + B_iK_j)^T P]x - 2x^T P B_{eij}\bar{e} \\ &+ 2x^T P B_{di} d + x^T W_i^T P W_i x\} \end{aligned} \tag{6-4-30}$$

and

$$\begin{aligned} \mathcal{L}V_2 = &\sum_{i=1}^{r} h_i(\mu) \{[\bar{e}^T(\bar{P}R_i + R_i^T\bar{P})\bar{e} - 2\bar{e}^T\bar{P}L_{si}u_s + 2\bar{e}^T\bar{P}TJ_1\ddot{f}] \\ &+ x^T\bar{W}_i^T T^T \bar{P} T \bar{W}_i x\} \end{aligned} \tag{6-4-31}$$

Then we have

$$\begin{aligned} \mathcal{L}V &= \mathcal{L}V_1 + \mathcal{L}V_2 \\ &= \textstyle\sum_{i=1}^{r} h_i(\mu) \sum_{j=1}^{r} h_j(\mu) \{x^T[P(A_i + B_iK_j) + (A_i + B_iK_j)^T P]x - 2x^T P B_{eij}\bar{e} \\ &\quad + 2x^T P B_{di} d + x^T W_i^T P W_i x + \bar{e}^T(\bar{P}R_i + R_i^T\bar{P})\bar{e} - 2\bar{e}^T\bar{P}L_i u_s \\ &\quad + 2\bar{e}^T\bar{P}TJ_1\ddot{f} + x^T\bar{W}_i^T T^T \bar{P} T \bar{W}_i x\} \end{aligned} \tag{6-4-32}$$

For all $\in \mathcal{R}^{l_f}$, it can be noticed that $s^T sgn(s) = \sum_{i=1}^{l_f}|s_i|$ and $\|s\| \leq \sum_{i=1}^{l_f}|s_i|$. Since we choose $L_{si} = TJ_1$, we can obtain

$$\begin{aligned} \textstyle\sum_{i=1}^{r} h_i(\mu)(-2\bar{e}^T\bar{P}L_{si}u_s + 2\bar{e}^T\bar{P}TJ_1\ddot{f}) &= -2\bar{e}^T\bar{P}TJ_1(\delta + \varepsilon)sgn(s) + 2\bar{e}^T\bar{P}TJ_1\ddot{f} \\ &= 2s^T\ddot{f} - 2s^T(\delta + \varepsilon)sgn(s) \\ &\leq 2\|s\|\|\ddot{f}\| - 2(\delta + \varepsilon)\|s\| \\ &\leq -2\varepsilon\|s\| \end{aligned} \tag{6-4-33}$$

Hence it is shown that when $d = 0$

$$\mathcal{L}V \leq \textstyle\sum_{i=1}^{r} h_i(\mu) \sum_{j=1}^{r} h_j(\mu) \{x^T[P(A_i + B_iK_j) + (A_i + B_iK_j)^T P]x$$

$$-2x^T PB_{eij}\bar{e} + x^T W_i^T PW_i x + \bar{e}^T(\bar{P}R_i + R_i^T\bar{P})\bar{e} + x^T\bar{W}_i^T T^T\bar{P}T\bar{W}_i x - 2\varepsilon\|s\|\}$$

$$\leq \sum_{i=1}^{r} h_i(\mu)\sum_{j=1}^{r} h_j(\mu)\,[x^T \quad \bar{e}^T]\Pi_{ij}\begin{bmatrix} x \\ \bar{e}\end{bmatrix}\} - 2\varepsilon\|s\| \tag{6-4-34}$$

where $\Pi_{ij} = \begin{bmatrix}\Pi_{ij11} & -PB_{eij} \\ * & \Pi_{ij22}\end{bmatrix}$, $\Pi_{ij11} = P(A_i + B_iK_j) + (A_i + B_iK_j)^T P + W_i^T PW_i + \bar{W}_i^T T^T\bar{P}T\bar{W}_i$ and $\Pi_{ij22} = \bar{P}T\bar{A}_i + \bar{A}_i^T T^T\bar{P} - \bar{P}L_{i1}\bar{C} - \bar{C}^T L_{i1}^T\bar{P}$. From LMIs (6-4-26), we can see $\Pi_{ij} < 0$, indicating a positive scalar c_3 can be found such that

$$\mathcal{L}V < -c_3\|\tilde{x}\|^2 \tag{6-4-35}$$

According to *Lemma 6.4.1*, system (6-4-24) is stochastically exponentially stable in mean square.

When $d \neq 0$, let us move on to discuss the robustness of the system against unknown inputs. Consider the following performance index:

$$\Gamma = \mathbb{E}\{\int_0^{Tf}[y_c^T(\tau)y_c(\tau) - \gamma^2 d^T(\tau)d(\tau)]d\tau\} \tag{6-4-36}$$

Then adding and subtracting $\mathbb{E}(\int_0^t \mathcal{L}V\, d\tau)$ to (6-4-36)yields:

$$\Gamma \leq \mathbb{E}\{\int_0^{Tf}\sum_{i=1}^{r} h_i(\mu)\sum_{j=1}^{r} h_j(\mu)\,[x^T \quad d^T \quad \bar{e}^T]\Omega_{ij}\begin{bmatrix} x \\ d \\ \bar{e}\end{bmatrix}d\tau\} - \mathbb{E}(\int_0^{Tf}\mathcal{L}V\, d\tau) \tag{6-4-37}$$

where $\Omega_{ij} = \begin{bmatrix}\Omega_{ij11} & PB_{di} & -PB_{eij} + C^T D_e \\ * & -\gamma^2 I_{ld} & 0 \\ * & * & \Omega_{ij33}\end{bmatrix}$, $\Omega_{ij11} = P(A_i + B_iK_j) + (A_i + B_iK_j)^T P + W_i^T PW_i + \bar{W}_i^T T^T\bar{P}T\bar{W}_i + C^T C$, $\Omega_{ij33} = \bar{P}T\bar{A}_i + \bar{A}_i^T T^T\bar{P} - \bar{P}L_{i1}\bar{C} - \bar{C}^T L_{i1}^T\bar{P} + D_e^T D_e$.

It is not hard to find $\mathbb{E}(\int_0^{Tf}\mathcal{L}V\, d\tau) = \mathbb{E}(V) > 0$. Thus if $\Omega_{ij} < 0$, we get $\Gamma < 0$, leading to $\mathbb{E}(\|y_c\|_{Tf}^2) < \gamma^2\mathbb{E}(\|d\|_{Tf}^2)$.

As a results, LMIs (6-4-26) can guarantee the stochastically exponentially stability in mean square of system (6-4-24)and satisfy performance $\mathbb{E}(\|y_c\|_{Tf}^2) < \gamma^2\mathbb{E}(\|d\|_{Tf}^2)$. This completes the proof.

It is noticed that both the system dynamics and error dynamics are subject to state Brownian fluctuation, which makes it challenging to design observer and controller gains simultaneously. In order to simplify the challenging matrix problem, the following theorem is proposed.

Theorem 6.4.2

The closed-loop system (6-4-24) is stochastic stable in mean square and satisfy $\mathbb{E}(\|y_c\|_{Tf}^2) < \gamma^2 \mathbb{E}(\|d\|_{Tf}^2)$, if $\forall\ i,j$

1. There are positive matrix P, matrices K_j, and positive scalars σ and γ_1, where $\gamma_1 < \gamma$ such that

$$\begin{bmatrix} \Lambda_{ij} & PB_{di} \\ * & -\gamma^2 I_{ld} \end{bmatrix} < \begin{bmatrix} -\sigma PP & 0 \\ * & -\gamma_1^2 I_{ld} \end{bmatrix} \tag{6-4-38}$$

where $\Lambda_{ij} = P(A_i + B_i K_j) + (A_i + B_i K_j)^T P + W_i^T P W_i + C^T C$, $i,j = 1,2,\dots r$.

2. There are positive matrix $\bar{P}$, matrices L_{i1}, N such that

$$\begin{bmatrix} -\sigma PP + \bar{W}_i^T T^T \bar{P} T \bar{W}_i & 0 & -PB_{eij} + C^T D_e \\ * & -\gamma_1^2 I_{ld} & 0 \\ * & * & \Omega_{ij33} \end{bmatrix} < 0 \tag{6-4-39}$$

and

$$J_1^T T^T \bar{P} = N\bar{C} \tag{6-4-40}$$

where P and K_j are obtained from solving (6-4-38), $i,j = 1,2,\dots r$.

Proof

According to inequality (6-4-38), $\forall i,j$, $\begin{bmatrix} -\sigma PP & 0 \\ * & -\gamma_1^2 I_{ld} \end{bmatrix} + \Theta < 0$ implies that $\begin{bmatrix} \Lambda_{ij} & PB_{di} \\ * & -\gamma^2 I_{ld} \end{bmatrix} + \Theta < 0$, where Θ is a semi-positive symmetric matrix. Therefore,

$$\Omega_{ij} = \begin{bmatrix} \Lambda_{ij} & PB_{di} & 0 \\ * & -\gamma^2 I_{ld} & 0 \\ * & * & 0 \end{bmatrix} + \begin{bmatrix} \bar{W}_i^T T^T \bar{P} T \bar{W}_i & 0 & -PB_{eij} + C^T D_e \\ * & 0 & 0 \\ * & * & \Omega_{ij33} \end{bmatrix}$$

$$\leq \begin{bmatrix} -\sigma PP & 0 & 0 \\ * & -\gamma_1^2 I_{ld} & 0 \\ * & * & 0 \end{bmatrix} + \begin{bmatrix} \bar{W}_i^T T^T \bar{P} T \bar{W}_i & 0 & -PB_{eij} + C^T D_e \\ * & 0 & 0 \\ * & * & \Omega_{ij33} \end{bmatrix}$$

$$= \begin{bmatrix} -\sigma PP + \bar{W}_i^T T^T \bar{P} T \bar{W}_i & 0 & -PB_{eij} + C^T D_e \\ * & -\gamma_1^2 I_{ld} & 0 \\ * & * & \Omega_{ij33} \end{bmatrix} \quad (6\text{-}4\text{-}41)$$

So (6-4-38) and (6-4-39) indicate $\Omega_{ij} < 0$, which meet LMIs (6-4-26). This completes the poof.

In this way, a sequential design approach can be obtained to reduce the complication for solving observer and controller gains by *Theorem 6.4.2*. Nevertheless, it can be noticed that LMIs (6-4-38) and (6-4-39)are nonlinear. In order to transform it into linear range, the following theorem is proposed.

Theorem 6.4.3

The closed loop system (6-4-24) are stochastically stable in mean square and satisfy $\mathbb{E}(\|y_c\|_{Tf}^2) < \gamma^2 \mathbb{E}(\|d\|_{Tf}^2)$, if $\forall\ i, j$

1. There are positive matrix P, matrices K_j, and positive scalars σ and γ_1, where $\gamma_1 < \gamma$ such that

$$\begin{bmatrix} \Psi_{ij} & XW_i^T & XC^T & PB_{di} \\ * & -X & 0 & 0 \\ * & * & -I_n & 0 \\ * & * & * & (\gamma_1^2 - \gamma^2) I_{ld} \end{bmatrix} < 0 \quad (6\text{-}4\text{-}42)$$

where $X = P^{-1}$, $\Psi_{ij} = A_i X + X A_i + B_i Y_j + Y_i^T B_i^T + \sigma I_n$, $Y_j = K_j X$ .Then the control gains can be selected as $K_j = Y_j X^{-1}$.

2. There are positive matrix $\bar{P}$, matrices Q_i, N such that

$$\begin{bmatrix} -\sigma PP + \bar{W}_i^T T^T \bar{P} T \bar{W}_i & 0 & -PB_{eij} + C^T D_e \\ * & -\gamma_1^2 I_{ld} & 0 \\ * & * & \Phi_{ij33} \end{bmatrix} < 0 \quad (6\text{-}4\text{-}43)$$

and

$$J_1^T T^T \bar{P} = N \bar{C} \quad (6\text{-}4\text{-}44)$$

where $\Phi_{ij33} = \bar{P} T \bar{A}_i + \bar{A}_i^T T^T \bar{P} - Q_i \bar{C} - \bar{C}^T Q_i^T + D_e^T D_e$. And the observer gains $L_{i1} = \bar{P}^{-1} Q_i$.

Proof

Inequality (6-4-38) can be rewritten as:

$$\begin{bmatrix} \Lambda_{ij} + \sigma PP & PB_{di} \\ * & (\gamma_1^2 - \gamma^2)I_{ld} \end{bmatrix} < 0 \tag{6-4-45}$$

Multiplying $\begin{bmatrix} P^{-T} & 0 \\ 0 & I_{ld} \end{bmatrix}$ on the left side and $\begin{bmatrix} P^{-1} & 0 \\ 0 & I_{ld} \end{bmatrix}$ on the right side of (6-4-45) we can have

$$\begin{bmatrix} \Psi_{ij} + XW_i^T X^{-1} W_i X + XC^T CX & PB_{di} \\ * & (\gamma_1^2 - \gamma^2)I_{ld} \end{bmatrix} < 0 \tag{6-4-46}$$

where $X = P^{-1}$, $\Psi_{ij} = A_i X + XA_i + B_i Y_j + Y_i^T B_i^T + \sigma I_n$, $Y_j = K_j X$. Based on Schur complement, (6-4-46) is equivalent to

$$\begin{bmatrix} \Psi_{ij} & XW_i^T & XC^T & PB_{di} \\ * & -X & 0 & 0 \\ * & * & -I_n & 0 \\ * & * & * & (\gamma_1^2 - \gamma^2)I_{ld} \end{bmatrix} < 0 \tag{6-4-47}$$

By using $Q_i = \bar{P}L_{i1}$, (6-4-39) can be rewritten as

$$\begin{bmatrix} -\sigma PP + \bar{W}_i^T T^T \bar{P} T \bar{W}_i & 0 & -PB_{eij} + C^T D_e \\ * & -\gamma_1^2 I_{ld} & 0 \\ * & * & \Phi_{ij33} \end{bmatrix} < 0 \tag{6-4-48}$$

This completes the proof.

Until now, sufficient conditions have been proposed for stochastically exponentially stability in mean square of system (6-4-24). However, (6-4-44) in *Theorem 6.4.3* is a matrix equality which is difficulty to be solved by available software toolbox directly. In order to simplify this problem, equation (6-4-44) can be rewritten as

$$J_1^T T^T \bar{P} - N\bar{C} = 0 \tag{6-4-49}$$

which can also be represented by

$$trace\{(J_1^T T^T \bar{P} - N\bar{C})^T (J_1^T T^T \bar{P} - N\bar{C})\} = 0 \tag{6-4-50}$$

Then we introduce the following condition:

$$(J_1^T T^T \bar{P} - N\bar{C})^T (J_1^T T^T \bar{P} - N\bar{C}) < \theta I \tag{6-4-51}$$

where θ is a positive scalar. According to Schur complement, (6-4-51) is equivalent with:

$$\begin{bmatrix} -\theta I & (J_1^T T^T \bar{P} - N\bar{C})^T \\ (J_1^T T^T \bar{P} - N\bar{C}) & -I \end{bmatrix} < 0 \tag{6-4-52}$$

As a result, condition (6-4-42), (6-4-43) and (6-4-44) can be converted into searching a global solution of the following problem:

$$\min \theta, \text{ subject to (6-4-42), (6-4-43), and (6-4-52)} \qquad (6\text{-}4\text{-}53)$$

which can be solved by employing Solvers $mincx$ in LMI toolbox of Matlab.

6.4.3 Reachability of the sliding mode surface

The above sections present the approaches to design robust estimator-based fault tolerant control scheme. Now let us look at the reachability of the sliding mode surface. It is known from [143] that the solution of $\bar{e}$ is given by

$$\bar{e} = \sum_{i=1}^{r} h_i(\mu) \{\int_0^t [R_i\bar{e}(\tau) - L_{si}u_s(\tau) + TJ_1\ddot{f}(\tau)]d\tau + \int_0^t T\bar{W}_i x(\tau)dw(\tau)\}$$

(6-4-54)

Substituting it into (6-4-16), we have

$$s = \sum_{i=1}^{r} h_i(\mu) \{\int_0^t J_1^T T^T \bar{P}[R_i\bar{e}(\tau) - L_{si}u_s(\tau) + TJ_1\ddot{f}(\tau)d\tau] + \int_0^t J_1^T T^T \bar{P} T\bar{W}_i x(\tau)dw(\tau)\}$$

(6-4-55)

If the following condition holds:

$$J_1^T T^T \bar{P} T\bar{W}_i = 0 \qquad (6\text{-}4\text{-}56)$$

we can yield

$$s = \sum_{i=1}^{r} h_i(\mu) \int_0^t J_1^T T^T \bar{P}[R_i\bar{e}(\tau) - L_{si}u_s(\tau) + TJ_1\ddot{f}(\tau)]d\tau \qquad (6\text{-}4\text{-}57)$$

which implies

$$\dot{s} = \sum_{i=1}^{r} h_i(\mu) J_1^T T^T \bar{P}(R_i\bar{e} - L_{si}u_s + TJ_1\ddot{f}) \qquad (6\text{-}4\text{-}58)$$

Remark 6.4.4

From condition (6-4-56), the stochastic influences have been removed from the sliding mode surface, which means $s(t) = 0$ is not stochastic.

In order to satisfy equation (6-4-55), which is equivalent to

$$trace\{(J_1^T T^T \bar{P} T\bar{W}_i)^T (J_1^T T^T \bar{P} T\bar{W}_i)\} = 0 \qquad (6\text{-}4\text{-}59)$$

By employing the same parameter θ in *Theorem 6.4.1*, we have

$$(J_1^T T^T \bar{P} T \bar{W}_i)^T (J_1^T T^T \bar{P} T \bar{W}_i) < \theta I \tag{6-4-60}$$

Applying Schur complement, (6-4-60) can be rewritten as:

$$\begin{bmatrix} -\theta I & (J_1^T T^T \bar{P} T \bar{W}_i)^T \\ J_1^T T^T \bar{P} T \bar{W}_i & -I \end{bmatrix} < 0 \tag{6-4-61}$$

Then equality (6-4-56) can also be converted into a minimization problem as

$$\min \theta, \text{ subject to (6-4-61)} \tag{6-4-62}$$

Remark 6.4.5

It is shown that both specified sliding surface and desired sliding mode control law can be constructed via convex optimization problem, which can be handled by LMI toolbox of Matlab.

Finally, we can generate the following theorem to design observer and controller gains.

Theorem 6.4.4

For system (6-4-2), there exists a tolerant observer-based controller in the form of (6-4-7), (6-4-19) and (6-4-22), ensuring that

1. The closed-loop system (6-4-24) is stochastically exponentially stable in mean square ;
2. The error trajectories $\bar{e}$ can be globally driven onto the sliding surface $s(t) = 0$ in probability.
3. The compensated output satisfies $\mathbb{E}(\|y_c\|_{Tf}^2) < \gamma^2 \mathbb{E}(\|d\|_{Tf}^2)$;

   if $\forall\, i, j$, we can find a global solution of the following optimization problem:

$$\min \theta, \text{ subject to (6-4-42), (6-4-43), (6-4-52) and (6-4-61)} \tag{6-4-63}$$

Proof

According to *Theorem 6.4.3*, conditions 1 and 3 can be guaranteed by optimization problem (6-4-63). Now let us prove condition 2. Consider the following Lyapunov candidate for sliding mode surface $s(t) = 0$:

$$V_3 = \frac{1}{2} s^T (J_1^T T^T \bar{P} T J_1)^{-1} s \tag{6-4-64}$$

Its derivative can be obtained as:

$$\dot{V}_3 = \sum_{i=1}^{r} h_i(\mu)\, s^T (J_1^T T^T \bar{P} T J_1)^{-1} J_1^T T^T \bar{P} (R_i \bar{e} - L_{si} u_s + T J_1 \ddot{f}) \tag{6-4-65}$$

It can be calculated that

$$\sum_{i=1}^{r} h_i(\mu)\, s^T (J_1^T T^T \bar{P} T J_1)^{-1} J_1^T T^T \bar{P}(-L_{si} u_s + T J_1 \ddot{f})$$

$$= s^T (J_1^T T^T \bar{P} T J_1)^{-1} J_1^T T^T \bar{P} T J_1 [-(\delta + \varepsilon) sgn(s) + \ddot{f}]$$

$$= s^T \left[-(\delta + \varepsilon) sgn(s) + \ddot{f}\right]$$

$$\leq -(\delta + \varepsilon)\|s\| + \|s\|\|\ddot{f}\|$$

$$\leq -\varepsilon\|s\| \tag{6-4-66}$$

Then we have

$$\dot{V}_3 \leq \sum_{i=1}^{r} h_i(\mu)\, [s^T (J_1^T T^T \bar{P} T J_1)^{-1} (J_1^T T^T \bar{P} R_i \bar{e})] - \varepsilon\|s\|$$

$$\leq \sum_{i=1}^{r} h_i(\mu)\|s\|\, [\|Z_i\|\mathbb{E}(\|\bar{e}\|) - \varepsilon] \tag{6-4-67}$$

where $Z_i = (J_1^T T^T \bar{P} T J_1)^{-1} (J_1^T T^T \bar{P} R_i)$.

Define the following variables:

$$\rho\big(h_i(\mu)\big) = \sum_{i=1}^{r} h_i(\mu)\, \|Z_i\| \tag{6-4-68}$$

It is easy to find the upper bounds ρ_0 to make $\rho\big(h_i(\mu)\big) < \rho_0$. Hence

$$\dot{V}_3 < \rho_0\|s\|\mathbb{E}(\|\bar{e}\|) - \varepsilon\|s\|$$

$$= -\|s\|[\varepsilon - \rho_0\mathbb{E}(\|\bar{e}\|)] \tag{6-4-69}$$

We define the following domain:

$$\Omega(\rho_0) = \{\mathbb{E}(\|\bar{e}\|) < \frac{\varepsilon}{\rho_0}\} \tag{6-4-70}$$

then

$$\dot{V}_3 < 0 \tag{6-4-71}$$

Since the error and original systems are stable, the trajectory of $\bar{e}$ enter in $\Omega(\rho_0)$ remains there, which means condition 2 is satisfied by optimization problem (6-4-71).

On the basis of the above theorems, the design procedures of integrated observer-based fault estimation and the corresponding fault tolerant control can be summarized as follows:

Procedure 6.4.1 *fault estimator-based fault tolerant control of Takagi-Sugeno fuzzy systems*

i) Construct the augmented system in the form of (6-4-5) for stochastic T-S fuzzy systems in presence of faults and unknown inputs

ii) Select matrix H^* in the form of (6-4-14), and T can be yielded as $T = I_{\bar{n}} - H\bar{C}$

iii) Solve LMIs (6-4-42) to obtain matrices X and Y_j, and calculate $P = X^{-1}$, $K_j = Y_j X^{-1}$

iv) Select the sliding mode control gains as $L_{si} = TJ_1$

v) Solve optimization problem

$$\min \theta, \text{ subject to (6-4-43), (6-4-52) and (6-4-61)}$$

by submitting P and K_j to obtain matrices $\bar{P}$, Q_i, N, and the observer gains can be derived as $L_{i1} = \bar{P}^{-1}Q_i$

vi) Calculate the other observer gains R_i and L_{i2} following the formulas (6-4-10) and (6-4-12), respectively.

vii) Implement the robust sliding mode unknown input observer (6-4-7) with the sliding term $u_s = (\delta + \varepsilon)sgn(s)$, where $s = Ny - N\bar{C}\hat{\bar{x}}$, and obtain the augmented estimate $\hat{\bar{x}}$, leading to simultaneous estimates of system states and faults $\hat{x}$ and $\hat{f}$.

viii) Implement control law $u = \sum_{j=1}^{r} h_j(\mu)\, \bar{K}_j \hat{\bar{x}}$ and sensor compensation output $y_c = y - D_f \hat{f}$, where $\bar{K}_j = [K_j \quad 0 \quad K_f]$ and $K_f = -B_h^{+} B_{fh}$.

Example 6.4.1

In this section, the obtained results are validated by the following nonlinear system represented by T-S fuzzy models, where the system coefficients are given as follows:

$$A_1 = \begin{bmatrix} -5 & -1.5 & 0 \\ 2 & -1 & -3 \\ 0 & 3 & -3 \end{bmatrix}, A_2 = \begin{bmatrix} -5 & 1.5 & 0 \\ 2 & -1 & 3 \\ 0 & -3 & -3 \end{bmatrix},$$

$$B_1 = \begin{bmatrix} 1 \\ 0.5 \\ 0 \end{bmatrix}, B_2 = \begin{bmatrix} 0.4 \\ 1 \\ 0 \end{bmatrix},$$

$$W_1 = \begin{bmatrix} 0.01 & 0 & -0.004 \\ 0 & -0.001 & 0 \\ 0 & 0 & 0.0001 \end{bmatrix},$$

$$W_2 = \begin{bmatrix} 0.001 & 0 & 0.002 \\ 0 & 0.001 & 0 \\ 0 & 0 & 0.0002 \end{bmatrix}, C = \begin{bmatrix} 1 & 0 & 0 \\ 0 & 1 & 0 \\ 0 & 0 & 1 \end{bmatrix}$$

with initial condition to be $x_0 = [0.001 \quad -0.003 \quad 0.002]^T$. And the membership functions are $h_1 = \frac{m_1}{m_1+m_2}, h_2 = \frac{m_2}{m_1+m_2}$, where $m_1 = \frac{1}{2}(1+\frac{x_1}{3})$ and $m_2 = \frac{1}{2}(1-\frac{x_1}{3})$.

The actuator fault taken into account is of the following value:

$$f_a = \begin{cases} 0 & 0s \le t < 8s \\ -0.5t + 4 & 8s \le t < 10s \\ 0.25\sin(8t) - 0.5 & 10s \le t < 12s \\ 0.5t - 7 & 12s \le t < 14s \\ 0 & t \ge 14s \end{cases} \tag{6-4-72}$$

with $B_{f_{a1}} = B_1, B_{f_{a2}} = B_2$. Concerned sensor fault f_s is 50% deviation of the first output, and $D_{f_s} = [1 \quad 0 \quad 0]^T$. By representing $f = [f_a^T \quad f_s^T]^T$, we have $B_{f1} = [B_{fa1} \quad 0]$, $B_{f2} = [B_{fa2} \quad 0]$ and $D_f = [0 \quad D_{f_s}]$. Unknown input signal is supposed to be random noises from -0.1 and 0.1, with $B_{d1} = B_{d2} = [0.1 \quad 0.2 \quad -0.1]^T$. The reference input is given as $u_r = 2$. Observer gain H can be solved by (6-4-14). Choosing $\gamma = 2$, $\gamma_1 = 0.1$, $\sigma = 0.1$, and solving LMI problem (6-4-63), the controller and observer gains can be calculated as follows:

$$K_1 = K_2 = [1.3890 \quad -7.1197 \quad -3.1549]$$

$$L_{11} = 10^4 \times \begin{bmatrix} 0.10472 & 0.7072 & 0.1337 \\ -0.1789 & 0.6036 & 0.2109 \\ -0.4836 & 0.4102 & 0.1937 \\ -971.53 & 3292.3 & 1573.5 \\ 33614 & 73369 & 128343 \\ -480.52 & 2284.8 & 797.62 \\ 3.8710 & -3.6337 & -1.4867 \end{bmatrix}$$

$$L_{21} = 10^4 \times \begin{bmatrix} 0.1213 & 1.2778 & 0.2340 \\ -0.1634 & 1.1410 & 0.3051 \\ -0.4727 & 0.7872 & 0.2599 \\ -850.26 & 7474.7 & 23.8.2 \\ 33591 & 72580 & 128205 \\ -419.95 & 4373.4 & 1164.6 \\ 3.7763 & -6.9014 & -2.0603 \end{bmatrix}$$

And we can obtain $\theta = 10^{-9}$, which means conditions $J_1^T T^T \bar{P} = N\bar{C}$ and $J_1^T T^T \bar{P} T \bar{W}_i = 0$ hold. Other observer gains K_{f1}, K_{f2}, $\bar{K}_1$, $\bar{K}_2$, T, L_{12}, L_{22}, R_1 and R_2 can be calculated according to (6-4-10) to (6-4-12) and (6-4-20) as follows:

$$K_{f1} = K_{f2} = [-1 \quad 0],$$

$$\bar{K}_1 = \bar{K}_2 = [1.3890 \quad -7.1197 \quad -3.1549 \quad 0 \quad 0 \quad -1 \quad 0]$$

$$T = \begin{bmatrix} 1 & 0 & 0 & 0 & 0 & 0 & 0 \\ 0 & 1 & 0 & 0 & 0 & 0 & 0 \\ -0.1 & 0.2 & 1.15 & 0 & 0 & 0 & -0.1 \\ 0 & 0 & 0 & 1 & 0 & 0 & 0 \\ 0 & 0 & 0 & 0 & 1 & 0 & 0 \\ 0 & 0 & 0 & 0 & 0 & 1 & 0 \\ 0 & 0 & 0 & 0 & 0 & 0 & 0 \end{bmatrix},$$

$$L_{12} = 10^4 \times \begin{bmatrix} -0.0134 & 0.0267 & 0.0201 \\ 0.0211 & 0.0421 & 0.0316 \\ -0.0194 & 0.0388 & 0.0291 \\ -157.35 & 314.70 & 236.02 \\ -12834 & 25669 & 19251 \\ -79.762 & 159.52 & 119.64 \\ 0.1487 & -0.2974 & -0.2230 \end{bmatrix},$$

$$L_{22} = 10^4 \times \begin{bmatrix} -0.0234 & 0.0468 & 0.0351 \\ -0.0305 & 0.0610 & 0.0457 \\ -0.0260 & 0.0520 & 0.0390 \\ -230.82 & 461.63 & 346.22 \\ -12820 & 25641 & 19231 \\ -116.46 & 232.91 & 174.68 \\ 0.2060 & -0.4121 & -0.3091 \end{bmatrix},$$

$$R_1 = 10^4 \times$$

$$\begin{bmatrix} -0.1052 & -0.7074 & 0.0134 & 0 & 0 & 10^{-4} & -0.1047 \\ 0.1791 & -0.6037 & -0.2106 & 0 & 0 & 5 \times 10^{-5} & 0.1789 \\ 0.4837 & -0.4099 & -0.1940 & 0 & -10^{-5} & 0 & 0.4836 \\ 971.53 & -3292.3 & -1573.5 & 0 & 0 & 0 & 971.53 \\ -33614 & -73369 & -128343 & 0 & 0 & 0 & -33614 \\ 480.52 & -2284.8 & -797.62 & 10^{-4} & 0 & 0 & 480.52 \\ -3.871 & 3.633 & 1.486 & 0 & 10^{-4} & 0 & -3.871 \end{bmatrix}$$

$$R_2 = 10^4 \times$$

$$\begin{bmatrix} -0.1218 & -1.2776 & -0.2340 & 0 & 0 & 4 \times 10^{-5} & -0.1213 \\ 0.1636 & -1.1411 & -0.3048 & 0 & 0 & 10^{-4} & 0.1634 \\ 0.4728 & -0.7876 & -0.2601 & 0 & -10^{-5} & 1.6 \times 10^{-5} & 0.4727 \\ 850.26 & -7474.7 & -2308.2 & 0 & 0 & 0 & 850.26 \\ -33591 & -72580 & -128205 & 0 & 0 & 0 & -33591 \\ 419.95 & -4373.4 & -1164.6 & 10^{-4} & 0 & 0 & 419.95 \\ -3.776 & 6.901 & 2.0603 & 0 & 10^{-4} & 0 & -3.776 \end{bmatrix}$$

The sliding mode controller gain can be obtained as $L_{si} = TJ_1$. Select $\rho_0 = 0.00001$, and $\varepsilon = 0.00001$, and using the Euler–Maruyama method to simulate the standard Brownian motions (with 5 Brownian paths), one can obtain the simultaneous estimation results of full system states and the means of concerned faults as shown in Figs. 6.4.1-6.4.5. Fig. 6.4.6 compares the output with and without signal compensations.

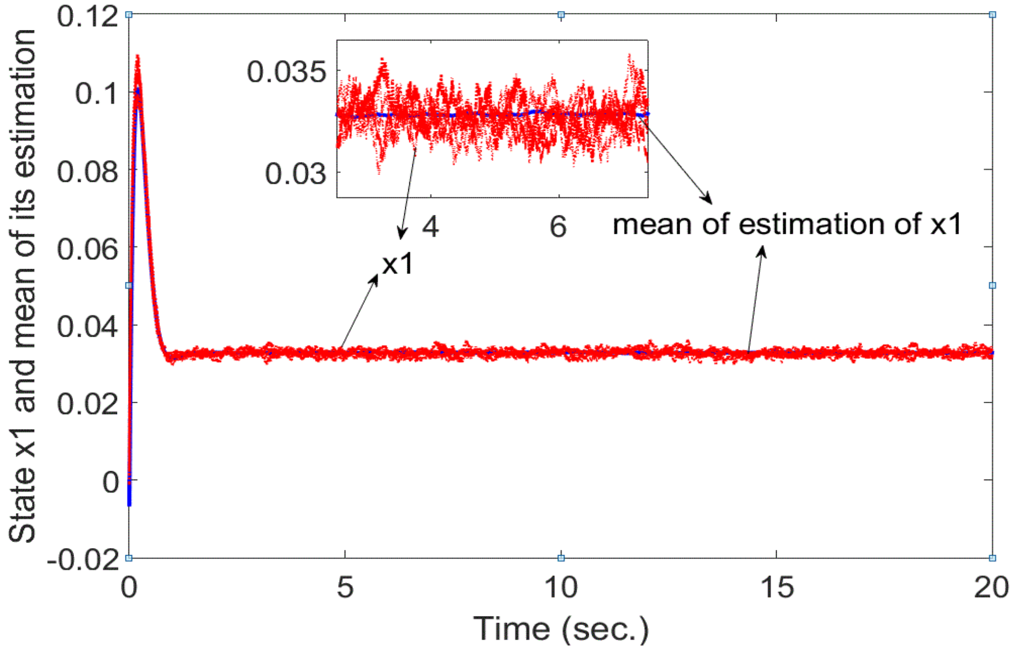

Fig. 6.4.1. x_1 and the mean of its estimation

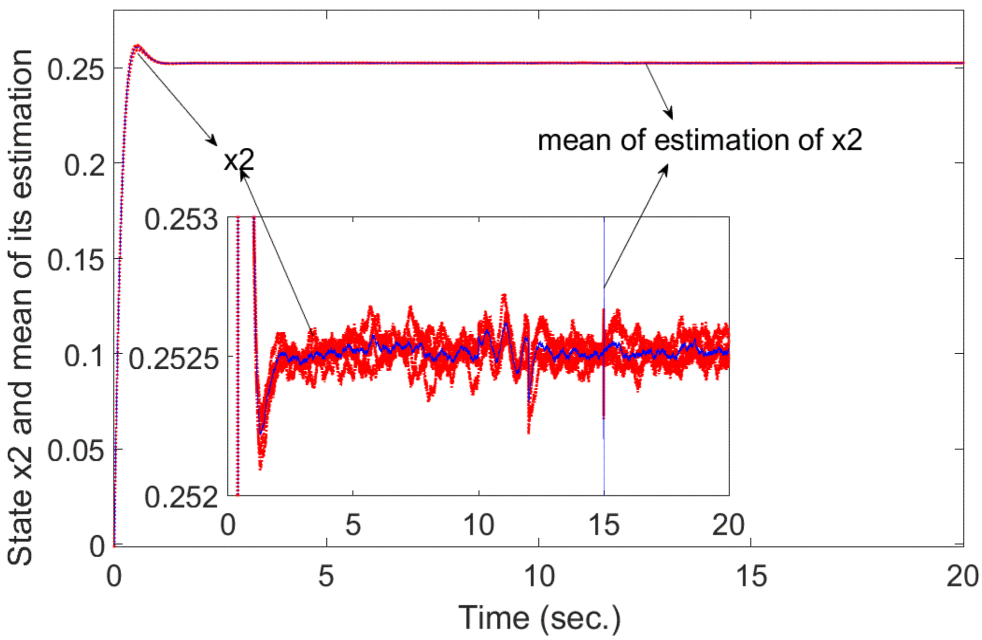

Fig. 6.4.2. x_2 and the mean of its estimation

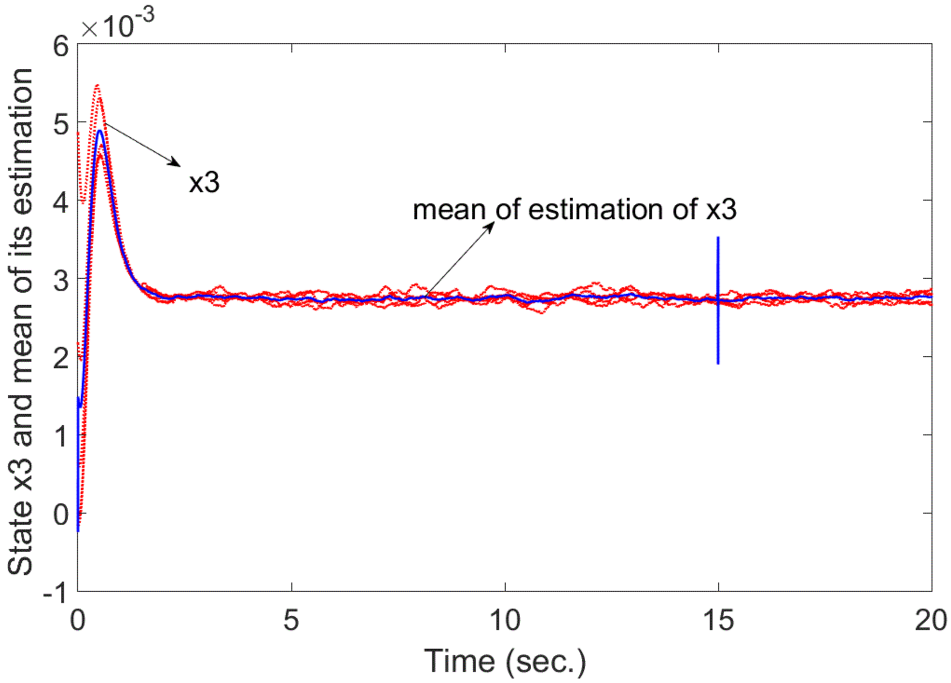

Fig. 6.4.3. x_3 and the mean of its estimation

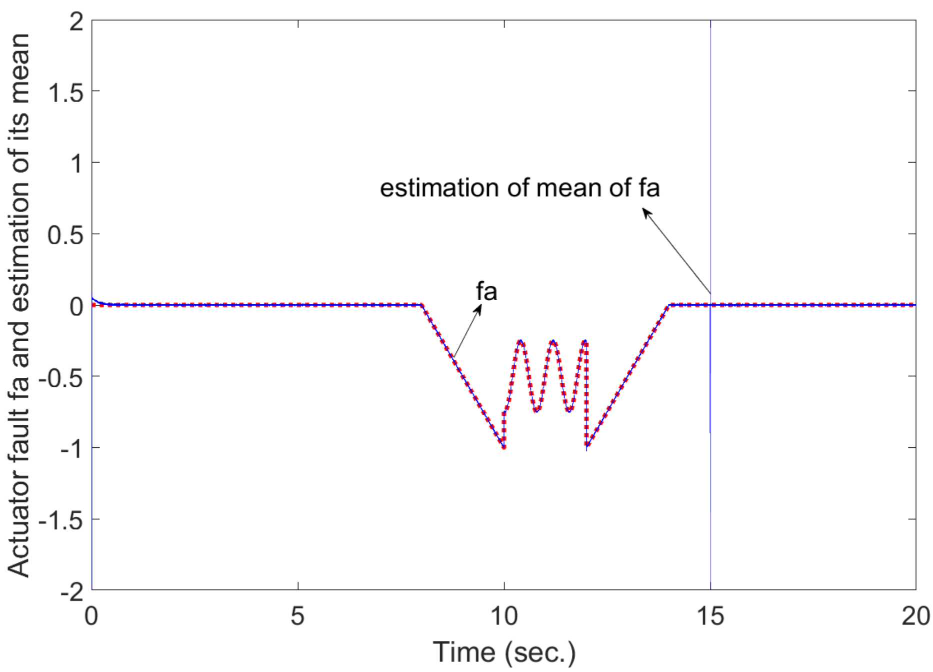

Fig. 6.4.4. f_a and its estimation

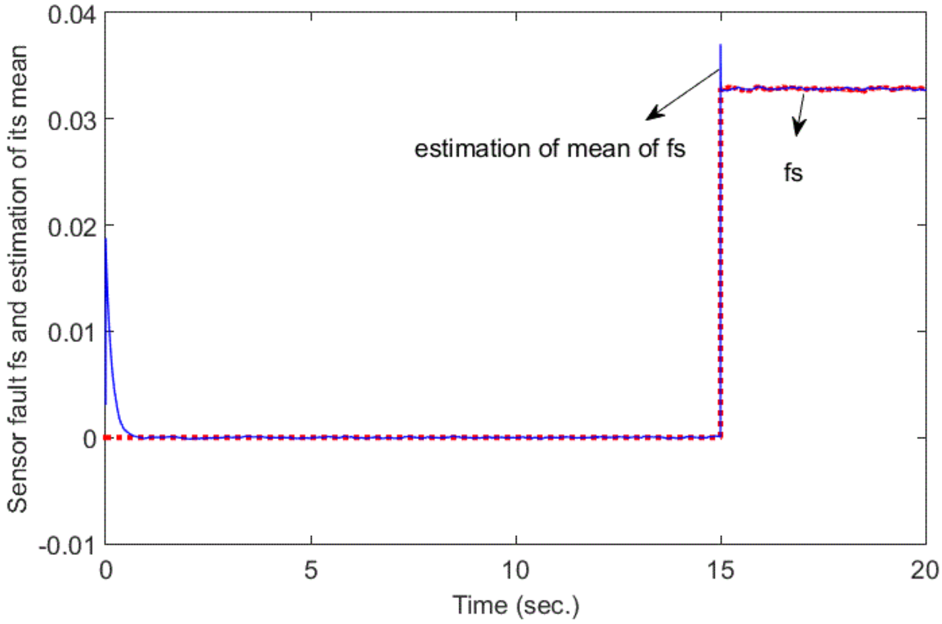

Fig. 6.4.5. f_s and its estimation

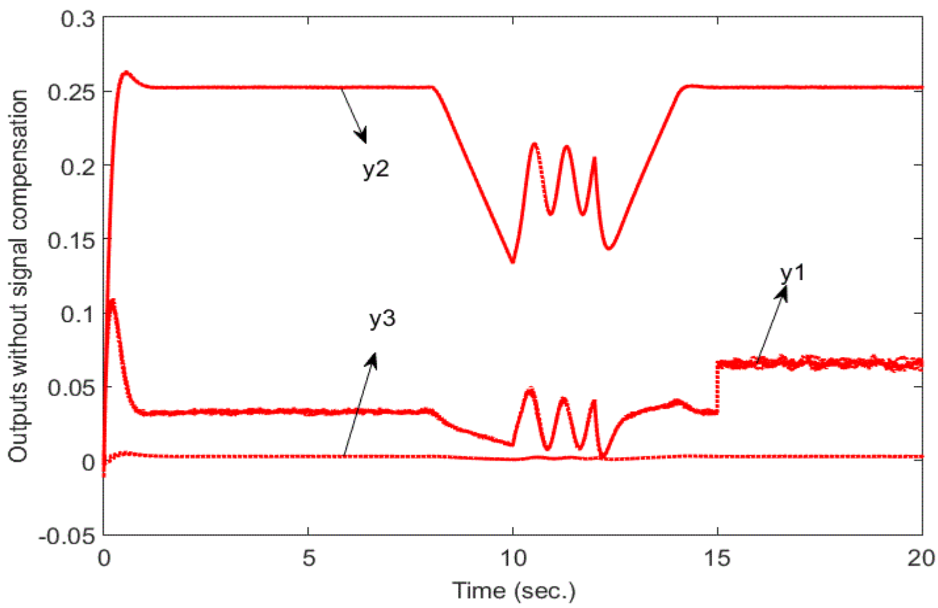

Fig. 6.4.6(a) outputs response without signal compensation

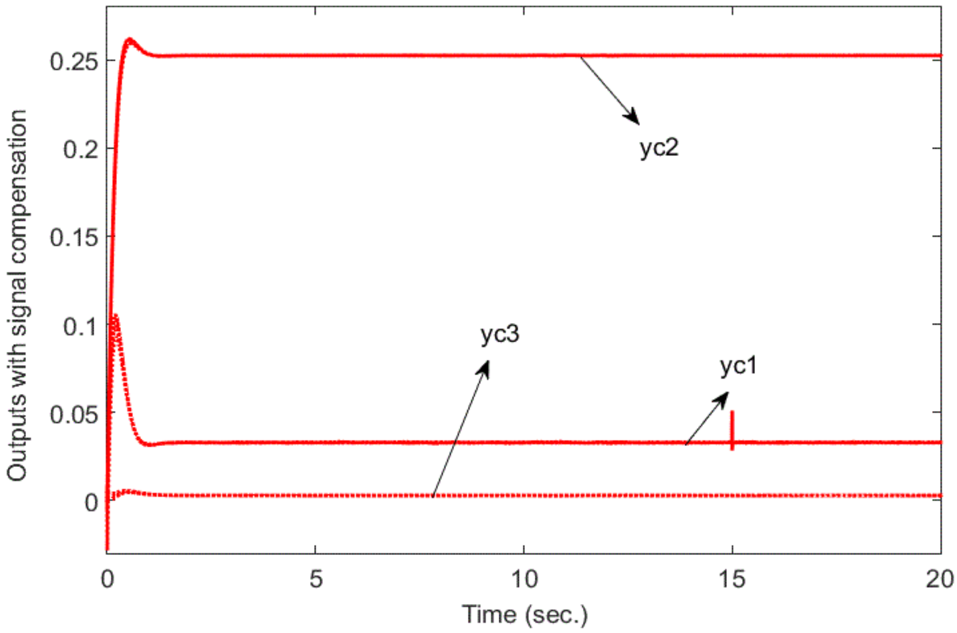

Fig. 6.4.6(b) outputs response with signal compensation

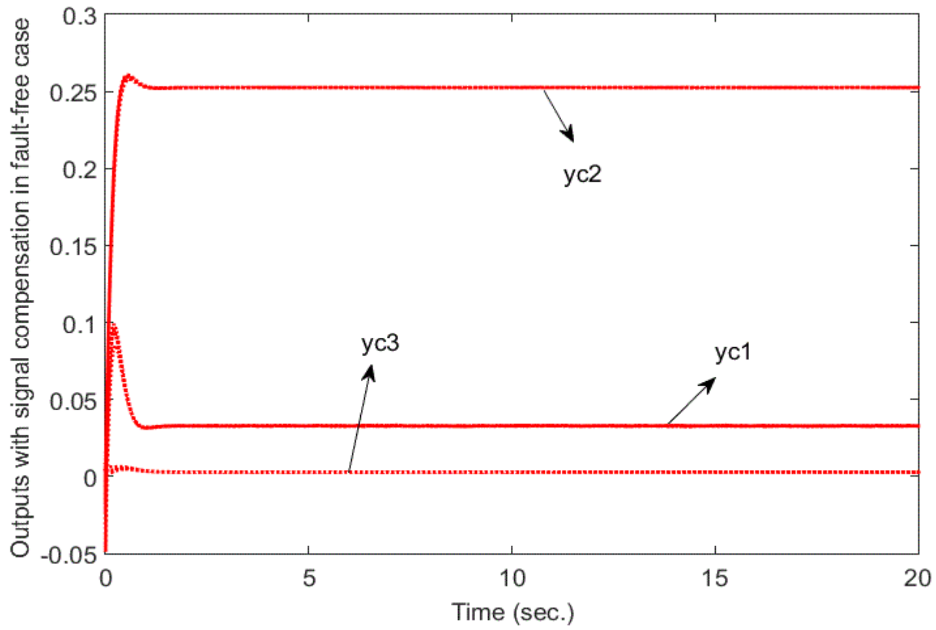

Fig. 6.4.6(c) output response with signal compensation in fault-free case

From Figs 6.4.1-6.4.5, the estimation performance of both the system states and considered faults are satisfactory. Fig. 6.4.6a shows the system outputs are distorted by the faults. Fig. 6.4.6b and Fig. 6.4.6c are consistent, which means the system can work well no matter the faults happen or not.

6.5 Summary

In this chapter, an integrated robust fault estimation and tolerant control technique has been developed for stochastic systems subjected to Brownian parameter perturbations, partially decoupled unknown inputs, and unexpected faults. Specifically, augmented system approach and UIO are integrated to achieve the robust state/fault estimation. The design of the tolerant controller can make the overall closed-loop system stochastically input-to-state stable, the influences of the unknown inputs are either decoupled by the UIO, or attenuated by the LMI, and the adverse effects from the faults to the system and output dynamics are eliminated by using signal compensations. Simulation studies have well demonstrated the effectiveness of the proposed fault estimation and tolerant control techniques. The proposed approach would have great potentials in applications to complex industrial processes with high nonlinearities and stochastic parameter perturbations.

Chapter 7

Case study on benchmark wind turbine

In this chapter, the developed robust fault estimation and fault tolerant control techniques are applied to wind turbines for enhancing system reliability and safety even the turbines are working under faulty scenario. Specifically, section 7.1 introduces the construction of a benchmark wind turbine. Since the overall system is highly nonlinear, section 7.2 illustrates the T-S fuzzy process of the nonlinear wind turbine. Based on the built T-S fuzzy model, section 7.3 applies the developed UIO-based fault estimation and fault tolerant control strategies to estimate all system states, actuator fault and sensor faults simultaneously, and compensate occurred faults, making the original wind turbine system have reliable outputs in both fault-free and faulty scenarios. In section 7.4, the robust fault estimator-based fault tolerant control approach is to be applied to stochastic drive train system in presence of Brownian perturbations, followed by section 7.5 to summarize this chapter.

7.1 System overview of benchmark wind turbine

A wind turbine converts wind energy to electrical energy. A benchmark model was designed in [81], based on a generic three blade horizontal wind turbine driven by variable speed, shown in Fig. 7.1.1, with a full converter coupling and a rated power of 4.8 MW.

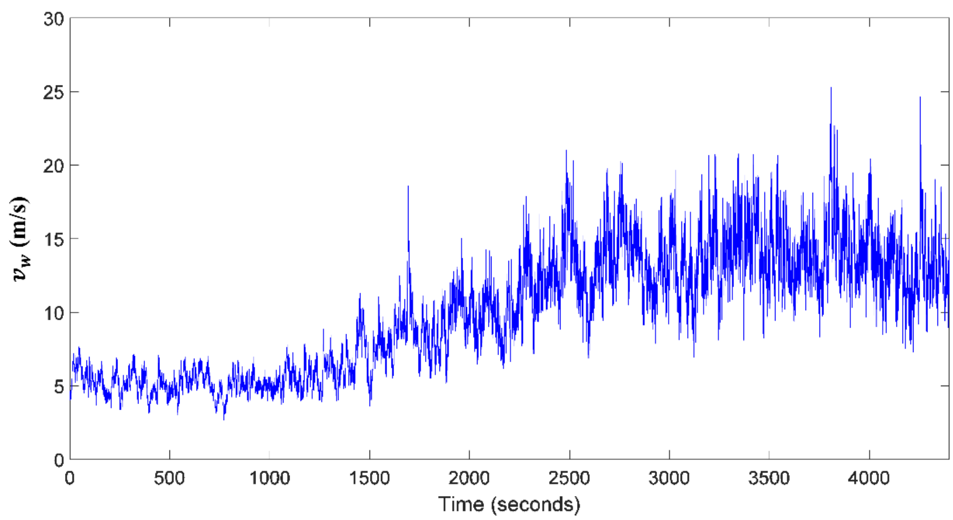

Fig. 7.1.1 Wind speed sequence used in benchmark model

The overall benchmark model is obtained by interconnecting the models of individual subsystems, including blade and pitch systems, drive train, generator and convertor, and controller, as shown in Fig. 7.1.2.

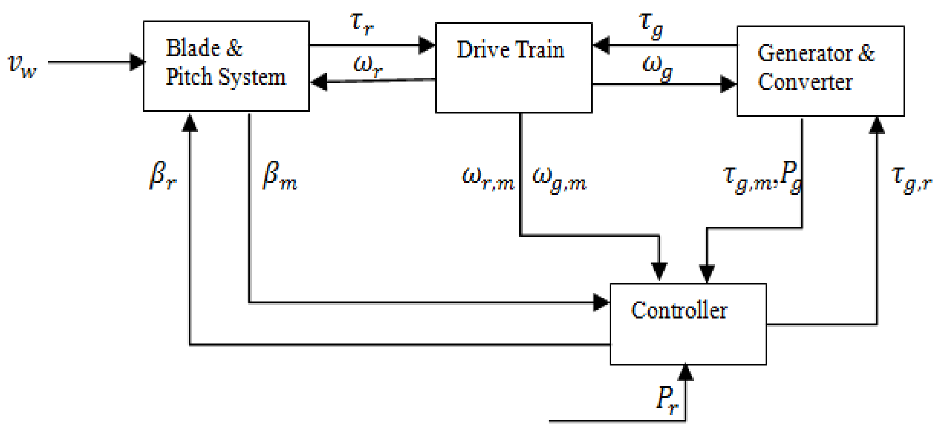

Fig. 7.1.2. Block diagram of wind turbine benchmark model [81]

7.1.1. Blade and pitch system

The blades connected to the rotor shaft are facing the wind direction. The wind energy is transformed to mechanical energy through the rotation of blades by the wind. Through pitching the blades or by controlling the rotation speed, we can control the aerodynamic torque modelled as

$$\tau_r(t) = \frac{1}{2}\rho\pi R^3 C_q(\lambda(t), \beta(t))v_w^2 \tag{7-1-1}$$

where ρ is the air density, R is the radius of the rotor, C_q is the torque coefficient which is a function of the pitch angle β and tip-speed-ratio λ given by:

$$\lambda(t) = \frac{R\omega_r(t)}{v_w(t)} \tag{7-1-2}$$

where ω_r is the turbine rotor angular speed. If the rotor speed is kept constant, then any change in the wind speed will change the tip-speed ratio, leading to the change of C_q, as illustrated in Fig. 7.1.3, as well as the generated power out of the wind turbine. If, however, the rotor speed is adjusted according to the wind speed variation, then the tip-speed ratio can be maintained as an optimal point, which will yield maximum power output from the system.

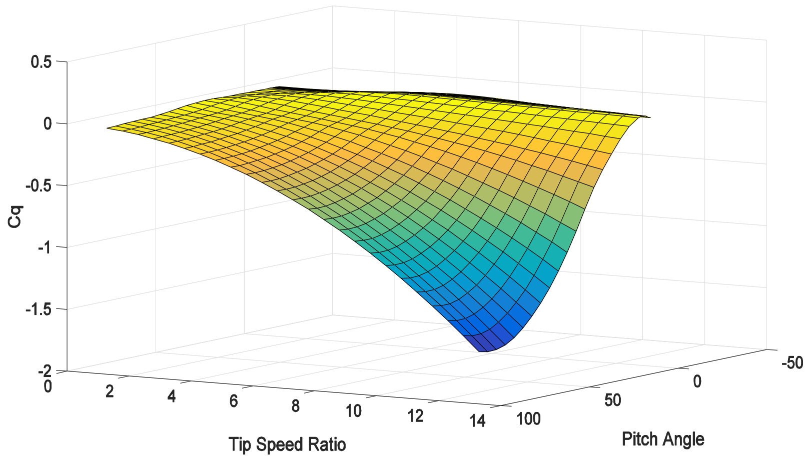

Fig. 7.1.3. Torque coefficient C_q as a function of the tip speed ratio λ and pitch angle β

The pitch systems considered in this model is three hydraulic pitch systems. The closed loop dynamic of each pitch system is described by a second-order system:

$$\frac{\beta(s)}{\beta_r(s)} = \frac{\omega_n^2}{s^2+2\xi\omega_n s+\omega_n^2} \tag{7-1-3}$$

where β_r is the pitch reference provided by the controller.

7.1.2. Drive train model

The drive train is responsible to increase the rotational speed from the rotor to generator. The model includes low and high speed shafts linked together by a gearbox modeled as a gear ratio, and the state space model is given by:

$$\begin{bmatrix} \dot{\omega_r}(t) \\ \dot{\omega_g}(t) \\ \dot{\theta}_\Delta(t) \end{bmatrix} = A_{DT} \begin{bmatrix} \omega_r(t) \\ \omega_g(t) \\ \theta_\Delta(t) \end{bmatrix} + B_{DT} \begin{bmatrix} \tau_r(t) \\ \tau_g(t) \end{bmatrix} \tag{7-1-4}$$

where τ_g is the generator torque, ω_g is the generator rotating speed and θ_Δ is the torsion angle of drive train. The state space matrices are:

$$A_{DT} = \begin{bmatrix} -\frac{B_{dt}+B_r}{J_r} & \frac{B_{dt}}{N_g J_r} & -\frac{K_{dt}}{J_r} \\ \frac{\eta_{dt} B_{dt}}{N_g J_g} & \frac{-\frac{\eta_{dt} B_{dt}}{N_g^2} - B_g}{J_g} & \frac{\eta_{dt} K_{dt}}{N_g J_g} \\ 1 & -\frac{1}{N_g} & 0 \end{bmatrix},$$

$$B_{DT} = \begin{bmatrix} \frac{1}{J_r} & 0 \\ 0 & -\frac{1}{J_g} \\ 0 & 0 \end{bmatrix},$$

where J_r and J_g are the rotor and generator moment of inertia, B_r and B_g are the rotor and generator external damping, B_{DT} is the torsion damping coefficient, N_g and η_{dt} are the gear ratio and efficiency of drive train, and K_{dt} is the torsion stiffness.

7.1.3. Generator and converter model

A generator fully coupled to a converter is used to convert mechanical energy to electricity. On a system level of wind turbine, the generator and converter dynamics can be modelled by a first-order transfer function:

$$\frac{\tau_g(s)}{\tau_{g,r}(s)} = \frac{\alpha_{gc}}{s+\alpha_{gc}} \tag{7-1-5}$$

where α_{gc} is the generator and converter model parameter. The convertor can be used to set the generator torque, which consequently can be used to control the rotational speed of generator and rotor can be controlled.

The power produced by the generator is given by:

$$P_g = \eta_g \omega_g(t) \tau_g(t) \tag{7-1-6}$$

where $\eta_g$is the efficiency of the generator.

7.1.4. Controller

The controller is designed to make the system track a given power reference. A simple control scheme such as PID controller is often used in wind turbine systems.

More details and numerical values of the parameters mentioned above can be found in [81]. For the simplification of description, in the rest of this chapter, we omit t in vector.

By integrating the subsystems together, the global wind turbine model can be described in the state-space form:

$$\begin{cases} \dot{x} = A(x)x + Bu \\ y = Cx \end{cases} \tag{7-1-7}$$

where $x = \begin{bmatrix} w_r & w_g & \theta_\Delta & \dot{\beta} & \beta & \tau_g \end{bmatrix}^T$ is the state vector, $u = [\tau_{g,r} \quad \beta_r]^T$ is the control input vector obtained from the predesigned controller,

$$A(x) = \begin{bmatrix} A_{11} & \frac{B_{dt}}{N_g J_r} & -\frac{K_{dt}}{J_r} & 0 & 0 & 0 \\ \frac{\eta_{dt} B_{dt}}{N_g J_g} & \frac{-\frac{\eta_{dt} B_{dt}}{N_g^2} - B_g}{J_g} & \frac{\eta_{dt} K_{dt}}{N_g J_g} & 0 & 0 & -\frac{1}{J_g} \\ 1 & -\frac{1}{N_g} & 0 & 0 & 0 & 0 \\ 0 & 0 & 0 & -2\varsigma\omega_n & -\omega_n^2 & 0 \\ 0 & 0 & 0 & 1 & 0 & 0 \\ 0 & 0 & 0 & 0 & 0 & -\alpha_{gc} \end{bmatrix}$$

$$B = \begin{bmatrix} 0 & 0 & 0 & 0 & 0 & \alpha_{gc} \\ 0 & 0 & 0 & \omega_n & 0 & 0 \end{bmatrix}^T, C = \begin{bmatrix} 1 & 0 & 0 & 0 & 0 & 0 \\ 0 & 1 & 0 & 0 & 0 & 0 \\ 0 & 0 & 0 & 0 & 1 & 0 \\ 0 & 0 & 0 & 0 & 0 & 1 \end{bmatrix},$$

where $A_{11} = -\frac{B_{dt}+B_r}{J_r} + \frac{1}{2J_r\lambda^2}\rho\pi R^5 C_q(\lambda,\beta)w_r$. It is noticed that only A_{11} depends on x.

The physical meanings of the wind turbine parameters are shown in Table 7.1.1.

Table 7.1.1. Parameter symbols of benchmark wind turbines

w_r	Rotor angular speed	β_r	Pitch reference
θ_Δ	Torsion angle	N_g	Gear ratio
w_g	Generator rotating speed	J_r	Rotor moment of inertia
β	Pitch angle	K_{dt}	Torsion stiffness
α_{gc}	Generator and converter parameter	J_g	Generator moment of inertia
B_g	Generator external damping	η_{dt}	Efficiency of drive train
ω_n	Natural frequency	τ_g	Generator torque
λ	Tip-speed-ratio	R	Rotor radius
ς	Damping ration	C_q	Torque coefficient

$\tau_{g,r}$	Generator torque reference	B_{dt}	Torsion damping coefficient
B_r	Rotor external damping	ρ	Air density

7.2 Takagi-Sugeno modelling of benchmark wind turbine

Although some subsystems are modelled as linear systems, the global model is highly nonlinear due to the wind turbine aerodynamic, which brings difficulties to the observer design. Thus it is motivated to rebuild the nonlinear wind turbine systems by T-S fuzzy models to reduce the complexity. In existing work about T-S fuzzy modelling of benchmark model, the details of local models and corresponding membership functions were not provided. Therefore, a new T-S fuzzy model is developed in this project.

In order to handle the nonlinearities in system (7-1-7), three parameters w_r, β and λ are selected as the premise variables for building the fuzzy wind turbine model. A set of local operation mode $[W_l \quad N_\tau \quad V_k]^T$ are chosen, where $l = 1,2$, $\tau = 1,2,3,4$, $k = 1,2,3$ and $W_1 = 0.0591$, $W_2 = 2.5$, $N_1 = -2$, $N_2 = 5$, $N_3 = 35$, $N_4 = 70$, $V_1 = 1$, $V_2 = 7$, $V_3 = 13$. Therefore, the nonlinear model (7-1-7) can be approximated by a set of IF-THEN rules as follows:

IF w_r is W_l, β is N_τ and λ is V_k, THEN

$$\begin{cases} \dot{x} = A_{l\tau k}x + B_{l\tau k}u \\ y = C_{l\tau k}x \end{cases} \tag{7-2-1}$$

where $A_{l\tau k}$ is $A(x)$ by replacing A_{11} by $A_{l\tau k11} = -\frac{B_{dt}+B_r}{J_r} + \frac{1}{2J_r\lambda^2}\rho\pi R^5 C_q(M_{3l\tau k}, M_{2l\tau k})M_{1l\tau k}$, $B_{l\tau k} = B$,$C_{l\tau k} = C$.

Now let us consider to define proper membership functions to make the T-S fuzzy model approximate the original plant accurately, which can be accessed by defining the sub-membership functions for the three decision parameters separately, and the global membership functions can be yielded by multiplying them together. Specifically, $a_1(w_r)$ and $a_2(w_r)$ are two membership functions representing the possibility of in the range of two local models W_1 and W_2. They can be defined as $a_1(w_r) = \frac{-w_r+W_2}{W_2-W_1}$, and $a_2(w_r) = \frac{-W_1+w_r}{W_2-W_1}$. We can easily verify that $a_1(w_r), a_2(w_r) \in [0,1]$, and $a_1(w_r) + a_2(w_r) = 1$. As a result, $a_1(w_r)$ and $a_2(w_r)$ can be the sub-membership functions of any given w_r in terms of W_1 and W_2.

Since four values of β are chosen to build T-S fuzzy model, we have $b_1(\beta)$, $b_2(\beta)$, $b_3(\beta)$ and $b_4(\beta)$ as the membership functions representing the possibility in the range of four local models N_1, N_2, N_3 and N_4, which are defined as follows

$$b_1(\beta) = \frac{-\beta+N_2}{2(N_2-N_1)} \cdot sgn(-\beta+N_2) + \frac{-\beta+N_2}{2(N_2-N_1)},$$

$$b_2(\beta) = \frac{-N_1+\beta}{2(N_2-N_1)} \cdot sgn(-\beta+N_2) + \frac{-N_1+\beta}{2(N_2-N_1)} + \frac{-\beta+N_3}{2(N_3-N_2)}$$

$$\cdot\, sgn(-N_2+\beta) \cdot\, sgn(-\beta+N_3) + \frac{-\beta+N_3}{2(N_3-N_2)},$$

$$b_3(\beta) = \frac{-N_2+\beta}{2(N_3-N_2)} \cdot sgn(-\beta+N_3) \cdot sgn(-N_2+\beta)$$

$$+ \frac{-N_2+\beta}{2(N_3-N_2)} + \frac{-\beta+N_4}{2(N_4-N_3)} \cdot sgn(-N_3+\beta) + \frac{-\beta+N_4}{2(N_4-N_3)},$$

$$b_4(\beta) = \frac{-N_3+\beta}{2(N_4-N_3)} \cdot sgn(-N_3+\beta) + \frac{-N_3+b_3}{2(N_4-N_3)}.$$

where

$$sgn(\sigma) = \begin{cases} -1 & \sigma < 0 \\ 0 & \sigma = 0 \\ 1 & \sigma > 0 \end{cases} \tag{7-2-2}$$

It is easy to verity that $b_1(\beta)$, $b_2(\beta)$, $b_3(\beta)$ and $b_4(\beta)$ match convex sum properties.

Similarly, we can have the membership functions of V_1, V_2 and V_3 in the following form:

$$c_1(\lambda) = \frac{-\lambda+V_2}{2(V_2-V_1)} \cdot sgn(-\lambda+V_2) + \frac{-\lambda+V_2}{2(V_2-V_1)},$$

$$c_2(\lambda) = \frac{-V_1+\lambda}{2(V_2-V_1)} \cdot sgn(-\lambda+V_2) + \frac{-V_1+\lambda}{2(V_2-V_1)} + \frac{-\lambda+V_3}{2(V_3-V_2)}$$

$$\cdot\, sgn(-V_2+\lambda) + \frac{-\lambda+V_3}{2(V_3-V_2)},$$

$$c_3(\lambda) = \frac{-V_2+\lambda}{2(V_3-V_2)} \cdot sgn(-V_2+\lambda) + \frac{-V_2+\lambda}{2(V_3-V_2)}$$

Finally, we can define $h_{l\tau k}(\mu) = a_l \cdot b_\tau \cdot c_k$, where $\mu = [w_r \quad \beta \quad \lambda]^T$, as global membership functions of the T-S fuzzy models and it is easy to verify that $h_{l\tau k}(\mu)$ also satisfy the convex sum conditions $0 \leq h_{l\tau k}(\mu) \leq 1$ and $\sum_{l=1}^{2}\sum_{\tau=1}^{4}\sum_{k=1}^{3} h_{l\tau k}(\mu) = 1$.

The final T-S fuzzy model can be inferred as:

$$\begin{cases} \dot{x} = \sum_{l=1}^{2}\sum_{\tau=1}^{4}\sum_{k=1}^{3} h_{l\tau k}(\mu)\,(A_{l\tau k}x + B_{l\tau k}u) \\ y = \sum_{l=1}^{2}\sum_{\tau=1}^{4}\sum_{k=1}^{3} h_{l\tau k}(\mu)\,C_{l\tau k}x \end{cases} \tag{7-2-3}$$

In order to evaluate the modelling performance, we can compare the outputs of T-S fuzzy model with the original plant outputs. The Simulink block diagrams and fuzzy system coefficients are presented in Appendix 2 and Appendix 3, respectively. Figs. 7.2.1-7.2.4 show the consistency between original outputs and T-S fuzzy outputs in the fault-free case. We can see the T-S fuzzy model built by the presented approach can track all the four original system outputs well, in spite of some modelling errors. It should be noted that practically, system (7-2-3) cannot be exactly the same as the actual plant (7-1-7) due to modelling error. Let ε_1 and ε_2 be the errors of state and output equations, respectively. The system (7-1-7) is thus described by the T-S fuzzy model with uncertainties:

$$\begin{cases} \dot{x} = \sum_{l=1}^{2}\sum_{\tau=1}^{4}\sum_{k=1}^{3} h_{l\tau k}(\mu)\,(A_{l\tau k}x + B_{l\tau k}u + E_1\varepsilon_1) \\ y = \sum_{l=1}^{2}\sum_{\tau=1}^{4}\sum_{k=1}^{3} h_{l\tau k}(\mu)\,(C_{l\tau k}x + E_2\varepsilon_2) \end{cases} \tag{7-2-4}$$

where E_1 and E_2 are constant matrices composed of 0 and 1, with 0 denoting no error whereas 1 denoting an error on a variable. It is noticed that in the benchmark model, the nonlinear parts only exist in the first state w_r thus the modelling errors influence w_r directly. In other words, for this model, the error only exists in the first state w_r, thus $E_1 = [1 \quad 0 \quad 0 \quad 0 \quad 0 \quad 0]^T$, and $E_2 = 0$.

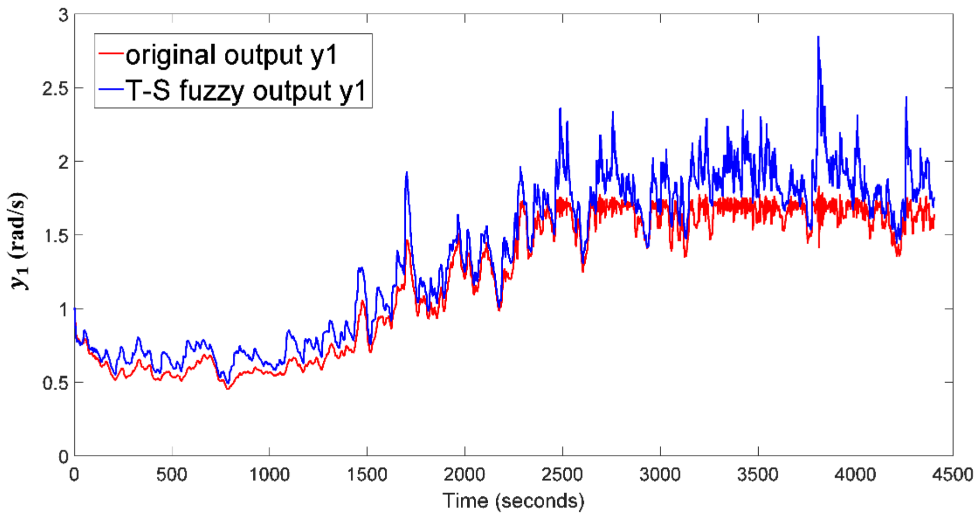

Fig. 7.2.1. T-S fuzzy modelling performance of y_1

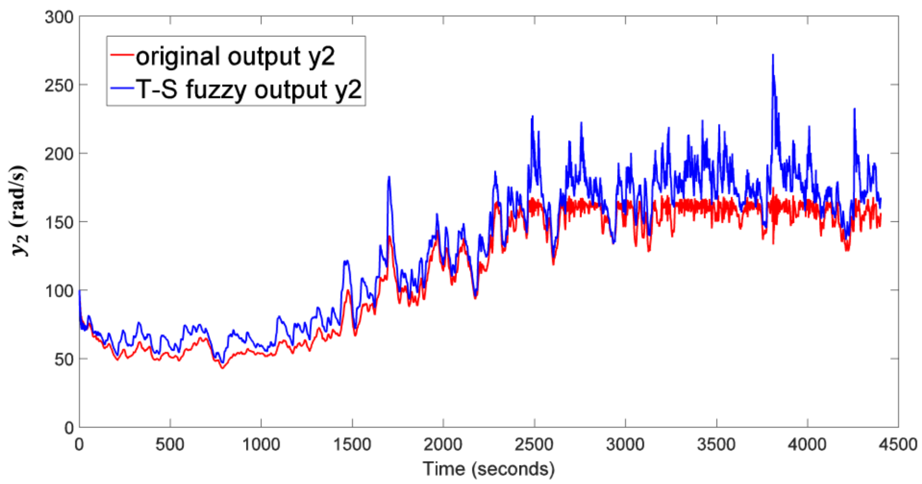

Fig. 7.2.2. T-S fuzzy modelling performance of y_2

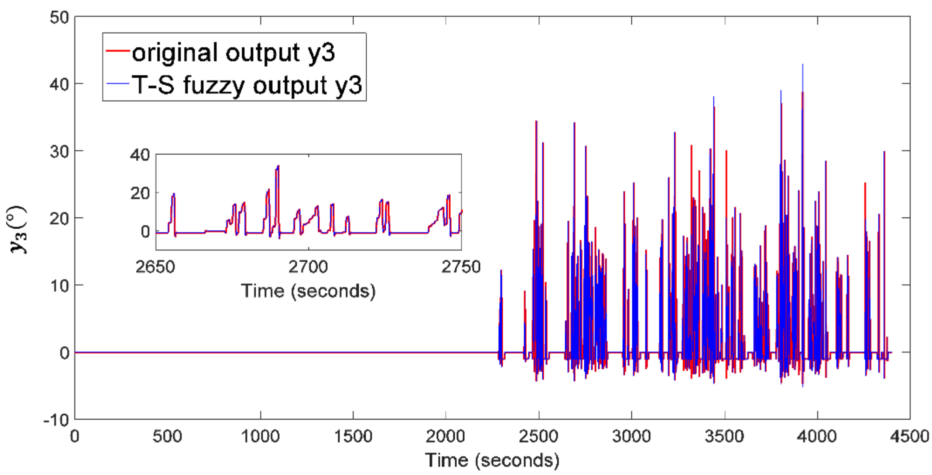

Fig. 7.2.3. T-S fuzzy modelling performance of y_3

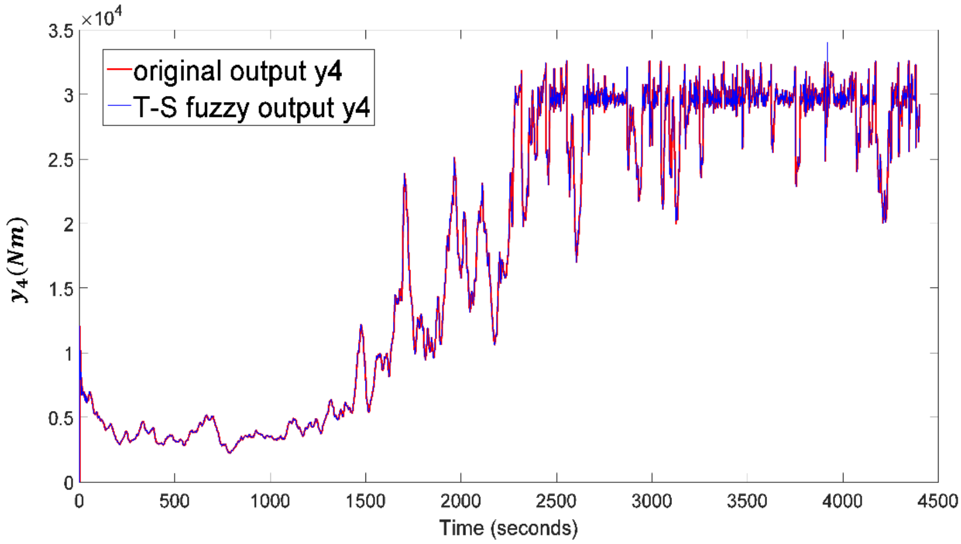

Fig. 7.2.4. T-S fuzzy modelling performance of y_4

Remark 7.2.1

In the wind turbine model, we use multi subscripts "$l\tau k$" to denote parameters of local model. By using single "i" to cover all different combinations of the subscripts, the fuzzy system with extra perturbations can be rewritten in the following form:

$$\begin{cases} \dot{x} = \sum_{i=1}^{r} h_i(\mu)\,(A_i x + B_i u + B_{ui} d_u + E_1 \varepsilon_1) \\ y = \sum_{i=1}^{r} h_i(\mu)\,(C_i x + D_{ui} d_{su} + E_2 \varepsilon_2) \end{cases} \tag{7-2-5}$$

where $r = 24$, $d_u \in \mathcal{R}^{l_{d_u}}$ and $d_{su} \in \mathcal{R}^{l_{d_{su}}}$ are extra perturbations of the plant and measurement, respectively, B_{ui} and D_{ui} are the coefficients with appropriate dimensions.

As the T-S fuzzy representation is an approximate of the real model, the modelling error can be regarded as a part of unknown inputs. In other words, by defining $d = [\varepsilon_1^T \quad d_u^T]^T$, $d_w = [\varepsilon_2^T \quad d_{su}^T]^T$, $B_{di} = [E_1 \quad B_{ui}]$ and $D_{di} = [E_2 \quad D_{ui}]$, the original nonlinear systems can be represented by plant

$$\begin{cases} \dot{x} = \sum_{i=1}^{r} h_i(\mu)\,(A_i x + B_i u + B_{di} d) \\ y = \sum_{i=1}^{r} h_i(\mu)\,(C_i x + D_{di} d_w) \end{cases} \tag{7-2-6}$$

Until now, the procedures to build the T-S fuzzy models for nonlinear systems can be summarized as follows:

Procedure 7.2.1 *T-S fuzzy modelling*

i) Find variables $\{\mu_j, j = 1,2,..,q\}$ that play dominant roles on nonlinear behaviors of the systems as premise decision variables.

ii) Choose a set of valid operating points M_{ji}, $i = 1,2,..,r$, $j = 1,2,..,q$ depending on the decision vector $\mu = \{\mu_j,\ j = 1,2,..,q\}$, which are representatives to reflect the several working conditions of the system.

iii) Determine the membership functions $h_i(\mu)$, $i = 1,2,..,r$ of any given working condition to represent its weight in each space divided by the chosen premise variables.

iv) The local linear models are built by substituting the parameters that valid around each operating points.

v) Obtain the global model (7-2-5) by combining local models weighted by the corresponding membership functions, and find where the modeling errors exist, such that E_1 and E_2 and can be determined.

vi) Obtain $B_{di} = [E_1 \quad B_{ui}]$ and $D_{di} = [E_2 \quad D_{ui}]$ as the coefficients of the unknown inputs, including external disturbances and modelling errors. Hence B_{di1}, B_{di2} and $\bar{B}_M$ can be obtained readily, and the system can be represented as plant (7-2-6).

It should be pointed out that in addition to wind turbines, the *Procedure* 7.2.1 is suitable for a variety of practical nonlinear industrial systems.

7.3 Fault estimation and signal compensation of wind turbine

Faulty components in wind turbine can cause high loses in energy production and possible damage to the wind turbines. Thus, the purpose of this section is to apply the advanced fault estimation and signal compensation techniques developed in Chapter 4 to benchmark wind turbines with faults.

The actuator of the power converter for controlling the generator torque could be faulty due to either faults in the converter electronics or an off-set on the converter torque. In this case study, the fault is considered to be 50% loss of actuation effectiveness from 1000s to 2000s. In this case, the coefficient of actuator fault is $B_{fa} = [0 \quad 0 \quad 0 \quad 0 \quad 0 \quad \alpha_{gc}]^T$. For an actual wind turbine, the sensors can be faulty resulting from electrical or mechanical failures. Here, the sensor fault is assumed to be 50% deviation of the real output of sensor 1. Thus, the coefficient of the sensor fault should be $D_{fs} = [1 \quad 0 \quad 0 \quad 0]^T$. Consequently, the fault vector considered is $f = [f_a \quad f_s]^T$ with $B_f = [B_{fa} \quad 0]$ and $D_f = [0 \quad D_{fs}]$. Then the nonlinear benchmark wind turbine subject to these two faults can be described by T-S fuzzy system (4-2). So the developed UIO-based fault estimation and signal compensation techniques developed for (4-2) can be implemented on the wind turbine.

It should be notice that the fuzzy observer-based estimation and fault tolerant control is implemented to the original nonlinear benchmark wind turbine rather than the developed fuzzy model. This meets practical requirement. Moreover, the modelling errors can be decoupled by the developed observer.

7.3.1. Fault estimation/reconstruction

The unknown inputs and the corresponding coefficients are given as: $d_{u1} = 0.01\sin(t)$, $d_{u2} = 0.03\sin(2t)$, $d_{su1} = \text{rand}(-0.02,0.02)$, $d_{su2} = \text{rand}(-0.2,0.2)$, $d_{su3} = 0.01\sin(\text{t})$, $d_{su4} = 0.2\sin(5\text{t})$, $B_{ui} = \begin{bmatrix} 0.2 & 0.25 & 0 & 0 & -0.3 & 0.4 \\ 0.4 & 0.5 & 0 & 0 & -0.6 & 0.8 \end{bmatrix}^T$, $D_{ui} = I$. Choosing $\gamma = 1.25$, we can obtain the observer gains by solving LMIs (4-13) so that the modelling error ε_1 is decoupled and the influences of d_u and d_w are attenuated.

Block diagram of simulation can be found in Appendix 4. The curves displayed in Figs. 7.3.1-7.3.8 exhibit the estimation performance for all system states, actuator fault and sensor fault, respectively. From these figures, one can see the estimation performance is excellent. The T-S fuzzy modelling error and external disturbances have been attenuated effectively. Hence the proposed fault estimation approach can successfully estimate the faults and system states robustly.

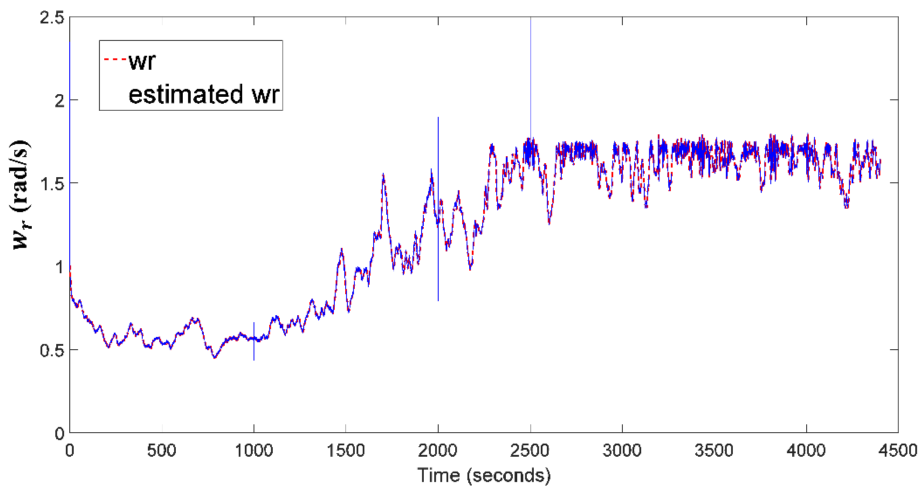

Fig. 7.3.1. w_r and its estimation

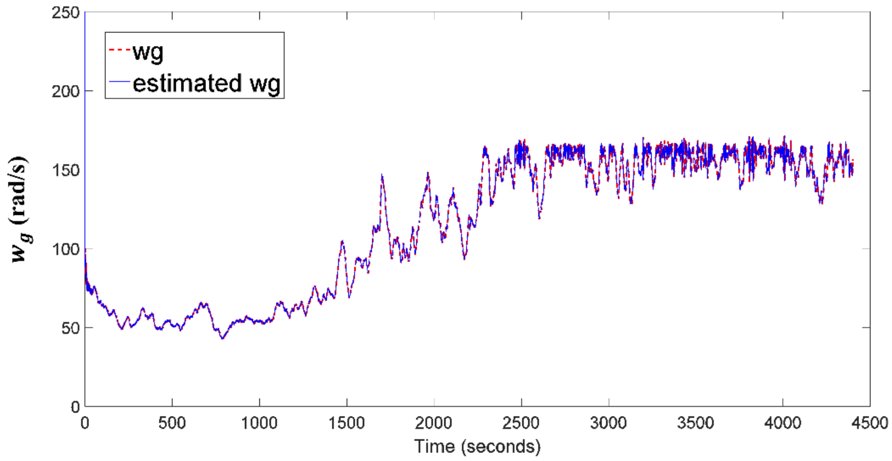

Fig. 7.3.2. w_g and its estimation

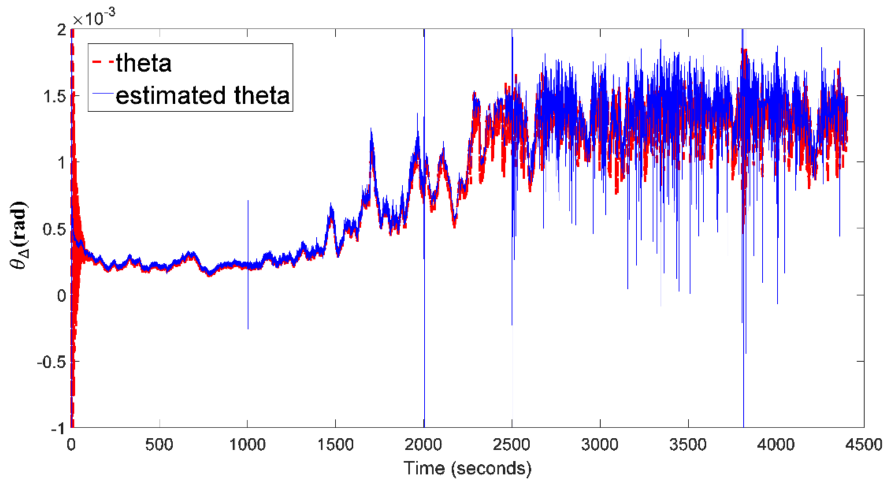

Fig. 7.3.3. θ_Δ and its estimation

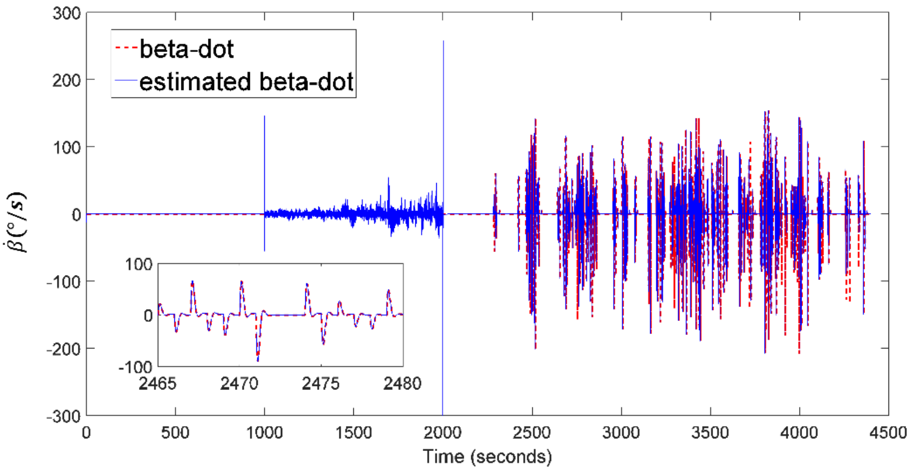

Fig. 7.3.4. $\dot{\beta}$ and its estimation

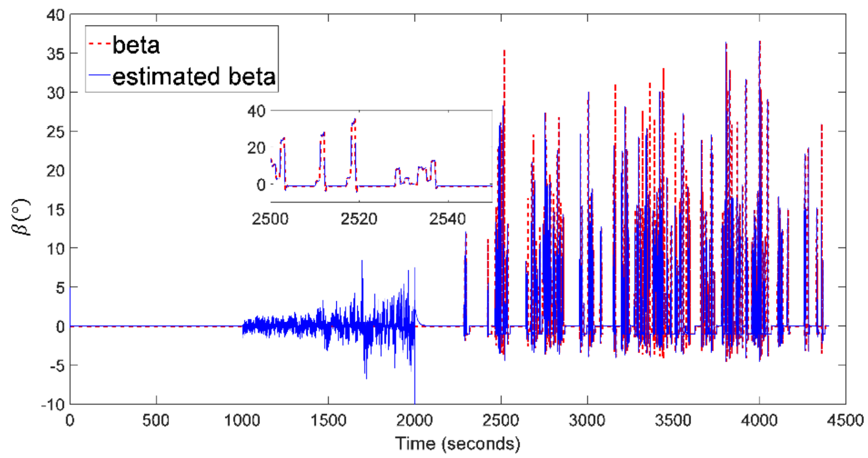

Fig. 7.3.5. β and its estimation

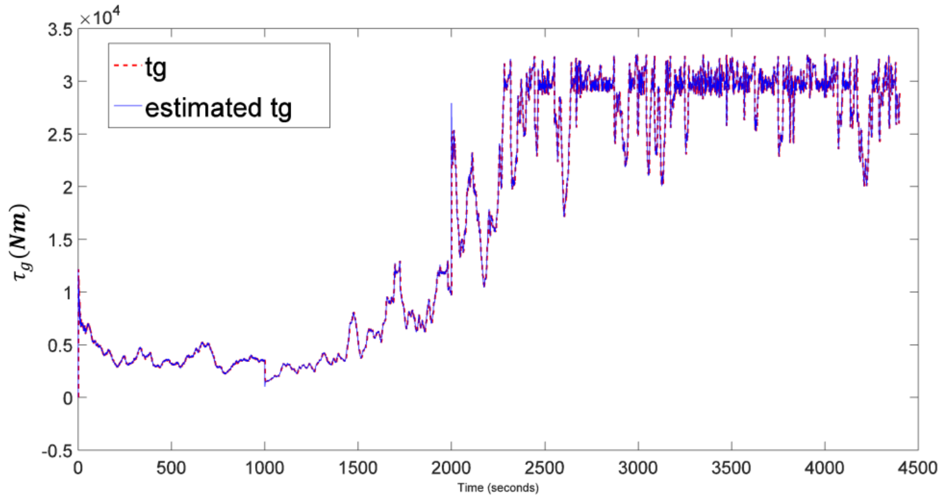

Fig. 7.3.6. τ_g and its estimation

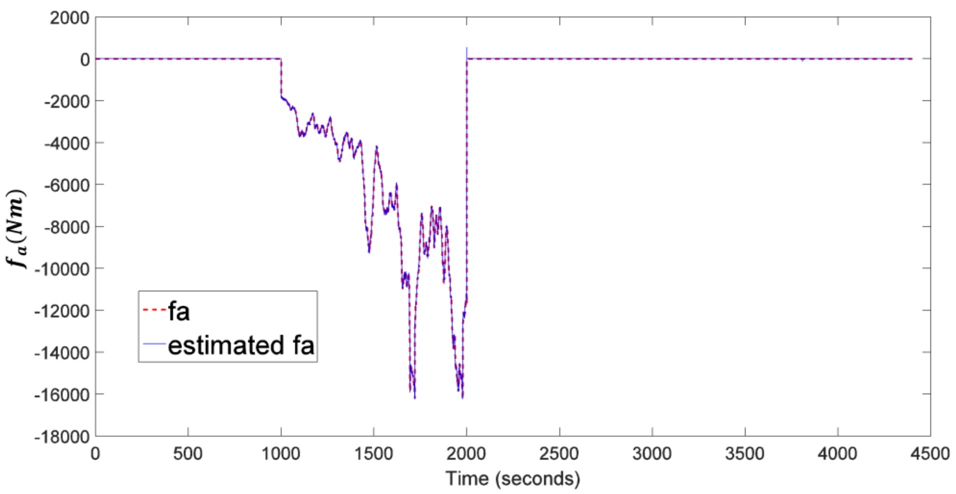

Fig. 7.3.7. f_a and its estimation

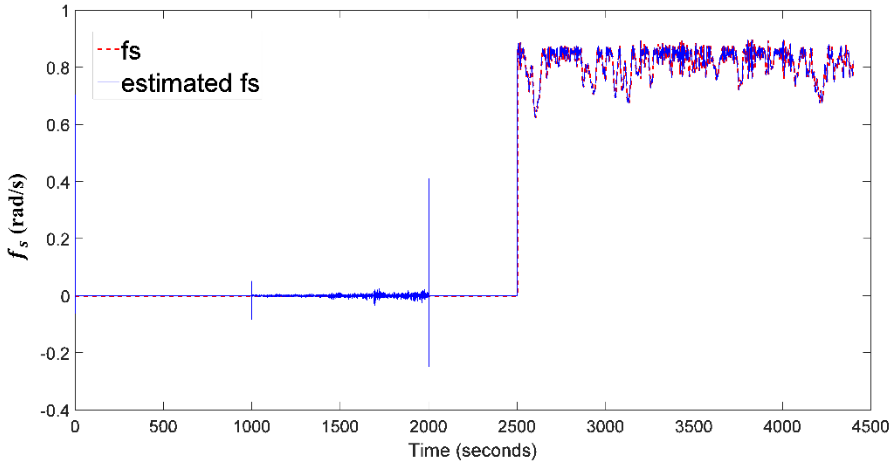

Fig. 7.3.8. f_s and its estimation

7.3.2. Fault tolerance by signal compensation

Based on the robust fault estimations, signal compensation techniques are applied to remove effects caused by faults. Block diagram of simulation is shown in Appendix 5. Figs. 7.3.9-7.3.13 show the simulated results, which compare the outputs with and without signal compensation. One can see that the compensated outputs for the wind turbines under faulty conditions can track the system output without faults. As a result, the tolerance of the wind turbine systems is realized.

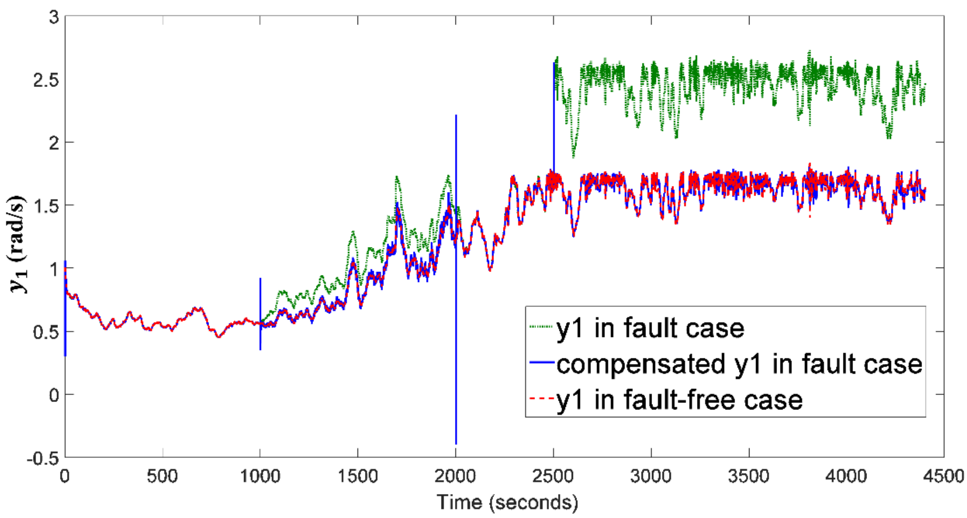

Fig. 7.3.9. y_1 with and without compensation

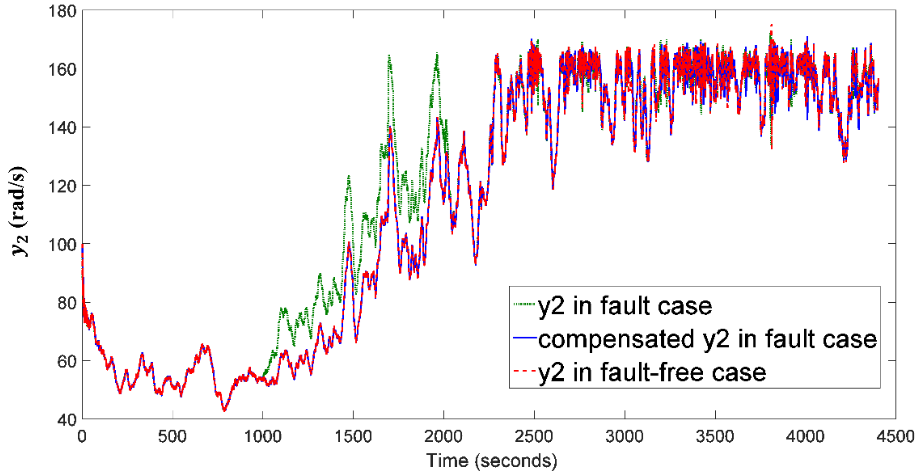

Fig. 7.3.10. y_2 with and without compensation

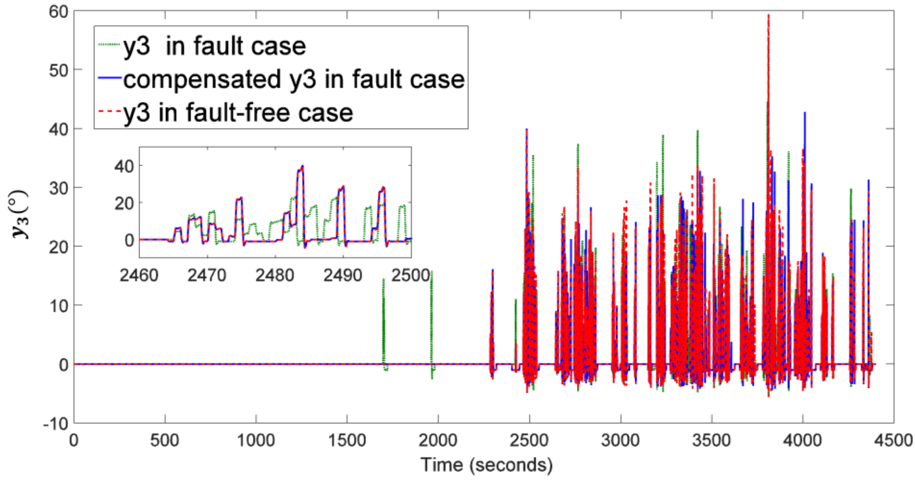

Fig. 7.3.11. y_3 with and without compensation

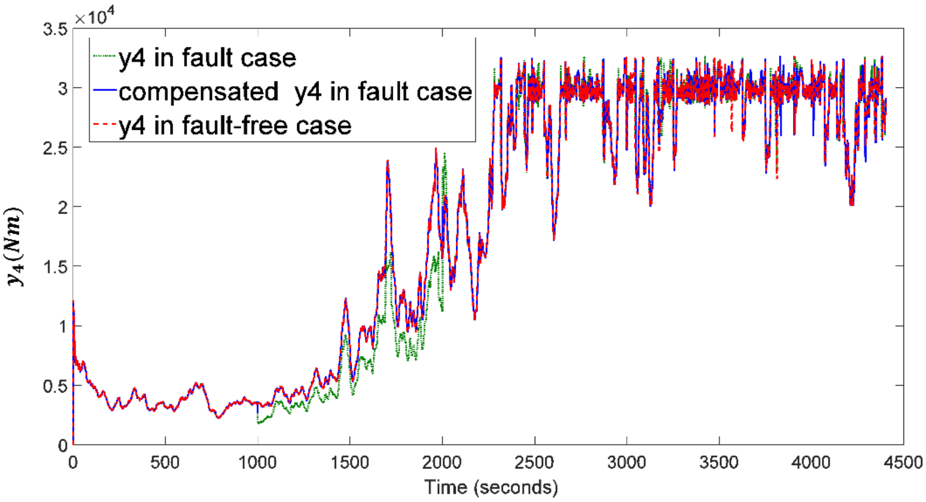

Fig. 7.3.12. y_4 with and without compensation

7.4 Robust fault estimation and fault tolerant control for drive train system subject to stochastic perturbations

The drive train is responsible for increasing the rotational speed from the rotor to generator. The model includes low and high speed shafts linked together by a gearbox modelled as a gear ratio. When the system is affected stochastic parameter perturbations, the state space model is given by:

$$\begin{cases} d\omega_r = \left(-\dfrac{B_{dt}+B_r}{J_r}\omega_r + \dfrac{B_{dt}}{N_g J_r}\omega_g - \dfrac{K_{dt}}{J_r}\theta_\Delta + \dfrac{1}{J_r}\tau_r\right)dt + 0.02\omega_r dw \\ d\omega_g = \left(\dfrac{\eta_{dt}B_{dt}}{N_g J_g}\omega_r + \dfrac{-\dfrac{\eta_{dt}B_{dt}}{N_g^2} - B_g}{J_g}\omega_g + \dfrac{\eta_{dt}K_{dt}}{N_g J_g}\theta_\Delta - \dfrac{1}{J_g}\tau_g\right)dt + 0.05\omega_g dw \\ d\theta_\Delta = \left(\omega_r - \dfrac{1}{N_g}\omega_g\right)dt + 0.01\theta_\Delta dw \\ y_1 = \omega_r \\ y_2 = \omega_g \end{cases} \quad (7\text{-}4\text{-}1)$$

When the plant (7-4-1) is subject to faults and unknown input disturbances, it can be represented by system (6-1-1) with $x = [\omega_r \quad \omega_g \quad \theta_\Delta]^T$ corrupted by random noises; $u = [\tau_r \quad \tau_g]^T$, where τ_r and τ_g take references from pitch system and generator system of the benchmark wind turbine, respectively. We consider $d = [d_1 \quad d_2 \quad d_3]^T$, and d_1, d_2 and d_3 are random signals with range from -10^{-2} to 10^{-2}; actuator fault f_a is 50% loss of actuation effectiveness for τ_g from 2000 seconds to 3500 seconds and the coefficients are as follows:

$$A = \begin{bmatrix} -\frac{B_{dt}+B_r}{J_r} & \frac{B_{dt}}{N_g J_r} & -\frac{K_{dt}}{J_r} \\ \frac{\eta_{dt}B_{dt}}{N_g J_g} & \frac{-\frac{\eta_{dt}B_{dt}}{N_g^2} - B_g}{J_g} & \frac{\eta_{dt}K_{dt}}{N_g J_g} \\ 1 & -\frac{1}{N_g} & 0 \end{bmatrix}, B = \begin{bmatrix} \frac{1}{J_r} & 0 \\ 0 & -\frac{1}{J_g} \\ 0 & 0 \end{bmatrix},$$

$$C = \begin{bmatrix} 1 & 0 & 0 \\ 0 & 1 & 0 \end{bmatrix}, \ W = \begin{bmatrix} 0.02 & 0 & 0 \\ 0 & 0.05 & 0 \\ 0 & 0 & 0.01 \end{bmatrix},$$

$$B_f = \begin{bmatrix} 0 \\ -\frac{1}{J_g} \\ 0 \end{bmatrix}, B_d = \begin{bmatrix} -0.6 & 0.04 & -0.08 \\ 0.2 & -0.02 & 0.04 \\ -0.3 & -0.01 & 0.02 \end{bmatrix} \text{ and } D_f = \begin{bmatrix} 0 \\ 0 \\ 0 \end{bmatrix}.$$

Since the drive train system is already a stable dynamic with desired response, we let control gain K to be zero. Selecting $\gamma_1 = 10$ and $\gamma_2 = 5$, and solving LMIs (6-1-21) and (6-1-22), the observer gain L_1 can be calculated as

$$L_1 = \begin{bmatrix} 539.86 & -2271.4 \\ -1618.7 & 6827.8 \\ 229.79 & -1047.9 \\ -14181 & 24558 \\ 11792 & 25226 \end{bmatrix}$$

Therefore R and L_2 can be obtained following the formulas (6-1-6) and (6-1-8), respectively.

Using the Euler–Maruyama method to simulate the standard Brownian motion, one can obtain the simulated curves of the stochastic state responses (here we give 5 state trajectories). Figures 7.4.1-7.4.4 exhibit the estimation performance for full system states and the means of actuator fault, respectively. Figures 7.4.5 and 7.4.6 compare the system outputs with and without tolerant control, and healthy outputs in fault-free cases.

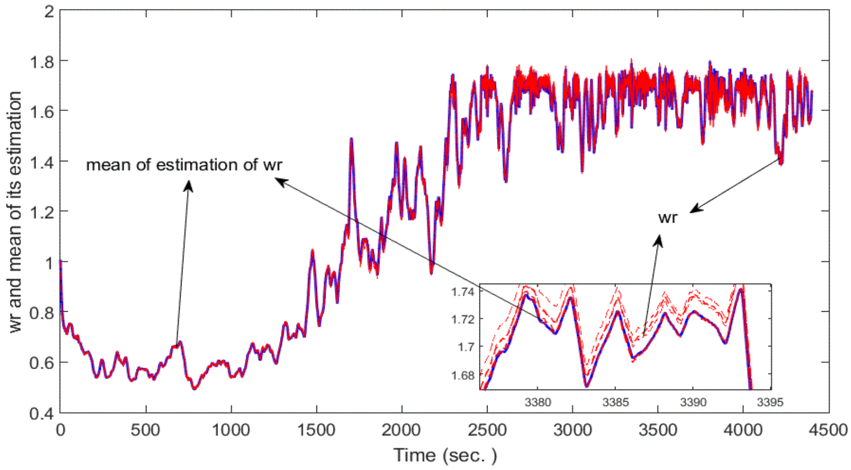

Figure 7.4.1. Rotor angular speed and the mean of its estimate (rad/s): wind turbine.

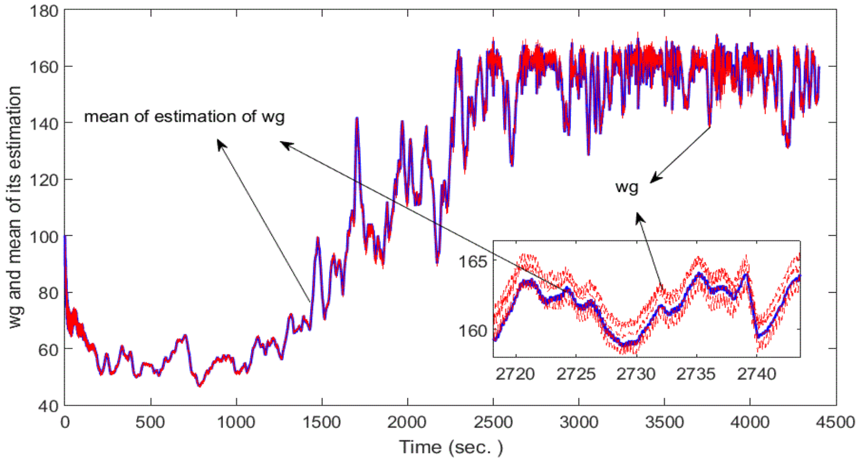

Figure 7.4.2. Generator rotating speed and the mean of its estimate (rad/s): wind turbine.

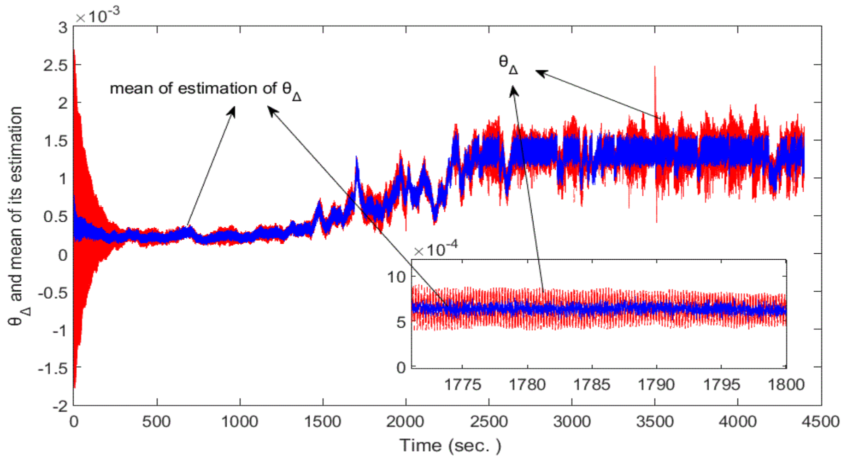

Figure 7.4.3. Torsion angle and the mean of its estimate (rad): wind turbine.

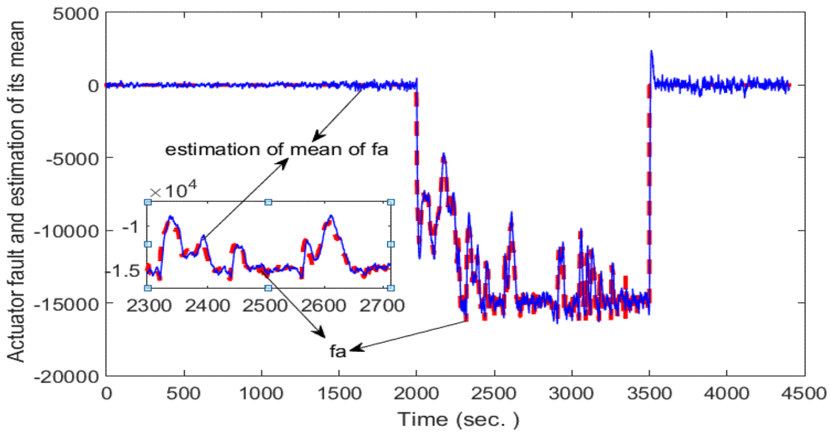

Figure 7.4.4. Generator torque fault and the estimate of its mean(Nm): wind turbine.

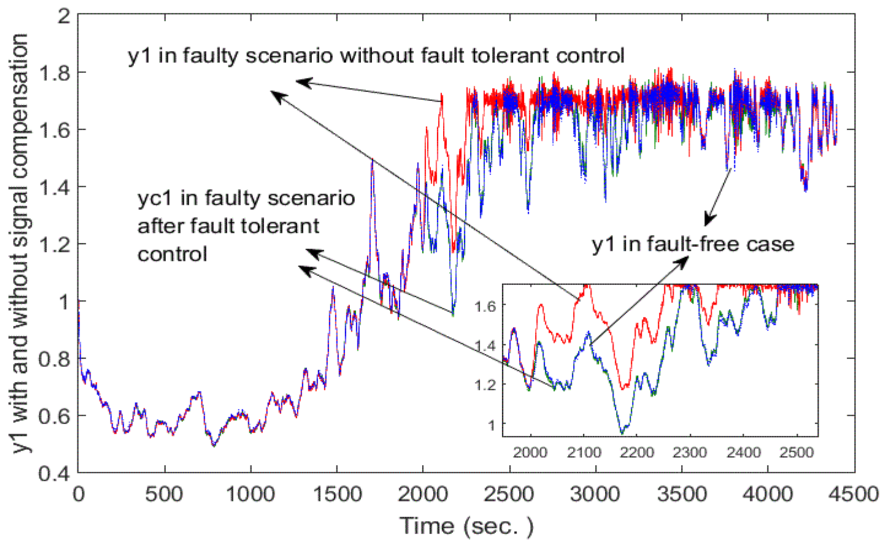

Figure 7.4.5. Comparisons of the first output (rad/s): fault-free output y_1, output $y_1$subjected to faults without tolerant control, and output subjected to faults after tolerant control denoted by y_{c1}: wind turbine.

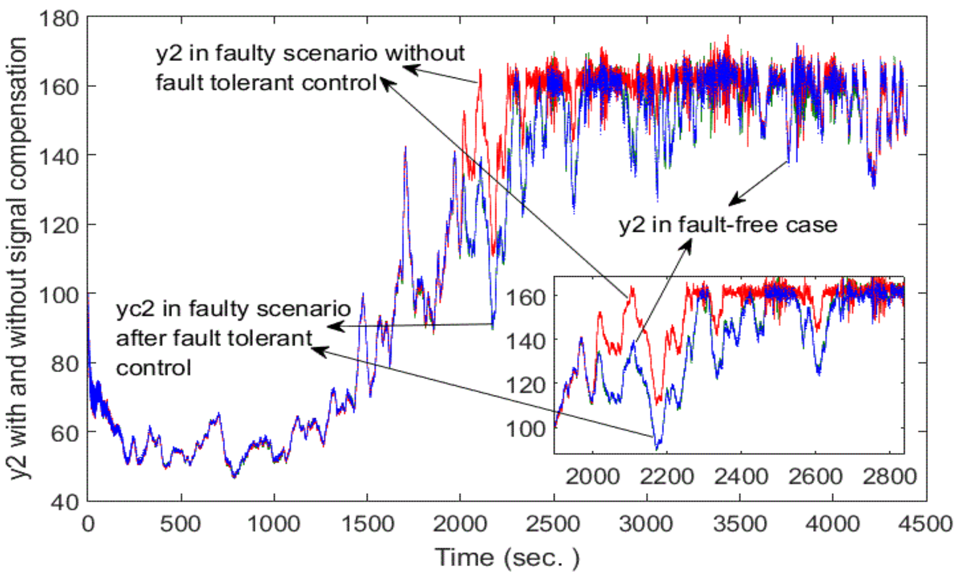

Figure 7.4.6. Comparisons of the second output (rad/s): fault-free output y_2, output $y_2$subjected to faults without tolerant control, and output subjected to faults after tolerant control denoted by y_{c2}: wind turbine.

From the Figures 7.4.1-7.4.4, we can see that both the system states and actuator fault are estimated satisfactorily, and the influences of the unknown inputs are decoupled/attenuated successfully. Moreover, we can find in Figures 7.4.5 and 7.4.6 that the actuator fault will make the deviation of the outputs. However, after tolerant control, the deviation is eliminated/offset successfully, as one can see the compensated outputs are consistent with the fault-free outputs. As a result, the proposed fault estimation-based fault tolerant control techniques are effective.

At present, limited work has been recorded in terms of the overall nonlinear wind turbine. Compared with existing work, the presented techniques can achieve robustness against more general types of unknown inputs. In addition, fault tolerant control can be achieved without replacing pre-designed controller. Furthermore, no existing effort has been made on robust fault estimation and fault tolerant control of stochastic wind turbine drive trains.

7.5 Summary

This chapter is a case study about robust fault estimation and fault tolerant control for wind turbines. The benchmark wind turbine with 4.8 MW electrical power output has been under study. Takagi-Sugeno modelling algorithms have been employed to handle the high-nonlinear natures of the wind turbine, then the designed UIO-based fault estimation and signal compensation approach has been applied to the whole benchmark wind turbine characterized by T-S fuzzy model. To be mentioned that the modelling errors have been considered as a part of unknown inputs.

Moreover, for stochastic wind turbine drive train in presence of Brownian perturbations, the integrated fault tolerant control technique designed for stochastic systems has been applied to remove actuation loss of effectiveness fault. All the implementation results have well validated the fault estimation and fault tolerant control performance of the developed methods.

Chapter 8

Conclusions

8.1 Thesis summary

This thesis focuses on developing robust fault estimation and fault tolerant control strategies, which can be applied to wind turbines and other industrial systems. Augmented system approach, unknown input observer method, and optimization technique have been integrated to achieve robust estimates of the system states and the faults concerned. Based on the estimates, robust fault tolerant control strategies have been developed by using actuator and sensor signal compensation techniques. The major contributions can be summarized as follows:

- Fault/state estimation with robustness against partially decoupled unknown inputs

  In contrast to existing results, partially decoupled rather than completely decoupled unknown inputs have been investigated in this thesis. Through augmented approach, simultaneous estimation of system states and concerned faults can be obtained. Unknown input observer technique jointly with optimization method have been utilized to eliminate the influences of unknown inputs on the estimation. Specifically, UIO was capable to decouple a part of unknown inputs. Since the unknown inputs were partially decoupled, those cannot be decoupled by the UIO still influenced the estimation. LMI was then combined to attenuate their influences such that expected robustness performance can be achieved. Moreover, the existence condition of such an unknown input observer has been proposed. The novel UIO-based fault estimation has been developed for linear systems, Lipschitz nonlinear systems (Chapter 3) and Takagi-Sugeno fuzzy nonlinear systems (Chapter 4).

- Fault estimation-based signal compensation for fault tolerant control

  After implementing the novel UIO-based fault estimation, signal compensation method combined with a pre-designed controller has been developed, such that the occurred faults can be removed from the system. It is worthy to notice that the pre-designed controller can guarantee the function of plant under fault-free scenario, and signal compensation approach can remove adverse effects of faults without changing the pre-designed controller. Therefore, the integrated fault tolerant control scheme can work reliably under both faulty and fault-free scenarios. This part of work has been presented in Chapter 4.

- Stochastically input-to-state stability based fault estimation and fault tolerant control for stochastic systems with Brownian motions

  Lyapunov-based criteria of stochastically input-to-state stability and finite-time stochastically input-to-state stability have been proposed with rigorous and completed proof. On this basis, UIO-based fault estimation techniques have been proposed for stochastic nonlinear systems. This part of work has been shown in Chapter 5. It is worthy to be mentioned that the estimation error was also influenced by stochastic perturbations, and the magnitude of stochastic perturbations was determined by system states due to the existence of Brownian motions. Hence, in the design of fault tolerant control, observer-based controller has been adopted to drive the overall closed-loop dynamic systems (consisting both original system after signal compensation and the estimation error system) to be stable with satisfied robustness performance. The systems under investigation can be linear, Lipschitz nonlinear, quadratic inner-bounded nonlinear, and T-S fuzzy nonlinear. This part of work can be found in Chapter 6.

- Application of designed integrated fault tolerant control to benchmark wind turbine

  Two scenarios have been provided in the case study of 4.8 MW benchmark wind turbine, i.e. deterministic nonlinear benchmark wind turbine and stochastic linear drive train in benchmark wind turbine. In both two cases, we consider the systems were subject to partially decoupled unknown inputs. In the first scenario, the nonlinear benchmark wind turbine has been modeled by a T-S fuzzy system with 24 fuzzy rules. The fuzzy modelling results have been compared with original plant to validate the effectiveness. Then the modelling errors have been recognized as a part of unknown inputs to be decoupled or attenuated by the novel UIO. To be pointed out that the procedure of T-S fuzzy model for general nonlinear systems has been proposed, which can also be applied to other nonlinear engineering systems. Based on well-developed T-S fuzzy model, the designed fault estimation and fault tolerant have been implemented to the original nonlinear wind turbine with generator toque actuator fault and rotor angle speed sensor fault. In the second scenario, drive train system in presence of stochastic Brownian motions has been investigated. Integrated fault tolerant control designed for stochastic systems has been implemented to remove generator toque actuator fault. The experimental results for both two scenarios have well validated the performance of integrated fault tolerant control. This case study has been demonstrated in Chapter 7.

To summarize, the novel UIO-based fault estimation designed in our work can achieve robustness against more general unknown inputs compared with previous results, i.e. either completely decoupled or partially decoupled. In addition, the designed fault estimation and fault tolerant control techniques are applicable for various types of engineering systems, including linear systems, Lipschitz nonlinear systems, quadratic inner-bounded nonlinear systems, and Takagi-Sugeno fuzzy nonlinear systems. Furthermore, the above mentioned systems can be either deterministic or stochastic with Brownian motions. Therefore, the proposed methodologies have wide application in practical dynamics.

8.2 Further research

Based on the PhD work mentioned above, it is motivated to keep on doing the research about the following problems.

- Application of integrated fault tolerant control for stochastic nonlinear benchmark wind turbine

  In the case study, fault estimation and fault tolerant control methods have been applied to deterministic nonlinear wind turbine modelled through T-S fuzzy logic and stochastic linear drive train system. On the other hand, integrated fault tolerant control techniques for stochastic T-S fuzzy systems have been designed in Chapter 6, which are potential to be applied to stochastic nonlinear wind turbines. Before implementation of fault tolerant control, stochastic modelling of the benchmark wind turbine, which is still an open problem, should be considered as a part of future work. Moreover, how to make linear matrix inequality less conservative and more solvable for designing observer gains and control gains is another interest for investigation.

- Finite-time robust fault estimation and fault tolerant control design for stochastic nonlinear systems

Convergence time is an important concern for observer-based control. Hence, it is of interest to investigate finite-time robust fault estimation and fault tolerant control design for stochastic nonlinear systems. The objective is to make the overall closed-loop system convergent in finite time through proper observer and controller design. To the best of our knowledge, no effort has been made on this topic, but worthy of future research.

- Estimation and control for pitch angle delay of wind turbine

Delays caused by hydraulic pressure driven units in wind turbines can lead to degradation of the whole wind turbine system. Estimation of the delays and compensation of their adverse influences is also a research interest in the future work.

Appendix 1

System coefficients of *Example 5.5.3*

$$A_1 = \begin{bmatrix} 0.0152 & 1.484\times10^{-7} & -49.0909 & 0 & 0 & 0 \\ 0.0203 & -0.1171 & 7.0688\times10^{4} & 0 & 0 & -0.0026 \\ 1 & -0.0105 & 0 & 0 & 0 & 0 \\ 0 & 0 & 0 & -13.332 & -123.4321 & 0 \\ 0 & 0 & 0 & 1 & 0 & 0 \\ 0 & 0 & 0 & 0 & 0 & -50 \end{bmatrix}$$

$$A_2 = \begin{bmatrix} 0.0017 & 1.484\times10^{-7} & -49.0909 & 0 & 0 & 0 \\ 0.0203 & -0.1171 & 7.0688\times10^{4} & 0 & 0 & -0.0026 \\ 1 & -0.0105 & 0 & 0 & 0 & 0 \\ 0 & 0 & 0 & -13.332 & -123.4321 & 0 \\ 0 & 0 & 0 & 1 & 0 & 0 \\ 0 & 0 & 0 & 0 & 0 & -50 \end{bmatrix}$$

$$A_3 = \begin{bmatrix} -2.115\times10^{-5} & 1.484\times10^{-7} & -49.0909 & 0 & 0 & 0 \\ 0.0203 & -0.1171 & 7.0688\times10^{4} & 0 & 0 & -0.0026 \\ 1 & -0.0105 & 0 & 0 & 0 & 0 \\ 0 & 0 & 0 & -13.332 & -123.4321 & 0 \\ 0 & 0 & 0 & 1 & 0 & 0 \\ 0 & 0 & 0 & 0 & 0 & -50 \end{bmatrix}$$

$$A_4 = \begin{bmatrix} 0.0187 & 1.484\times10^{-7} & -49.0909 & 0 & 0 & 0 \\ 0.0203 & -0.1171 & 7.0688\times10^{4} & 0 & 0 & -0.0026 \\ 1 & -0.0105 & 0 & 0 & 0 & 0 \\ 0 & 0 & 0 & -13.332 & -123.4321 & 0 \\ 0 & 0 & 0 & 1 & 0 & 0 \\ 0 & 0 & 0 & 0 & 0 & -50 \end{bmatrix}$$

$$A_5 = \begin{bmatrix} 0.0013 & 1.484\times10^{-7} & -49.0909 & 0 & 0 & 0 \\ 0.0203 & -0.1171 & 7.0688\times10^{4} & 0 & 0 & -0.0026 \\ 1 & -0.0105 & 0 & 0 & 0 & 0 \\ 0 & 0 & 0 & -13.332 & -123.4321 & 0 \\ 0 & 0 & 0 & 1 & 0 & 0 \\ 0 & 0 & 0 & 0 & 0 & -50 \end{bmatrix}$$

$$A_6 = \begin{bmatrix} 1.311\times10^{-4} & 1.484\times10^{-7} & -49.0909 & 0 & 0 & 0 \\ 0.0203 & -0.1171 & 7.0688\times10^{4} & 0 & 0 & -0.0026 \\ 1 & -0.0105 & 0 & 0 & 0 & 0 \\ 0 & 0 & 0 & -13.332 & -123.4321 & 0 \\ 0 & 0 & 0 & 1 & 0 & 0 \\ 0 & 0 & 0 & 0 & 0 & -50 \end{bmatrix}$$

$$A_7 = \begin{bmatrix} 0.0292 & 1.484\times10^{-7} & -49.0909 & 0 & 0 & 0 \\ 0.0203 & -0.1171 & 7.0688\times10^{4} & 0 & 0 & -0.0026 \\ 1 & -0.0105 & 0 & 0 & 0 & 0 \\ 0 & 0 & 0 & -13.332 & -123.4321 & 0 \\ 0 & 0 & 0 & 1 & 0 & 0 \\ 0 & 0 & 0 & 0 & 0 & -50 \end{bmatrix}$$

$$A_8 = \begin{bmatrix} -0.0035 & 1.484\times10^{-7} & -49.0909 & 0 & 0 & 0 \\ 0.0203 & -0.1171 & 7.0688\times10^{4} & 0 & 0 & -0.0026 \\ 1 & -0.0105 & 0 & 0 & 0 & 0 \\ 0 & 0 & 0 & -13.332 & -123.4321 & 0 \\ 0 & 0 & 0 & 1 & 0 & 0 \\ 0 & 0 & 0 & 0 & 0 & -50 \end{bmatrix}$$

$$A_9 = \begin{bmatrix} -0.0036 & 1.484\times10^{-7} & -49.0909 & 0 & 0 & 0 \\ 0.0203 & -0.1171 & 7.0688\times10^{4} & 0 & 0 & -0.0026 \\ 1 & -0.0105 & 0 & 0 & 0 & 0 \\ 0 & 0 & 0 & -13.332 & -123.4321 & 0 \\ 0 & 0 & 0 & 1 & 0 & 0 \\ 0 & 0 & 0 & 0 & 0 & -50 \end{bmatrix}$$

$$A_{10} = \begin{bmatrix} 0.6432 & 1.484\times10^{-7} & -49.0909 & 0 & 0 & 0 \\ 0.0203 & -0.1171 & 7.0688\times10^{4} & 0 & 0 & -0.0026 \\ 1 & -0.0105 & 0 & 0 & 0 & 0 \\ 0 & 0 & 0 & -13.332 & -123.4321 & 0 \\ 0 & 0 & 0 & 1 & 0 & 0 \\ 0 & 0 & 0 & 0 & 0 & -50 \end{bmatrix}$$

$$A_{11} = \begin{bmatrix} 0.0717 & 1.484\times10^{-7} & -49.0909 & 0 & 0 & 0 \\ 0.0203 & -0.1171 & 7.0688\times10^{4} & 0 & 0 & -0.0026 \\ 1 & -0.0105 & 0 & 0 & 0 & 0 \\ 0 & 0 & 0 & -13.332 & -123.4321 & 0 \\ 0 & 0 & 0 & 1 & 0 & 0 \\ 0 & 0 & 0 & 0 & 0 & -50 \end{bmatrix}$$

$$A_{12} = \begin{bmatrix} -3.07\times10^{-4} & 1.484\times10^{-7} & -49.0909 & 0 & 0 & 0 \\ 0.0203 & -0.1171 & 7.0688\times10^{4} & 0 & 0 & -0.0026 \\ 1 & -0.0105 & 0 & 0 & 0 & 0 \\ 0 & 0 & 0 & -13.332 & -123.4321 & 0 \\ 0 & 0 & 0 & 1 & 0 & 0 \\ 0 & 0 & 0 & 0 & 0 & -50 \end{bmatrix}$$

$$A_{13} = \begin{bmatrix} 0.7916 & 1.484\times10^{-7} & -49.0909 & 0 & 0 & 0 \\ 0.0203 & -0.1171 & 7.0688\times10^{4} & 0 & 0 & -0.0026 \\ 1 & -0.0105 & 0 & 0 & 0 & 0 \\ 0 & 0 & 0 & -13.332 & -123.4321 & 0 \\ 0 & 0 & 0 & 1 & 0 & 0 \\ 0 & 0 & 0 & 0 & 0 & -50 \end{bmatrix}$$

$$A_{14} = \begin{bmatrix} 0.0555 & 1.484\times10^{-7} & -49.0909 & 0 & 0 & 0 \\ 0.0203 & -0.1171 & 7.0688\times10^{4} & 0 & 0 & -0.0026 \\ 1 & -0.0105 & 0 & 0 & 0 & 0 \\ 0 & 0 & 0 & -13.332 & -123.4321 & 0 \\ 0 & 0 & 0 & 1 & 0 & 0 \\ 0 & 0 & 0 & 0 & 0 & -50 \end{bmatrix}$$

$$A_{15} = \begin{bmatrix} 0.0061 & 1.484\times10^{-7} & -49.0909 & 0 & 0 & 0 \\ 0.0203 & -0.1171 & 7.0688\times10^{4} & 0 & 0 & -0.0026 \\ 1 & -0.0105 & 0 & 0 & 0 & 0 \\ 0 & 0 & 0 & -13.332 & -123.4321 & 0 \\ 0 & 0 & 0 & 1 & 0 & 0 \\ 0 & 0 & 0 & 0 & 0 & -50 \end{bmatrix}$$

$$A_{16} = \begin{bmatrix} 1.2369 & 1.484\times10^{-7} & -49.0909 & 0 & 0 & 0 \\ 0.0203 & -0.1171 & 7.0688\times10^{4} & 0 & 0 & -0.0026 \\ 1 & -0.0105 & 0 & 0 & 0 & 0 \\ 0 & 0 & 0 & -13.332 & -123.4321 & 0 \\ 0 & 0 & 0 & 1 & 0 & 0 \\ 0 & 0 & 0 & 0 & 0 & -50 \end{bmatrix}$$

$$A_{17} = \begin{bmatrix} -0.1484 & 1.484\times10^{-7} & -49.0909 & 0 & 0 & 0 \\ 0.0203 & -0.1171 & 7.0688\times10^{4} & 0 & 0 & -0.0026 \\ 1 & -0.0105 & 0 & 0 & 0 & 0 \\ 0 & 0 & 0 & -13.332 & -123.4321 & 0 \\ 0 & 0 & 0 & 1 & 0 & 0 \\ 0 & 0 & 0 & 0 & 0 & -50 \end{bmatrix}$$

$$A_{18} = \begin{bmatrix} -0.1525 & 1.484\times10^{-7} & -49.0909 & 0 & 0 & 0 \\ 0.0203 & -0.1171 & 7.0688\times10^{4} & 0 & 0 & -0.0026 \\ 1 & -0.0105 & 0 & 0 & 0 & 0 \\ 0 & 0 & 0 & -13.332 & -123.4321 & 0 \\ 0 & 0 & 0 & 1 & 0 & 0 \\ 0 & 0 & 0 & 0 & 0 & -50 \end{bmatrix}$$

$$B_i = \begin{bmatrix} 0 & 0 \\ 0 & 0 \\ 0 & 0 \\ 0 & 123.4321 \\ 0 & 0 \\ 50 & 0 \end{bmatrix}, i = 1,2, \dots 18$$

$$C_i = \begin{bmatrix} 1 & 0 & 0 & 0 & 0 & 0 \\ 0 & 1 & 0 & 0 & 0 & 0 \\ 0 & 0 & 0 & 0 & 1 & 0 \\ 0 & 0 & 0 & 0 & 0 & 1 \end{bmatrix}, i = 1,2, \dots 18$$

$$D_i = \begin{bmatrix} 0 & 0 \\ 0 & 0 \\ 0 & 0 \\ 0 & 0 \end{bmatrix}, i = 1,2, \dots 18$$

$$B_{di} = \begin{bmatrix} 0 & 0.2 & 0.4 \\ 0 & 0.25 & 0.5 \\ 0 & 0 & 0 \\ 0 & 0 & 0 \\ 1 & -0.3 & -0.6 \\ 0 & 0.4 & 0.8 \end{bmatrix}, i = 1,2, \dots 18$$

$$D_{di} = \begin{bmatrix} 1 & 0 & 0 & 0 \\ 0 & 1 & 0 & 0 \\ 0 & 0 & 1 & 0 \\ 0 & 0 & 0 & 1 \end{bmatrix}, i = 1,2, \dots 18$$

Appendix 2

Simulink blocks of T-S fuzzy modelling

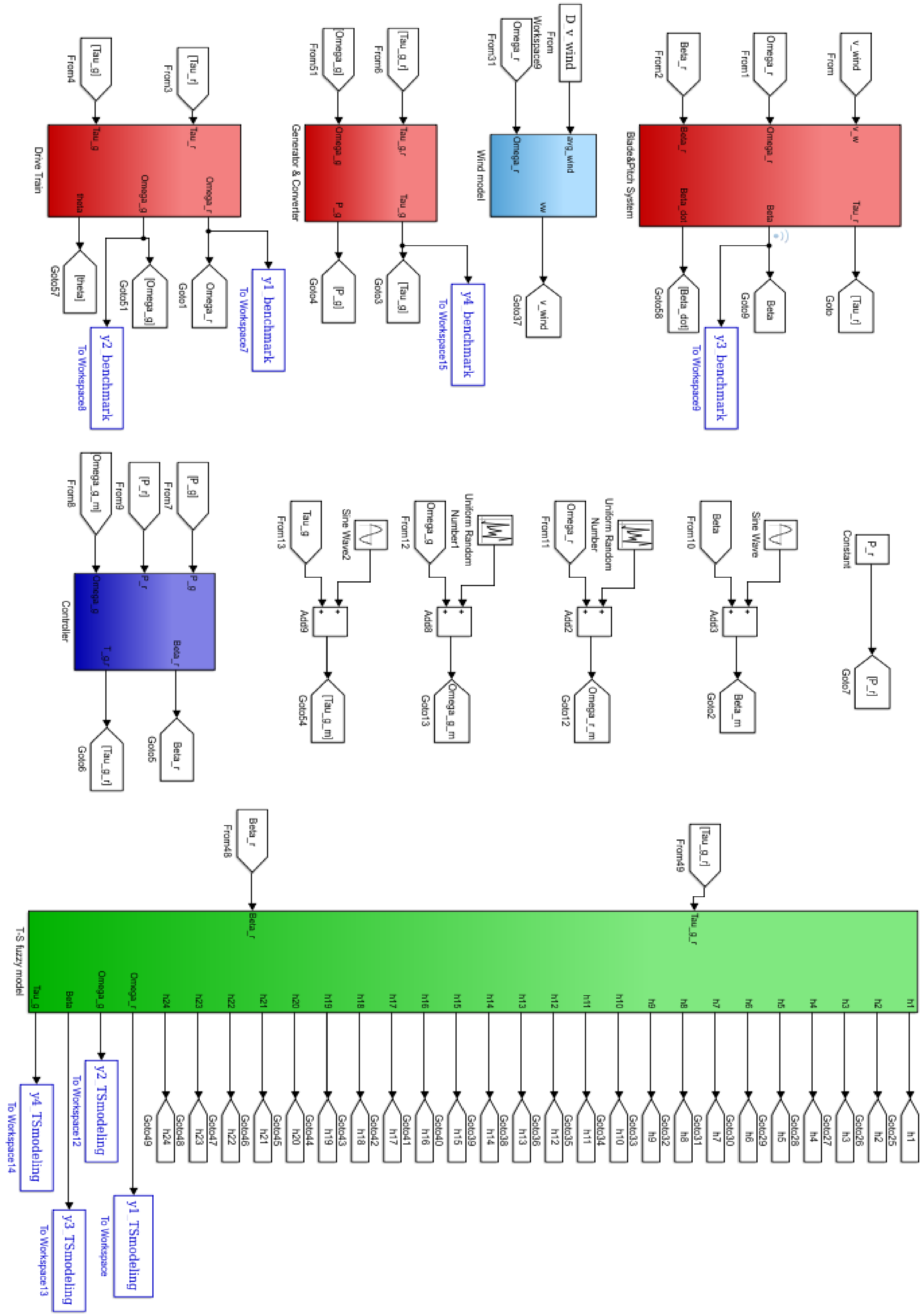

Simulink blocks of benchmark wind turbine and T-S fuzzy modelling

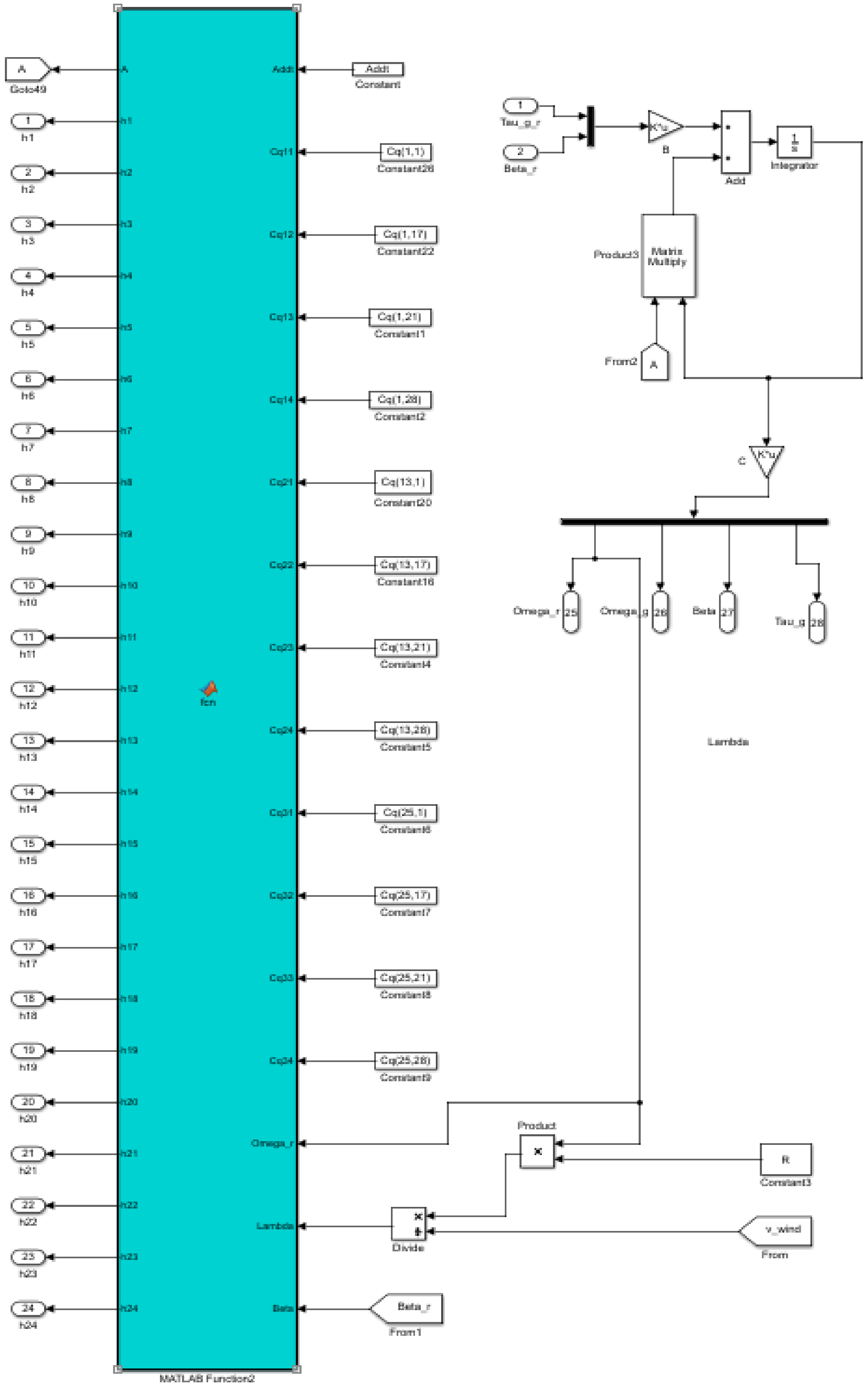

Simulink blocks of T-S fuzzy modelling

Appendix 3

System coefficients of benchmark wind turbine characterized by T-S fuzzy model

$$A_{111} = \begin{bmatrix} 0.0152 & 1.484\times10^{-7} & -49.0909 & 0 & 0 & 0 \\ 0.0203 & -0.1171 & 7.0688\times10^{4} & 0 & 0 & -0.0026 \\ 1 & -0.0105 & 0 & 0 & 0 & 0 \\ 0 & 0 & 0 & -13.332 & -123.4321 & 0 \\ 0 & 0 & 0 & 1 & 0 & 0 \\ 0 & 0 & 0 & 0 & 0 & -50 \end{bmatrix}$$

$$A_{112} = \begin{bmatrix} 0.0017 & 1.484\times10^{-7} & -49.0909 & 0 & 0 & 0 \\ 0.0203 & -0.1171 & 7.0688\times10^{4} & 0 & 0 & -0.0026 \\ 1 & -0.0105 & 0 & 0 & 0 & 0 \\ 0 & 0 & 0 & -13.332 & -123.4321 & 0 \\ 0 & 0 & 0 & 1 & 0 & 0 \\ 0 & 0 & 0 & 0 & 0 & -50 \end{bmatrix}$$

$$A_{113} = \begin{bmatrix} -2.115\times10^{-5} & 1.484\times10^{-7} & -49.0909 & 0 & 0 & 0 \\ 0.0203 & -0.1171 & 7.0688\times10^{4} & 0 & 0 & -0.0026 \\ 1 & -0.0105 & 0 & 0 & 0 & 0 \\ 0 & 0 & 0 & -13.332 & -123.4321 & 0 \\ 0 & 0 & 0 & 1 & 0 & 0 \\ 0 & 0 & 0 & 0 & 0 & -50 \end{bmatrix}$$

$$A_{121} = \begin{bmatrix} 0.0222 & 1.484\times10^{-7} & -49.0909 & 0 & 0 & 0 \\ 0.0203 & -0.1171 & 7.0688\times10^{4} & 0 & 0 & -0.0026 \\ 1 & -0.0105 & 0 & 0 & 0 & 0 \\ 0 & 0 & 0 & -13.332 & -123.4321 & 0 \\ 0 & 0 & 0 & 1 & 0 & 0 \\ 0 & 0 & 0 & 0 & 0 & -50 \end{bmatrix}$$

$$A_{122} = \begin{bmatrix} -2.768\times10^{-4} & 1.484\times10^{-7} & -49.0909 & 0 & 0 & 0 \\ 0.0203 & -0.1171 & 7.0688\times10^{4} & 0 & 0 & -0.0026 \\ 1 & -0.0105 & 0 & 0 & 0 & 0 \\ 0 & 0 & 0 & -13.332 & -123.4321 & 0 \\ 0 & 0 & 0 & 1 & 0 & 0 \\ 0 & 0 & 0 & 0 & 0 & -50 \end{bmatrix}$$

$$A_{123} = \begin{bmatrix} -9.4166\times10^{-4} & 1.484\times10^{-7} & -49.0909 & 0 & 0 & 0 \\ 0.0203 & -0.1171 & 7.0688\times10^{4} & 0 & 0 & -0.0026 \\ 1 & -0.0105 & 0 & 0 & 0 & 0 \\ 0 & 0 & 0 & -13.332 & -123.4321 & 0 \\ 0 & 0 & 0 & 1 & 0 & 0 \\ 0 & 0 & 0 & 0 & 0 & -50 \end{bmatrix}$$

$$A_{131} = \begin{bmatrix} 0.0327 & 1.484\times10^{-7} & -49.0909 & 0 & 0 & 0 \\ 0.0203 & -0.1171 & 7.0688\times10^{4} & 0 & 0 & -0.0026 \\ 1 & -0.0105 & 0 & 0 & 0 & 0 \\ 0 & 0 & 0 & -13.332 & -123.4321 & 0 \\ 0 & 0 & 0 & 1 & 0 & 0 \\ 0 & 0 & 0 & 0 & 0 & -50 \end{bmatrix}$$

$$A_{132} = \begin{bmatrix} -0.0045 & 1.484\times10^{-7} & -49.0909 & 0 & 0 & 0 \\ 0.0203 & -0.1171 & 7.0688\times10^{4} & 0 & 0 & -0.0026 \\ 1 & -0.0105 & 0 & 0 & 0 & 0 \\ 0 & 0 & 0 & -13.332 & -123.4321 & 0 \\ 0 & 0 & 0 & 1 & 0 & 0 \\ 0 & 0 & 0 & 0 & 0 & -50 \end{bmatrix}$$

$$A_{133} = \begin{bmatrix} -0.0048 & 1.484\times10^{-7} & -49.0909 & 0 & 0 & 0 \\ 0.0203 & -0.1171 & 7.0688\times10^{4} & 0 & 0 & -0.0026 \\ 1 & -0.0105 & 0 & 0 & 0 & 0 \\ 0 & 0 & 0 & -13.332 & -123.4321 & 0 \\ 0 & 0 & 0 & 1 & 0 & 0 \\ 0 & 0 & 0 & 0 & 0 & -50 \end{bmatrix}$$

$$A_{141} = \begin{bmatrix} -0.0234 & 1.484\times10^{-7} & -49.0909 & 0 & 0 & 0 \\ 0.0203 & -0.1171 & 7.0688\times10^{4} & 0 & 0 & -0.0026 \\ 1 & -0.0105 & 0 & 0 & 0 & 0 \\ 0 & 0 & 0 & -13.332 & -123.4321 & 0 \\ 0 & 0 & 0 & 1 & 0 & 0 \\ 0 & 0 & 0 & 0 & 0 & -50 \end{bmatrix}$$

$$A_{142} = \begin{bmatrix} -0.0118 & 1.484\times10^{-7} & -49.0909 & 0 & 0 & 0 \\ 0.0203 & -0.1171 & 7.0688\times10^{4} & 0 & 0 & -0.0026 \\ 1 & -0.0105 & 0 & 0 & 0 & 0 \\ 0 & 0 & 0 & -13.332 & -123.4321 & 0 \\ 0 & 0 & 0 & 1 & 0 & 0 \\ 0 & 0 & 0 & 0 & 0 & -50 \end{bmatrix}$$

$$A_{143} = \begin{bmatrix} -0.0114 & 1.484\times10^{-7} & -49.0909 & 0 & 0 & 0 \\ 0.0203 & -0.1171 & 7.0688\times10^{4} & 0 & 0 & -0.0026 \\ 1 & -0.0105 & 0 & 0 & 0 & 0 \\ 0 & 0 & 0 & -13.332 & -123.4321 & 0 \\ 0 & 0 & 0 & 1 & 0 & 0 \\ 0 & 0 & 0 & 0 & 0 & -50 \end{bmatrix}$$

$$A_{211} = \begin{bmatrix} 0.7204 & 1.484\times10^{-7} & -49.0909 & 0 & 0 & 0 \\ 0.0203 & -0.1171 & 7.0688\times10^{4} & 0 & 0 & -0.0026 \\ 1 & -0.0105 & 0 & 0 & 0 & 0 \\ 0 & 0 & 0 & -13.332 & -123.4321 & 0 \\ 0 & 0 & 0 & 1 & 0 & 0 \\ 0 & 0 & 0 & 0 & 0 & -50 \end{bmatrix}$$

$$A_{212} = \begin{bmatrix} 0.0803 & 1.484\times10^{-7} & -49.0909 & 0 & 0 & 0 \\ 0.0203 & -0.1171 & 7.0688\times10^{4} & 0 & 0 & -0.0026 \\ 1 & -0.0105 & 0 & 0 & 0 & 0 \\ 0 & 0 & 0 & -13.332 & -123.4321 & 0 \\ 0 & 0 & 0 & 1 & 0 & 0 \\ 0 & 0 & 0 & 0 & 0 & -50 \end{bmatrix}$$

$$A_{213} = \begin{bmatrix} -3.4213\times10^{-4} & 1.484\times10^{-7} & -49.0909 & 0 & 0 & 0 \\ 0.0203 & -0.1171 & 7.0688\times10^{4} & 0 & 0 & -0.0026 \\ 1 & -0.0105 & 0 & 0 & 0 & 0 \\ 0 & 0 & 0 & -13.332 & -123.4321 & 0 \\ 0 & 0 & 0 & 1 & 0 & 0 \\ 0 & 0 & 0 & 0 & 0 & -50 \end{bmatrix}$$

$$A_{221} = \begin{bmatrix} 1.0529 & 1.484\times10^{-7} & -49.0909 & 0 & 0 & 0 \\ 0.0203 & -0.1171 & 7.0688\times10^{4} & 0 & 0 & -0.0026 \\ 1 & -0.0105 & 0 & 0 & 0 & 0 \\ 0 & 0 & 0 & -13.332 & -123.4321 & 0 \\ 0 & 0 & 0 & 1 & 0 & 0 \\ 0 & 0 & 0 & 0 & 0 & -50 \end{bmatrix}$$

$$A_{222} = \begin{bmatrix} -0.0125 & 1.484\times10^{-7} & -49.0909 & 0 & 0 & 0 \\ 0.0203 & -0.1171 & 7.0688\times10^{4} & 0 & 0 & -0.0026 \\ 1 & -0.0105 & 0 & 0 & 0 & 0 \\ 0 & 0 & 0 & -13.332 & -123.4321 & 0 \\ 0 & 0 & 0 & 1 & 0 & 0 \\ 0 & 0 & 0 & 0 & 0 & -50 \end{bmatrix}$$

$$A_{223} = \begin{bmatrix} -0.0440 & 1.484\times10^{-7} & -49.0909 & 0 & 0 & 0 \\ 0.0203 & -0.1171 & 7.0688\times10^{4} & 0 & 0 & -0.0026 \\ 1 & -0.0105 & 0 & 0 & 0 & 0 \\ 0 & 0 & 0 & -13.332 & -123.4321 & 0 \\ 0 & 0 & 0 & 1 & 0 & 0 \\ 0 & 0 & 0 & 0 & 0 & -50 \end{bmatrix}$$

$$A_{231} = \begin{bmatrix} 1.5516 & 1.484\times10^{-7} & -49.0909 & 0 & 0 & 0 \\ 0.0203 & -0.1171 & 7.0688\times10^{4} & 0 & 0 & -0.0026 \\ 1 & -0.0105 & 0 & 0 & 0 & 0 \\ 0 & 0 & 0 & -13.332 & -123.4321 & 0 \\ 0 & 0 & 0 & 1 & 0 & 0 \\ 0 & 0 & 0 & 0 & 0 & -50 \end{bmatrix}$$

$$A_{232} = \begin{bmatrix} -0.2104 & 1.484 \times 10^{-7} & -49.0909 & 0 & 0 & 0 \\ 0.0203 & -0.1171 & 7.0688 \times 10^{4} & 0 & 0 & -0.0026 \\ 1 & -0.0105 & 0 & 0 & 0 & 0 \\ 0 & 0 & 0 & -13.332 & -123.4321 & 0 \\ 0 & 0 & 0 & 1 & 0 & 0 \\ 0 & 0 & 0 & 0 & 0 & -50 \end{bmatrix}$$

$$A_{233} = \begin{bmatrix} -0.2289 & 1.484 \times 10^{-7} & -49.0909 & 0 & 0 & 0 \\ 0.0203 & -0.1171 & 7.0688 \times 10^{4} & 0 & 0 & -0.0026 \\ 1 & -0.0105 & 0 & 0 & 0 & 0 \\ 0 & 0 & 0 & -13.332 & -123.4321 & 0 \\ 0 & 0 & 0 & 1 & 0 & 0 \\ 0 & 0 & 0 & 0 & 0 & -50 \end{bmatrix}$$

$$A_{241} = \begin{bmatrix} -1.1083 & 1.484 \times 10^{-7} & -49.0909 & 0 & 0 & 0 \\ 0.0203 & -0.1171 & 7.0688 \times 10^{4} & 0 & 0 & -0.0026 \\ 1 & -0.0105 & 0 & 0 & 0 & 0 \\ 0 & 0 & 0 & -13.332 & -123.4321 & 0 \\ 0 & 0 & 0 & 1 & 0 & 0 \\ 0 & 0 & 0 & 0 & 0 & -50 \end{bmatrix}$$

$$A_{242} = \begin{bmatrix} -0.5598 & 1.484 \times 10^{-7} & -49.0909 & 0 & 0 & 0 \\ 0.0203 & -0.1171 & 7.0688 \times 10^{4} & 0 & 0 & -0.0026 \\ 1 & -0.0105 & 0 & 0 & 0 & 0 \\ 0 & 0 & 0 & -13.332 & -123.4321 & 0 \\ 0 & 0 & 0 & 1 & 0 & 0 \\ 0 & 0 & 0 & 0 & 0 & -50 \end{bmatrix}$$

$$A_{243} = \begin{bmatrix} -0.5404 & 1.484 \times 10^{-7} & -49.0909 & 0 & 0 & 0 \\ 0.0203 & -0.1171 & 7.0688 \times 10^{4} & 0 & 0 & -0.0026 \\ 1 & -0.0105 & 0 & 0 & 0 & 0 \\ 0 & 0 & 0 & -13.332 & -123.4321 & 0 \\ 0 & 0 & 0 & 1 & 0 & 0 \\ 0 & 0 & 0 & 0 & 0 & -50 \end{bmatrix}$$

$$B_{l\tau k} = \begin{bmatrix} 0 & 0 \\ 0 & 0 \\ 0 & 0 \\ 0 & 123.4321 \\ 0 & 0 \\ 50 & 0 \end{bmatrix}, l = 1,2, \tau = 1,2,3,4, k = 1,2,3$$

$$C_{l\tau k} = \begin{bmatrix} 1 & 0 & 0 & 0 & 0 & 0 \\ 0 & 1 & 0 & 0 & 0 & 0 \\ 0 & 0 & 0 & 0 & 1 & 0 \\ 0 & 0 & 0 & 0 & 0 & 1 \end{bmatrix}, l = 1,2, \tau = 1,2,3,4, k = 1,2,3$$

Appendix 4

Simulink blocks of fault estimation of benchmark wind turbine

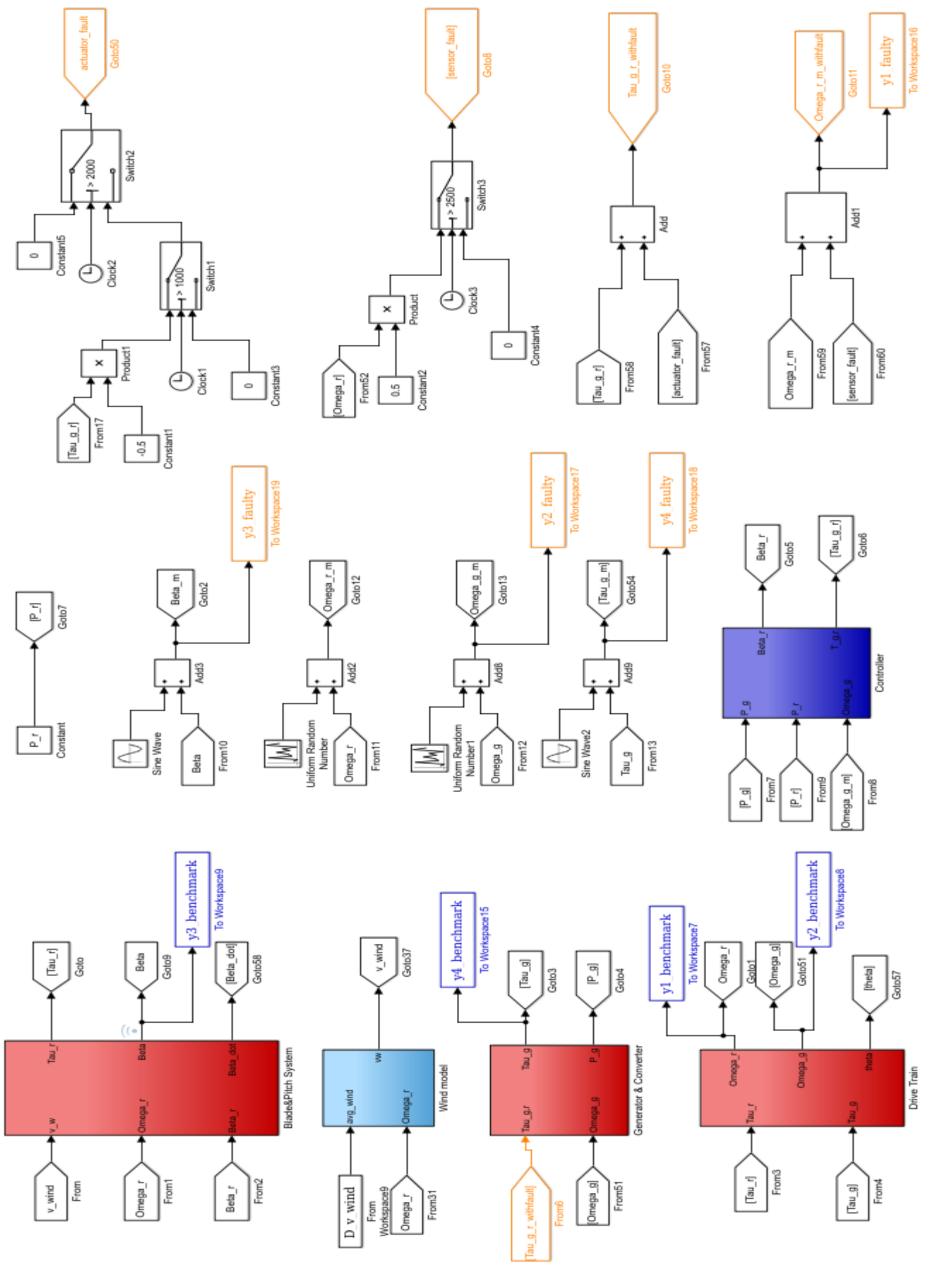

Simulink blocks of benchmark wind turbine with faults

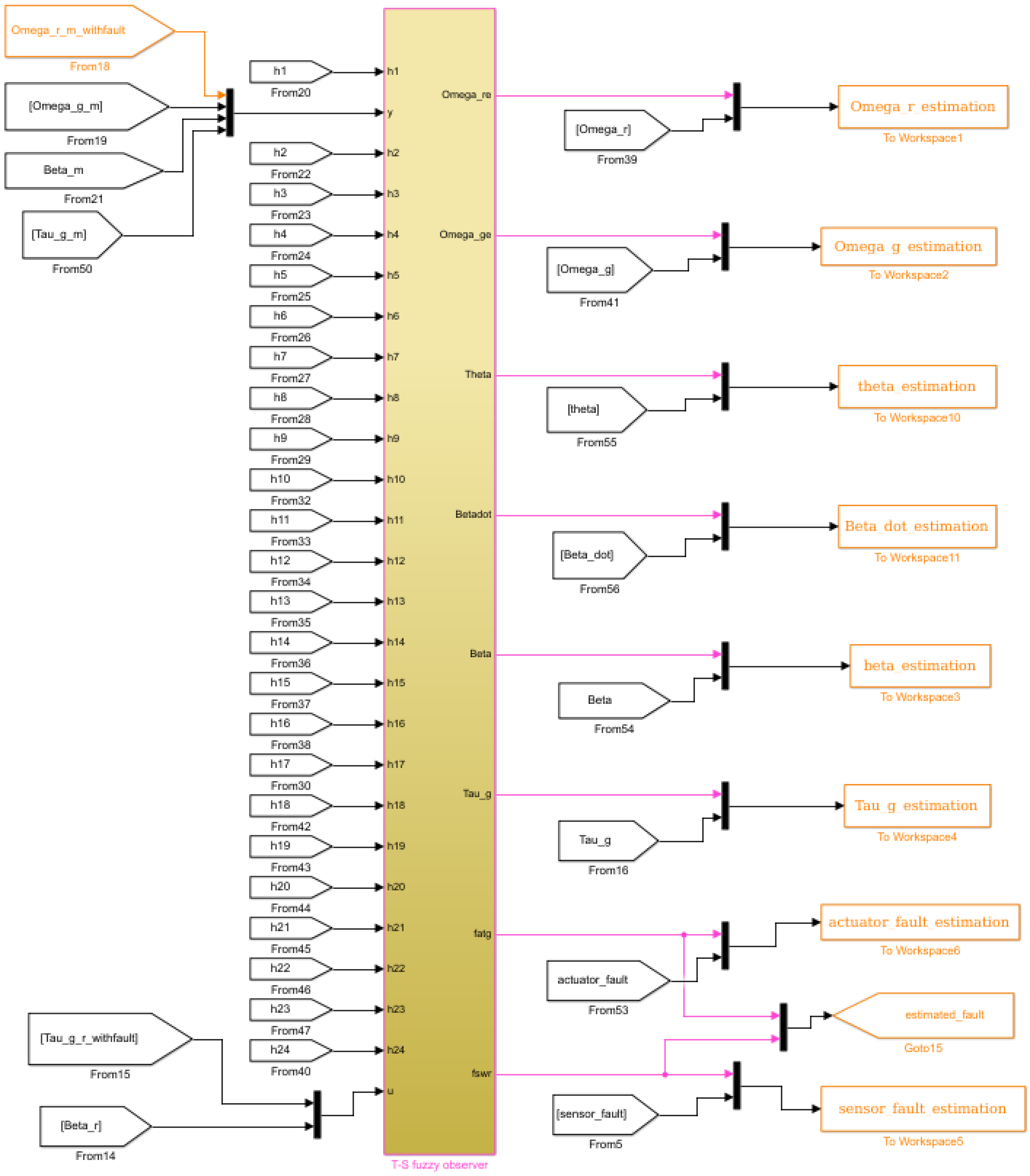

Simulink blocks of fault estimation

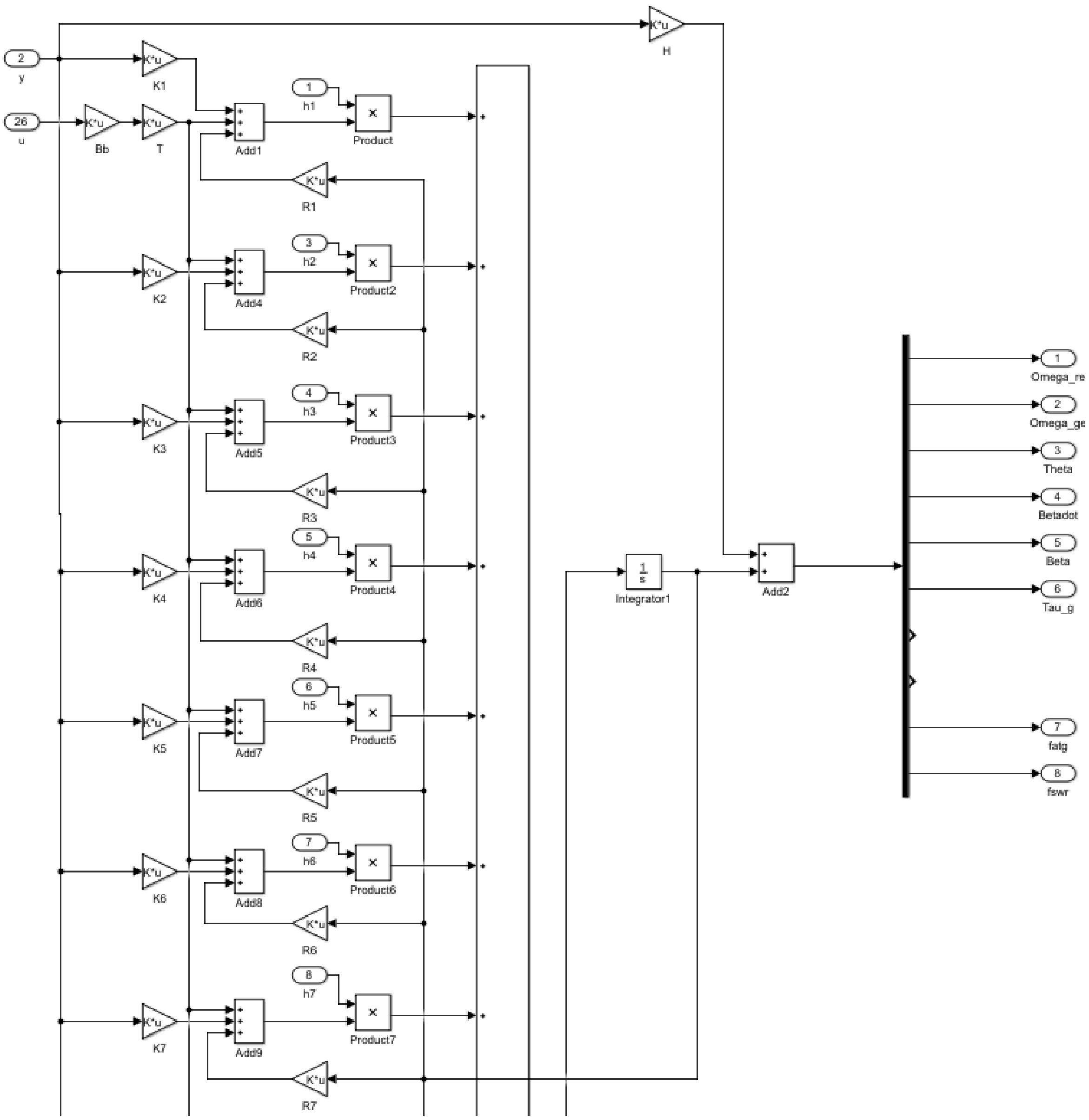

Simulink blocks of unknown input observer (24 individual observers are combined by fuzzy logic, only 7 have been shown due to the limited space.)

Appendix 5

Simulink blocks of signal compensation of benchmark wind turbine

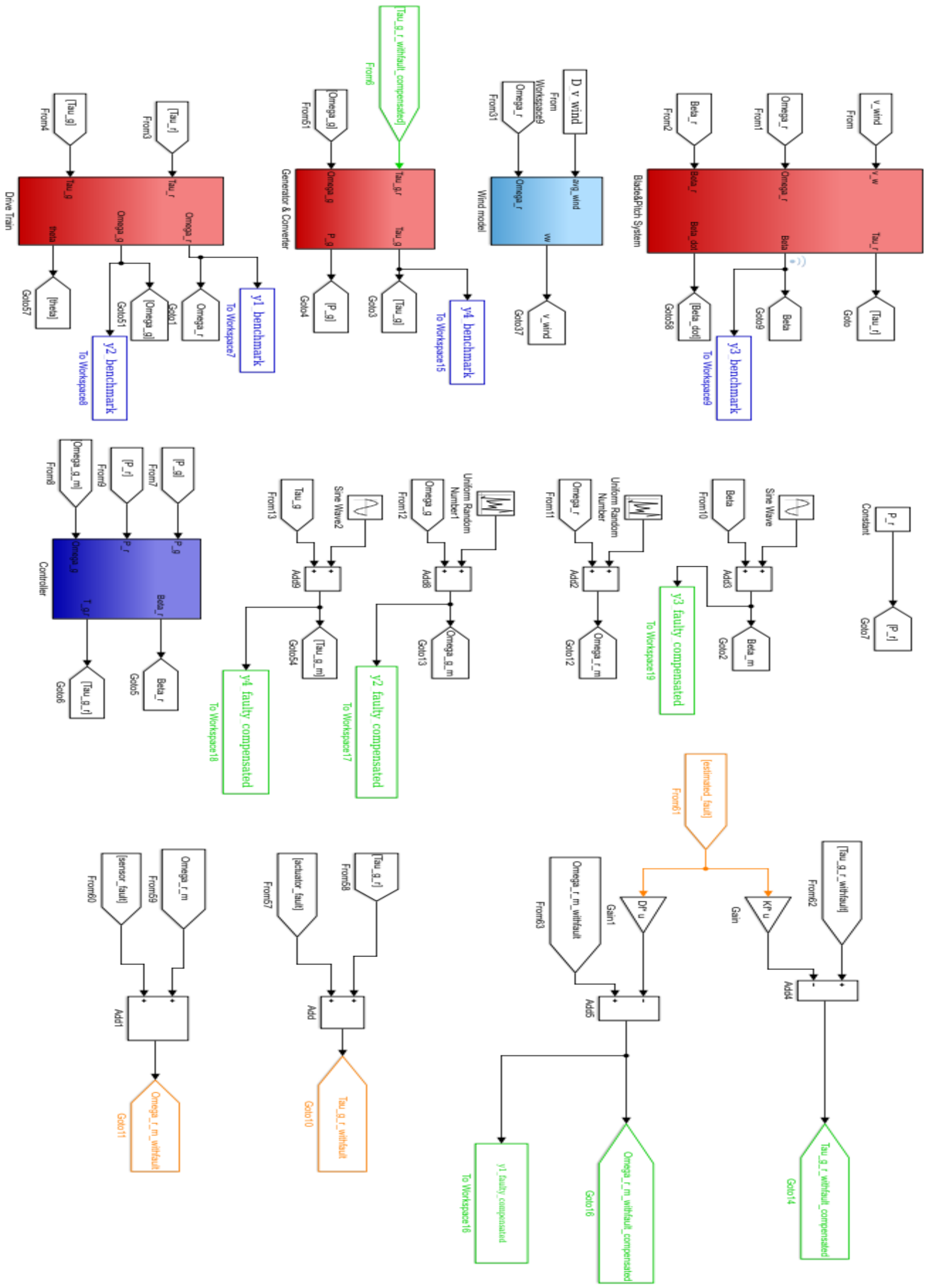

Simulink blocks of signal compensation

References

[1] Z. Gao, C. Cecati and S. X. Ding, “A Survey of fault diagnosis and fault-tolerant techniques part I: fault diagnosis with model- and signal-based approaches,” *IEEE Trans. Ind. Electron*., vol. 62, no. 6, pp. 3575-3767, Jun. 2015.

[2] Z. Gao, C. Cecati and S. X. Ding, “A Survey of fault diagnosis and fault-tolerant techniques part II: fault diagnosis with knowledge-based and hybrid/active approaches,” *IEEE Trans. Ind. Electron*., vol. 62, no. 6, pp. 3768-3774, Jun. 2015.

[3] B. Shafai, C.T. Pi and S. Nork, “Simultaneous disturbance attenuation and fault detection using proportional integral observers,” in *Proc. Amer. Control Conf.*, pp. 1647-1649, Anchorage, AK, May 2002.

[4] X. Yan and C. Edwards, “Adaptive sliding-mode-observer-based fault reconstruction for nonlinear systems with parametric uncertainties,” *IEEE Trans. Ind. Electron.*, vol.55, no.11, pp. 4029-4036, Nov. 2008.

[5] H. Alwi and C. Edwards, “An adaptive sliding mode differentiator for actuator oscillatory failure case reconstruction,” *Automatica*, vol. 49, no. 2, pp. 642-651, Feb. 2013.

[6] Z. Gao and S. X. Ding, “Sensor fault reconstruction and sensor compensation for a class of nonlinear state-space systems via a descriptor system approach,” *IET Control Theory Appl.*, vol. 1, no. 3, pp. 578-585, May 2007.

[7] R. Mehra and J. Peschon, “An innovation approach to fault detection and diagnosis in dynamic systems,” *Automatica*, vol. 7, no. 5, pp. 637-640, Sep. 1971.

[8] L. Mironovski, “Functional diagnosis of linear dynamic systems,” *Autom. Remote Control*, vol. 40, no. 8, pp. 1198-1205, Aug. 1980.

[9] E. Chow and A. Willsky, “Analytical redundancy and the design of robust detection systems,” *IEEE Trans. Autom. Control*, vol. 29, no. 7, pp. 603-614, Jul. 1984.

[10] C. Bakiotis, J. Raymond and A. Pault, “Parameter and discriminant analysis for jet engine mechanical state diagnosis,” in *Proc. Conf. Decision Control*, pp. 648-650, Fort Lauderdale, FL, USA, Dec. 1979.

[11] J. Chen and R. J. Patton, Robust Model-Based Fault Diagnosis for Dynamic Systems, Boston: Kuwer Academic Publishers, 1999.

[12] R. Patton and J. Chen, "On eigenstructure assignment for robust fault diagnosis," *Int. J. Robust Nonlinear Control*, vol. 10, no. 14, pp. 1193-1208, Dec. 2000.

[13] M. Zhong, S. X. Ding, J. Lam and H. Wang, "An LMI approach to design robust fault detection filter for uncertain LTI systems," *Automatica*, vol. 39, no. 3, pp. 543-550, Mar. 2003.

[14] B. Chen and S. Nagarajaiah, "H_{-}/H_{∞} structural damage detection filter design using an iterative linear matrix inequality approach," *Smart Mater. Struct.*, vol. 17, no. 3, pp. 1-9, Apr. 2008.

[15] J. Chen, R. J. Patton and H. Y. Zhang, "Design of unknown input observers and robust fault detection filters," *Int. J. Contr.*, vol. 63, no. 1, pp. 85-105, Jan. 1996.

[16] A. Pertew, H. Marquez and Q. Zhao, "Design of unknown input observers for lipschitz nonlinear systems," in *Proc. American Contr. Conf.*, pp. 4198-4203, Portland, USA, Jun. 2005.

[17] W. Chen and M. Saif, "Unknown input observer design for a class of nonlinear systems: an LMI approach," in *Proc. American Contr. Conf.*, pp. 834-838, Minnesota, USA, Jun. 2006.

[18] Z. Wang, "Unknown input observer based fault class isolation and estimation," in *Proc. Chinese Contr. Conf.*, pp. 3963-3968, Beijing, China, Jul. 2010.

[19] T. Sedighi, A. Koshkouei and K. Burnham, "Nonlinear unknown input observer design for nonlinear systems: A new method," in *Proc. IFAC World Congress*, pp. 11067-11072, Milano, Italy, Aug. 2011.

[20] J. Zari and E. Shokri, "Robust sensor fault detection based on nonlinear unknown input observer," *Measurement*, vol. 48, no. 2, pp. 355-367, Feb. 2014.

[21] R. Fonod, D. Henry, C. Charbonnely and E. Bornschleglz, "A class of nonlinear unknown input observer for fault diagnosis: application to fault tolerant control of an autonomous spacecraft," in *Proc. UKACC Int. Conf. Contr.*, pp. 19-24, Loughborgh, UK, Jul. 2014.

[22] L. Imsland, T. Johansen, H. Grip and T. Fossen, “On nonlinear unknown input observers – applied to lateral vehicle velocity estimation on banked roads,” *Int. J. Contr.*, vol. 80, no. 11, pp. 1741-1750, Nov. 2007.

[23] O. Hrizi, B. Boussaid, A. Zouinkhi and M. Abdelkrim, “Robust unknown input observer based fast adaptive fault estimation: application to unicycle robot,” in *Proc. Int. Conf. Automation, Contr. Eng. Comput. Sci.*, pp. 186-194, Monastir, Tunisia, Mar. 2014.

[24] X. Sun and R. J. Patton, “Robust actuator multiplicative fault estimation with unknown input decoupling for a wind turbine system,” in *Proc. Conf. Contr. Fault-Tolerant Syst.*, pp. 263-268, Nice, France, Oct. 2013.

[25] H. Wang, Z. J. Huang and S. Daley, “On the use of adaptive updating rules for actuator and sensor fault diagnosis,” *Automatica*, vol. 33, no. 2, pp. 217-225, Feb. 1997.

[26] H. Alwi and C. Edwards, “Robust fault reconstruction for linear parameter varying systems using sliding mode observers,” *Int. J. Robust Nonlin. Contr.*, vol. 24, no. 14, pp. 1947-1968, Sep. 2014.

[27] Z. Gao and H. Wang, “Descriptor observer approaches for multivariable systems with measurement noises and application in fault detection and diagnosis,” *Syst. Contr. Lett.*, vol. 55, no. 4, pp. 304-313, Apr. 2006.

[28] Z. Gao, S. Ding and Y. Ma, “Robust fault estimation approach and its application in vehicle lateral dynamic systems,” *Opt. Contr. App. Meth.*, vol. 28, no. 3, pp. 143-156, May/Jun. 2007.

[29] Z. Gao and S. Ding, “Sensor fault reconstruction and sensor compensation for a class of nonlinear state-space systems via a descriptor system approach,” *IET Contr. Theory Appli.*, vol. 1, no. 3, pp. 578-585, May 2007.

[30] Z. Gao, T. Breikin and H. Wang, “High-gain estimator and fault-tolerant design with application to a gas turbine dynamic system,” *IEEE Trans. Contr. Syst. Tech.*, vol. 15, no. 4, pp. 740-753, Jul. 2007.

[31] Z. Gao and S. X. Ding, “State and disturbance estimator for time-delay systems with application to fault estimation and signal compensation,” *IEEE Trans. Signal Process.*, vol. 55, no. 12, pp. 5541-5551, Dec. 2007.

[32] S. Bezzaoucha, B. Marx, D. Maquin and J. Ragot, “On the unknown input observer design : A decoupling class approach,” in *Proc. IEEE Int. Conf. Contr. Automation*, pp. 602-607, Santiago, Chile, Dec. 2011.

[33] H. Ting, J. Chang and Y. Chen, “Proportional-derivative unknown input observer design using descriptor system approach for non-minimum phase systems,” *Int. J. Contr. Automat. Sys.*, vol. 9, no. 5, pp. 850-856, May 2011.

[34] T. Takagi and M. Sugeno, “Fuzzy identification of systems and its applications to modeling and control,” *IEEE Trans. Syst. Man, Cybern.*, vol. SMC-15, no. 1, pp. 116-132, Jan. -Feb. 1985.

[35] M. Liu and P. Shi, “Sensor fault estimation and tolerant control for Itˆo stochastic systems with a descriptor sliding mode approach,” *Automatica*, vol. 49, no. 5, pp. 1242-1250, May 2013.

[36] M. Liu, X. Cao and P. Shi, “Fuzzy-model-based fault tolerant design for nonlinear stochastic systems against simultaneous sensor and actuator faults,” *IEEE Tran. Fuzzy Syst.*, vol. 21, no. 5, pp. 789-799, Oct. 2013.

[37] S. Simani, S. Farsoni and P. Castaldi, “Fault diagnosis of a wind turbine benchmark via identified fuzzy models,” *IEEE Trans. Ind. Electron.*, vol. 62, no. 6, pp. 3775-3782, Jun. 2015.

[38] Z. Gao, X. Shi and S. Ding, “Fuzzy state/disturbance observer design for T–S fuzzy systems with application to sensor fault estimation,” *IEEE Trans. Syst. Man, Cybern., Part B (Cybernetics)*, vol. 38, no. 3, pp. 875-880, Jun. 2008.

[39] S. Guo, F. Zhu and L. Xu, “Unknown input observer design for Takagi-Sugeno fuzzy stochastic system,” *Int. J. Control Automat. Syst.*, vol. 13, no. 4, pp. 1003-1009, Aug. 2015.

[40] M. Chadli and H. Karimi, “Robust observer design for unknown inputs Takagi–Sugeno models,” *IEEE Trans. Fuzzy Syst.*, vol. 21, no. 1, pp. 158-164, Feb. 2013.

[41] W. Chen and M. Saif, “Design of a TS based fuzzy nonlinear unknown input observer with fault diagnosis applications,” in *Proc. Amer. Control Conf.*, pp. 2545-2550, New York City, USA, Jul. 2007.

[42] K. Guelton, S. Delprat and T. Guerra, “An alternative to inverse dynamics joint torques estimation in human stance based on a Takagi-Sugeno unknown-inputs observer in the descriptor form,” *Control Eng. Pract.*, vol. 16. no. 12, pp. 1414-1426, Dec. 2008.

[43] T. Bessaoudi, F. Hmida and C. Hsieh, “Robust state and fault estimation for linear descriptor stochastic systems with disturbances: a DC motor application,” *IET Control Theory Appl.*, vol. 11, no. 5, pp. 601-610, Mar. 2017.

[44] S. H. Mousavi and H. J. Marquez, “Integral-based event triggering controller design for stochastic LTI systems via convex optimisation,” *International Journal of Control*, vol. 89, no. 7, pp. 1416-1427, Jul. 2016.

[45] H. Li, P. Shi and D. Yao, “Adaptive sliding-mode control of Markov jump nonlinear systems with actuator faults,” *IEEE Trans. Automat. Contr.*, vol. 62, no. 4, pp. 1933-1939, Apr. 2017.

[46] Q. Zhang, L. Li, X. Yan and S. K. Spurgeon, “Sliding mode control for singular stochastic Markovian jump systems with uncertainties,” *Automatica*, vol. 79, pp. 27-34, May 2017.

[47] L. Yao, J. Qin, H. Wang and B. Jiang, “Design of new fault diagnosis and fault tolerant control scheme for non-Gaussian singular stochastic distribution systems,” *Automatica*, vol. 48, no. 9, pp. 2305-2313, Sep. 2012.

[48] X. Mao, Stochastic differential equations and applications, London: Woodhead Publishing, 1997.

[49] Z. Gao and X. Shi, “Observer-based controller design for stochastic descriptor systems with Brownian motions,” *Automatica*, vol. 49, no. 7, pp. 2229-2235, Jul. 2013.

[50] H. Chen and S. Lu, “Fault diagnosis digital method for power transistors in power converters of switched reluctance motors,” *IEEE Trans. Ind. Electron.*, vol. 60, no. 2, pp. 749-763, Feb. 2013.

[51] M. Shahbazi, E. Jamshidpour, P. Poure, S. Saadate and M. Zolghadri, "Open and short-circuit switch fault diagnosis for nonisolated dc–dc converters using field programmable gate array," *IEEE Trans. Ind. Electron.*, vol. 60, no. 9, pp. 4136-4145, Sep. 2013.

[52] L. Hong and J. Dhupia, "A time domain approach to diagnose gearbox fault based on measured vibration signals," *J. Sound Vib.*, vol. 333, no. 7, pp. 2164-2180, Mar. 2014.

[53] M. Shahriar, T. Ahsan and U. Chong, "Fault diagnosis of induction motors utilizing local binary pattern-based texture analysis," *EURASIP J. Image Video Process.*, vol. 2013, no. 1, pp. 1-11, May 2013.

[54] D. Zappalá, P. Tavner, C. Crabtree and S. Sheng, "Side-band algorithm for automatic wind turbine gearbox fault detection and diagnosis," *IET Renew. Power Gener.*, vol. 8, no. 4, pp. 380-389, May 2014.

[55] S. Nandi, T. Ilamparithi, S. Lee and D. Hyun, "Detection of eccentricity faults in induction machines based on nameplate parameters," *IEEE Trans. Ind. Electron.*, vol. 58, no. 5, pp. 1673-1683, May 2011.

[56] Y. Gritli, L. Zarri, C. Rossi, F. Filippetti, G. Capolino and D. Casadei, "Advanced diagnosis of electrical faults in wound-rotor induction machines," *IEEE Trans. Ind. Electron.*, vol. 60, no. 9, pp. 4012-4024, Sep. 2013.

[57] R. Yan and R. Gao, "Hilbert–Huang transform-based vibration signal analysis for machine health monitoring," *IEEE Trans. Instrum. Meas.*, vol. 55, no. 6, pp. 2320-2329, Dec. 2006.

[58] R. Burnett, J. Watson and S. Elder, "The application of modern signal processing techniques for use in rotor fault detection and location within three-phase induction motors," *Signal Process.*, vol. 49, no. 1, pp. 57-70, Feb. 1996.

[59] E. Henley, "Application of expert systems to fault diagnosis," in *Proc. AICHE Annu. Meet.*, San Francisco, CA, USA, 1984.

[60] S. Yin, S. Ding, A. Haghani, H. Hao and P. Zhang, "A comparison study of basic data-driven fault diagnosis and process monitoring methods on the benchmark

Tennessee Eastman process," *Journal of Process Control*, vol. 22, no. 9, pp. 1567-1581, Oct. 2012.

[61] Y. Shatnawi and M. Al-Khassaweneh, "Fault diagnosis in internal combustion engines using extension neural network," *IEEE Trans. Ind. Electron.*, vol. 61, no. 3, pp. 1434-1443, Mar. 2014.

[62] F. Zidani, D. Diallo, M. Benbouzid and R. Nait-Said, "A fuzzy-based approach for the diagnosis of fault modes in a voltage-fed PWM inverter induction motor drive," *IEEE Trans. Ind. Electron.*, vol. 55, no. 2, pp. 586-593, Feb. 2008.

[63] M. Schlechtingen, I. Santos and S. Achiche, "Wind turbine condition monitoring based on SCADA data using normal behaviour models. Part 1: system description," *Appl. Soft Computing*, vol. 13, no. 1, pp. 259-270, Jan. 2013.

[64] J. Scott, R. Finderisen, R. Braatz and D. Raimondo, "Input design for guaranteed fault diagnosis using zonotopes," *Automatica*, vol. 50, no. 6, pp. 1580-1589, Jun. 2014.

[65] J. Scott, G. Marseglia, L. Magni, R. Braatz and D. Raimondo, "A hybrid stochastic-deterministic input design method for active fault diagnosis," in *Proc. IEEE Conf. Decision Control*, pp. 5656-5661, Florence, Italy, Dec. 2013.

[66] M. Simandl and I. Puncochar, "Active fault detection and control: Unified formulation and optimal design," *Automatica*, vol. 45, no. 9, pp. 2052-2059, Sep. 2009.

[67] A. Ashari, R. Nikoukhah and S. Campbell, "Active robust fault detection in closed-loop systems: Quadratic optimization approach," *IEEE Trans. Autom. Control*, vol. 57, no. 10, pp. 2532-2544, Oct. 2012.

[68] B. Hahn, M. Durstewitz and K. Rohrig, "Reliability of Wind Turbines," pp. 329-332, Springer-Verlag Berlin/Heidelberg, Germany, 2007.

[69] T. Verbruggen, "Wind turbine operation & maintenance based on condition monitoring," *ECN Wind Energy,* Tech. Rep. ECN-C-03-047, Petten, The Netherlands, Apr. 2003.

[70] W. Qiao and D. Lu, “A survey on wind turbine condition monitoring and fault diagnosis-part I: components and subsystems,” *IEEE Tans. Ind. Electron.*, vol. 62, no. 10, pp. 6536-6545, Oct. 2015.

[71] M. Drewry and G. Georgiou, “A review of NDT techniques for wind turbines,” *Insight*, vol. 49, no. 3, pp. 137-141, Mar. 2007.

[72] Y. Amirat, M. Benbouzid, E. Al-Ahmar, B. Bensaker and S. Turri, “A brief status on condition monitoring and fault diagnosis in wind energy conversion systems,” *Renew. Sustain. Energy Rev.*, vol. 13, no. 9, pp. 2629-2636, Dec. 2009.

[73] S. Aval and A. Ahadi, “Wind turbine fault diagnosis techniques and related algorithms,” *Int. J. Renew. Energ. Res.*, vol. 6, no. 1, pp. 80-89, Jan. 2016.

[74] Z. Hameed, Y. Hong, Y. Cho, S. Ahn and C. Song, “Condition monitoring and fault detection of wind turbines and related algorithms: A review,” *Renew. Sustain. Energy Rev.*, vol. 13, no. 1, pp. 1-39, Jan. 2009.

[75] B. Lu, Y. Li, X. Wu and Z. Yang, “A review of recent advances in wind turbine condition monitoring and fault diagnosis,” in *Proc. IEEE Symp. Power Electron. Mach. Wind Appl.*, pp. 1-7, Lincoln, NE, USA, Jun. 2009.

[76] F. Márquez, A. Tobias, J. Pérez and M. Papaelias, “Condition monitoring of wind turbines: Techniques and methods,” *Renew. Energ.*, vol. 46, pp. 169-178, Oct. 2012.

[77] S. Sharma and D. Mahto, “Condition monitoring of wind turbines: a review,” *Int. J. Sci. Eng. Res.*, vol. 4, no. 8, pp. 35-50, Aug. 2013.

[78] P. Tchakoua, R. Wamkeue, M. Ouebec, F. Slaoui-Hasnaoui, T. Tameghe and G. Ekemb, “Wind turbine condition monitoring: state-of-the-art review, new trends, and future challenges,” *Energies*, vol. 7, no. 4, pp. 2595-2630, Apr. 2014.

[79] W. Liu, B. Tang, J. Han, X. Lu and Z. He, “The structure healthy condition monitoring and fault diagnosis methods in wind turbines: a review,” *Renew. Sust. Energ. Rev.*, vol. 44, pp. 466-472, Apr. 2015.

[80] W. Qiao and D. Lu, “A survey on wind turbine condition monitoring and fault diagnosis-part II: signals and signal processing methods,” *IEEE Tans. Ind. Electron.*, vol. 62, no. 10, pp. 6546-6557, Oct. 2015.

[81] P. Odgaard, J. Stoustrup and M. Kinnaert, “Fault tolerant control of wind turbines – a benchmark model,” in *Proceedings of the 7th IFAC symposium on fault detection, supervision and safety of technical processes*, pp. 155-160, Barcelona, Spain, June 30-July 3, 2009.

[82] P. Odgaard, J. Stoustrup and M. Kinnaert, “Fault-tolerant control of wind turbines: a benchmark model,” *IEEE Trans. Contr. Syst. Tech.*, vol. 21, no. 4, pp. 1168-1182, Jul. 2013.

[83] P. Odgaard and K. Johnson, “Wind turbine fault detection and fault tolerant control-an enhanced benchmark challenge,” in *Proc. ACC*, pp. 4447-4452, Washington, DC, USA, Jun. 2013.

[84] J. Ekanayake, L. Holdsworth, X. Wu and N. Jenkins, “Dynamic modelling of doubly fed induction generator wind turbines,” *IEEE. Trans. Power Syst.*, vol. 18, no. 2, pp. 803-809, May 2003.

[85] X. Wei, M. Verhaegen and T. Engelen, “Sensor fault detection and isolation for wind turbines based on subspace identification and Kalman filter techniques,” *Int. J. Adapt. Control Signal Process*, vol. 24, no. 8, pp. 687-707, Aug. 2010.

[86] P. Anderson and A. Bose, “Stability simulation of wind turbine systems,” *IEEE Trans. Power App. Sys.*, vol. PAS-102, no. 12, pp. 3791-3795, Dec. 1983.

[87] S. Kim and E. Kim, “PSCAD/EMTDC-based modelling and analysis of a gearless variable speed wind turbine,” *IEEE. Trans. Energy Convers.*, vol. 22, no. 2, pp. 421-430, Jun. 2007.

[88] M. Rahnavard, M. Yazdi and M.Ayati, “On the development of a sliding mode observer-based fault diagnosis scheme for a wind turbine benchmark model,” *Energy Equipment and Systems*, vol. 5, no. 1, pp. 13-26, Mar. 2017.

[89] P. Odgaard and J. Stoustrup, “Unknown Input Observer Based Scheme for Detecting Faults in a Wind Turbine Converter,” in *Proceedings of the 7th IFAC symposium on fault detection, supervision and safety of technical processes*, pp. 161-166, Barcelona, Spain, June 30-July 3, 2009.

[90] M. Shaker and R. Pattern, “Active sensor fault tolerance output feedback tracking control for wind turbine systems via T-S fuzzy model,” *Eng. Appl. Artif. Intell.,* vol. 34, pp. 1-12, Sep. 2014.

[91] S. Dey, P. Pisu and B. Ayalew, “A comparitive study of three fault diagnosis schemes for wind turbines,” *IEEE Trans. Control Syst. Technol.*, vol. 23, no. 5, pp. 1853-1868, Sep. 2015.

[92] M. Cao, Y. Qiu, Y. Feng, H. Wang and D. Li, “Study of wind turbine fault diagnosis based on unscented Kalman filter and SCADA data,” *Energies*, vol. 9, no. 10, pp. 847-864, Oct. 2016.

[93] P. Guo, D. Infield and X. Yang, “Wind turbine generator condition monitoring using temperature trend analysis,” *IEEE Trans. Sustain. Energy*, vol. 3, no. 1, pp. 124-133, Jan. 2012.

[94] H. Badihi, Y. Zhang and K. Hong, “Wind turbine fault diagnosis and fault-tolerant torque load control against actuator faults,” *IEEE. Tans. Contr. Syst. Technol.*, vol. 23, no. 4, pp. 1351-1372, Jul. 2015.

[95] J. Chen, L. Jiang, W. Yao and Q. Wu, “Perturbation estimation based nonlinear adaptive control of a full-rated converter wind turbine for fault ride-through capability enhancement,” *IEEE. Trans. Power Syst.*, vol. 29, no. 6, pp. 2733-2743, Nov. 2014.

[96] R. Gao and Z. Gao, “Pitch control for wind turbine systems using optimization, estimation and compensation,” *Renew. Energ.*, vol. 91, pp. 501-515, Jun. 2016.

[97] S. Simani and P. Castaldi, “Active actuator fault-tolerant control of a wind turbine benchmark model,” *Int. J. Robust Nonlinear Control*, vol. 24, nos. 8-9, pp. 1283-1303, May-Jun. 2014.

[98] Y. Vidal, C. Tutive´n, J. Rodellar and L. Acho, “Fault diagnosis and fault tolerant control of wind turbines via a discrete time controller with disturbance compensator,” *Energies*, vol. 8, pp. 4300-4316, May 2015.

[99] F. Shi and R. Patton, “An active fault tolerant control approach to an offshore wind turbine model,” *Renew. Energ.*, vol. 75, pp. 788-798, Mar. 2015.

[100] P. Odgaard and J. Stoustrup, “A benchmark evaluation of fault tolerant wind turbine control concepts,” *IEEE Tans. Contr. Technol.*, vol. 23, no. 3, pp. 1221-1228, May 2015.

[101] S. Simani and P. Castaldi, “Data-driven and adaptive control applications to a wind turbine benchmark model,” *Control Eng. Practice*, vol. 21, no. 12, pp. 1678-1693, Dec. 2013.

[102] F. Shi and R. Patton, “An active fault tolerant control approach to an offshore wind turbine model,” *Renew. Energ.*, vol. 75, pp. 788-798, Mar. 2015.

[103] W. Teng, F. Wang, K. Zhang, Y. Liu and X. Ding, “Pitting fault detection of a wind turbine gearbox using empirical mode decomposition,” *J. Mech. Eng.*, vol. 60, no. 1, pp. 12-20, 2014.

[104] J. Chen, J. Pan, Z. Li, Y. Zi and X. Chen, “Generator bearing fault diagnosis via empirical wavelet transform using measured vibration signals,” *Renew. Energ.*, vol. 89, pp. 80-92, Apr. 2016.

[105] P. Tamilselvan, P. Wang, S. Sheng and J. Twomey, “A two-stage diagnosis frame work for wind turbine gearbox condition monitoring,” *Int. J. Prognost. Health Mang.*, vol. 4, pp. 21-31, May 2013.

[106] D. Zappalá, P. Tavner, C. Crabtree and S. Sheng, “Side-band algorithm for automatic wind turbine gearbox fault detection and diagnosis,” *IET Renew. Power Gener.*, vol. 8, no. 4, pp. 380-389, May 2014.

[107] F. Pozo and Y. Vidal, “Wind turbine fault detection through principal component analysis and statistical hypothesis testing,” *Energies*, vol. 9, no. 3, pp. 1-20, Dec. 2015.

[108] J. Wang, R. Gao and R. Yan, “Intergration of EEMD and ICA for wind turbine gearboc diagnosis,” *Wind Energ.*, vol. 17, no. 5, pp. 757-773, May 2014.

[109] G. Wang and Z. Huang, “Data-driven fault tolerant control design for wind turbines with robust residual generator,” *IET Contr. Theory Appl.*, vol. 9, no. 7, pp. 1173-1179, Apr. 2015.

[110] J. Lou, H. Lu, J. Xu and Z. Qu, "A data-mining approach for wind turbine power generation performance monitoring based on power curve," *Int. J. Smart Home*, vol. 10, no. 2, pp. 137-152, Feb. 2016.

[111] N. Yampikulsakul, E. Byon, S. Huang, S. Sheng and M. You, "Condition monitoring of wind power system with nonparametric regression analysis," *IEEE. Trans. Energ. Convers.*, vol. 29, no. 2, pp. 288-299, Jun. 2014.

[112] P. Santos, L. Villa, A. Ren˜ones, A. Bustillo and J. Maudes, "An SVM-based solution for fault detection in wind turbines," *Sensors*, vol. 15, no. 3, pp. 5627-5648, Mar. 2015.

[113] M. Schlechtingen and I. Santos, "Comparative analysis of neural network and regression based condition monitoring approaches for wind turbine fault detection," *Mechanical Systems and Signal Processing*, vol. 25, no. 5, pp. 1849-1875, Jul. 2011.

[114] Z. Yang, X. Wang and J. Zhong, "Representational learning for fault diagnosis of wind turbine equipment: a multi-layered extreme learning machines approach," *Energies*, vol. 9, no. 6, pp. 379-395, May 2016.

[115] A. Kusiak, H. Zheng and Z. Song, "Models for monitoring wind farm power," *Renew. Energ.*, vol. 34, no. 3, pp. 583-590, Mar. 2009.

[116] H. Toubakh and M. Sayed-Mouchaweh, "Hybrid dynamic data-driven approach for drift-like fault detection in wind turbines," *Evolving Syst.*, vol. 6, no. 2, pp. 115-129, Jun. 2015.

[117] R. Fernandes-Canti, J. Blesa, S. Tornil-Sin and V. Puig, "Fault detection and isolation for a wind turbine benchmark using a mixed Bayesian/set-membership approach," *Annual Reviews in Control*, vol. 40, pp. 59-69, Oct. 2015.

[118] L. Bessa, R. Palhares, M. Dangelo and J. Filho, "Data-driven fault detection and isolation scheme for a wind turbine benchmark," *Renew. Energ.*, vol. 87, no. 1, pp. 634-645, Mar. 2016.

[119] N. Lao, S. Othman, M. Alamir and N. Sheibat-Othman, "Combination of model-based observer and support vector machines for fault detection of wind turbines," *Int. J. Auto. Comput.*, vol. 11, no. 3, pp. 274-287, Jun. 2014.

[120] M. Entezami, S. Hillmansen, P. Weston and M. Papaelias, “Fault detection and diagnosis within a wind turbine mechanical braking system using condition monitoring,” *Renew. Energ.*, vol. 47, pp. 175-182, Nov. 2012.

[121] S. Yin, G. Wang and H. Karimi, “Data-driven design of robust fault detection systems for wind turbines,” *Mechatronics*, vol. 24, no. 4, pp. 298-306, Jun. 2014.

[122] Z. Du, X. Chen, H. Zhang and R. Yan, “Sparse feature identification based on union of redundant dictionary for wind turbine gearbox fault diagnosis,” *IEEE Trans. Ind. Electron.*, vol. 62, no. 10, pp. 6594-6605, Oct. 2015.

[123] Y. Jiang, B. Tang, Y. Qin and W. Liu, “Feature extraction method of wind turbine based on adaptive Morlet wavelet and SVD,” *Renew. Energ.*, vol. 36, no. 8, pp. 2146-2153, Aug. 2011.

[124] W. Liu, Z. Wang, J. Han and G. Wang, “Wind turbine fault diagnosis method based on diagonal spectrum and clustering binary tree SVM,” *Renew. Energy*, vol. 50, pp. 1-6, Feb. 2013.

[125] L. Li, Y. Jia, J. Du and S. Yuan, “Robust L_2-L_∞ control for uncertain singular systems with time-varying delay,” *Prog. Natur. Sci.*, vol. 18, no. 8, pp. 1015-1021, Aug. 2008.

[126] S. Boyd, L. E. Ghaoui, E. Feron and V. Balakrishnan, Linear matrix inequalities in system and control theory, Philadelphia: Society for Industrial and Applied Mathematics, 1994.

[127] S. Daley and H. Wang, “Fault detection using reduced order models,” *Proceedings of the Institution of Mechanical Engineers, Part I: J. Syst. Contr. Eng.*, vol. 207, no. 3, pp. 153-164, Jul. 1993.

[128] S. Ibrir, W. Xie, and C. Su, “Observer-based control of discrete-time Lipschitzian non-linear systems: application to one-link flexible joint robot,” *Int. J. Contr.*, vol. 78, no. 6, pp. 385-395, Apr. 2005.

[129] R. Rajamani and Y.M. Cho, “Existence and design of observers for nonlinear systems: relation to distance to unobservability,” *Int. J. Contr.*, vol. 65, no. 5, pp. 717-731, May 1998.

[130] E. D. Sontag, “Smooth stabilization implies coprime factorization,” *IEEE Trans. Auto. Contr.*, vol. 34, no. 4, pp. 435-443, Apr. 1989.

[131] E. D. Sontag and Y. Wang, “New characterization of input-to-state stability,” *IEEE Trans. Auto. Contr.*, vol. 41, no. 9, pp. 1283-1294, Sep. 1996.

[132] M. Arcak and P. Kokotovic, “Nonlinear observer: a circle criterion design and robustness analysis,” *Automatica*, vol. 37, no. 12, pp. 1923-1930, Dec. 2001.

[133] H. Shim, J. H. Seo and A. R. Teel, “Nonlinear observer design via passivation of the error dynamics,” *Automatica*, vol. 39, no. 5, pp. 885-892, May 2003.

[134] M. A. Muller and D. Liberzon, “Input/output-to-state stability and state-norm estimators for switched nonlinear systems,” *Automatica*, vol. 48, no. 9, pp. 2029-2039, Sep. 2012.

[135] D. Liberzon and D. Nesic, “Input-to-state stabilization of linear systems with quantized state measurements,” *IEEE Trans. Auto. Contr.*, vol. 52, no. 5, pp. 767-781, May 2007.

[136] J. Tsinias, “Stochastic input-to-state stability and applications to global feedback stabilization,” *Int. J. Contr.*, vol. 71, no. 5, pp. 907-930, May 1998.

[137] S. J. Liu, J. F. Zhang and Z. P. Jiang, “A notion of stochastic input-to-state stability and its application to stability of cascaded stochastic nonlinear systems,” *Acta Math. Appl. Sin., Engl. Ser.*, vol. 24, no. 1, pp. 141-156, Jan. 2008.

[138] P. Zhao, W. Feng and Y. Kang, “Stochastic input-to-state stability of switched stochastic nonlinear systems,” *Automatica*, vol. 48, no. 10, pp. 2569-2576, Oct. 2012.

[139] S. P. Bhat and D. S. Bernstein, “Finite-time stability of continuous autonomous systems,” *SIAM J. Contr. Opt.*, vol. 38, no. 3, pp. 751-766, 2000.

[140] P. Zhao, W. Feng, Y. Zhao and Y. Kang, “Finite-time stochastic input-to-state stability of switched stochastic nonlinear systems,” *Applied Mathematics and Computation*, vol. 268, pp. 1038-1054, Oct. 2015.

[141] W. T. Zha, J. Y. Zhai, S. M. Fei and Y. J. Wang, “Finite-time stabilization for a class of stochastic nonlinear systems via output feedback,” *ISA Trans.*, vol. 53, no. 3, pp. 709-716, May 2014.

[142] Z. D. Ai and G. D. Zong, “Finite-time stochastic input-to-state stability of impulsive switched stochastic nonlinear systems,” *Appl. Math. Comput.*, vol. 245, pp. 462-473, Oct. 2014.

[143] R. Situ, Theory of stochastic differential equations with jumps and applications: mathematical and analysis techniques with applications to engineering, New York, USA: Springer, 2005.

[144] W. Hahn, Stability of motion, Berlin: Springer-Verlag, 1967.

[145] M. Krstić and H. Deng, Stabilization of nonlinear uncertain systems, London: Springer-Verlag, 1998.

[146] X. Mao, Stochastic differential equations and applications, 2nd ed. Chichester, U. K.: Horwood, 2007.

[147] M. Abbaszadeh and H. J. Marquez, “Nonlinear observer design for one-sided Lipschitz systems,” in *Proc. IEEE American Contr. Conf.*, pp. 5284-5289, Baltimore, MD, USA, June 30-July 2, 2010.

[148] D. Higham, “An algorithmic introduction to numerical simulation of stochastic differentail equations,” *SIAM Review*, vol. 43, no. 3, pp. 525-546, 2001.

[149] M. Chilali and P. Gahinet, “H_∞ design with pole placement constraints: an LMI approach,” *IEEE Trans. Automat. Contr.*, vol. 41, no. 3, pp. 358-367, Mar. 1996.

[150] D. Zhou, X. He, Z. Wang, G. Liu and Y. Ji, “Leakage fault diagnosis for an internet-based three-tank system: An experimental study,” *IEEE Trans. Control Syst. Technol.*, vol. 20, no. 4, pp. 857-870, Jul. 2012.